

POWER OPTIMIZATION, NETWORK CODING AND DECISION FUSION IN  
MULTI-ACCESS RELAY NETWORKS

by  
KAYHAN ERİTMEN

Submitted to the Graduate School of Engineering and  
Natural Sciences in partial fulfillment of  
the requirements for the degree of  
Doctor of Philosophy

Sabancı University  
August 2014

POWER OPTIMIZATION, NETWORK CODING AND DECISION FUSION IN  
MULTI-ACCESS RELAY NETWORKS

APPROVED BY:

Associate Prof. Dr. Mehmet Keskinöz (Thesis Advisor): .....

Prof. Dr. Murat Uysal : .....

Prof. Dr. Ersin Göğüş: .....

Associate Prof. Dr. Ali Koşar: .....

Associate Prof. Dr. Yücel Saygın: .....

DATE OF APPROVAL: .....

© Kayhan Eritmen 2014

All Rights Reserved

## ABSTRACT

Multi-access relay (MAR) assisted communication appears in various applications such as hierarchical wireless sensor networks (WSN), two-way relay channels (TWRC) etc. since it provides a high speed and reliable communication with considerably large coverage. In this thesis, we develop the optimal power allocation, network coding and information fusion techniques to improve the performance of MAR channel by considering certain criterion (e.g., minimizing the average symbol error rate (SER) or maximizing the average sum-rate. For this purpose, we first derive optimal information fusion rules for hierarchical WSNs with the use of complete channel state information (CSI) and the partial CSI using channel statistics (CS) with the exact phase information. Later, we investigate the optimization of the MAR channel that employs complex field network coding (CFNC), where we have used two different metrics during the optimization: achievable sum rate and SER bound of the network under the assumption of receiver CSI. After that, we formulate the optimal power allocation problem to maximize the achievable sum rate of the MAR with decode and forward relaying while considering fairness among users in terms of their average achievable information rates under the constraints on the total power and network geometry. We show that this problem is non-convex and nonlinear, and obtain an analytical solution by properly dividing parameter space into four regions. Then, we derive an average SER bound for the CFNC coded MAR channel and aim to jointly optimize the CFNC and the relay power by minimizing SER bound under the total power constraint, which we prove as a convex program that cannot be solved analytically since the Karush-Khun-Tucker (KKT) conditions result in highly nonlinearity equations. Following that, we devise an iterative method to obtain SER optimal solutions which uses the information theoretical rate optimal analytical solution during the initialization and we show that this speeds up the convergence of the iterative method as compared to equal power allocation scheme. Next, we integrate CFNC

into WSNs that operate over non-orthogonal communication channel, and derive optimal fusion rule accordingly, combine the SER bound minimization and the average rate-fairness ideas to come up with an approximate analytical method to jointly optimize CFNC and the relay power. Simulation results show that the proposed methods outperform the conventional methods in terms of the detection probability, achievable average sum-rate or average SER.

## ÖZET

Çoklu erişimli röle (ÇER) destekli haberleşme kanalları, yüksek hızda güvenilir haberleşme ve oldukça geniş kapsama alanı sağlaması nedeniyle hiyerarşik kablosuz duyurga ağları (KDA) ve iki yönlü röle kanalları gibi uygulamalarda kullanılmaktadır. Bu tezde, belli kriterleri dikkate alarak (sembol hata oranını (SHO) en azlamak, veya ortalama toplam ulaşılabilir veri hızını en çoklamak gibi) ÇER kanala performansını artırmak için en uygun güç paylaşırma, şebeke kodlama ve bilgi tümleştirme teknikleri geliştirdik. Bu sebepten ilk olarak hiyerarşik KDAlar için en uygun bilgi tümleştirme kuralını, eksiksiz kanal durum bilgisi (KDB) ve tam faz bilgisi ile kanal istatistiği (KI) durumları için ayrı ayrı türettik. Sonra, alıcıların KDBye sahip oldukları varsayımı altında, ulaşılabilir toplam veri hızı ve şebekenin SHO üst sınırı en iyileme ölçülerini kullanarak, kompleks alan şebeke kodu (KAŞK) kullanan ÇER kanalın en iyilemesini inceledik. Daha sonra, çöz ve ilet aktarma kullanan ÇER için kullanıcılar arasında ortalama ulaşılabilir veri hızı açısından adil olan ve ulaşılabilir toplam veri hızını en çoklayan güç paylaşırma problemini toplam güç kısıtını ve şebeke geometrisini hesaba katarak formülize ettik. Bu problemin dışbükey ve doğrusal olmadığını gösterip, parametere uzayını uygun bir şekilde dört bölgeye bölerek analitik bir sonuç elde ettik. Ardından, KAŞK kodlanmış ÇER için ortalama bir SHO üst sınır türettik ve KAŞK ve röle güç değerlerini toplam güç kısıtı altında SHO üst sınırını en azlayacak şekilde ortaklaşa en iyilemeyi hedefledik ki bu problemin Karush-Kuhn-Tucker koşullarındaki yüksek doğrusalsızlık nedeni ile analitik olarak çözülemeyen bir dışbükey program olduğunu gösterdik. Bunun üzerine, ilklendirme sırasında veri hızını açısından en uygun olan analitik çözümü kullanan yinelemeli bir metod tasarladık ve bunun eşit güç paylaşımına göre yinelemeli sistemin yakınsamasını hızlandırdığını gördük. Ardından, KAŞKı dikey olmayan kanallar üzerinden çalışan KDAlara entegre ettik ve en uygun tümleştirme kuralını türettik; SHO üst sınırını en azlama ve ortalama veri hızı adaleti fikirlerini birleştirerek KAŞKı ve röle gücünü

birlikte en iyileyen yaklaşıp bir analitik metod önerdik. Benzetim sonuçları önerdiğimiz methodların geleneksel methodlara göre sezim olasılığı, ulaşılabilir ortalama toplam veri hızı ve ortalama SHO açısından üstün olduğunu gösterdi.

## **ACKNOWLEDGEMENTS**

I would like to offer my thanks and gratitude to my thesis advisor Associate Professor Mehmet Keskinöz for his technical and psychological support throughout this work.

I also would like to thank Professors Murat Uysal, Ersin Göğüş, Ali Koşar and Yücel Saygın for reading and commenting on this thesis.

Throughout my doctorate studies, I am financially supported by TUBITAK which helped me very much to concentrate on my thesis.

I would like to thank my colleagues, housemates and members of Sabancı University for creating an entertaining and inspirational atmosphere. Also, I would like to thank Gülfem for her presence.

Last but not the least; I am grateful to my beloved family -particularly my mother Müzeyyen Akın- for their endless support during my graduate study.

*Dedicated to Recep Akin ...*

## TABLE OF CONTENTS

1.	INTRODUCTION .....	1
1.1	Hierarchical WSNs.....	3
1.2	Two Way Relay Channel .....	6
1.3	Wireless Network Coding for Multi Source Communication .....	7
1.4	Literature Review.....	9
1.4.1	Decision Fusion .....	10
1.4.2	Wireless Network Coding.....	10
1.5	Scope of the thesis and Contributions .....	12
2.	Distributed Decision Fusion over Fading Channels in Hierarchical Wireless Sensor Networks.....	15
2.1	The System Model of a Hierarchical WSN for Distributed Detection.....	18
2.2	Likelihood Ratio Test (LRT) Based Fusion Rule under Perfect Channel State Information .....	20
2.3	LRT Based Fusion Rule under Channel Statistics .....	25
2.4	Computational Complexity Comparison between LRT-CSI and LRT-CS .....	36
2.5	Simulation Results .....	38
2.6	Conclusions .....	42
3.	A Rate-Optimal Power Adaption Policy with User Fairness for Non-Orthogonal Multi-Access Relay Channels.....	46
3.1	System Model for a Basic Non-Orthogonal Multi-Access Relay Channel .....	49
3.2	A Fair Power Optimization Based On Rate Maximization Under Decode and Forward Relaying.....	52
3.2.1	Partition 1: $0 < \alpha \leq \frac{\min(g_1 - \gamma_1, g_2 - \gamma_2)}{g_r}$ .....	57
3.2.2	Partition 2: $\frac{\min(g_1 - \gamma_1, g_2 - \gamma_2)}{g_r} \leq \alpha \leq \alpha_0$ .....	59
3.2.3	Partition 3: $\alpha_0 \leq \alpha \leq \frac{\max(g_1 - \gamma_1, g_2 - \gamma_2)}{g_r}$ .....	62
3.2.4	Partition 4: $\frac{\max(g_1 - \gamma_1, g_2 - \gamma_2)}{g_r} \leq \alpha$ .....	65
3.2.5	Justification of the Negligibility of the Cross-Term .....	67
3.3	Simulation Results .....	69
3.4	Conclusions .....	76
4.	Symbol-Error Rate Optimized Complex Field Network Coding for Mobile Communications.....	78
4.1	A Basic Complex Field Network Coded Relay Channel Model .....	79
4.2	Determination of SER-Optimized User-Signatures .....	81
4.3	Determination of an Approximate Solution for the Signature Powers.....	91
4.4	Bit Error Rate Simulation Results of The SER-optimized CFNC.....	95
4.5	Conclusions .....	102
5.	Joint Optimization of Complex-Field Network Coding and Relay Power for Multi-User Communications.....	104
5.1	System Model for A Basic CFNC Coded Multi-ACCESS Relay Channel.....	105
5.2	A Bound on Average SER under ML Detection and Receiver Channel State Information .....	108

5.3	Determination of SER-Optimized User-Signatures when Only Receivers Knows Channel State Information .....	118
5.4	An Information Theoretical Heuristic Initialization Method.....	130
5.5	Bit Error Rate Simulation Results For the SER-optimized CFNC Coded MAR-NOC Channel ..	135
5.6	Conclusions .....	143
6.	Distributed Detection in Wireless Sensor Networks Using Complex Field Network Coding.....	145
6.1	Overview of Classical Distributed Detection Over Orthogonal Communication Channels.....	147
6.2	Distributed Detection For Complex Field Network Coded Relay Assisted Communication Over Multi-access Channels .....	149
6.3	Determination Of Sensor Signatures and The Relay Power For Complex Field Network Coded Relay Assisted Communications in WSNs.....	153
6.3.1	Information Theoretical Determination of Individual Sensor Powers .....	163
6.4	Simulation Results .....	166
6.5	Conclusions .....	172
7.	Conclusion and Future Work.....	173
	References .....	176

## TABLE OF FIGURES

Figure 1-1. Solution of basic problems in wireless communication.....	3
Figure 1-2. Types of WSN topologies.....	5
Figure 1-3. Classical Relaying for a Serial Relay Network.....	7
Figure 1-4. Two Way Relay Channel.....	7
Figure 1-5. Network Coding Schemes for TWRC.....	8
Figure 1-6. Complex Field Network coding.....	8
Figure 2-1. A wireless sensor network in hierarchical topology with two cluster heads and a global fusion center.....	19
Figure 2-2. ROC curves for LRT-CSI and LRT-CS fusion rules under SNR= 5 dB, $N=4$ clusters of $K=4,8$ sensors with $P_{D_j}^m = 0.5$ , $P_{F_j}^m = 0.05$ .....	43
Figure 2-3. Global detection probability of LRT-CSI and LRT-CS as a function of SNR for a WSN with $N=4$ clusters each of $K=8$ sensors under global false alarm probability, $P_{F_0}$ , of 0.01.....	43
Figure 2-4. Global detection performance improvement of LRT-CSI over LRT-CS as a function of SNR for a WSN with $N=4$ clusters each of $K=8$ sensors under global false alarm probability, $P_{F_0}$ , of 0.01.....	44
Figure 2-5. ROC curves for LRT-CSI and LRT-CS fusion rules under SNR= 5 dB, $N=4$ clusters of $K=4,8$ sensors with different detection and false alarm probabilities.....	44
Figure 2-6. ROC curves for LRT-CSI and LRT-CS fusion rules under SNR= 5 dB, $N=4,8,100$ clusters of $K=250, 125, 10$ sensors with $P_{D_j}^m = 0.6$ , $P_{F_j}^m = 0.08$ .....	45
Figure 2-7. ROC curves for LRT-CSI and LRT-CS fusion rules under SNR= 5dB, $N=4$ for uniform and non-uniform clustering with $P_{D_j}^m = 0.6$ , $P_{F_j}^m = 0.08$ .....	45
Figure 3-1. Schematic of a basic CFNC-RAC channel with two users, one relay node and one destination node.....	52
Figure 3-2. Average BER as a function of SNR of ROFPA and EPA method for various location of relay	73
Figure 3-3. Average BER as a function of SNR of the proposed power optimization methods for cases $g_1=5.57$ dB, $g_2=1.70$ dB $g_r=6.43$ dB and $g_1=3.60$ dB, $g_2=3.60$ dB $g_r=7.27$ dB.....	74
Figure 3-4. BER of each user for cases $g_1=5.57$ dB, $g_2=1.70$ dB $g_r=6.43$ dB and $g_1=3.60$ dB, $g_2=3.60$ dB $g_r=7.27$ dB.....	74
Figure 3-5. Sum rate as a function of SNR of ROFPA and EPA method for various location of relay.....	75
Figure 3-6. Sum rate as a function of SNR of the proposed power optimization methods for cases $g_1=5.57$ dB, $g_2=1.70$ dB $g_r=6.43$ dB and $g_1=3.60$ dB, $g_2=3.60$ dB $g_r=7.27$ dB.....	75
Figure 3-7. Rate of each user as a function of SNR of the proposed power optimization methods for cases $g_1=5.57$ dB, $g_2=1.70$ dB $g_r=6.43$ dB and $g_1=3.60$ dB, $g_2=3.60$ dB $g_r=7.27$ dB.....	76
Figure 4-1 A basic complex field network coded relay channel with two users and one relay node.....	81
Figure 4-2 Average BER as a function of SNR of the optimized and non-optimized CFNC for $g_1=30$ dB, $g_2=0.14$ dB, $g_r=0.27$ dB and various $\gamma_2$ values.....	98
Figure 4-3. Average BER as a function of SNR of the optimized and non-optimized CFNC for $g_1=3.10$ dB, $g_2=20$ dB, $g_r=3.10$ dB and various $\gamma_2$ values.....	101
Figure 5-1. Schematic of a basic CFNC coded MAR-NOC channel with two users, one relay node and one destination node.....	107
Figure 5-2. PEP as a function of SNR for $\gamma_1=0$ dB $\gamma_2=0$ dB $g_1=g_2=3.60$ dB $g_r=7.27$ dB.....	116
Figure 5-3. Average SER as a function of SNR for $\gamma_1=0$ dB $\gamma_2=0$ dB $g_1=g_2=3.60$ dB $g_r=7.27$ dB.....	118
Figure 5-4. NMRS value at each iteration for the scenario $g_1=3.60$ dB, $g_2=3.60$ dB $g_r=7.27$ dB $\gamma_1=0$ dB $\gamma_2=0$ when only receivers have knowledge of CSI.....	134
Figure 5-5. NMRS value at each iteration for the scenario $g_1=2.72$ dB, $g_2=2.72$ dB $g_r=9.55$ dB $\gamma_1=0$ dB $\gamma_2=0$ when only receivers have knowledge of CSI.....	135
Figure 5-6. Average BER value of users for various location of relay.....	139
Figure 5-7. Average BER value of users for cases $g_1=5.57$ dB, $g_2=1.70$ dB $g_r=6.43$ dB and $g_1=3.60$ dB, $g_2=3.60$ dB $g_r=7.27$ dB.....	140

Figure 5-8. BER of each user for cases $g_1= 5.57$ dB, $g_2= 1.70$ dB $g_r= 6.43$ dB and $g_1= 3.60$ dB, $g_2= 3.60$ dB $g_r= 7.27$ dB.....	141
Figure 6-3 Probability of error versus $SNR$ curves of CFNC-DD and CDD for $N=2$ , $\gamma_1= \gamma_2=0$ dB, $g_1=$ $g_2=10.45$ dB, $g_r= 3.10$ dB.....	169
Figure 6-4. ROC curves of CFNC-DD and CDD under different $SNRs$ for $N=2$ , $\gamma_1= \gamma_2=0$ dB, $g_1= g_2=10.45$ dB, $g_r= 3.10$ dB .....	170
Figure 6-5. Probability of error versus $SNR$ curves of CFNC-DD and CDD under various $\gamma_2$ values for $N=2$ , $\gamma_1= 0$ dB $g_1= 10.45$ dB $g_2= 3.10$ dB $g_r= 3.10$ dB.....	170
Figure 6-6. ROC curves of CFNC-DD and CDD under various $\gamma_2$ values for $N=2$ , $\gamma_1= 0$ dB $g_1= 10.45$ dB $g_2= 3.10$ dB $g_r= 3.10$ dB and $SNR= -5$ dB.....	171
Figure 6-7. Probability of error versus $SNR$ curves of CFNC-DD and CDD under various $\gamma_4$ values for $N=4$ , $\gamma_1=0$ dB, $\gamma_2=0.91$ dB, $\gamma_3=0.91$ dB, and $g_1= g_2= g_3= g_4=13.98$ dB, $g_r= 0.91$ dB.....	171
Figure 6-8. ROC curves of CFNC-DD and CDD under various $\gamma_4$ values for $N=4$ , $\gamma_1=0$ dB, $\gamma_2=0.91$ dB, $\gamma_3=0.91$ dB, and $g_1= g_2= g_3= g_4=13.98$ dB, and $SNR=0$ dB.....	172

## TABLE OF TABLES

Table 2-1. On-line computational complexity comparison of LRT-CSI and LRT-CS for each channel realizations .....	38
Table 3-1. The optimal user and relay powers obtained by ROFPA policy for various locations of relay ....	73
Table 3-2. The optimal user and relay powers obtained by ROFPA for various location of relay.....	73
Table 4-1. The SER-optimized signature powers for $g_1 = 30$ dB, $g_2 = 0.14$ dB, $g_r = 0.27$ dB and various $\gamma_2$ values .....	97
Table 4-2. BERs of Individual Users , the average BER and Its improvement at the destination with and without optimized CFNC for $\gamma_2 = 3$ dB .....	99
Table 4-3. BERs of Individual Users , the average BER and Its improvement at the destination with and without optimized CFNC for $\gamma_2 = 6$ dB .....	100
Table 4-4. The SER-optimized signature powers for $g_1 = 3.10$ dB, $g_2 = 20$ dB, $g_r = 3.10$ dB and various $\gamma_2$ values .....	100
Table 4-5. BERs of Individual Users, the average BER and Its improvement at the destination with and without optimized CFNC for $\gamma_2 = 1.94$ DB .....	101
Table 4-6. BERs of Individual Users , the average BER and Its improvement at the destination with and without optimized CFNC for $\gamma_2 = 4.44$ dB .....	102
Table 5-1. SER Optimum Signature powers and $\alpha$ for various location of relay node.....	139
Table 5-2. SER Optimum Signature powers and $\alpha$ for various location of relay node.....	140
Table 5-3. BER of users with Optimized Angle.....	143
Table 5-4. BER of users with Non-Optimized Angle.....	143
Table 5-5. BER improvement of Angle Optimization.....	143

# 1. INTRODUCTION

The growth of wireless communication industry continues to increase day by day with the help of advances in the communication theory and hardware technologies, and also due to its widespread use in internet connectivity, multimedia and data transfer, web-based applications such as Youtube, Twitter and Facebook etc. [1]. As a result of an enormous increase in the multimedia traffic, people demand for a high-rate and power efficient wireless connectivity. However, satisfying the quality of service (QoS) requirements of the numerous users or wireless devices in these high-speed wireless links is hindered by several degradations: path loss, multipath fading multi-user interference, shadowing, path loss, and receiver electronics noise etc [2].

Firstly, information carrying electromagnetic signals in wireless medium experience a reduction in their strengths or powers, which increases proportional to the distance they travel, and is referred as “path-loss” [2]. Secondly, the transmitted signal reflect from the obstacles (e.g., buildings, plantation, vehicles) in the wireless environment, and a bunch of signals possibly with different delays, amplitude and Doppler shifts arrive to the receiver. The superposition of these signals results in another phenomenon called “fading”, which is another source of degradation that affects the wireless system performance. Due to mobility of users, and the changes in the surrounding medium from time to time, the transmitted signal may not be “heard” from the receiver, this situation is called deep fading.

Therefore, researchers and system designers in wireless communications field should come up with new design ideas in order to satisfy QoS demands of users for reliable, efficient and high speed communications under these degradations while exploiting the limited resources in wireless systems well.

For example, diversity concept is proposed in literature [2] to overcome deep fading. Basically, diversity is achieved by transmitting the same signal over different channels that fade in an

uncorrelated fashion; consequently this decreases the deep fading probability. Diversity can be realized in different forms such as time, frequency, spatial and cooperative diversity [2], [3], [4]. Time diversity can be realized, for example, with the use of an error control code and interleaver [5]. Spatial diversity can be implemented by using space-time codes and multiple antennas at the transmitter and/or receiver [6]. Frequency diversity is done by transmitting the replicas of the information bearing signal through different frequency bands. In cooperative diversity, the information bearing signal of a specific user reaches the destination with the help of both the direct transmission and the relayed signaling, where other user(s) in the network act as relay(s) and the exchange of data between users relies on the broadcast nature of the wireless channel [4].

Actually, the main concept behind cooperative diversity based on the relay assisted communication channel is first introduced by Van Der Meulen [7], where there is one source, one receiver and a single relay node that helps the source transmit its data to the destination more reliably. In a more general setting, there may be more than one source or user, which get benefit of the relay assistance to transmit their data more reliably to a predetermined destination, and this system is referred as “ a multi-access relay (MAR) network”, which is proposed to overcome basic problems in multi user wireless communications as illustrated in Figure 1-1.

In a MAR network, there are essentially two classes of relaying: analog relaying and digital relaying [8], [9]. In the analog relaying, the relay amplifies the signal it receives and forwards it to the destination. Hence, the analog relaying decreases the amount of processing performed at the relay but it causes that the noise due to the electronics of the relay is also propagated to the destination. Contrary to the analog relaying, the relay in digital relaying first cleans the message from the noise by decoding or estimating the message, and then it re-encodes the decoded message and forwards it to the destination, in which the decoding or estimation errors result in incorrectness in the relayed message. Note that some relaying protocols existing in the current literature such as *amplify-and-forward* (AF) falls into analog relaying whereas *decode-and-forward* (DF) and *estimate and forward* (EF) policy are examples of digital relaying.

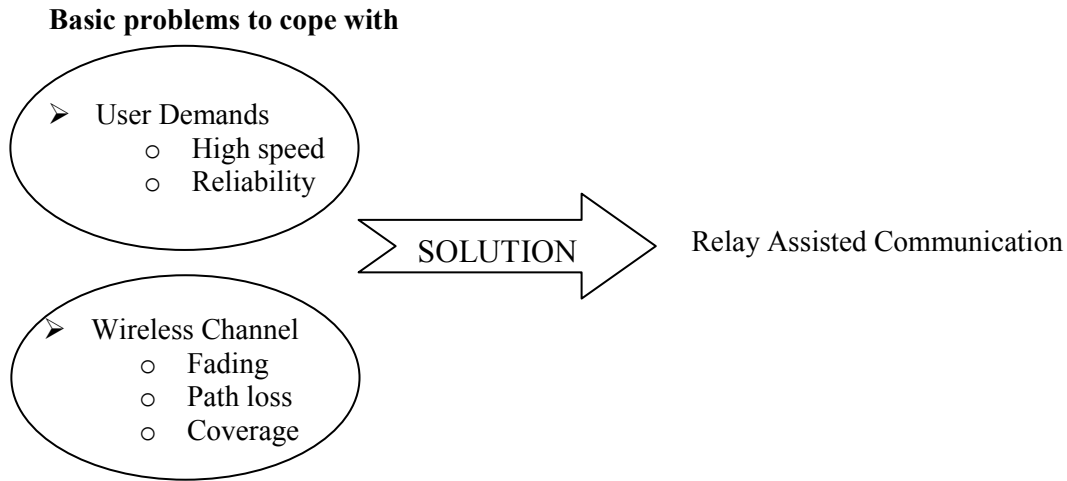


Figure 1-1. The relay assisted communication is useful to solve the basic problems in wireless communications

Moreover, error and outage probability analyses of relay assisted networks are investigated in [50]-[53]; capacity and power allocation for single user relay channels are addressed in [54]-[59]. In literature, there are some important examples of MAR channel such as hierarchical wireless sensor networks [10], [11] and two-way relay channels [12], which are subsequently explained in detail.

## 1.1 Hierarchical Wireless Sensor Networks (WSNs)

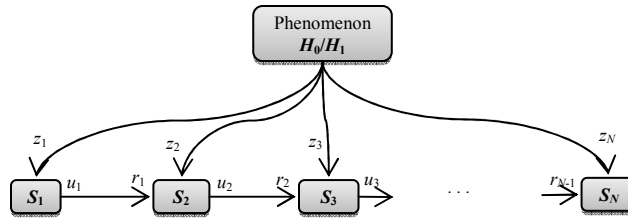
Conceptually, sensor nodes in a WSN are assumed to be simple and low powered devices with signal processing and transmission capabilities. They cooperatively try to make a decision about a phenomenon in the region of interest (ROI). Directly transmitting the raw sensor observations to a central unit is not wise since the transmission of the raw data consumes excessive power and sensors have low power. Therefore, each sensor first makes its own decision, which is called local decision, and then transmits this local decision to the nearest central unit. Lastly, a central unit called fusion center (FC) combines all the useful information coming from sensors and makes a

final decision, which is referred as “distributed detection” [10] and it is an instance of the MAR channel.

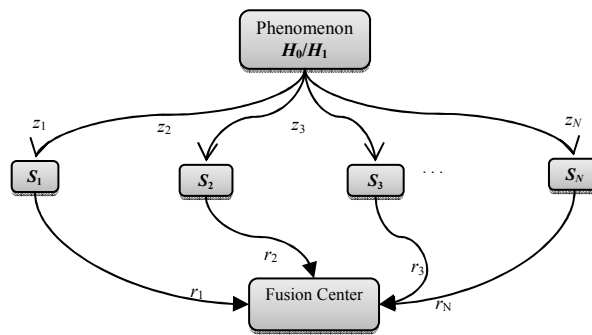
The distributed detection is conventionally handled over orthogonal channels, which can be realized by using time division multiple access (TDMA) or frequency division multiple access (FDMA) etc [2].

In general, WSNs can have different deployment topologies such as serial, parallel and hierarchical as depicted in Figure 1-2. In a serial topology, each sensor combines its observation with previous sensor's decision to make a local decision. Therefore, the last node in the network which can be considered as FC, makes the final decision. On the other hand, in parallel topology, sensors send their decisions directly to the FC, which combines the sensor signals and arrives at the final decision.

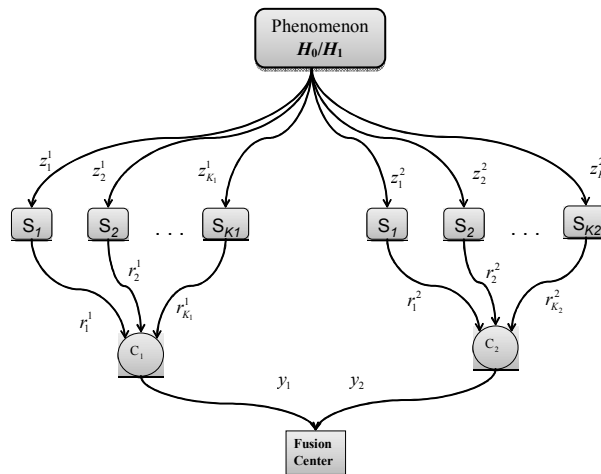
When a large number of sensors are randomly deployed in a large ROI, the serial topology cannot be applicable in practice since performing the serial distributed detection of large numbers of sensors increases the delay too much. The parallel topology is not viable for the case of a large ROI because sensors are low powered and the FC may not be in the direct transmission range of sensor nodes. On the other hand, the hierarchical topology is preferable to increase the coverage of the network when the ROI is large, in which the WSN is composed of clusters as shown in Figure 1-2-c, and each cluster has a cluster head (CLH) that acts as a relay, and each CLH fuses the local sensor decisions within its cluster to reach an intermediate decision to send to the global fusion center (GFC), which makes the final decision. Hence, applying this layered strategy in a hierarchical WSN presents a practical solution for the case of a large ROI since it can be covered with a low delay. Therefore, developing distributed detection and fusion methods for hierarchical WSNs are very useful for many practical applications.



a) Serial topology



b) Parallel topology



c) Hierarchical topology

Figure 1-2. Types of WSN topologies

## 1.2 Two-Way Relay Channel

Suppose two parties are not in the coverage of each other and aim to exchange their information through a relay node. Assuming that the communication is half-duplex [2] (i.e., only one node sends information at a time), a serial relay network in Figure 1-3 illustrates the way of exchanging information between the users, where the relay node  $R$  first receives the information symbol  $x_{s_1}$  of the user  $S_1$  and forwards it to the user  $S_2$  in the second time slot, and then the user  $S_2$  in the third time slot transmits its symbol  $x_{s_2}$  to the relay node  $R$  that forwards it to the user  $S_1$  in the fourth time slot. Consequently, the whole process of exchanging information between two users requires for time slots in total. Hence, the throughput of the serial relay network in terms of the number of symbols per source per channel use (sym/s/cu) is  $\frac{1}{4}$ . Therefore, the spectral efficiency of the classical relaying with half-duplex communication is low since one transmission period is divided into two time slots [13].

To increase throughput of the network, two-way relay (TWRC) channel protocols are proposed in [12], [13] and [18], where the user  $S_1$  and the user  $S_2$  transmit their symbols  $x_{s_1}$  and  $x_{s_2}$ , in the first and the second time slots, respectively, and subsequently the relay node decodes the user symbols and then forwards, for example, their modulo-2 sum,  $x_{s_1} \oplus x_{s_2}$ , in the next time slot as depicted in Figure 1-4. Hence, the exchange of user messages is completed in three time slots in TWRC, which provides a throughput of  $\frac{1}{3}$  sym/s/cu instead of  $\frac{1}{4}$  sym/s/cu of the classical relaying. Consequently, this TWRC protocol provides a higher spectral efficiency since the relay combines the user messages and forwards that combination of the user signals instead of sending them separately [13].

It is an important to note that the TWRC is a special case of a MAR channel where the source nodes and the destination nodes are the same. Also, the way of combining the user messages at

the relay node is called network coding (NC), which will be thoroughly explained in the next section.

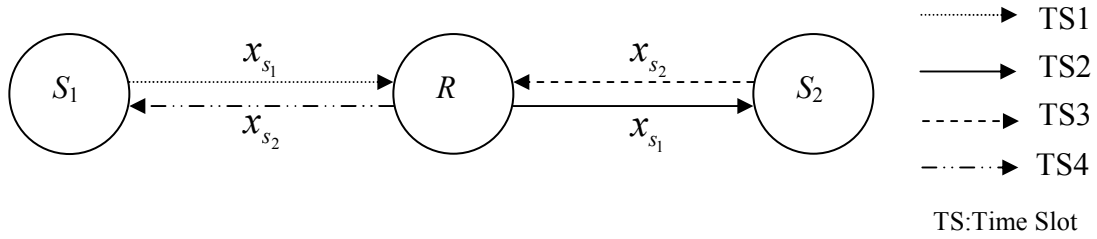


Figure 1-3. Classical Relaying for a Serial Relay Network

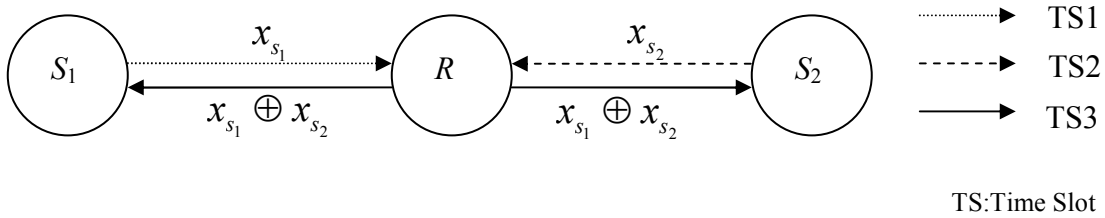


Figure 1-4. Two-way Relay Channel

### 1.3 Wireless Network Coding

Early works of the network coding focus more on wire-line communications where each source communicates with a relay node over an orthogonal channel that is assumed to be error free[14]. In contrast to wire-line channels, wireless channels allow the superposition of the transmitted signal in the “air” [8] thanks to its broadcast nature, which can be used to increase the throughput of the TWRC that employs modulo-2 (or XOR) network coding. Consequently, physical layer network coding (PNC) is proposed [15], where the users  $S_1$  and  $S_2$  simultaneously send their information signals  $x_{s_1}$  and  $x_{s_2}$  to the relay node in the first time slot, and the relay node experiences the superimposed signal  $x_{s_1} + x_{s_2}$  the because of the additive nature of wireless channels, and the relay node obtains an estimate of the superimposed signal,  $x_r$ , that is

broadcasted to both of the users in the second time slot (as illustrated in Figure 1-5). Hence the throughput of PNC becomes  $\frac{1}{2}$  sym/s/cu instead of  $\frac{1}{3}$  sym/s/cu of modulo-2 (or XOR) network coding over orthogonal channels. Note that PNC uses the multi-access nature of the wireless channel in the first time slot to improve the network throughput.

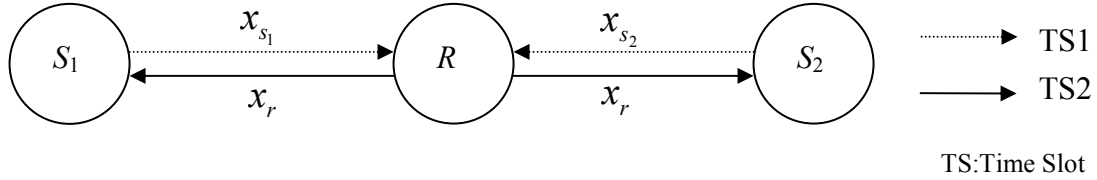


Figure 1-5. Physical Layer Network Coding for TWRC

Even though PNC achieves the throughput of  $\frac{1}{2}$  sym/s/cu, it is applicable for only TWRC. For a general MAR channel where the sources and destination nodes are different, PNC is not useful since the relay cannot uniquely decode the user messages, and this deteriorates the error performance of the system.

To remedy that, the complex field network coding (CFNC) has been proposed [20] as illustrated in, where each of  $N$  users is first assigned to a unique pre-determined complex number  $\theta_i$  for  $i=1,2,\dots,N$  that is referred as *signature*. Then, each user weights its message by its signature and then simultaneously broadcast them in the first time slot, which are superposed at both the relay and destination nodes. In the second time slot, the relay decodes each of the user messages from the superposed signal and estimates the noise-free CFNC symbol  $\theta_1 x_{s_1} + \theta_2 x_{s_2} + \dots + \theta_N x_{s_N}$ , which is then forwarded to the destination node in the second time slot. Finally, the destination node jointly decodes each of the user messages from the signals it has received in two time slots. Note that each user messages (assuming they are drawn from a finite constellation) can be uniquely decoded from the CFNC symbol  $\theta_1 x_{s_1} + \theta_2 x_{s_2} + \dots + \theta_N x_{s_N}$  as

long as  $\theta_i \neq \theta_j$  for  $i \neq j$ . Hence, CFNC uniquely allows decoding of user messages under multi-access interference (MAI) which is introduced due to the non-orthogonal communications, and provides a throughput of  $\frac{1}{2}$  symbol per source per channel-use. Moreover, it has also ability to provide full diversity irrespective from signal-to-noise-ratio (SNR) and the type of employed modulation [20]. Because of these nice features, in this thesis, we consider the CFNC as a network coding scheme.

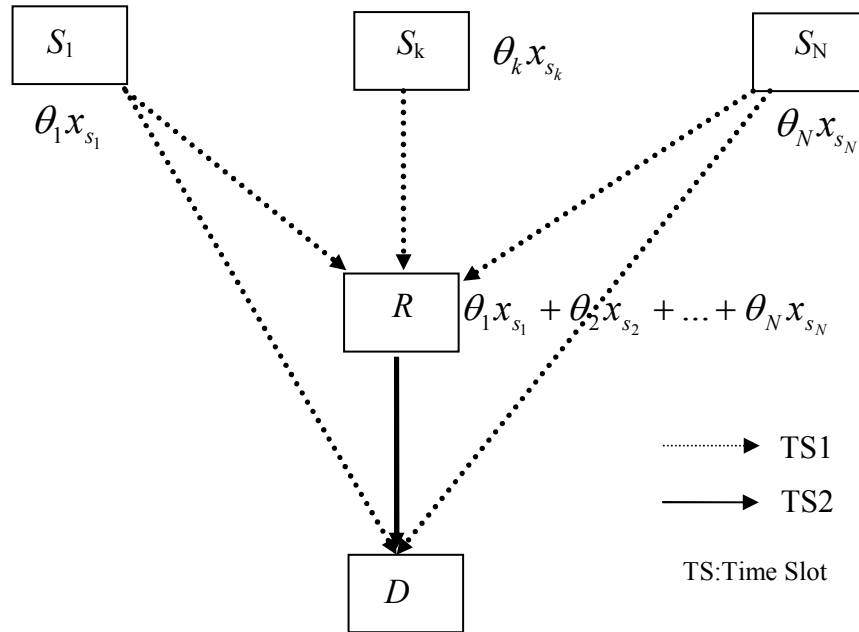


Figure 1-6. Complex Field Network coding

Diversity gain of network coding in wireless networks is analyzed in [60]. Also, practical implementation problems such as network layer issues, symbol and carrier phase asynchronies and channel coding-decoding strategies for network coding are investigated in [61]-[66].

## 1.4 Problem Definition and Related Literature

In this section, we give a literature overview regarding the issues throughout the thesis.

### **1.4.1** *Distributed Decision Fusion*

Early works of distributed decision fusion with multiple sensors goes back to early 80's. In the first works of this literature, the distributed decision fusion rules for WSNs are derived both under Bayes and Neyman-Pearson criteria, when the sensors have conditionally independent observations [21]-[26]. Then, authors in [27]-[32] analyzed how distributed decision fusion can be performed when sensor observations are correlated. Up to this point, aforementioned works was interested in optimally fusing the decisions of the sensors and they do not take the limitations on the communication resources into account. Therefore, the studies in [33]-[37] consider the communication constraints while performing distributed decision fusion. Also, authors in [38] included the communication errors during the decision fusion process, and the optimal decision fusion strategy under Bayes criterion is obtained for non-ideal communication channels in [39]. Channel-aware optimum and sub-optimum fusion rules are derived in [40] and [41] by considering wireless channel imperfections.

Thus far, the referred works regarding the distributed decision fusion assume that sensors are deployed in a parallel topology. However, a hierarchical topology is more practical to serve in a large ROI as mentioned in Section 1.1. Hence, the distributed decision fusion in hierarchical WSNs becomes crucial, which was analyzed in [42] and [43] by considering only the noise without taking the fading into account. Therefore, developing distributed decision fusion rules over fading channels in a hierarchical WSN is useful to be used in practical applications.

### **1.4.2** *Wireless Network Coding & Optimal Power Allocation*

As mentioned in Section 1.3, network coding is to combine data of several users and then send the resultant combination to the destination(s) to overcome bandwidth inefficiency of the multi-user communications, which is first proposed in [17] for wired networks. Then the first practical network coding strategy that is performed at the relay node is XOR method proposed in [18].

Eventually, PNC was proposed in [15] to increase the throughput of wired and wireless

channels. Although XOR method and PNC are efficient protocols for TWRC, they cannot be used for exchanging information among more than two users and for the case where the destination nodes are different from the source nodes. On the other hand, the complex field network coding (CFNC) proposed in [20] allows uniquely decoding of user messages as long as their signatures are distinct, which makes the CFNC be robust against multi-access interference (MAI) due to the simultaneous transmission of the user messages, and thus it achieves a throughput of 1/2 symbol per user per channel-use irrespective from the number of users in the network.

Therefore, the signature selection becomes an important issue for the CFNC coded MAR system. Wang *et.al.* [20] select signatures based on linear constellation precoding, which are purely complex exponential and distinctively rotates the constellation of each user. In contrast to [20], one can also employ signatures with non-unity magnitudes, and optimize them according to certain criterion (e.g., minimizing the average symbol error rate (SER) bound or maximization the total information rate under the average rate fairness) to enhance its performance by keeping the average transmit power of the network limited, which results in the optimizing the constellation and power of the users simultaneously. In addition to signature optimization, the performance of the system can be further improved by appropriately allocating the relay power. Hence, joint optimization of the user signatures and the relay power is an important problem to research for.

To best of our knowledge, there are a few studies in the context of power optimization in network coding. In [71], authors propose a constellation optimization method based on instantaneous CSI of users for TWRC which applies PNC where users apply QPSK modulation and relay uses denoise and forward relaying. Also, Zaidi *et.al.* [72] optimized the mapping at the relay in a way that maximizes the achievable sum rate of an orthogonal additive white Gaussian noise (AWGN) MAR channel which employs PNC. Last, Wang *et. al.* [73] investigated a special network with two sources, two destinations and a relay where PNC is applied and destinations cannot directly receive from their corresponding sources. They proposed a power adaptation method to maximize the achievable rate of the network under peak power constraint for sources and relay and

assuming that CSI of communication channels are available at each node.

Besides theory, RAC take its part in the standards of fourth generation (4G) communication networks like Long Term Evolution – Advanced (LTE-Advanced) [74]. In June 2013 “world’s first publicly available LTE-Advanced network” which applies relays with decode and forward capability is deployed by SK Telecom in South Korea [75]. These developments show that future generation communication networks will need RAC to satisfy customers’ data and speed demands.

In this thesis, we shall also consider CFNC coded MAR system and devise performance booster strategies, which are summarized in the next section.

## **1.5 Scope of the thesis and Contributions**

This thesis is organized as follows:

In Chapter 2, we consider WSNs which are a specialized usage of wireless technology to handle environmental monitoring and surveillance applications. For a WSN with hierarchical topology we investigated optimum fusion rules using exact channel state information (CSI) and exact phase knowledge with the envelope statistics. We show that even the fusion rule with exact CSI performs better in terms of detection performance; it is much more complex when compared to the fusion rule with exact phase knowledge with the envelope statistics. Hence, we confirm that when processing power is crucial for a WSN, fusion rule which uses exact phase knowledge with the envelope statistics become a good choice with a little detection performance degradation. We also show that, when the total number of sensors is constant preferring small clusters sizes have positive impact on detection probability regardless of fusion rule.

We introduce a power optimization problem for complex field network coded relay assisted communication (CFNC-RAC) channel which uses decode and forward for relaying in Chapter 3. We propose a power optimization method for users and relay which fairly maximizes information

rate. In detail, we define an optimization problem to maximize the average sum capacity of the users while considering fairness in information rate under a total power constraint. By portioning the parameter space we come up with an analytical solution to this problem which is non-linear and non-convex. Also, we give bit error rate (BER) performance of this proposed system, compare it with a non-optimized system and show its performance superiority.

Chapter 4 introduces upper bound for symbol error probability (SER) of users at destination node for CFNC-RAC. Then, we propose to choose complex signatures in a way that minimizes this SER upper bound considering a total power constraint over users. We define a convex optimization problem and using Krush-Kuhn-Tucker (KKT) conditions we find the condition that argument of each complex signature have to satisfy. Besides, we obtain a highly non-linear relation between absolute values of complex signatures of each user which cannot be solved analytically. Then using the result we obtained in Chapter 3 as initial values of user power, we obtained the optimum power allocation for users using Taylor expansion around this initial point. We give BER performances of this proposed power and signature optimization and show that it has better BER performance when compared to the non-optimized system.

In Chapter 5, we first derive SER upper bound under the assumption that relay power is adjustable. Then we jointly optimized the signature powers and angles of users and relay power using this upper bound. Again, the relationship between user signature powers and relay power is highly nonlinear and analytic solutions cannot be found. Hence we select solution that we obtained in Chapter 3 as initial point and used Sequential Quadratic Programming (SQP) where we can write each step analytically, to obtain the optimum solution. Then, we show BER performance of proposed power and argument selection method to quantify the performance improvement of the proposed method.

In Chapter 6, first we give some background information about classical distributed detection. Then, we propose to use CFNC in distributed detection in WSNs and introduce system model for CFNC assisted distributed detection. We derive SER upper bound at the destination under the

assumption that relay power is adjustable and symbol probabilities are not equal. We propose to choose signatures which minimize SER at destination in order to decrease communication errors in detection process and define the optimization problem which minimizes the SER upper bound at fusion center under total power constraint. Since we have a more complicated optimization problem when compared to previous chapters, we end up more complicated relations between user powers and relay power. For this case, we come up with another initial point selection method where we model all users as a one *super node*. We derive this *super node*'s pair wise error probability at destination and we obtain power value of this *super node* and relay by minimizing the worst case PEP. Finally, we give receiver operating characteristic and error performance curves for proposed method and show its supremacy over classical distributed detection.

We conclude and give possible future work in chapter 7.

## 2. Distributed Decision Fusion over Fading Channels in Hierarchical Wireless Sensor Networks

As we introduced in Chapter 1, in distributed detection local sensor nodes make their own decisions and then send these decisions to the nearest CLHs and CLHs send their decisions to the GFC. Since sensor nodes transmit their decisions instead of transmitting their raw observation data distributed detection is more reasonable for the networks with limited resources and it is preferable for WSN with limited resources [10]. In this chapter, we study distributed decision fusion problem for WSNs with hierarchical topology.

In the literature, the distributed detection problem in a WSN using Bayes or Neyman-Pearson (N-P) criterion has been investigated comprehensively by deriving fusion rules and detection techniques [22]- [26] under the assumption of conditional independence. Additionally, the decision fusion based on correlated observations has been analyzed in [27]-[32]. Some studies have been dedicated to distributed detection under communication resource constraints [33]-[37]. All the above-mentioned works assume the communication between the sensor nodes to the fusion center to be error-free. To relax this assumption, Thomopoulos and Zhang [38] have come up with the idea of distributed detection over non-ideal communication channels under the N-P criterion. They have only considered the effect of the noise and assumed that the communication channel between each sensor and the fusion center is binary symmetric channel (BSC). Then, they have employed person-by-person optimization to determine the optimal LRT thresholds for both the local sensor and the fusion center. Later, Chen and Willet [39] have shown that the local sensor decisions obtained through LRTs are also optimal using the Bayes criterion.

Unfortunately, in addition to noise, fading is also present as another source of degradation during the signal transmission and information fusion in a practical WSN. To address that, Chen *et. al.* [40] have derived optimum and sub-optimum fusion rules for noisy and Rayleigh faded WSN with parallel structure when the channel state (CSI) information (i.e., fading coefficient) is

exactly known at the fusion center. The work in [40] has later been extended by Niu *et. al.* [41] to derive optimal and sub-optimal fusion rules when exact phase information along with the envelope statistics of the fading coefficient is exactly known at the fusion center, which is referred as channel statistics (CS) based fusion rule.

All previously mentioned studies have derived the fusion rules for WSNs with the parallel topology, in which sensors send their local decision directly to the fusion center. While the parallel topology is theoretically important and analytically tractable, it may not realistically present the way a practical WSN operates. In most WSN applications, sensors have irreplaceable power supply, which limits the transmission range of each sensor. To increase the coverage of the network, the hierarchical topology is preferable, in which the local sensors send their decisions to the local fusion centers called cluster heads (CLHs) and each CLH fuses these local sensor decisions to reach an intermediate decision to send to the global fusion center (GFC), which makes the final decision.

Recently, the distributed detection for a hierarchically configured network has been analyzed in [42] and [43] by assuming that the communication links are degraded only by noise, for which BSC model is used. In [43], the majority voting fusion rule has been employed, which assigns the same weight to all communication links, participating in the fusion at each CLH or at the GFC, regardless of their individual reliabilities. Because of that, a heuristic weighting rule has also been proposed in [43] to improve the performance of the majority rule, which gives relatively higher weights to more reliable links. In [42], the optimal decision fusion policy for BSC has been shown to be weighted order statistics whose weights are positive integers and obtained according to the reliabilities of the links. In addition, the uniform clustering has been considered in [42] while the non-uniform clustering has also been analyzed in [43].

Authors in [42] and [43] have fused hard decisions of the sensors under the BSC model, which causes loss in information [43]. As pointed out in [43], a BSC model may not be the best modeling choice for a wireless communication link, which experiences fading in addition to

noise. Hence, in this chapter, we have the fading and noise together taken into account and proposed signal level fusion methods for a hierarchical topology. Specifically, our contributions can be summarized as follows.

- Under the knowledge of the complete fading channel state information (CSI), we develop likelihood ratio test (LRT) based optimal fusion rule referred as LRT-CSI. For this purpose, we obtain optimal weights of CLHs in terms of probability of detection and probability of false alarm by deriving the probability density functions of LRTs of all CLHs.
- We analyze the computational complexity of LRT-CSI and state that it requires many *on-line* computations.
- To devise a fusion rule with lower complexity, we utilize the exact phase with envelope statistics (CS) of the fading channel and develop optimal LRT based fusion rule called LRT-CS. During its development, we derive the probability density functions of LRTs of all CLHs in order to determine their optimal weights in terms of their probability of detection and probability of false alarm.
- We analyze the computational complexity of LRT-CS and show that the *on-line* computations of LRT-CS are less than that of LRT-CSI and most of the computationally intensive steps in LRT-CS can be done *off-line*, which makes it practically attractive.
- Finally, we investigate the performance of LRT-CSI and LRT-CS through extensive numerical simulations, where the effects of various parameters such as signal-to noise ratio (SNR), number of clusters and/or number of sensors per cluster, types of clustering (i.e., uniform and non-uniform clustering), false alarm and detection probabilities of sensors are evaluated extensively.

In the next section, we describe the WSN model with a hierarchical configuration, while we derive LRT based fusion rules using CSI in Section 2.2. After that, the LRT based fusion rule

using CS is given in Section 2.3. In Section 2.4, the computational complexity of the proposed detection methods are analyzed and their performance evaluations are investigated through numerical experiments in Section 2.5. Finally, our conclusions are summarized in Section 2.6.

## 2.1 The System Model of a Hierarchical WSN for Distributed Detection

In this section, we present a system model of the hierarchical WSN configuration, which considers the fading and noise during the data communication and distributed detection. For this topology, we assume that there are  $N$  clusters each with  $K$  sensors<sup>1</sup> and all the sensors in each cluster work collaboratively to distinguish two or more hypotheses and send their decisions to the associated cluster head for intermediate data detection. Following that, cluster heads send their decisions to the global fusion center in order to reach a final decision.

In this work, we focus on binary hypotheses:  $H_1$  and  $H_0$  (e.g., they may represent the existence and absence of a target respectively) at region of interest. As depicted in Figure 2-1, the  $j^{\text{th}}$  sensor in the  $m^{\text{th}}$  cluster acquires an observation  $z_j^m$ , and quantizes it to reach a local decision of binary 0 or 1. Then these decisions are modulated through Binary Phase Shift Keying (BPSK) to obtain the signal  $x_j^m$ , which is assumed to take values of -1 and 1 for decision 0 and decision 1 respectively. The modulated signal  $x_j^m$  is later sent to the  $m^{\text{th}}$  CLH over the flat fading channel. By employing phase-coherent detection, receiver eliminates the phase of the signal therefore the amplitude of the received signal at  $m^{\text{th}}$  CLH becomes

$$r_j^m = h_j^m x_j^m + n_m \quad (2.1)$$

where  $h_j^m$  is the gain of the Rayleigh fading channel between the  $j^{\text{th}}$  sensor and  $m^{\text{th}}$  CLH, and  $n_m$  is the additive white Gaussian noise (AWGN) sample that is assumed to be zero-mean and

<sup>1</sup> Although we have assumed clusters with equal size  $K$ , the expressions and derivations are still same for the case of clusters with different sizes. Specifically, it is enough to replace  $K$  with  $K_m$ , which denotes the size of the  $m^{\text{th}}$  cluster.

variance of  $\sigma^2$ .

After the  $m^{th}$  CLH acquires all the signals from the sensors within the associated cluster, it arrives at an intermediate decision, which is sent through BPSK modulated signal,  $s_m$ , to the GFC over another wireless link. Under the coherent detection at GFC, the amplitude signal from the  $m^{th}$  CLH becomes

$$y_m = g_m s_m + n_G \quad (2.2)$$

where  $g_m$  is the fading coefficient of the channel between the  $m^{th}$  CLH and the global fusion center, and  $n_G$  represents an AWGN noise source that has a mean of zero and a variance of  $\sigma^2$ .

Finally, GFC reaches a final decision by combining all signals from CLHs. Using the hierarchical WSN model explained above, the LRT fusion rules based on Neyman-Pearson (N-P) formulation will be derived in the following two sections, where the instantaneous CSI of all wireless communication links within the  $m^{th}$  cluster and the instantaneous CSI of all GFC-CLH communications are denoted by a vector  $\mathbf{h}_m = [h_1^m, h_2^m, \dots, h_K^m]$ , and  $\mathbf{g} = [g_1, g_2, \dots, g_N]$ , respectively. Also, in the subsequent developments, the vectors  $\mathbf{y} = [y_1, \dots, y_N]$  and  $\mathbf{r}_m = [r_1^m, r_2^m, \dots, r_K^m]$  show the received signal vector at the GFC and at the  $m^{th}$  CLH, respectively.

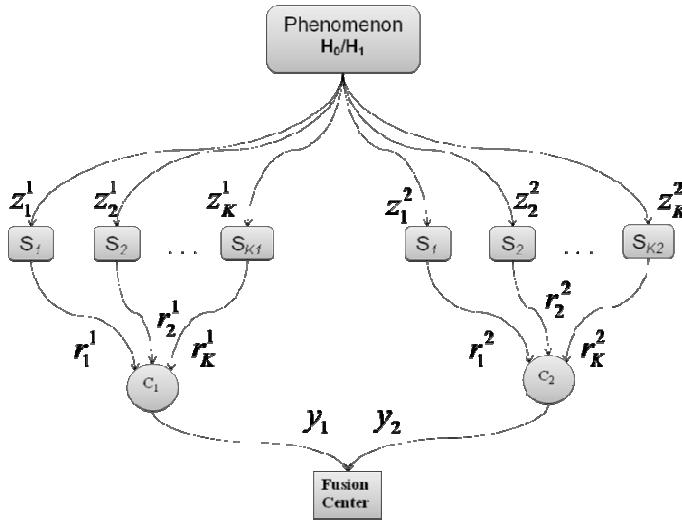


Figure 2-1. A wireless sensor network in hierarchical topology with two cluster heads and a global fusion center

## 2.2 Likelihood Ratio Test (LRT) Based Fusion Rule under Perfect Channel State Information

In this section, we assume that instantaneous CSI of all wireless communication channels in the network, namely,  $\mathbf{g} = [g_1, g_2, \dots, g_N]$  and  $\mathbf{h} = [\mathbf{h}_1, \mathbf{h}_2, \dots, \mathbf{h}_N]$  are known at GFC. Moreover, the  $m^{\text{th}}$  CLH is supposed to have only the knowledge of the CSI vector  $\mathbf{h}_m$ . Because of the conditional independence assumption, the optimal detection rule at both the GFC and each CLH is LRT based monotone threshold rule [44]. Therefore, LRT based global fusion rule in log-domain for the hierarchical structure can be expressed as

$$\Lambda_G(\mathbf{y}) = \log \frac{f(\mathbf{y}|H_1, \mathbf{h}, \mathbf{g})}{f(\mathbf{y}|H_0, \mathbf{h}, \mathbf{g})} = \sum_{m=1}^N \log \left\{ \frac{P_D(\mathbf{h}_m) e^{-\frac{(y_m - g_m)^2}{2\sigma^2}} + [1 - P_D(\mathbf{h}_m)] e^{-\frac{(y_m + g_m)^2}{2\sigma^2}}}{P_F(\mathbf{h}_m) e^{-\frac{(y_m - g_m)^2}{2\sigma^2}} + [1 - P_F(\mathbf{h}_m)] e^{-\frac{(y_m + g_m)^2}{2\sigma^2}}} \right\} \quad (2.3)$$

where  $P_D(\mathbf{h}_m)$  and  $P_F(\mathbf{h}_m)$  are detection and false alarm probabilities of the  $m^{\text{th}}$  CLH with CSI vector  $\mathbf{h}_m$ . It is important to note that there is a major distinction between the fusion rule in Eq. (2.3) and the channel-aware decision fusion developed in [40] for the parallel topology. That is both probability of false alarm and the probability of detection at each CLH change over the time since it is assumed that the fading coefficient of the wireless channel changes independently from symbol to symbol.

In order to use Eq. (2.3), GFC needs to determine the performance indices of the all CLHs namely  $P_D(\mathbf{h}_m)$  and  $P_F(\mathbf{h}_m)$  for  $1 \leq m \leq N$ , which also depend on the fusion rule employed at the CLHs. As mentioned above, the optimal network performance requires that each CLH performs LRT during the fusion of the decisions transmitted by the sensors within that cluster. Therefore, the log likelihood-ratio (LLR) performed at  $m^{\text{th}}$  CLH with CSI vector  $\mathbf{h}_m$  is given by

$$\Lambda_m(\mathbf{r}_m) = \log \frac{f(\mathbf{r}_m|H_1, \mathbf{h}_m)}{f(\mathbf{r}_m|H_0, \mathbf{h}_m)} = \sum_{j=1}^K \psi(r_j^m) \quad (2.4)$$

where the LLR of the received signal  $r_j^m$  under the complete information on the channel fading

coefficient  $h_j^m$  is represented by  $\psi(r_j^m)$  and defined as

$$\psi(r_j^m) = \log \frac{f(r_j^m | H_1, h_j^m)}{f(r_j^m | H_0, h_j^m)} = \log \left[ \frac{P_{D_j}^m e^{-\frac{(r_j^m - h_j^m)^2}{2\sigma^2}} + (1 - P_{D_j}^m) e^{-\frac{(r_j^m + h_j^m)^2}{2\sigma^2}}}{P_{F_j}^m e^{-\frac{(r_j^m - h_j^m)^2}{2\sigma^2}} + (1 - P_{F_j}^m) e^{-\frac{(r_j^m + h_j^m)^2}{2\sigma^2}}} \right] \quad (2.5)$$

where  $P_{F_j}^m = P(x_j^m = 1 | H_0)$  and  $P_{D_j}^m = P(x_j^m = 1 | H_1)$  are false alarm and detection probabilities of the  $j^{\text{th}}$  sensor in the the  $m^{\text{th}}$  cluster respectively.

The performance indices of the  $m^{\text{th}}$  CLH under the LRT based fusion rule can be determined as

$$\begin{aligned} P_F(\mathbf{h}_m) &= P(\Lambda_m(\mathbf{r}_m) > t_m | H_0, \mathbf{h}_m) = P\left(\sum_{j=1}^K \psi(r_j^m) > t_m | H_0\right) \\ P_D(\mathbf{h}_m) &= P(\Lambda_m(\mathbf{r}_m) > t_m | H_1, \mathbf{h}_m) = P\left(\sum_{j=1}^K \psi(r_j^m) > t_m | H_1\right) \end{aligned} \quad (2.6)$$

where  $t_m$  is the optimal threshold used by the  $m^{\text{th}}$  CLH in order to perform the LRT and it is dependent on the CSI vector  $\mathbf{h}_m$ . However, due to notational simplicity, we have let its dependence on  $\mathbf{h}_m$  be implicit.

The determination of the false and detection probabilities in Eq. (2.6) necessitates knowing the conditional distribution of  $\Lambda_m(\mathbf{r}_m)$  for each hypothesis. The calculations of these conditional probability density functions (pdfs) amount to the determination of the conditional pdf of  $\psi(r_j^m)$  for each hypothesis since they are conditionally independent random variables under  $H_1$  or  $H_0$ .

With this motivation, we have derived the conditional pdfs of  $\psi(r_j^m)$  under  $H_1$  and  $H_0$  as stated in the following theorem.

*Theorem 2-1:* For notational simplicity, let us drop the subscript and superscript of all variables

in Eq. (2.5) and obtain  $\psi = \log \left[ \frac{P_D e^{-\frac{(r-h)^2}{2\sigma^2}} + (1 - P_D) e^{-\frac{(r+h)^2}{2\sigma^2}}}{P_F e^{-\frac{(r-h)^2}{2\sigma^2}} + (1 - P_F) e^{-\frac{(r+h)^2}{2\sigma^2}}} \right]$ . The conditional pdfs  $f(\psi | H_1)$  and

$f(\psi | H_0)$  are given as

$$f(\psi | H_1) = \frac{\sigma e^\psi (P_D - P_F)}{2\sqrt{2\pi}h [1 - P_D - e^\psi (1 - P_F)] (e^\psi P_F - P_D)} \left[ P_D e^{-\frac{1}{2\sigma^2}(\rho_0 - h)^2} + (1 - P_D) e^{-\frac{1}{2\sigma^2}(\rho_0 + h)^2} \right]_{\rho_0 = \frac{\sigma^2}{2h} \log \left[ \frac{(1 - P_D) - e^\psi (1 - P_F)}{e^\psi P_F - P_D} \right]} \left[ U \left( \psi - \log \left( \frac{1 - P_D}{1 - P_F} \right) \right) - U \left( \psi - \log \left( \frac{P_D}{P_F} \right) \right) \right] \quad (2.7)$$

And

$$f(\psi | H_0) = \frac{\sigma e^\psi (P_D - P_F)}{2\sqrt{2\pi}h [1 - P_D - e^\psi (1 - P_F)] (e^\psi P_F - P_D)} \left[ P_F e^{-\frac{1}{2\sigma^2}(\rho_0 - h)^2} + (1 - P_F) e^{-\frac{1}{2\sigma^2}(\rho_0 + h)^2} \right]_{\rho_0 = \frac{\sigma^2}{2h} \log \left[ \frac{(1 - P_D) - e^\psi (1 - P_F)}{e^\psi P_F - P_D} \right]} \left[ U \left( \psi - \log \left( \frac{1 - P_D}{1 - P_F} \right) \right) - U \left( \psi - \log \left( \frac{P_D}{P_F} \right) \right) \right] \quad (2.8)$$

where  $U(x)$  is unit step function, which equals to one for  $x \geq 0$  and zero for  $x < 0$ .

*Proof of Theorem 2-1:* For simplicity, we drop the subscript and superscript of all variables in

Eq. (2.5) and obtain  $\psi = \log \left[ \frac{P_D e^{-\frac{(r-h)^2}{2\sigma^2}} + (1 - P_D) e^{-\frac{(r+h)^2}{2\sigma^2}}}{P_F e^{-\frac{(r-h)^2}{2\sigma^2}} + (1 - P_F) e^{-\frac{(r+h)^2}{2\sigma^2}}} \right]$  and  $r = hx + n$ . The conditional pdf

$f(\psi | H_1)$  and  $f(\psi | H_0)$ , can be derived using the conditional pdf  $f(r | H_1)$  and  $f(r | H_0)$

respectively together with the Jacobian transformation [5] as

$$f(\psi | H_i) = \sum_k \left. \frac{f(r | H_i)}{\left| \frac{d\psi(r)}{dr} \right|} \right|_{r=\rho_k} \quad \text{for } i = 0, 1 \quad (2.9)$$

where  $\rho_k$  represents the  $k^{\text{th}}$  root of  $r$  for a given  $\psi$ .

Given the CSI  $h$ , the conditional pdf  $f(r | H_1)$  can be determined as

$$\begin{aligned}
f(r|H_1) &= \sum_x f(r,x|H_1) = \sum_x f(r|x,H_1)f(x|H_1) \\
&= f(r|x=1,H_1)P_D + f(r|x=-1,H_1)(1-P_D) \\
&= f(r|x=1)P_D + f(r|x=-1)(1-P_D) \\
&= P_D \frac{1}{\sqrt{2\pi}\sigma} e^{-\frac{(r-h)^2}{2\sigma^2}} + (1-P_D) \frac{1}{\sqrt{2\pi}\sigma} e^{-\frac{(r+h)^2}{2\sigma^2}}
\end{aligned} \tag{2.10}$$

where we used the fact that  $f(r|x,H_1)$  does not depend on  $H_1$  for given decision  $x$ . Similar to that,  $f(r|H_0)$  can be obtained as

$$f(r|H_0) = P_F \frac{1}{\sqrt{2\pi}\sigma} e^{-\frac{(r-h)^2}{2\sigma^2}} + (1-P_F) \frac{1}{\sqrt{2\pi}\sigma} e^{-\frac{(r+h)^2}{2\sigma^2}} \tag{2.11}$$

To perform Eq.(2.9), the derivative of  $\psi$  with respect to  $r$  is needed and it can be derived as

$$\frac{d\psi}{dr} = \frac{2h(P_D - P_F)e^{-\frac{2rh}{\sigma^2}}}{\sigma^2 \left[ P_D + (1-P_D)e^{-\frac{2rh}{\sigma^2}} \right] \left[ P_F + (1-P_F)e^{-\frac{2rh}{\sigma^2}} \right]} \tag{2.12}$$

which is greater than zero for  $0 \leq P_F < P_D \leq 1$  and  $-\infty < r_j^m < \infty$ . Therefore, LLR $\psi$  is monotonically increasing function of  $r$  for  $0 \leq P_F < P_D \leq 1$ . The infimum and supremum of the  $\psi$  can be obtained as

$$\psi_{\text{inf}} = \lim_{r \rightarrow -\infty} \psi(r) = \log\left(\frac{1-P_D}{1-P_F}\right) \tag{2.13}$$

$$\psi_{\text{sup}} = \lim_{r \rightarrow \infty} \psi(r) = \log\left(\frac{P_D}{P_F}\right) \tag{2.14}$$

Therefore, the support of the  $\psi$  is  $\left(\log\left(\frac{1-P_D}{1-P_F}\right), \log\left(\frac{P_D}{P_F}\right)\right)$  for  $P_F < P_D$ . As a result of the

monotonicity of  $\psi$ , the root of  $r$  for a given  $\psi$  exists and is unique for

$\log\left(\frac{1-P_D}{1-P_F}\right) < \psi < \log\left(\frac{P_D}{P_F}\right)$ , which can be obtained as

$$\rho_0 = \frac{\sigma^2}{2h} \log\left[\frac{(1-P_D) - e^\psi(1-P_F)}{e^\psi P_F - P_D}\right] \text{ for } \log\left(\frac{1-P_D}{1-P_F}\right) < \psi < \log\left(\frac{P_D}{P_F}\right) \tag{2.15}$$

By combining Eqs. (2.9)-(2.15), we derive the conditional pdfs  $f(\psi | H_1)$  and  $f(\psi | H_0)$  as in Eq.(2.7) and (2.8), respectively.

∴ QED.

Using the result in *Theorem 2-1* together with the conditional independence of  $\psi(r_j^m)$ , the conditional pdfs of  $\Lambda_m(\mathbf{r}_m)$  in Eq.(2.4) can be calculated under  $H_0$  and  $H_1$  as

$$\begin{aligned} f(\Lambda_m(\mathbf{r}_m)|H_0) &= f(\psi(r_1^m)|H_0) * \dots * f(\psi(r_K^m)|H_0) \\ f(\Lambda_m(\mathbf{r}_m)|H_1) &= f(\psi(r_1^m)|H_1) * \dots * f(\psi(r_K^m)|H_1) \end{aligned} \quad (2.16)$$

where \* denotes the convolution operation.

By combining Eqs. (2.6) and (2.16), the false alarm and the detection probabilities of the  $m^{\text{th}}$  CLH can be determined as

$$\begin{aligned} P_F(\mathbf{h}_m) &= \int_{t_m}^{\infty} f(\Lambda_m(\mathbf{r}_m) | H_0, \mathbf{h}_m) d\Lambda_m \\ P_D(\mathbf{h}_m) &= \int_{t_m}^{\infty} f(\Lambda_m(\mathbf{r}_m) | H_1, \mathbf{h}_m) d\Lambda_m \end{aligned} \quad (2.17)$$

Thus, we can calculate each CLH's false alarm and the detection probabilities using Eq.(2.17) and then these probabilities are used to employ the optimal LRT test using global fusion rule in Eq. (3) as

$$\Lambda_G(\mathbf{y}) \underset{x_G=0}{\overset{x_G=1}{\geq}} t_G \quad (2.18)$$

where  $t_G$  is the decision threshold and  $x_G$  is the decision made at the GFC, which is 1 if the fusion rule is greater than the threshold and is otherwise zero. Note that both  $\Lambda_G(\mathbf{y})$  and  $t_G$  depend instantaneously on the CSI vectors  $\mathbf{g}$  and  $\mathbf{h}$ . Therefore, the global threshold value need to be optimized for each of CSI vectors to achieve a fixed false alarm probability  $P_F$  expressed below.

$$P_F = P(\Lambda_G(\mathbf{y}) > t_G | H_0) \quad (2.19)$$

Hence, using the optimal threshold value, the instantaneous detection probability at GFC can be determined as

$$P_D(\mathbf{g}, \mathbf{h}) = P(\Lambda_G(\mathbf{y}) > t_G | H_1) \quad (2.20)$$

where  $P_D(\mathbf{g}, \mathbf{h})$  denotes the instantaneous detection probability of the GFC. The overall detection capability of the network can be measured by determining the average detection probability  $\bar{P}_D$  as

$$\bar{P}_D = E_{\mathbf{g}, \mathbf{h}}[P_D(\mathbf{g}, \mathbf{h})] \quad (2.21)$$

where  $E_{\mathbf{g}, \mathbf{h}}[\cdot]$  represents the expectation operator with respect to CSI vectors  $\mathbf{g}$  and  $\mathbf{h}$ .

Although the LRT-CSI fusion rule is optimal, it requires to use the complete CSI of all communicating nodes and performance indices of CLHs in terms of their detection and false alarm probabilities for all time instants. Therefore, its computational demand is expected to be high (please see Section 2.4 for details).

Also, it is important to note that, CSIs between sensor nodes and CLHs have to be known by GFC to perform this fusion rule. Namely, CLHs have to transmit these CSIs to GFC before the calculation of Eq.(2.3). However, these CSIs can take any value between zero and infinity since they are assumed to be Rayleigh random variables therefore in practice they have to be quantized before transmission. Due to this quantization, GFC cannot have the complete CSI values and transmitting the quantized CSIs increases the communication burden of the WSN [5].

To reduce the computational complexity of the LRT-CSI and to save the resources, we relax the requirement of using complete CSI, in the next section, and derive a channel envelope statistics (CS) based fusion rule for the hierarchical topology.

### 2.3 LRT Based Fusion Rule under Channel Statistics

The phase-coherent detection used in the signal model (refer to Eq.(2.1)) requires the knowledge about the exact phase of fading coefficient, which can be obtained either by employing a first order Phase Locked Loop( PLL) that assumes slow fading, or by using a preamble symbol [42]. After having the fading phase, one can also estimate the fading envelope. However, the use of fading envelope directly leads to LRT-CSI, which is computationally expensive and resource

consuming (please see Section 2.4 for details). Therefore, in order to devise a fusion rule with lower complexity, we develop LRT based fusion rule, which uses only the exact phase information with channel envelope statistics (CS) for a hierarchical WSN. For this purpose, we first average the conditional distribution of the received signal over channel envelope statistics for each hypothesis and then perform LRT afterwards, which is referred as LRT-CS. Hence, LRT-CS based fusion rule at the GFC can be written as

$$\tilde{\Lambda}_G(\mathbf{y}) = \sum_{m=1}^N \log \left[ \frac{\int f(y_m | g_m, H_1) f(g_m) dg_m}{\int f(y_m | g_m, H_0) f(g_m) dg_m} \right] = \sum_{m=1}^N \log \left[ \frac{f(y_m | H_1)}{f(y_m | H_0)} \right] \quad (2.22)$$

The conditional pdfs needed to perform Eq. (2.22) can be determined in similar lines with the parallel topology [45] and be stated as

$$\begin{aligned} f(y_m | H_0) &= \frac{2\sigma}{\sqrt{2\pi}(\sigma_g^2 + \sigma^2)} e^{-\frac{y_m^2}{2\sigma^2}} \left\{ 1 + [P_{F_m} - Q(a_g y_m)] \sqrt{2\pi} a_g y_m e^{-\frac{(a_g y_m)^2}{2}} \right\} \\ f(y_m | H_1) &= \frac{2\sigma}{\sqrt{2\pi}(\sigma_g^2 + \sigma^2)} e^{-\frac{y_m^2}{2\sigma^2}} \left\{ 1 + [P_{D_m} - Q(a_g y_m)] \sqrt{2\pi} a_g y_m e^{-\frac{(a_g y_m)^2}{2}} \right\} \end{aligned} \quad (2.23)$$

where  $P_{F_m}$  and  $P_{D_m}$  denote the false alarm and detection probabilities of the  $m^{\text{th}}$  CLH under CS respectively, and  $2\sigma_g^2$  is the average power of each channel between the GFC and every CLH, and  $a_g = \left( \sigma_g / \sigma \sqrt{\sigma_g^2 + \sigma^2} \right)$ .

By combining Eqs. (2.22)-(2.23), the LRT-CS based fusion rule at GFC can be derived as

$$\tilde{\Lambda}_G(\mathbf{y}) = \sum_{m=1}^N \log \left\{ \frac{1 + [P_{D_m} - Q(a_g y_m)] \sqrt{2\pi} a_g y_m e^{-\frac{(a_g y_m)^2}{2}}}{1 + [P_{F_m} - Q(a_g y_m)] \sqrt{2\pi} a_g y_m e^{-\frac{(a_g y_m)^2}{2}}} \right\} \quad (2.24)$$

Similar to the above development, the following LRT-CS based rule for the  $m^{\text{th}}$  CLH can be written as

$$\tilde{\Lambda}_m(\mathbf{r}_m) = \sum_{j=1}^K \log \left[ \frac{\int f(r_j^m | h_j^m, H_1) f(h_j^m) dh_j^m}{\int f(r_j^m | h_j^m, H_0) f(h_j^m) dh_j^m} \right] = \sum_{j=1}^K \log \left[ \frac{f(r_j^m | H_1)}{f(r_j^m | H_0)} \right] \quad (2.25)$$

where the conditional pdfs of the signals received by the  $m^{\text{th}}$  CLH under each hypothesis can be obtained respectively as

$$f(r_j^m | H_0) = \frac{2\sigma}{\sqrt{2\pi}(\sigma_h^2 + \sigma^2)} e^{-\frac{r_j^{m2}}{2\sigma^2}} \left\{ 1 + [P_{F_j}^m - Q(a_h r_j^m)] \sqrt{2\pi} a_h r_j^m e^{-\frac{(a_h r_j^m)^2}{2}} \right\}$$

$$f(r_j^m | H_1) = \frac{2\sigma}{\sqrt{2\pi}(\sigma_h^2 + \sigma^2)} e^{-\frac{r_j^{m2}}{2\sigma^2}} \left\{ 1 + [P_{D_j}^m - Q(a_h r_j^m)] \sqrt{2\pi} a_h r_j^m e^{-\frac{(a_h r_j^m)^2}{2}} \right\} \quad (2.26)$$

where  $2\sigma_h^2$  is the average power of every channel between each sensor and the  $m^{\text{th}}$  CLH, and

$$a_h = \left( \sigma_h / \sigma \sqrt{\sigma_h^2 + \sigma^2} \right)$$

Therefore, the LRT-CS based fusion rule at the  $m^{\text{th}}$  CLH can be obtained through Eqs. (2.25)-(2.26) as

$$\tilde{\Lambda}_m(\mathbf{r}_m) = \sum_{j=1}^K \log \left\{ \frac{1 + [P_{D_j}^m - Q(a_h r_j^m)] \sqrt{2\pi} a_h r_j^m e^{-\frac{(a_h r_j^m)^2}{2}}}{1 + [P_{F_j}^m - Q(a_h r_j^m)] \sqrt{2\pi} a_h r_j^m e^{-\frac{(a_h r_j^m)^2}{2}}} \right\} \quad (2.27)$$

However, it is important to note that the global LRT-CS rule at the GFC in Eq. (2.24) requires the calculation of the false alarm and detection probabilities of all CLHs (i.e.,  $P_{F_m}$  and  $P_{D_m}$  respectively) before fusing the information. These probabilities can be determined as

$$P_{F_m} = P(\tilde{\Lambda}_m(\mathbf{r}_m) > \tilde{t}_m | H_0) = P\left( \sum_{j=1}^K \psi_{cs}(r_j^m) > \tilde{t}_m | H_0 \right)$$

$$P_{D_m} = P(\tilde{\Lambda}_m(\mathbf{r}_m) > \tilde{t}_m | H_1) = P\left( \sum_{j=1}^K \psi_{cs}(r_j^m) > \tilde{t}_m | H_1 \right) \quad (2.28)$$

where  $\tilde{t}_m$  is the optimal threshold and the LRT of the signal sent from the  $j^{\text{th}}$  sensor to the  $m^{\text{th}}$  CLH when CS is known, is denoted by  $\psi_{cs}(r_j^m)$  and can be written as

$$\psi_{cs}(r_j^m) = \log \left\{ \frac{1 + [P_{D_j}^m - Q(a_h r_j^m)] \sqrt{2\pi} a_h r_j^m e^{-\frac{(a_h r_j^m)^2}{2}}}{1 + [P_{F_j}^m - Q(a_h r_j^m)] \sqrt{2\pi} a_h r_j^m e^{-\frac{(a_h r_j^m)^2}{2}}} \right\} \quad (2.29)$$

Hence, the determination of the false alarm and detection probabilities of each CLH necessitates the conditional pdfs of  $\psi_{cs}(r_j^m)$  for each hypothesis, which we derive in the following theorem.

*Theorem 2-2:* For the sake of notational simplicity, we denote  $\psi_{cs}(r_j^m)$  as  $\psi_{cs}$ . The conditional pdfs  $f(\psi_{cs} | H_0)$  and  $f(\psi_{cs} | H_1)$  can be obtained as

$$\begin{aligned} f(\psi_{cs} | H_1) &= \frac{2\sigma e^{-\psi_{cs}}}{2\pi(\sigma_h^2 + \sigma^2)(P_{D_j}^m - P_{F_j}^m)a_h} \\ &\times \left\{ e^{\frac{\rho_0^2}{(\sigma_h^2 + \sigma^2)}} \left[ P_{D_j}^m \sqrt{2\pi} a_h \rho_0 + C(a_h \rho_0) \right]^3 \right\}_{\rho_0 = \frac{1}{a_h} g^{-1} \left( \frac{e^{\psi_{cs}} - 1}{(P_{D_j}^m - e^{\psi_{cs}} P_{F_j}^m) \sqrt{2\pi}} \right)} \\ &\times \left[ U(\psi_{cs}) - U \left( \psi_{cs} - \log \left( \frac{P_{D_j}^m}{P_{F_j}^m} \right) \right) \right] \\ &+ e^{\frac{\rho_0^2}{(\sigma_h^2 + \sigma^2)}} \left[ (P_{D_j}^m - 1) \sqrt{2\pi} a_h \rho_0 + C(a_h \rho_0) \right]^3 \left\{ \right. \\ &\left. U \left( \psi_{cs} - \log \left( \frac{1 - P_{D_j}^m}{1 - P_{F_j}^m} \right) \right) - U(\psi_{cs}) \right\} \Bigg|_{\rho_0 = \frac{1}{a_h} g^{-1} \left( \frac{e^{\psi_{cs}} - 1}{[(P_{D_j}^m - 1) - e^{\psi_{cs}} (P_{F_j}^m - 1)] \sqrt{2\pi}} \right)} \end{aligned} \quad (2.30)$$

where  $U(x)$  is unit step function, which equals to one for  $x \geq 0$  and is zero for  $x < 0$ ,  $g^{-1}(x)$  is

the inverse of the function  $g(x) = \frac{x}{C(x)}$  and  $C(x) = e^{-x^2/2} - |x| \sqrt{2\pi} Q(|x|)$ .

Similarly,

$$\begin{aligned}
f(\psi_{cs} | H_0) &= \frac{2\sigma e^{-\psi_{cs}}}{2\pi(\sigma_h^2 + \sigma^2)(P_{D_j}^m - P_{F_j}^m)a_h} \\
&\times \left\{ e^{\frac{\rho_0^2}{(\sigma_h^2 + \sigma^2)}} \left[ P_{F_j}^m \sqrt{2\pi} a_h \rho_0 + C(a_h \rho_0) \right]^3 \right\}_{\rho_0 = \frac{1}{a_h} g^{-1} \left( \frac{e^{\psi_{cs}} - 1}{(P_{D_j}^m - e^{\psi_{cs}} P_{F_j}^m) \sqrt{2\pi}} \right)} \\
&\left[ U(\psi_{cs}) - U \left( \psi_{cs} - \log \left( \frac{P_{D_j}^m}{P_{F_j}^m} \right) \right) \right] \\
&+ e^{\frac{\rho_0^2}{(\sigma_h^2 + \sigma^2)}} \left[ (P_{F_j}^m - 1) \sqrt{2\pi} a_h \rho_0 + C(a_h \rho_0) \right]^3 \left\{ \right. \\
&\left. U \left( \psi_{cs} - \log \left( \frac{1 - P_{D_j}^m}{1 - P_{F_j}^m} \right) \right) - U(\psi_{cs}) \right\} \Bigg|_{\rho_0 = \frac{1}{a_h} g^{-1} \left( \frac{e^{\psi_{cs}} - 1}{[(P_{D_j}^m - 1) - e^{\psi_{cs}} (P_{F_j}^m - 1)] \sqrt{2\pi}} \right)}
\end{aligned} \tag{2.31}$$

In order to derive the results of *Theorem 2-2*, we first prove the next two lemmas.

*Lemma 2-1:*  $\psi_{cs}$  in Eq. (2.29) is a monotonically increasing function of  $r_j^m$  for  $0 \leq P_{F_j}^m < P_{D_j}^m \leq 1$

and  $-\infty < r_j^m < \infty$ , and its support is  $\left( \log \left( \frac{1 - P_{D_j}^m}{1 - P_{F_j}^m} \right), \log \left( \frac{P_{D_j}^m}{P_{F_j}^m} \right) \right)$ . Also,  $\psi_{cs}$  satisfies

that  $\psi_{cs} > 0$  for  $r_j^m > 0$ ,  $\psi_{cs} = 0$  for  $r_j^m = 0$  and  $\psi_{cs} < 0$  for  $r_j^m < 0$ .

*Proof of Lemma 2-1:*

The derivative of  $\psi_{cs}$  with respect to  $r_j^m$  can be obtained given as

$$\frac{d\psi_{cs}}{dr_j^m} = \sqrt{2\pi} a_h e^{\frac{(a_h r_j^m)^2}{2}} \frac{(P_{D_j}^m - P_{F_j}^m)}{\left\{ 1 + [P_{D_j}^m - Q(a_h r_j^m)] \sqrt{2\pi} a_h r_j^m e^{\frac{(a_h r_j^m)^2}{2}} \right\} \left\{ 1 + [P_{F_j}^m - Q(a_h r_j^m)] \sqrt{2\pi} a_h r_j^m e^{\frac{(a_h r_j^m)^2}{2}} \right\}}
\tag{2.32}$$

Now, let us consider the following function with parameter  $\omega$  as

$$f(x) = 1 + [\omega - Q(x)]\sqrt{2\pi x}e^{\frac{x^2}{2}} \text{ for } -\infty < x < \infty \text{ and } 0 \leq \omega \leq 1 \quad (2.33)$$

It is well known that  $Q(x) < \frac{1}{\sqrt{2\pi x}}e^{-x^2/2}$  for  $x \geq 0$  [5]. Using this property, it is clearly obvious

that  $f(x)$  positive for  $x \geq 0$  and  $0 \leq \omega \leq 1$ . For  $x < 0$ , we can obtain  $Q(x) < 1 + \frac{1}{\sqrt{2\pi x}}e^{-x^2/2}$  by

using the fact that  $Q(x) = 1 - Q(-x)$ , and then the bound on  $f(x)$  can be determined as

$$f(x) > (\omega - 1)\sqrt{2\pi x}e^{\frac{x^2}{2}} \quad (2.34)$$

Since  $\omega$  is between zero and one,  $(\omega - 1)\sqrt{2\pi x}$  is greater than or equal to zero for  $x < 0$ , which makes  $f(x)$  is positive for  $x < 0$ . Hence,  $f(x)$  is always positive for all  $x$  and  $\omega$ .

Let us now define  $f(x, \omega)$  as  $f(x)$  with parameter  $\omega$ , which is nonnegative and less than one.

The denominator of Eq. (2.32) can be written as  $f(a_h r_j^m, P_{D_j}^m) \times f(a_h r_j^m, P_{F_j}^m)$  which is strictly

positive for all values of  $r_j^m$ ,  $P_{D_j}^m$  and  $P_{F_j}^m$ . The numerator of Eq. (2.32) is strictly positive for

$P_{F_j}^m < P_{D_j}^m$ . Hence,  $\psi_{cs}$  in Eq. (2.29) is a monotonically increasing function of  $r_j^m$  for

$0 \leq P_{F_j}^m < P_{D_j}^m \leq 1$  and  $-\infty < r_j^m < \infty$ .

Since  $\psi_{cs}$  is a monotonically increasing function with  $\psi_{cs}(0) = 0$ , it should also satisfy the following equation

$$\begin{aligned} \psi_{cs} &> 0 \text{ for } r_j^m > 0 \\ \psi_{cs} &= 0 \text{ for } r_j^m = 0 \\ \psi_{cs} &< 0 \text{ for } r_j^m < 0 \end{aligned} \quad (2.35)$$

The infimum and supremum of the  $\psi_{cs}(r_j^m)$  can be obtained as

$$\psi_{cs}(r_j^m)_{\inf} = \lim_{r_j^m \rightarrow -\infty} \psi_{cs}(r_j^m) = \log\left(\frac{1 - P_{D_j}^m}{1 - P_{F_j}^m}\right) \quad (2.36)$$

$$\psi_{cs} \left( r_j^m \right)_{\text{sup}} = \lim_{r_j^m \rightarrow \infty} \psi_{cs} \left( r_j^m \right) = \log \left( \frac{P_{D_j}^m}{P_{F_j}^m} \right) \quad (2.37)$$

Thus, the support of the  $\psi_{cs} \left( r_j^m \right)$  is  $\left( \log \left( \frac{1-P_D}{1-P_F} \right), \log \left( \frac{P_D}{P_F} \right) \right)$  for  $P_{F_j}^m < P_{D_j}^m$ .

∴ QED.

As a result of *Lemma 2-1*, we have proved that the root of  $r_j^m$  for a given  $\psi_{cs}$  in Eq (2.29) does exist and is unique for  $\psi_{cs} \in \left( \log \left( \frac{1-P_D}{1-P_F} \right), \log \left( \frac{P_D}{P_F} \right) \right)$ . However, a closed-form solution to find the root is not possible directly from Eq.(2.29). Instead of determining a closed form solution, one can numerically obtain the root by finding the inverse of the function  $\psi_{cs}$ , for which one may employ a curve-fitting algorithm such as the Levenberg–Marquardt algorithm [46] that has complexity of  $O(n^3)$  [47]. However, since the inverse of  $\psi_{cs}$  also depends on  $P_{D_j}^m$  and  $P_{F_j}^m$ , we obtain different curves with regard to the inverse for various values of  $P_{D_j}^m$  and  $P_{F_j}^m$ . Consequently, this approach can be very exhaustive and impractical to implement. Therefore, we need a way to determine the root of  $r_j^m$ , which should work for any  $P_{D_j}^m$  and  $P_{F_j}^m$  and be practically simple to employ. For this, we propose a method in *Lemma 2-2*.

*Lemma 2-2*: The root of  $r_j^m$  for any  $\psi_{cs}$ ,  $P_{D_j}^m$  and  $P_{F_j}^m$  can be obtained as

$$\rho_0 = \begin{cases} \frac{1}{a_h} g^{-1} \left( \frac{e^{\psi_{cs}} - 1}{(P_{D_j}^m - e^{\psi_{cs}} P_{F_j}^m) \sqrt{2\pi}} \right) & \text{for } \psi_{cs} \geq 0 \\ \frac{1}{a_h} g^{-1} \left( \frac{e^{\psi_{cs}} - 1}{[(P_{D_j}^m - 1) - e^{\psi_{cs}} (P_{F_j}^m - 1)] \sqrt{2\pi}} \right) & \text{for } \psi_{cs} < 0 \end{cases}$$

where  $g^{-1}(x)$  is the inverse of the function  $g(x) = \frac{x}{C(x)}$  and  $C(x) = e^{-x^2/2} - |x| \sqrt{2\pi} Q(|x|)$ .

*Proof of Lemma 2-2:*

Let us consider the following well-known asymptotic approximation of  $Q(x)$  [5]

$$Q(x) \cong \begin{cases} \frac{1}{\sqrt{2\pi x}} e^{-x^2/2} & \text{for } x > 3 \\ 1 + \frac{1}{\sqrt{2\pi x}} e^{-x^2/2} & \text{for } x < -3 \end{cases} \quad (2.38)$$

where we have used the fact that  $Q(-x) = 1 - Q(x)$ .

This equation can be re-written alternatively as

$$e^{-x^2/2} \cong \begin{cases} \sqrt{2\pi x} Q(x) & \text{for } x > 3 \\ \sqrt{2\pi x} Q(x) - \sqrt{2\pi x} & \text{for } x < -3 \end{cases} \quad (2.39)$$

Note that the approximation in Eq.(2.39) is very accurate for  $|x| > 3$  but it is otherwise inaccurate. To obtain more accurate results, we express the quadratic exponential  $e^{-x^2/2}$  in terms of  $Q(x)$  and add a correction function  $C(x)$  so that for all values  $x$ , Eq.(2.39) can be re-written with an exact equality as

$$e^{-x^2/2} = \begin{cases} x\sqrt{2\pi}Q(x) + C(x) & \text{for } x \geq 0 \\ x\sqrt{2\pi}Q(x) - x\sqrt{2\pi} + C(x) & \text{for } x < 0 \end{cases} \quad (2.40)$$

The correction function  $C(x)$  can be obtained from Eq.(2.40) as

$$C(x) = \begin{cases} e^{-x^2/2} - x\sqrt{2\pi}Q(x) & \text{for } x \geq 0 \\ e^{-x^2/2} - x\sqrt{2\pi}Q(x) + x\sqrt{2\pi} & \text{for } x < 0 \end{cases} \quad (2.41)$$

which can be shown to be an even function of  $x$  and is always positive. The correction function  $C(x)$  in Eq.(2.41) is a decreasing function of  $|x|$  and has also the following limits:  $\lim_{x \rightarrow 0} C(x) = 1$  and  $\lim_{x \rightarrow \mp\infty} C(x) = 0$ .

The function  $f(x)$  in Eq.(2.33) can be put in an alternative form by expressing  $Q(x)\sqrt{2\pi x}$  in terms of quadratic exponential and the correction function using Eq.(2.40) as

$$f(x) = \begin{cases} 1 + \left[ \omega\sqrt{2\pi x} - \left( e^{-\frac{x^2}{2}} - C(x) \right) \right] e^{\frac{x^2}{2}} & \text{for } x \geq 0 \\ 1 + \left[ \omega\sqrt{2\pi x} - \left( e^{-\frac{x^2}{2}} - C(x) + \sqrt{2\pi x} \right) \right] e^{\frac{x^2}{2}} & \text{for } x < 0 \end{cases} \quad (2.42)$$

This equation can be further simplified as

$$f(x) = \begin{cases} \left( \omega\sqrt{2\pi x} + C(x) \right) e^{\frac{x^2}{2}} & \text{for } x \geq 0 \\ \left[ (\omega - 1)\sqrt{2\pi x} + C(x) \right] e^{\frac{x^2}{2}} & \text{for } x < 0 \end{cases} \quad (2.43)$$

By utilizing the approximation in Eq. (2.40) and using Eqs. (2.33), (2.43),  $\psi_{cs}$  in Eq (2.29) can

be re-written as

$$\begin{aligned} \psi_{cs}(r_j^m) &= \log \left[ \frac{f(a_h r_j^m, P_{D_j}^m)}{f(a_h r_j^m, P_{F_j}^m)} \right] \\ &= \begin{cases} \log \left[ \frac{P_{D_j}^m \sqrt{2\pi} a_h r_j^m + C(a_h r_j^m)}{P_{F_j}^m \sqrt{2\pi} a_h r_j^m + C(a_h r_j^m)} \right] & \text{for } r_j^m \geq 0 \\ \log \left[ \frac{(P_{D_j}^m - 1)\sqrt{2\pi} a_h r_j^m + C(a_h r_j^m)}{(P_{F_j}^m - 1)\sqrt{2\pi} a_h r_j^m + C(a_h r_j^m)} \right] & \text{for } r_j^m < 0 \end{cases} \end{aligned} \quad (2.44)$$

where  $f(x, \omega)$  denotes  $f(x)$  with parameter  $\omega$ .

Fortunately now, handling Eq.(2.44) to find the inverse of  $\psi_{cs}$  is easier as compared to Eq.

(2.29) since it just depends on the correction function  $C(x)$  and  $x$  where  $x = a_h r_j^m$ . By using Eq.

(2.35) and by elaborating Eq. (2.44), we come up with the following expression

$$\frac{a_h r_j^m}{C(a_h r_j^m)} = \begin{cases} \frac{e^{\psi_{cs}} - 1}{(P_{D_j}^m - e^{\psi_{cs}} P_{F_j}^m) \sqrt{2\pi}} & \text{for } \psi_{cs} \geq 0 \\ \frac{e^{\psi_{cs}} - 1}{\left[ (P_{D_j}^m - 1) - e^{\psi_{cs}} (P_{F_j}^m - 1) \right] \sqrt{2\pi}} & \text{for } \psi_{cs} < 0 \end{cases} \quad (2.45)$$

The left-hand side of Eq. (2.45) can be expressed using the following function

$$g(x) = \frac{x}{C(x)} \quad (2.46)$$

The function  $g(x)$  is an odd function of  $x$ , and therefore its derivative is an even function, which can be obtained as

$$g'(x) = \frac{d}{dx} \left( \frac{x}{C(x)} \right) = \frac{1}{C(x)} - \frac{C'(x)}{C^2(x)} x \quad (2.47)$$

Since for  $x > 0$ ,  $C'(x)$  is negative and  $C(x)$  is positive,  $g'(x)$  is clearly positive for  $x \geq 0$ . Also,  $g'(x)$  is positive for  $x < 0$  because of the evenness of  $g'(x)$ . Hence,  $g(x)$  is a monotonically increasing function of  $x$  for  $-\infty < x < \infty$ , and therefore its inverse  $g^{-1}(x)$  does exist, which is also a monotonically increasing odd function.

Therefore, the root of  $r_j^m$  for a given  $\psi_{cs}$  can be derived by combining  $g^{-1}(x)$  in Eq. (2.49) and Eq.(2.45) as

$$\rho_0 = \begin{cases} \frac{1}{a_h} g^{-1} \left( \frac{e^{\psi_{cs}} - 1}{\left( P_{D_j}^m - e^{\psi_{cs}} P_{F_j}^m \right) \sqrt{2\pi}} \right) & \text{for } \psi_{cs} \geq 0 \\ \frac{1}{a_h} g^{-1} \left( \frac{e^{\psi_{cs}} - 1}{\left[ \left( P_{D_j}^m - 1 \right) - e^{\psi_{cs}} \left( P_{F_j}^m - 1 \right) \right] \sqrt{2\pi}} \right) & \text{for } \psi_{cs} < 0 \end{cases} \quad (2.48)$$

Combining the results of *Lemma 2-1*, and *Lemma 2-2* yields the conditional pdfs  $f(\psi_{cs} | H_0)$  and  $f(\psi_{cs} | H_1)$  as stated in *Theorem 2-2*.

Note that although  $g(x)$  in *Theorem 2-2* can be analytically written, we cannot find a closed form expression for its inverse. However,  $g^{-1}(x)$  can be numerically expressed by employing a curve-fitting algorithm. For this purpose, we have applied the Levenberg–Marquardt algorithm [46] to approximate  $g^{-1}(x)$  as

$$g^{-1}(x) \cong \begin{cases} -1.598[\log(1+|x|)]^{0.4856} + 1.391 & \text{for } x < -2.5 \\ -0.6583[\log(1+|x|)]^{0.7327} & \text{for } -2.5 \leq x < 0 \\ 0.6583[\log(1+|x|)]^{0.7327} & \text{for } 0 \leq x \leq 2.5 \\ 1.598[\log(1+|x|)]^{0.4856} - 1.391 & \text{for } 2.5 < x \end{cases} \quad (2.49)$$

Thus, the conditional pdf of  $\tilde{\Lambda}_m$  given the hypothesis  $H_0$  or  $H_1$  can be calculated using the fact that  $\psi_{cs}(r_j^m)$  terms are conditionally independent random variables with the pdfs stated in *Theorem 2-2*. Finally, the detection and false alarm probabilities of the  $m^{\text{th}}$  CLH can be determined using Eq. (2.28) for the optimal threshold  $\tilde{t}_m$ , and these probabilities are then put in Eq. (2.24) to calculate the optimal CS based global fusion, which is finally used to perform the following LRT:

$$\tilde{\Lambda}_G(\mathbf{y}) \underset{x_G=0}{\overset{x_G=1}{\gtrless}} \tilde{t}_G \quad (2.50)$$

where  $\tilde{t}_G$  is the threshold used at the GFC when CS is known, and this threshold value does not rely on the instantaneous channel state information and just depends on the desired false alarm probability  $P_f$  as

$$P_f = P(\tilde{\Lambda}_G(\mathbf{y}) > \tilde{t}_G | H_0) \quad (2.51)$$

Hence, the detection performance of the network with the LRT-CS,  $\tilde{P}_D$ , can be determined as

$$\tilde{P}_D = P(\tilde{\Lambda}_G(\mathbf{y}) > \tilde{t}_G | H_1) \quad (2.52)$$

It is important to notice that although we assume clusters of the same size  $K$ , the expressions and derivations throughout the manuscript are still valid by replacing  $K$  by  $K_m$  in order to account for different cluster sizes where  $K_m$  denotes the size of the  $m^{\text{th}}$  cluster. The reason for this is that the decisions of CLHs have already different weights in terms of detection and false alarm probabilities of CLHs, which are dependent on the cluster size  $K_m$ , for the proposed fusion rules. Hence, the derived LRT-CSI and LRTCS fusion rules inherently weight the CLHs' decisions, and there is no need for an additional weighing strategy as proposed in [43], where the majority voting fusion rule has been employed. Note that since the majority rule assigns same weights to

all CLHs regardless of their individual reliabilities, a heuristic weighting rule is proposed in [43] to improve its performance, which gives higher weights to more reliable CLHs.

After having pointed out that we devote the next section to examine the computational complexities of the proposed detection methods for the hierarchical topology.

## 2.4 Computational Complexity Comparison between LRT-CSI and LRT-CS

In this part, we analyze the computational complexities of LRT-CSI and LRT-CS. During our analysis, we count a division operation as a multiplication and a subtraction operation as an addition. In addition, we have assumed that the complexities of functions  $\log(x)$  and  $e^x$  are the same.

It is critical to note that all computations regarding LRT-CSI should be performed *on-line*. Hence, we need to perform the following operations in LRT-CSI for each realization of CSI vectors  $\mathbf{g}$  and  $\mathbf{h}$  :

Calculation of LLR per cluster per sensor expressed in Eq.(2.5) requires 9 multiplications , 6 additions, 3 exponential operations. Hence, we need  $9K$  multiplications,  $6K$  additions and  $3K$  exponential operations to evaluate the LLR per CLH in Eq.(2.4).

- (i) Determination of the pdf per cluster per sensor in Eqs(2.7) and (2.8) demands 15 multiplications, 7 additions and 3 exponential operations. So, there is a need of  $15K$  multiplications,  $7K$  additions and  $3K$  exponential operations to calculate the pdf of sensors' LLR for each cluster
- (ii) We need to run  $2(K-1)$  convolutions at each CLH in order to determine the pdf of its LLR in Eq.(2.16).
- (iii) For each CLH, the determination of the performance indices in Eq. (2.17) necessitates 2 numerical integrations.

- (iv) At the GFC, we need  $9N$  multiplications,  $6N$  additions and  $3N$  exponential operations to evaluate its LLR in Eq.(2.3).
- (v) There is a need of  $15N$  multiplications,  $7N$  additions and  $3N$  exponential operations to calculate the pdf of CLHs' at the GFC.
- (vi) In order to calculate the false alarm probability at GFC , which is subsequently used to determine the optimal threshold, we need to run  $N-1$  convolutions for the pdf of LLR at the GFC under  $H_0$ .
- (vii) We need 1 numerical integration to determine the optimal threshold value at the GFC for the desired false alarm probability.
- (viii) Since we have  $N$  clusters each with  $K$  sensors, in total,  $24(NK+N)$  multiplications,  $13(NK+N)$  additions,  $6(NK+N)$  exponential function evaluations,  $2NK-1$  convolution operations and  $2N+1$  numerical integrations are needed.

It is important to note that we need to re-do the operations summarized in (ix) *on-line* to obtain the fusion result for every realization of CSI vectors  $\mathbf{g}$  and  $\mathbf{h}$  . In addition, the CSI vector  $\mathbf{h}$  should be transmitted from the CLHs to GFC, which consumes the communication resources. Contrary to LRT-CSI, the most of the computationally intensive steps in LRT-CS can be performed *off-line* just once before the fusion: (a) determination of the pdf per cluster per sensor in Eqs. (2.30) - (2.31); (b) determination of pdf of each CLH's LLR ; (c) the determination of CLHs' performance indices in Eq. (2.28) ; (d) the determination of the optimal thresholds at CLHs and GFC. Additionally, we perform the following *on-line* computations during the execution of LRT-CS.

- (i) Calculation of LLR per cluster per sensor expressed in Eq.(2.29) requires 5 multiplications, 4 additions, 3 exponential and 2  $Q(x)$  operations. Hence, we need  $5K$  multiplications,  $4K$  additions,  $3K$  exponential and  $2K$   $Q(x)$  operations to evaluate the LLR per cluster.
- (ii) At the GFC, we need  $5N$  multiplications,  $4N$  additions,  $3N$  exponential and  $2N$   $Q(x)$  operations to evaluate its LLR in Eq.(2.24).

(iii) Since we have  $N$  clusters each with  $K$  sensors,  $5(NK+N)$  multiplications,  $4(NK+N)$  additions,  $3(NK+N)$  exponential and  $2(NK+N)$   $Q(x)$  function evaluations are needed in total.

We summarized the *on-line* computations required by LRT-CSI and LRT-CS in Table 2-1. Hence, the *on-line* computational complexity needed to run LRT-CS is much less than that of LRT-CSI since the number of operations in LRT-CS is smaller and a convolution operation and numerical integration in LRT-CSI are computationally more intensive than a  $Q(x)$  function evaluation in LRT-CS. In contrast to LRT-CSI, LRT-CS does not need to have the CSI vector  $\mathbf{h}$  at the GFC, and therefore extra communication resources are not spent to transmit it.

In the subsequent section, we investigate the performance of fusion rules we have developed via simulations.

Table 2-1. On-line computational complexity comparison of LRT-CSI and LRT-CS for each channel realizations

Detection Method	# of Multiplications	# of Additions	# of Exponential Function Evaluations.	# of $Q(\cdot)$ Evaluations	# of Convolutions	# of Numerical Integrations
LRT-CSI	$24(NK+N)$	$13(NK+N)$	$6(NK+N)$	--	$2NK-1$	$2N+1$
LRT-CS	$5(NK+N)$	$4(NK+N)$	$3(NK+N)$	$2(NK+N)$	--	--

## 2.5 Simulation Results

In this section, through extensive numerical experiments, we evaluate the performance of the proposed CSI and CS based fusion rules: LRT-CSI and LRT-CS. Throughout our discussion, we suppose that sensors observe a DC + AWGN noise signal to determine the presence or absence of a target at the region of interest. Mathematically, the sensor measurements can be expressed as

$$z_j^m = \begin{cases} \mu + v_j^m, & H_1 \\ v_j^m, & H_0 \end{cases} \quad (2.53)$$

where  $\mu$  is the level of DC signal to be detected that is assumed to be 1,  $v_j^m$  is zero mean AWGN with its variance of  $\sigma_o^2$  which is taken to be 0.3696 as in [40].

We also assume that unit power Rayleigh fading channel is available between all communicating nodes and we define the average signal-to-noise ratio (SNR) as

$$\text{SNR (dB)} = 10 \log_{10} \left( \frac{1}{\sigma^2} \right) \quad (2.54)$$

In the subsequent LRT-CSI simulations, the optimal values of the thresholds at CLHs and GFC are determined using Eq. (2.19) in order to achieve a desired false alarm probability,  $P_F$ , for each of the channel realizations via exhaustive search to obtain the best instantaneous detection performance at GFC using Eq. (2.20). Then, the receiver operating characteristics (ROC) curve for the LRT-CSI rule is obtained by plotting the average detection probability,  $\bar{P}_D$ , using Eq.(2.21) versus the desired false alarm probability  $P_F$ . Contrary to LRT-CSI, the optimal thresholds for the LRT-CS method are determined once employing exhaustive search using Eq. (2.51) since they do not depend on the CSI vectors. Then, we produce the ROC curve for LRT-CS by sketching  $\tilde{P}_D$ , which is calculated by Eq.(2.52), as a function of  $P_F$ .

We first obtain the receiver operating characteristics (ROC) curves of the global fusion rules as depicted in Figure 2-2 for a hierarchical WSN with  $N=4$  clusters each with  $K=4$  and 8 local sensors under SNR of 5 dB. For this experiment, we have adjusted the local threshold of all sensors in order to have their performance indices as  $P_{F_j}^m = 0.05$  and  $P_{D_j}^m = 0.5$ . As seen from this figure, LRT-CSI outperforms the LRT-CS for the same number of sensors per cluster. Specifically, for the false alarm probability of  $10^{-2}$ , LRT-CSI results in detection performance improvement of 10.91% and 21.05 % over LRT-CS for  $K=4$  and  $K=8$  respectively. Similarly, for the target false alarm probability of  $10^{-3}$ , the detection performance of the networks gets better

by utilizing LRT-CSI compared to LRT-CS with a factor of 19.7% and 30% for  $K=4$  and  $K=8$  respectively. Also, when the number of sensors per cluster is increased from 4 to 8, the detection performance of LRT-CSI or LRT-CS gets improved because of the increased amount of cooperation obtained by employing more sensors while keeping the average transmit power of the network the same. For the false alarm probability of  $10^{-2}$ , the detection probabilities of the LRT-CSI and LRT-CS become better by 12.3% and 12.7% for the network with clusters of 8 sensors instead of 4 sensors respectively. As observed from this figure, if we decrease the false alarm probability down to  $10^{-3}$ , the detection probability of LRT-CSI is higher than that of LRT-CS by 3.7% and 4.1% for  $K = 4$  and  $K = 8$  respectively.

Next, for a network employing four clusters each with eight sensors and global false probability of 0.01, we obtain the detection performance of LRT-CSI over LRT-CS as in Figure 2-3 under various SNR values. For detection probability of 0.9, LRT-CSI provides SNR gain of 0.7 dB over LRT-CS. For this case, we have also calculated the percentage increase in detection performance by employing LRT-CSI rather than using LRT-CS, which we refer as the detection performance improvement, and have plotted it as a function of SNR in Figure 2-4. As seen from this figure, improvements of 52.8%, 30.2%, 31%, 27.9%, 13.5% and 5% are obtained for SNR of -4.5 dB, -2 dB, 0.5 dB, 3 dB, 5.5 dB and 8 dB, respectively. At very high SNR, the improvement is negligible or not observed since both fusion rules operate well. Similarly, LRT-CSI and LRT-CS cannot function reliably at very low SNR region, and no improvement can be seen in the Figure 2-4 for these SNR values.

After that, we have assigned different false alarm and detection probabilities to sensor nodes by changing their local thresholds. We select the thresholds of sensors by dividing the interval  $[t_{\min}, t_{\max}]$  into  $NK$  equally separated numbers where  $t_{\min}$  and  $t_{\max}$  represent the minimum and maximum threshold values respectively, and each of numbers is assigned randomly to the  $j^{th}$  sensor of the  $m^{th}$  cluster uniquely as its threshold,  $t_j^m$ . During this experiment, we let  $t_{\min} = 0$  and

$t_{\max} = \frac{3\mu}{2}$ . Then the false alarm and the detection probabilities of the sensors are generated as

$$P_{F_j}^m = Q\left(\frac{t_j^m}{\sigma_o}\right) \text{ and } P_{D_j}^m = Q\left(\frac{t_j^m - \mu}{\sigma_o}\right) \text{ respectively, which is according to the observation model in}$$

Eq.(2.53). Following that, we obtain ROC curves of LRT-CSI and LRT-CS fusion rules in Figure 2-5 for a WSN with  $N = 4$  clusters each with  $K=4$  and 8 local sensors under SNR of 5 dB. As seen from this figure, for the false alarm probability of  $10^{-2}$ , LRT-CSI has a detection performance improvement over LRT-CS by 10.33% and 13.26% for  $K = 4$  and  $K = 8$  respectively. For false alarm probability of  $10^{-3}$ , the detection performance of LRT-CSI is higher than LRT-CS by 20.10% and 31.74% for  $K = 4$  and  $K = 8$  respectively. Hence, LRT-CSI still performs better than LRT-CS under inhomogeneity of local performance indices of the sensors.

Afterwards, we consider a large-scale WSN of 1000 sensor nodes and change the number of sensors per cluster while keeping the total number of sensors in the network the same. For this, consider the following  $(N, K)$  pairs: (4, 250), (8, 125), (100, 10) and obtained the ROC curves of LRT-CSI and LRT-CS in Figure 2-6. As seen from this figure, for a false alarm probability of  $10^{-2}$ , increasing number of clusters improves the detection performance of LRT-CSI by 34.82% and 67.23% for  $N=8$  and  $N=100$  respectively when compared to  $N=4$ . Similarly, LRT-CS performs better in detection probability by 29.82% and 56.84% for  $N=8$  and  $N=100$  respectively when compared to  $N=4$ . This is because we have higher spatial diversity among communication links between CLHs and GFC by increasing the number of clusters. For this scenario, LRT-CSI has a detection performance improvement by 30.94%, 36.03% and 39.67% compared to LRT-CS for  $N=4, 8$  and 100 respectively.

Finally, we investigate the effect of uniform and non-uniform cluster sizes on the performance of the network for which we consider a WSN of  $N=4$  clusters and 1000 sensor nodes each with  $P_{D_j}^m = 0.6$  and  $P_{F_j}^m = 0.08$ . Let  $K_m$  denote the cluster size of the the  $m^{\text{th}}$  cluster for  $1 \leq m \leq 4$ , which can be represented by a row vector  $\mathbf{K}=[K_1 K_2 K_3 K_4]$ . For non-uniform clustering, we choose the

cluster sizes as  $K_1=50$ ,  $K_2=100$ ,  $K_3=150$  and  $K_4=700$ , whereas uniform clustering assumes  $K_1=K_2=K_3=K_4=250$ . Then, we obtain ROC curves of uniform and non-uniform clustering in Figure 2-7, from which one can see that the uniform clustering outperforms the non-uniform clustering in terms of detection probability for each fusion rule (i.e, LRT-CSI or LRT-CS). This is reasonable because when the information signal sent from the CLH of a large cluster is highly degraded, it is more likely that the GFC makes incorrect decision since a relatively high reliability weight to that CLH has been assigned during the fusion. As seen from Figure 2-7, for a false alarm probability of  $10^{-2}$ , using uniform clustering instead of employing non-uniform results in a detection performance improvement of 39.94% and 44.30% for LRT-CSI and LRT-CS respectively. Also, LRT-CSI has a detection performance increase by 34.97% over LRT-CS under non-uniform clustering.

## 2.6 Conclusions

In this chapter, we have investigated the distributed detection over fading channels for a hierarchical WSN. We have derived two LRT based fusion rules: the first one is LRT-CSI, which uses the complete channel state information (CSI), and the second one is LRT-CS, which only utilizes the exact phase information with the envelope statistics of the channel. While numerical results shows that LRT-CSI performs better than LRT-CS in terms of probability of detection for various parameters such as false alarm probabilities, SNR regimes, number of clusters and/or number of sensors per cluster and types of clustering (i.e., uniform and non-uniform clustering), the complexity analysis reveals that LRT-CS is much simpler to implement compared to LRT-CSI.

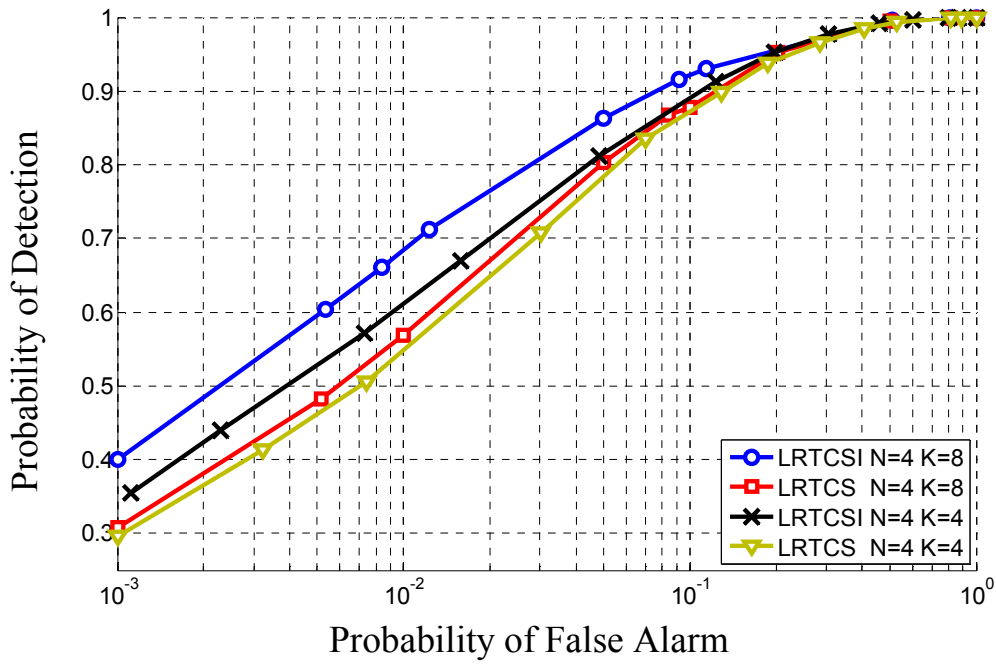


Figure 2-2. ROC curves for LRT-CSI and LRT-CS fusion rules under SNR= 5 dB,  $N=4$  clusters of  $K=4,8$  sensors with  $P_{D_j}^m = 0.5$ ,  $P_{F_j}^m = 0.05$

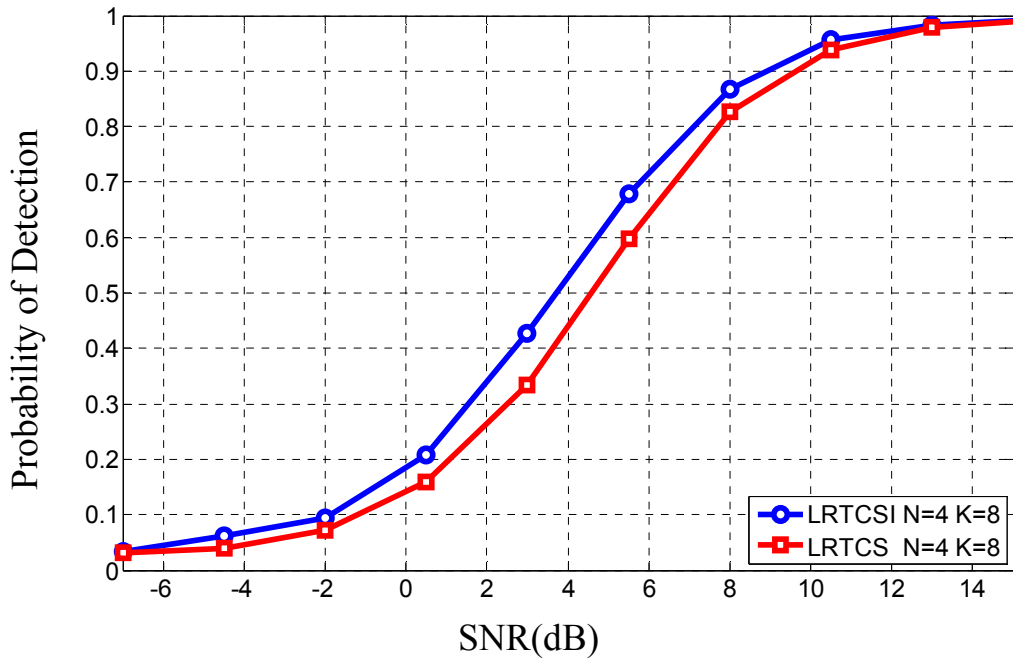


Figure 2-3. Global detection probability of LRT-CSI and LRT-CS as a function of SNR for a WSN with  $N=4$  clusters each of  $K=8$  sensors under global false alarm probability,  $P_{F_0}$ , of 0.01.

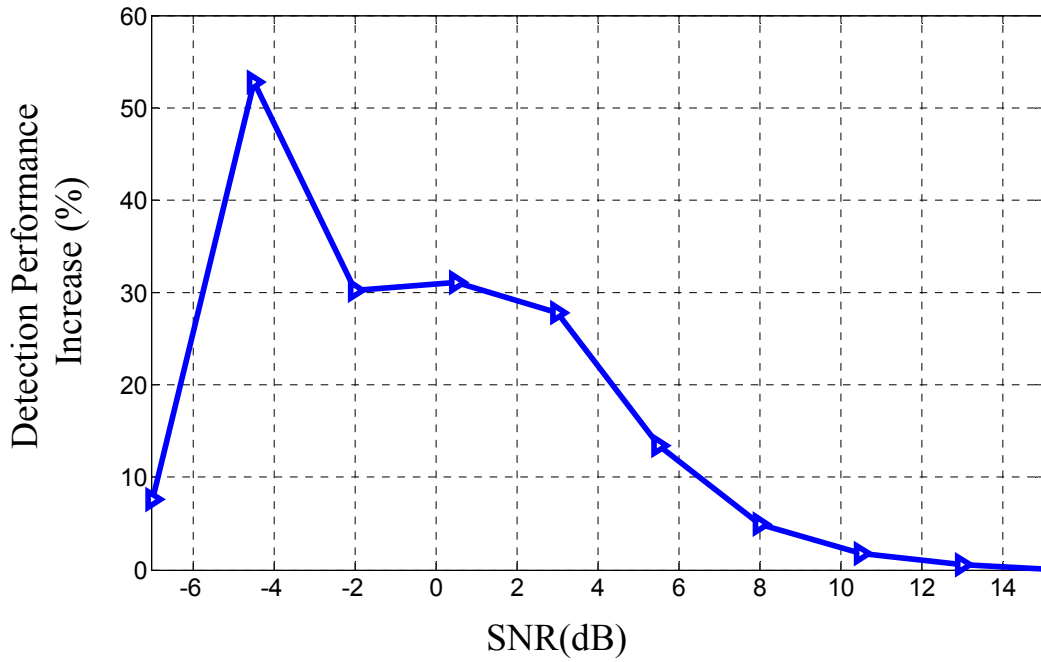


Figure 2-4. Global detection performance improvement of LRT-CSI over LRT-CS as a function of SNR for a WSN with  $N=4$  clusters each of  $K=8$  sensors under global false alarm probability,  $P_{F_0}$ , of 0.01.

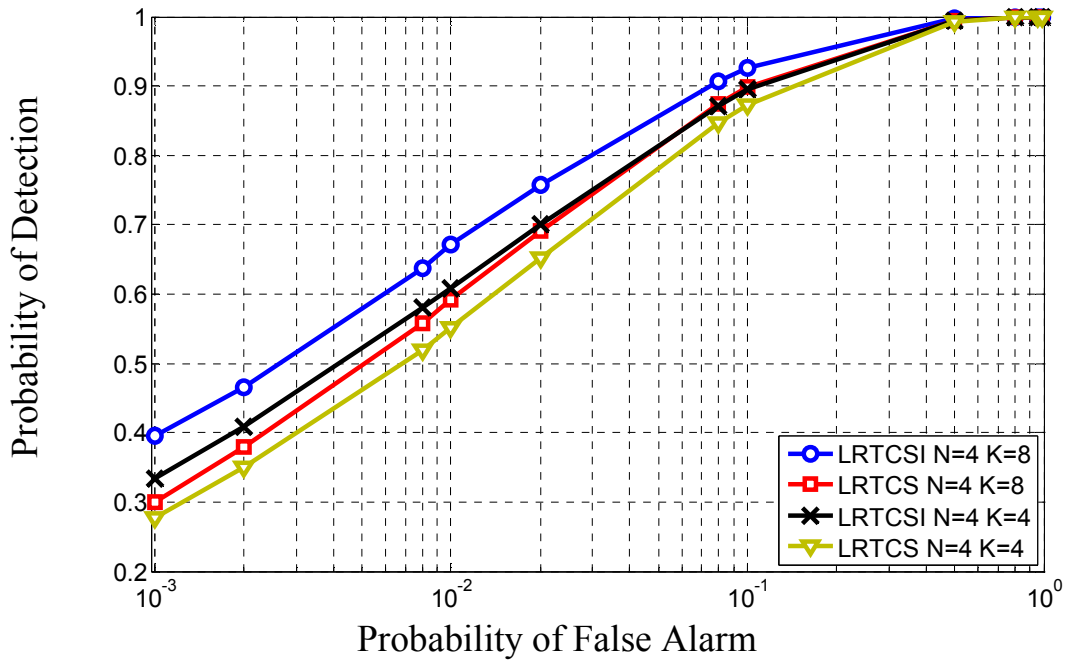


Figure 2-5. ROC curves for LRT-CSI and LRT-CS fusion rules under  $SNR=5$  dB,  $N=4$  clusters of  $K=4,8$  sensors with different detection and false alarm probabilities.

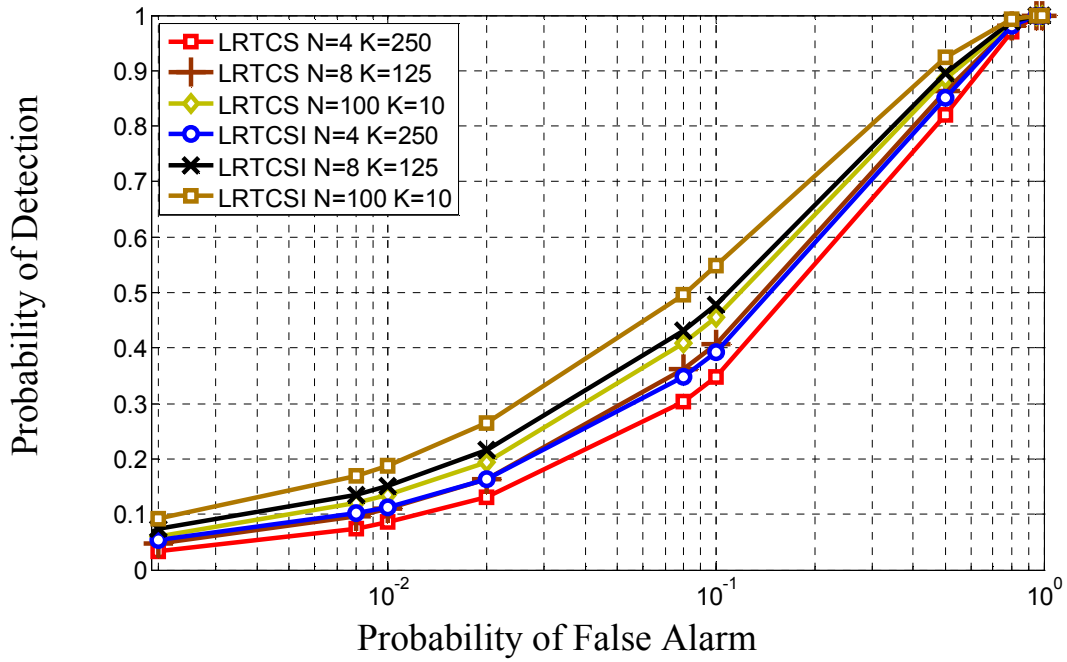


Figure 2-6 ROC curves for LRT-CSI and LRT-CS fusion rules under SNR= 5 dB,  $N=4,8,100$  clusters of  $K=250, 125, 10$  sensors with  $P_{D_j}^m = 0.6$ ,  $P_{F_j}^m = 0.08$

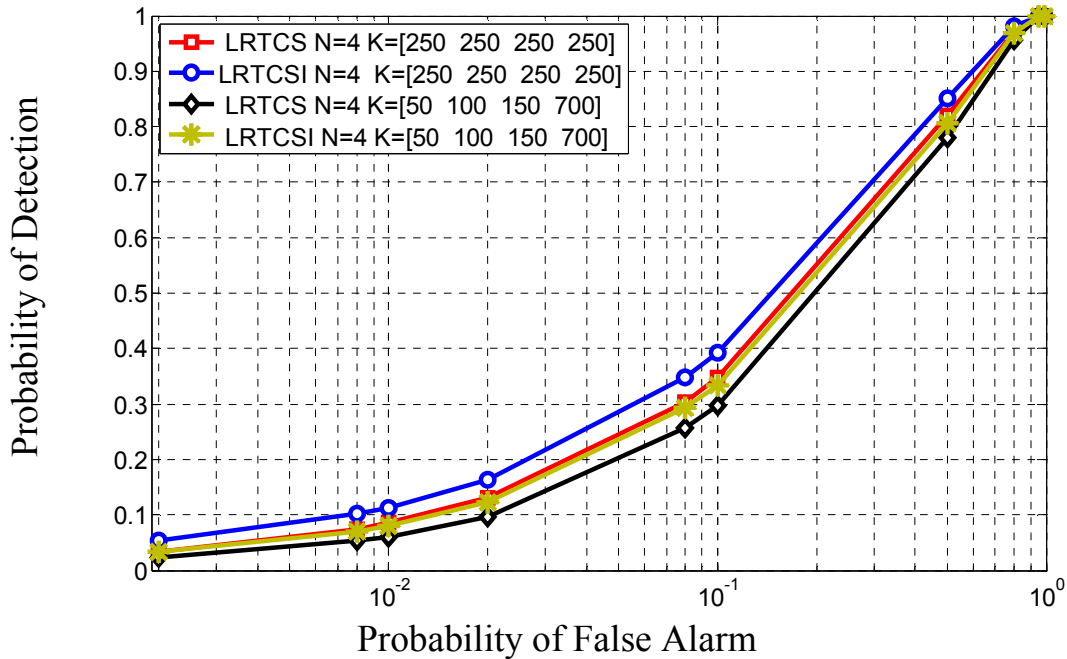


Figure 2-7. ROC curves for LRT-CSI and LRT-CS fusion rules under SNR= 5dB,  $N=4$  for uniform and non-uniform clustering with  $P_{D_j}^m = 0.6$ ,  $P_{F_j}^m = 0.08$

### 3. A Rate-Optimal Power Adaption Policy with User Fairness for Non-Orthogonal Multi-Access Relay Channels

In previous chapter, we studied hierarchical WSNs (which can be considered as an example of relay assisted communication (RAC) channels) in the distributed decision fusion context. In this chapter, we change our paradigm and begin to analyze RAC channels in the communication context. To be specific, in this chapter, we study optimum power allocation problem for maximizing the achievable rate of multi-access relay channel which is also an example of RAC channels.

Recently, single user relay channels (which is also an example of RAC) have attracted much attention as a means to achieve cooperative diversity [16], [48] and [49] where the user first sends the information over wireless medium and then both the relay node and the destination node receive the information bearing signals of the users thanks to the broadcast nature of the wireless channel. After that, the relay nodes extract some useful information about the user messages from the received signals. Finally, they forward the inferred information to the destination node by employing a relaying protocol such as *amplify-and-forward* (AF), *decode-and-forward* (DF) and *estimate and forward* (EF) policy etc [48]. Thus, the relay nodes cooperate with the users to help the destination node for successfully decoding the user messages. Numerous works address the resource (e.g., power and bandwidth) allocation issue in single user relay channels [9], [50]-[59].

To improve the throughput of RAC channel, various network coding (NC) methods have been proposed in [60]-[66] such as XOR method, physical layer network coding (PNC) (a.k.a analog network coding), complex field network coding (CFNC) etc. Among the NC techniques, CFNC uniquely allows decoding of user messages under multi-access interference (MAI), which is introduced due to the simultaneous data transmission of the users in the network, and provides the highest throughput ( $1/2$  symbol per user per channel-use) compared to PNC and XOR coding

methods [20]. Furthermore, it has also the ability to provide full diversity irrespective from signal-to-noise-ratio (SNR) and the type of employed modulation [20]. Because of these desired features, we consider CFNC coded relay assisted communication (CFNC-RAC) channel, where each user is first assigned to a unique pre-determined complex number, which we refer as *signature*. Then, each user weights its message by its signature, which enables a receiving node (e.g., the relay or destination node) to decode each user data uniquely, and thus, provides robustness against MAI in CFNC-RAC. Wang *et.al.* [20] selected signatures based on linear constellation precoding, which is designed for multi-input multi-output (MIMO) systems. There, the signature of the  $i^{\text{th}}$  user in a CFNC-RAC network of  $N$  users is taken to be  $\theta_i = e^{j\pi(4n-1)(i-1)/(2N)}$  for  $N = 2^k$  and  $\theta_i = e^{j\pi(6n-1)(i-1)/(3N)}$  for  $N = 3 \times 2^k$  for any  $n = 1, \dots, N$ , which is purely complex exponential and distinctively rotates the constellation of each user.

One way to improve the performance of the CFNC-RAC under MAI is to optimally allocate the power of the users and the relay according to their channel conditions. While developing an optimal power adaptation policy for the CFNC-RAC channel, maintaining the fairness among users is also very crucial in realizing a practical multi-user communication system [3], which ensures that the access of any user to the network is not denied or overly penalized [67]. For resource allocation in communication systems, various fairness criteria are considered in the literature such as max-min fairness [68], proportional fairness [69] and fairness in information rate (a.k.a symmetric capacity) [70]. Since the symmetric capacity represents the fairest maximum common rate [70], we consider a fairness criterion based on the notion of symmetric capacity and aim to develop a fair power allocation policy for CFNC-RAC channel in this study.

In the context of power allocation for network coding, Zaidi *et.al.* [72] considered an orthogonal additive white Gaussian noise (AWGN) multiple access relay channel employing PNC and then optimized the PNC by controlling the power of each user to maximize the achievable sum rate under the average power constraint of relay node, which was solved by a fixed point iteration

method. Recently, Wang *et. al.*[73] considered a communication scenario, in which each destination node receives only the information of a single user in the first time slot while the PNC coded signal from the relay node that uses *amplify-and-forward* (AF) relaying is observed at all destination nodes in the second time slot. They developed a joint rate and power adaptation scheme to maximize the symmetric-rate bound of each user under the peak power constraint by assuming that the complete channel state information (CSI) of communicating nodes is known at all nodes (i.e., transmitter CSI and receiver CSI are available).

In order to devise a fair power allocation policy for CFNC-RAC channel, we first consider a basic CFNC-RAC channel, which consists of two users, one relay node and one destination node each with a single transmit and/or a receive antenna, under the decode and forward (DF) relaying. Then we develop a rate-optimal fair power adaptation (ROFPA) policy for CFNC-RAC channel, for which we assume that the transmitting nodes (e.g., the user nodes and relay node) have knowledge only on the path-losses dictated by the network geometry, while the receiving nodes (e.g., the relay and destination nodes) have complete knowledge on both path-losses and the channel state information (CSI) due to Rayleigh fading. The proposed ROFPA technique maximizes the information theoretical ergodic or average sum-rate bounds of the users (since we assume receiver-CSI) while maintaining the symmetric-rate fairness among the users on the average and keeping the total transmit power of nodes fixed.

Compared to the previously mentioned studies in [72]-[73], our work is completely different in many ways. Firstly, we assume that the receiving nodes (i.e., the relay node or the destination node) solely know the CSI, whereas the transmitting nodes do not have such knowledge, which is more practical to implement since it does not require any feedback from the receiving node to the transmitting node(s). Secondly, the channel model we have considered (also in[20]), is equivalent to a multi-access channel (MAC) in both time slots since both the relay and destination node observe the superposed signal in all these slots, and thus, it has completely different signal and error characteristics compared to [72]-[73]. Thirdly, *decode-and-forward* (DF) has been

considered in our work, whereas Wang *et. al.* [73] utilized *amplify-and-forward* (AF) relaying in their work.

Our main contribution in this work can be summarized as follows:

We first formulate a rate-optimal fair power adaptation (ROFPA) policy as an optimization problem for CFNC-RAC channel under receiver CSI, and the constraint on the total power budget and the network geometry.

We show that our formulation for ROFPA policy is a non-convex and non-linear program, whose solution is cumbersome, since a standard approach such as Geometric Programming (GP) [85] is not directly applicable.

To solve the optimization problem in the ROFPA policy, we divide the parameter space into four disjoint regions and determine the optimal feasible solution over each segment. Then, ROFPA policy is analytically determined by finding the power values giving the highest achievable sum-rate among the fair optimum solutions over all segments.

Finally, we investigate the performance of ROFPA policy through extensive numerical simulations, where the effects of various parameters such as signal-to noise ratio (SNR) and network geometry are evaluated extensively.

In the next section, we describe the basic system model for CFNC-RAC. After that, we derive a rate-optimal fair power adaptation method (ROFPA) in Section 3.2. In Section 3.3, the performance evaluation of the proposed power allocation method is investigated through numerical experiments. Finally, our conclusions are summarized in Section 3.4.

### **3.1 System Model for a Basic Non-Orthogonal Multi-Access Relay Channel**

In this work, we consider a basic CFNC-RAC channel (as depicted in Figure 3-1), where there are two users  $S_1$  and  $S_2$ , one relay node  $R$  and one destination node  $D$ . As seen from this figure, users first generate their information symbols (denoted as  $x_{s_1}[n]$  and  $x_{s_2}[n]$  for the user  $S_1$  and user  $S_2$ ,

respectively), which are assumed to be drawn from a constellation with average unit-energy. To achieve CFNC, user messages are then multiplied by the previously assigned signatures (expressed by  $\theta_1$  and  $\theta_2$  for users  $S_1$  and  $S_2$ , respectively), which are subsequently scaled according to their individual average powers (denoted as  $P_1$  and  $P_2$  for the user  $S_1$  and user  $S_2$ , respectively) in order to facilitate a power adaptation mechanism. Afterwards, the resultant signals are simultaneously sent over multi-access communication (MAC) channels in time slot 1, which cause multiuser interference at both the relay and the destination. Based on the maximum likelihood (ML) relaying policy, the relay node sends its estimate to the destination node in time slot 2. In this figure, the path-loss coefficients of  $S_1$ -to-destination link,  $S_2$ -to-destination link,  $S_1$ -to-relay link,  $S_2$ -to-relay link and relay-to-destination link are represented by  $\gamma_1, \gamma_2, g_1, g_2$  and  $g_r$ , respectively. Under the flat-fading wireless communications, the received signals at relay node and destination node in time slot 1 (represented by  $y_r[n]$  and  $y_{sd}[n]$ , respectively) and the signal acquired by the destination due to the relaying in time slot 2 (denoted as  $y_{rd}[n]$ ) can be expressed as:

$$y_r[n] = \sqrt{g_1} h_{s_1r} \sqrt{P_1} \theta_1 x_{s_1}[n] + \sqrt{g_2} h_{s_2r} \sqrt{P_2} \theta_2 x_{s_2}[n] + z_r[n] \quad (3.1)$$

$$y_{sd}[n] = \sqrt{\gamma_1} h_{s_1d} \sqrt{P_1} \theta_1 x_{s_1}[n] + \sqrt{\gamma_2} h_{s_2d} \sqrt{P_2} \theta_2 x_{s_2}[n] + z_d[n] \quad (3.2)$$

$$y_{rd}[n] = \sqrt{g_r} h_{rd} \sqrt{\alpha} x_r[n] + z_d[n] \quad (3.3)$$

where  $h_{s_1r}, h_{s_2r}, h_{s_1d}, h_{s_2d}$  and  $h_{rd}$  are fading coefficients for  $S_1$ - $R$ ,  $S_2$ - $R$ ,  $S_1$ - $D$ ,  $S_2$ - $D$ ,  $R$ - $D$  links, respectively, which are modeled as complex Gaussian random variables with zero mean and unit variance. The parameter  $\alpha$  controls the relay power and determines the power allocated to the relay as a fraction of the total transmit power of all users, while  $\gamma_k, g_k$  and  $g_r$  are the path-loss coefficients of  $S_k$ - $D$ ,  $S_k$ - $R$ , and  $R$ - $D$  links for  $k=1,2$ , respectively,  $z_r[n]$  and  $z_d[n]$  represent the noise at the relay node and destination node, respectively, which are modeled as additive white Gaussian noise (AWGN) with zero mean and variance of  $N_0/2$  per dimension.

To reduce the computational burden on the relay node, we just consider the ML relaying policy instead of the optimum maximum a posteriori probability (MAP) relaying (ML is equivalent to MAP as long as the prior probabilities are same) [5], in which the user messages are estimated as:

$$(\hat{x}_{s_1}[n], \hat{x}_{s_2}[n]) = \arg \min_{x_{s_1}[n], x_{s_2}[n]} \left\| y_r[n] - \sqrt{g_1} h_{s_1 r} \sqrt{P_1} \theta_1 x_{s_1}[n] - \sqrt{g_2} h_{s_2 r} \sqrt{P_2} \theta_2 x_{s_2}[n] \right\|^2 \quad (3.4)$$

Then, the relay signal is generated by incorporating the ML estimates of user messages as:

$$x_r[n] = \sqrt{P_1} \theta_1 \hat{x}_{s_1}[n] + \sqrt{P_2} \theta_2 \hat{x}_{s_2}[n] \quad (3.5)$$

where the relay node encodes the user messages by using the same modulation and CFNC signatures as in the user nodes and thereafter forwards their power scaled CFNC coded signal  $x_r[n]$  in time slot 2 to the destination according to Eq.(3.3). The destination node decodes user messages using signals coming from users and relay using ML detectors as :

$$\begin{aligned} (\hat{x}_{s_1}[n], \hat{x}_{s_2}[n]) = \arg \min_{x_{s_1}[n], x_{s_2}[n]} & \left\| y_{sd}[n] - \sqrt{\gamma_1} h_{s_1 d} \sqrt{P_1} \theta_1 x_{s_1}[n] - \sqrt{\gamma_2} h_{s_2 d} \sqrt{P_2} \theta_2 x_{s_2}[n] \right\|^2 \\ & + \left\| y_{rd}[n] - \sqrt{g_r} h_{rd} \sqrt{\alpha} (\sqrt{P_1} \theta_1 x_{s_1}[n] + \sqrt{P_2} \theta_2 x_{s_2}[n]) \right\|^2 \end{aligned} \quad (3.6)$$

In this work, the channel state information (CSI) of fading gains is assumed to be known only at the receiving nodes (i.e., the relay node and the destination node), and the transmitting nodes solely have knowledge on the path-loss coefficients owing to the network geometry. For the sake of simplicity, we also assume that the average energy of fading gains for all communicating nodes is unity.

In the next section, we shall devise a fair power allocation strategy, which considers all the system parameters and path gains and aims at achieving user fairness to improve the performance of the CFNC-RAC channel in Figure 3-1.

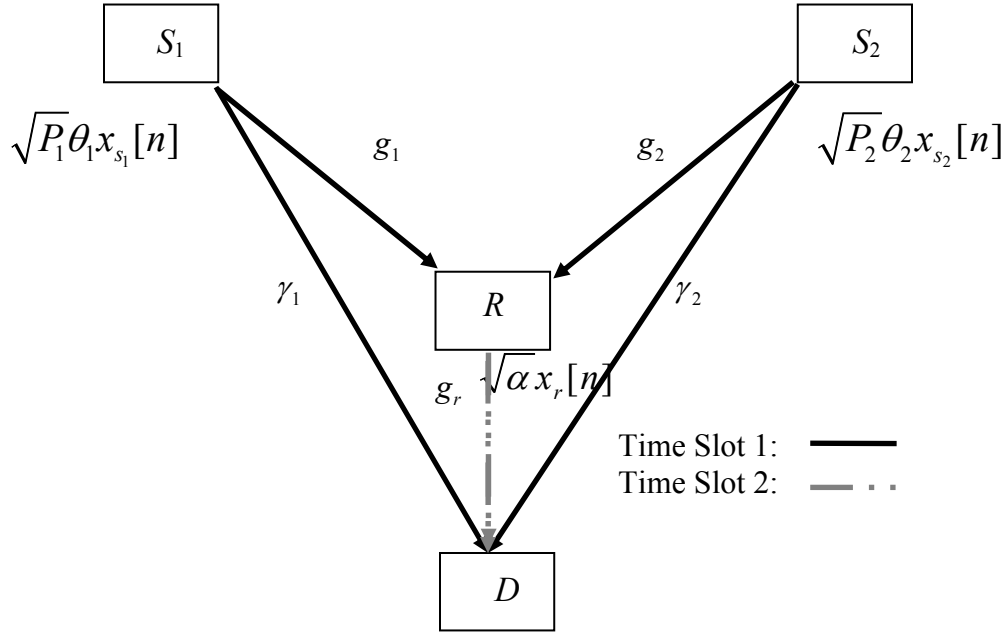


Figure 3-1. Schematic of a basic CFNC-RAC channel with two users, one relay node and one destination node

### 3.2 A Fair Power Optimization Based On Rate Maximization Under Decode and Forward Relaying

In this section, we develop a novel power allocation policy for the system considered, which maximizes the achievable sum-rate bound of CFNC-RAC channel and ensures fairness among users. In sequel, for the sake of simplicity, we assume that the transmitting nodes do not know CSI due to the Rayleigh fading and do only know the path gains perfectly whereas the receiving nodes have knowledge about full CSI. However, the derived expressions during the subsequent analysis can be straightforwardly extended to the case of the full CSI at the transmitter.

For this purpose, we first consider the users-to-relay channel, which is a MAC channel, and thus, the achievable sum-rate of users (the rates of user  $S_1$  user  $S_2$  are denoted by  $R_1$  and  $R_2$ , respectively) at the relay is upper bounded as:

$$\begin{aligned}
R_1 + R_2 &\leq \frac{1}{2} E \left\{ \log \left( 1 + \frac{g_1 P_1 |h_{s_1,r}|^2 + g_2 P_2 |h_{s_2,r}|^2}{2\sigma^2} \right) \right\} \\
&\leq \frac{1}{2} \log \left( 1 + \frac{g_1 P_1 E \{ |h_{s_1,r}|^2 \} + g_2 P_2 E \{ |h_{s_2,r}|^2 \}}{2\sigma^2} \right) \\
&= \frac{1}{2} \log \left( 1 + \frac{g_1 P_1 + g_2 P_2}{2\sigma^2} \right)
\end{aligned} \tag{3.7}$$

Note that the first line of Eq. (3.7) is because of the ergodic sum-capacity of the MAC channel, while the second line follows from the Jensen's inequality since the ergodic sum-capacity is a log-concave function, and the third line is a resultant from the assumption of independently identically distribution (i.i.d) fading gains with unit energy. Also, the factor of  $\frac{1}{2}$  in the rate calculations results from the normalization due to the use of two time-slots during the communications.

Hence, the single user rate bounds can be obtained as:

$$R_1 \leq \frac{1}{2} \log \left( 1 + \frac{g_1 P_1}{2\sigma^2} \right) \tag{3.8}$$

$$R_2 \leq \frac{1}{2} \log \left( 1 + \frac{g_2 P_2}{2\sigma^2} \right) \tag{3.9}$$

Assuming that the relay decodes the user messages perfectly (which can be, achieved by adjusting the user powers appropriately), the signals received at the destination in both time slots (see Eq. (3.2) and Eq.(3.5)) can be written as:

$$\underbrace{\begin{bmatrix} y_{sd}[n] \\ y_{rd}[n] \end{bmatrix}}_{\mathbf{y}} = \underbrace{\begin{bmatrix} \sqrt{\gamma_1} h_{s_1d} & \sqrt{\gamma_2} h_{s_2d} \\ \sqrt{g_r \alpha} h_{rd} & \sqrt{g_r \alpha} h_{rd} \end{bmatrix}}_{\mathbf{H}} \underbrace{\begin{bmatrix} \sqrt{P_1} \theta_1 x_{s_1}[n] \\ \sqrt{P_2} \theta_2 x_{s_2}[n] \end{bmatrix}}_{\mathbf{x}} + \underbrace{\begin{bmatrix} z_d[n] \\ z_d[n] \end{bmatrix}}_{\mathbf{z}} \tag{3.10}$$

where  $\mathbf{y}$  is the received signal vector at destination;  $\mathbf{H}$  is the channel gain matrix;  $\mathbf{x}$  is the user signal vector and  $\mathbf{z}$  is the AWGN noise vector;  $\alpha$  is a parameter, which controls the relay power and determines the power allocated to the relay as a fraction of the total transmit power of all users (i.e.,  $\alpha \triangleq \frac{P_r}{P_1 + P_2}$  or equivalently  $P_r = \alpha(P_1 + P_2)$ ). Therefore, the CFNC-RAC channel can

be modeled as a  $2 \times 2$  *Virtual*-MIMO system, since we consider the dependency of the relayed signal on the user messages in Eq.(3.5) under the assumption of perfect relay decoding.

The single-user and the joint-user rate-bounds of users  $S_1$  and  $S_2$  at the destination are obtained as:

$$R_1 \leq \frac{1}{2} \log \left( 1 + \frac{\gamma_1 P_1 + g_r \alpha P_1}{2\sigma^2} \right) \quad (3.11)$$

$$R_2 \leq \frac{1}{2} \log \left( 1 + \frac{\gamma_2 P_2 + g_r \alpha P_2}{2\sigma^2} \right) \quad (3.12)$$

$$\begin{aligned} R_1 + R_2 &\leq \frac{1}{2} E \left\{ \log \left( \det \left( \mathbf{I} + \frac{\mathbf{HSH}^\dagger}{2\sigma^2} \right) \right) \right\} \leq \frac{1}{2} \log \left( \det \left( \mathbf{I} + \frac{E\{\mathbf{HSH}^\dagger\}}{2\sigma^2} \right) \right) \\ &= \frac{1}{2} \log \left( 1 + \frac{\gamma_1 P_1 + \gamma_2 P_2 + g_r \alpha \left( P_1 + P_2 + P_1 P_2 (\sqrt{\gamma_2} - \sqrt{\gamma_1})^2 \right)}{2\sigma^2} \right) \end{aligned} \quad (3.13)$$

where  $\dagger$  denotes the conjugate-transpose operation,  $\mathbf{S} = E[\mathbf{xx}^T]$  is the input covariance matrix, which is a diagonal matrix with  $P_1$  and  $P_2$  on its diagonal.

By combining Eqs. (3.7)-(3.8) with Eqs. (3.11)-(3.13), the single user and joint-user rate bounds in CFNC-RAC channel can be derived as:

$$R_1 \leq \min \left\{ \frac{1}{2} \log \left( 1 + \frac{\gamma_1 P_1 + g_r \alpha P_1}{2\sigma^2} \right), \frac{1}{2} \log \left( 1 + \frac{g_1 P_1}{2\sigma^2} \right) \right\} \quad (3.14)$$

$$R_2 \leq \min \left\{ \frac{1}{2} \log \left( 1 + \frac{\gamma_2 P_2 + g_r \alpha P_2}{2\sigma^2} \right), \frac{1}{2} \log \left( 1 + \frac{g_2 P_2}{2\sigma^2} \right) \right\} \quad (3.15)$$

$$R_1 + R_2 \leq \min \left\{ \frac{1}{2} \log \left( 1 + \frac{\gamma_1 P_1 + \gamma_2 P_2 + g_r \alpha \left( P_1 + P_2 + P_1 P_2 (\sqrt{\gamma_2} - \sqrt{\gamma_1})^2 \right)}{2\sigma^2} \right), \frac{1}{2} \log \left( 1 + \frac{g_1 P_1 + g_2 P_2}{2\sigma^2} \right) \right\} \quad (3.16)$$

Since our aim is to determine an information theoretical optimum power allocation policy, which considers fairness among users, we equalize the maximum rate bounds of users in Eqs. (3.14) and (3.15) as:

$$\min \left\{ \frac{1}{2} \log \left( 1 + \frac{\gamma_1 P_1 + g_r \alpha P_1}{2\sigma^2} \right), \frac{1}{2} \log \left( 1 + \frac{g_1 P_1}{2\sigma^2} \right) \right\} = \min \left\{ \frac{1}{2} \log \left( 1 + \frac{\gamma_2 P_2 + g_r \alpha P_2}{2\sigma^2} \right), \frac{1}{2} \log \left( 1 + \frac{g_2 P_2}{2\sigma^2} \right) \right\} \quad (3.17)$$

Since our aim is to develop an optimum power allocation policy, which not only maximizes the achievable sum -rate in CFNC-RAC channel but also achieves fairness among users under the total power constraint  $P_T - (1 + \alpha) \sum_{k=1}^2 P_k = 0$ , we end up with the following optimization problem:

$$\text{maximize}_{P_1, P_2, \alpha} w_0(P_1, P_2, \alpha) = \min \left\{ \frac{1}{2} \log \left( 1 + \frac{\gamma_1 P_1 + \gamma_2 P_2 + g_r \alpha (P_1 + P_2 + P_1 P_2 (\sqrt{\gamma_2} - \sqrt{\gamma_1})^2)}{2\sigma^2} \right), \right. \\ \left. \frac{1}{2} \log \left( 1 + \frac{g_1 P_1 + g_2 P_2}{2\sigma^2} \right) \right\}$$

such that

$$\begin{aligned} w_1(P_1, P_2, \alpha) &= P_T - (1 + \alpha) \sum_{k=1}^2 P_k = 0 \\ w_2(P_1, P_2, \alpha) &= P_1 > 0 \\ w_3(P_1, P_2, \alpha) &= P_2 > 0 \\ w_4(P_1, P_2, \alpha) &= \alpha > 0 \\ w_5(P_1, P_2, \alpha) &= \min \left\{ \frac{1}{2} \log \left( 1 + \frac{\gamma_1 P_1 + g_r \alpha P_1}{2\sigma^2} \right), \frac{1}{2} \log \left( 1 + \frac{g_1 P_1}{2\sigma^2} \right) \right\} \\ &\quad - \min \left\{ \frac{1}{2} \log \left( 1 + \frac{\gamma_2 P_2 + g_r \alpha P_2}{2\sigma^2} \right), \frac{1}{2} \log \left( 1 + \frac{g_2 P_2}{2\sigma^2} \right) \right\} = 0 \end{aligned} \tag{3.18}$$

where the objective function  $w_0(P_1, P_2, \alpha)$  represents the sum-rate of users , which can be obtained by taking the minimum of sum-rates at the relay and the destination;  $w_1(P_1, P_2, \alpha)$  is the total power constraint;  $w_2(P_1, P_2, \alpha)$ ,  $w_3(P_1, P_2, \alpha)$  are power constraints of users  $S_1$  and  $S_2$  , respectively, which are strictly greater than zero because the users actively send information all the time;  $w_4(P_1, P_2, \alpha)$  implies the non-negativity of the relay power, which is because the relay node is assumed to be positioned between the users and the destination; is stated according to the fairness constraint in Eq.(3.17).

It is important to note that the optimization problem in Eq. (3.18) cannot be solved directly by using the Geometric Programming (GP) approach [85] since the equality constraints (i.e., total

power constraint and fairness constraints) shall result in posynomials rather than monomials when  $\log(\cdot)$  transformation is applied to the optimization parameters.

During our study of the program in Eq.(3.18), we realized that the cross-term  $P_1 P_2 (\sqrt{\gamma_2} - \sqrt{\gamma_1})^2$  in sum-rate bound of the destination is negligible compared to  $P_1 + P_2$ , which shall be justified in subsection **E**, and it complicates our analysis to find out a solution. Hence, for the sake simplicity, we eliminate the cross-term  $P_1 P_2 (\sqrt{\gamma_2} - \sqrt{\gamma_1})^2$  in the objective and re-express Eq. (3.18) as:

$$\begin{aligned}
& \underset{P_1, P_2, \alpha}{\text{maximize}} w_0(P_1, P_2, \alpha) = \min \{ \gamma_1 P_1 + \gamma_2 P_2 + g_r \alpha (P_1 + P_2), g_1 P_1 + g_2 P_2 \} \\
& \text{such that} \\
& w_1(P_1, P_2, \alpha) = P_T - (1 + \alpha) \sum_{k=1}^2 P_k = 0 \\
& w_2(P_1, P_2, \alpha) = P_1 > 0 \\
& w_3(P_1, P_2, \alpha) = P_2 > 0 \\
& w_4(P_1, P_2, \alpha) = \alpha > 0 \\
& w_5(P_1, P_2, \alpha) = \min \{ \gamma_1 P_1 + g_r \alpha P_1, g_1 P_1 \} - \min \{ \gamma_2 P_2 + g_r \alpha P_2, g_2 P_2 \} = 0
\end{aligned} \tag{3.19}$$

The optimization problem in Eq.(3.19) is non-linear and non-convex, for which it is difficult to obtain an analytical solution directly because of the minimum operation(s) both in the objective function and fairness constraint.

In order to find the results of these minimum operations, we first propose to partition the parameter space based on solely  $\alpha$  into four disjoint regions. Then we determine an exact analytical solution of the optimization problem over each partition. Finally, the optimal solution is found by determining the partition, which gives the maximum value of the objective function among all partitions. In each of these partitions, the parameter  $\alpha$  is assumed to be in a certain interval, whose boundary is dependent on the channel parameters. Thus, we perform a constrained optimization over each segment by putting additional constraints on parameter  $\alpha$  due to the boundary conditions of each partition to determine the optimal  $(P_1, P_2, \alpha)$  tuple. Therefore, we give these partitions and analyze their associated solutions in detail for the optimal fair

allocation problem in CFNC-RAC channel.

$$\mathbf{3.2.1} \quad \textit{Partition 1: } 0 < \alpha \leq \frac{\min(g_1 - \gamma_1, g_2 - \gamma_2)}{g_r}$$

For this interval, the objective function becomes  $w_0(P_1, P_2, \alpha) = \gamma_1 P_1 + \gamma_2 P_2 + g_r \alpha (P_1 + P_2)$ , whose monotonicity is stated below.

*Lemma 3-1:* Within this interval of parameter  $\alpha$ , the objective function  $w_0(P_1, P_2, \alpha) = \gamma_1 P_1 + \gamma_2 P_2 + g_r \alpha (P_1 + P_2)$  is a monotonically increasing function of  $\alpha$  with the following user powers, which are determined by using the total power and fairness constraints as:

$$\begin{aligned} P_1 &= \frac{(\gamma_2 + g_r \alpha) P_T}{(1 + \alpha)(\gamma_1 + 2g_r \alpha + \gamma_2)} \\ P_2 &= \frac{(\gamma_1 + g_r \alpha) P_T}{(1 + \alpha)(\gamma_1 + 2g_r \alpha + \gamma_2)} \end{aligned} \quad (3.20)$$

*Proof of Lemma 3-1:*

Within this partition, the following inequalities hold

$$\begin{aligned} \gamma_1 + g_r \alpha &\leq g_1 \\ \gamma_2 + g_r \alpha &\leq g_2 \\ (\gamma_1 + g_r \alpha) P_1 + (\gamma_2 + g_r \alpha) P_2 &\leq g_1 P_1 + g_2 P_2 \end{aligned} \quad (3.21)$$

Therefore, the objective function and the fairness constraint in Eq. (3.19) can be re-written as:

$$\begin{aligned} w_0(P_1, P_2, \alpha) &= \gamma_1 P_1 + \gamma_2 P_2 + g_r \alpha (P_1 + P_2) \\ w_5(P_1, P_2, \alpha) &= (\gamma_1 + g_r \alpha) P_1 - (\gamma_2 + g_r \alpha) P_2 = 0 \end{aligned} \quad (3.22)$$

The users powers for this partition can be determined using the total power constraint and fairness constraint as:

$$\begin{aligned} P_1 &= \frac{(\gamma_2 + g_r \alpha) P_T}{(1 + \alpha)(\gamma_1 + 2g_r \alpha + \gamma_2)} \\ P_2 &= \frac{(\gamma_1 + g_r \alpha) P_T}{(1 + \alpha)(\gamma_1 + 2g_r \alpha + \gamma_2)} \end{aligned} \quad (3.23)$$

The derivative of the objective function with respect to  $\alpha$  becomes:

$$\begin{aligned} \frac{\partial w_0(P_1, P_2, \alpha)}{\partial \alpha} &= (\gamma_1 - \gamma_2) \frac{g_r P_T (1 + \alpha) (\gamma_1 + 2g_r \alpha + \gamma_2) - (\gamma_2 + g_r \alpha) P_T ((\gamma_1 + 2g_r \alpha + \gamma_2) + (1 + \alpha) 2g_r)}{(1 + \alpha)^2 (\gamma_1 + 2g_r \alpha + \gamma_2)^2} \\ &\quad + \frac{(g_r - \gamma_2) P_T (\gamma_1 + 2g_r \alpha + \gamma_2)^2}{(1 + \alpha)^2 (\gamma_1 + 2g_r \alpha + \gamma_2)^2} \end{aligned} \quad (3.24)$$

After some manipulations, the derivative in Eq.(3.24) can be put into the following form

$$\frac{\partial w_0(P_1, P_2, \alpha)}{\partial \alpha} = \frac{P_T (A\alpha^2 + B\alpha + C)}{(1 + \alpha)^2 (\gamma_1 + 2g_r \alpha + \gamma_2)^2}$$

where

$$A = 2g_r^2 (2g_r - \gamma_1 - \gamma_2) \quad (3.25)$$

$$B = 4g_r (g_r (\gamma_1 + \gamma_2) - 2\gamma_1 \gamma_2)$$

$$C = g_r (\gamma_1 - \gamma_2)^2 + (\gamma_1 + \gamma_2) (g_r (\gamma_1 + \gamma_2) - 2\gamma_1 \gamma_2)$$

Since  $\gamma_1 < g_r$  and  $\gamma_2 < g_r$  hold,  $A$  in Eq.(3.25) is clearly positive. To prove the positivity of  $B$  and  $C$ , we need to use the result of the following claim.

*Claim* : For  $\gamma_1 < g_r$  and  $\gamma_2 < g_r$ ,  $(g_r (\gamma_1 + \gamma_2) - 2\gamma_1 \gamma_2)$  is strictly greater than zero.

*Proof*: Assume  $\gamma_1 \leq \gamma_2$  is true. Then this implies  $2\gamma_1 \leq \gamma_1 + \gamma_2$ , and since  $\gamma_2 < g_r$ ,  $g_r (\gamma_1 + \gamma_2) > 2\gamma_1 \gamma_2$  holds. By proceeding similarly for the case of  $\gamma_2 \leq \gamma_1$ , we end up with the same result.

Therefore, the coefficients  $B$  and  $C$  in Eq.(3.25) are also strictly positive, and  $w_0(P_1, P_2, \alpha)$  is an increasing function of  $\alpha$ .

Because of *Lemma 3-1*, the optimal value of  $\alpha$  and corresponding user powers in Eq. (3.20) for this partition can be found as:

$$\begin{aligned}
\alpha &= \min\left(\frac{g_1 - \gamma_1}{g_r}, \frac{g_2 - \gamma_2}{g_r}\right) \\
P_1 &= \frac{P_T}{\left(1 + \min\left(\frac{g_1 - \gamma_1}{g_r}, \frac{g_2 - \gamma_2}{g_r}\right)\right)} \frac{\min(g_1 - \gamma_1 + \gamma_2, g_2)}{\min(2g_1 - \gamma_1 + \gamma_2, 2g_2 - \gamma_2 + \gamma_1)} \\
P_2 &= \frac{P_T}{\left(1 + \min\left(\frac{g_1 - \gamma_1}{g_r}, \frac{g_2 - \gamma_2}{g_r}\right)\right)} \frac{\min(g_1, g_2 - \gamma_2 + \gamma_1)}{\min(2g_1 - \gamma_1 + \gamma_2, 2g_2 - \gamma_2 + \gamma_1)}
\end{aligned} \tag{3.26}$$

**3.2.2 Partition 2:**  $\frac{\min(g_1 - \gamma_1, g_2 - \gamma_2)}{g_r} \leq \alpha \leq \alpha_0$

For this partition, the maximum value of  $\alpha$ , which is denoted as  $\alpha_0$ , is determined by equating the sum-rate bounds at the relay and destination under the fairness constraint as

$$\alpha_0 = \frac{-(\gamma_1 + \gamma_2) + \sqrt{(\gamma_1 + \gamma_2)^2 - 4(\gamma_1\gamma_2 - g_1g_2)}}{2g_r} \tag{3.27}$$

*Lemma 3-2:* Over **Partition 2**, the objective function becomes  $w_0(P_1, P_2, \alpha) = \gamma_1 P_1 + \gamma_2 P_2 + g_r \alpha (P_1 + P_2)$  and is a monotonically increasing function of  $\alpha$  with the following user powers, which are obtained from the power and fairness constraints:

$$\begin{aligned}
P_1 &= \begin{cases} \frac{(\gamma_2 + g_r \alpha) P_T}{(1 + \alpha)(g_1 + \gamma_2 + g_r \alpha)} & \text{for } g_1 - \gamma_1 \leq g_2 - \gamma_2 \\ \frac{g_2 P_T}{(1 + \alpha)(g_2 + \gamma_1 + g_r \alpha)} & \text{for } g_2 - \gamma_2 \leq g_1 - \gamma_1 \end{cases} \\
P_2 &= \begin{cases} \frac{(\gamma_1 + g_r \alpha) P_T}{(1 + \alpha)(g_2 + g_r \alpha + \gamma_1)} & \text{for } g_1 - \gamma_1 \leq g_2 - \gamma_2 \\ \frac{g_1 P_T}{(1 + \alpha)(g_1 + g_r \alpha + \gamma_2)} & \text{for } g_2 - \gamma_2 \leq g_1 - \gamma_1 \end{cases}
\end{aligned} \tag{3.28}$$

*Proof of Lemma 3-2:* For this interval, the objective function is  $w_0(P_1, P_2, \alpha) = \gamma_1 P_1 + \gamma_2 P_2 + g_r \alpha (P_1 + P_2)$  since the value of  $\alpha$  is less than  $\alpha_0$ , at which sum-rate bounds at the relay and destination become the same under fairness constraint. The value of  $\alpha_0$  is determined as follows.

Assume  $g_1 - \gamma_1 \leq g_2 - \gamma_2$ . Then the following inequalities are valid:

$$\begin{aligned} g_1 &\leq \gamma_1 + g_r \alpha \\ \gamma_2 + g_r \alpha &\leq g_2 \end{aligned} \quad (3.29)$$

Therefore, the fairness constraint becomes

$$w_5(P_1, P_2, \alpha) = g_1 P_1 - (\gamma_2 + g_r \alpha) P_2 = 0 \quad (3.30)$$

Hence, the following expression is valid at  $\alpha = \alpha_0$ .

$$\gamma_1 P_1 + \gamma_2 P_2 + g_r \alpha_0 (P_1 + P_2) - (g_1 P_1 + g_2 P_2) = 0 \quad (3.31)$$

By combining Eq.(3.30) with Eq. (3.31),  $\alpha_0$  should satisfy

$$g_r^2 \alpha_0^2 + (\gamma_1 g_r + \gamma_2 g_r) \alpha_0 - g_1 g_2 + \gamma_1 \gamma_2 = 0 \quad (3.32)$$

The positive root of this equation can be found as:

$$\alpha_0 = \frac{-(\gamma_1 + \gamma_2) + \sqrt{(\gamma_1 + \gamma_2)^2 - 4(\gamma_1 \gamma_2 - g_1 g_2)}}{2g_r} \quad (3.33)$$

For  $g_2 - \gamma_2 \leq g_1 - \gamma_1$ , we end up with the same quadratic relation as in Eq.(3.32), and therefore, the same root in Eq.(3.33) is obtained.

After finding the value of  $\alpha_0$ , we are now ready to show the monotonicity of the objective function over this interval.

For  $g_1 - \gamma_1 \leq g_2 - \gamma_2$ , the user powers can be derived as :

$$\begin{aligned} P_1 &= \frac{(\gamma_2 + g_r \alpha) P_T}{(1 + \alpha)(g_1 + g_r \alpha + \gamma_2)} \\ P_2 &= \frac{g_1 P_T}{(1 + \alpha)(g_1 + g_r \alpha + \gamma_2)} \end{aligned} \quad (3.34)$$

By using Eq. (3.34), the derivative of the objective function can be determined as:

$$\begin{aligned} &\frac{\partial w_0(P_1, P_2, \alpha)}{\partial \alpha} \\ &= (\gamma_1 - \gamma_2) \frac{g_r P_T (1 + \alpha)(g_1 + g_r \alpha + \gamma_2) - (\gamma_2 + g_r \alpha) P_T ((g_1 + g_r \alpha + \gamma_2) + (1 + \alpha) g_r)}{(1 + \alpha)^2 (g_1 + g_r \alpha + \gamma_2)^2} + \frac{(g_r - \gamma_2) P_T}{(1 + \alpha)^2} \end{aligned} \quad (3.35)$$

After some manipulations, Eq. (3.35) can be put into the following form:

$$\frac{\partial w_0(P_1, P_2, \alpha)}{\partial \alpha} = \frac{P_r (A\alpha^2 + B\alpha + C)}{(1+\alpha)^2 (g_1 + g_r \alpha + \gamma_2)^2}$$

where

$$A = g_r^2 (g_r - \gamma_1) \quad (3.36)$$

$$B = 2g_r (\gamma_2 (g_r - \gamma_1) + g_1 (g_r - \gamma_2))$$

$$C = (\gamma_1 - \gamma_2) (g_r g_1 - g_1 \gamma_2 - \gamma_2^2) + (g_r - \gamma_2) (g_1 + \gamma_2)^2$$

It is clear that  $A, B > 0$  because of  $\gamma_1 < g_r$  and  $\gamma_2 < g_r$ . The positivity of the coefficient  $C$  is not

obvious at first glance. After some manipulations,  $C$  can be obtained as:

$$\begin{aligned} C &= (\gamma_1 - \gamma_2) (g_r g_1 - g_1 \gamma_2 - \gamma_2^2) + (g_r - \gamma_2) (g_1 + \gamma_2)^2 \\ &= (g_r - \gamma_2) (g_1 (\gamma_1 - \gamma_2) + (g_1 + \gamma_2)^2) - \gamma_2^2 (\gamma_1 - \gamma_2) \\ &= (g_r - \gamma_2) (g_1 \gamma_1 + g_1 \gamma_2 + g_1^2 + \gamma_2^2) - \gamma_2^2 (\gamma_1 - \gamma_2) \\ &= (g_r - \gamma_2) g_1 (\gamma_1 + \gamma_2 + g_1) + \gamma_2^2 (g_r - \gamma_2 - (\gamma_1 - \gamma_2)) \\ &= (g_r - \gamma_2) g_1 (\gamma_1 + \gamma_2 + g_1) + \gamma_2^2 (g_r - \gamma_1) \end{aligned} \quad (3.37)$$

Each term in Eq. (3.37) is positive, so is the coefficient  $C$ .

For  $g_2 - \gamma_2 \leq g_1 - \gamma_1$ , the fairness constraint becomes  $w_5(P_1, P_2, \alpha) = \gamma_1 P_1 + g_r \alpha P_1 - g_2 P_2 = 0$ , and

we perform the same analysis as we did in the case of  $g_1 - \gamma_1 \leq g_2 - \gamma_2$ . Then the user powers

can be obtained as:

$$\begin{aligned} P_1 &= \frac{g_2 P_r}{(1+\alpha)(\gamma_1 + g_r \alpha + g_2)} \\ P_2 &= \frac{(\gamma_1 + g_r \alpha) P_r}{(1+\alpha)(\gamma_1 + g_r \alpha + g_2)} \end{aligned} \quad (3.38)$$

Hence, the derivative of the objective function can be derived as:

$$\frac{\partial w_0(P_1, P_2, \alpha)}{\partial \alpha} = \frac{P_r (A\alpha^2 + B\alpha + C)}{(1+\alpha)^2 (\gamma_1 + g_r \alpha + g_2)^2}$$

where

$$A = g_r^2 (g_r - \gamma_2) \quad (3.39)$$

$$B = 2g_r (\gamma_1 (g_r - \gamma_2) + g_2 (g_r - \gamma_1))$$

$$C = (\gamma_2 - \gamma_1) (g_r g_2 - g_2 \gamma_1 - \gamma_1^2) + (g_r - \gamma_1) (g_2 + \gamma_1)^2$$

$$= (g_r - \gamma_1) g_2 (\gamma_1 + \gamma_2 + g_2) + \gamma_1^2 (g_r - \gamma_2)$$

Therefore, we have shown that the objective function is an increasing function of the variable

$\alpha$  within **Partition 2**. Since the objective function  $w_0(P_1, P_2, \alpha)$  is an increasing function, the optimal solution over this segment becomes:

$$\alpha = \frac{-(\gamma_1 + \gamma_2) + \sqrt{(\gamma_1 + \gamma_2)^2 - 4(\gamma_1\gamma_2 - g_1g_2)}}{2g_r}$$

$$P_1 = \begin{cases} \frac{(\gamma_2 + g_r\alpha)P_T}{(1+\alpha)(g_1 + \gamma_2 + g_r\alpha)} & \text{for } g_1 - \gamma_1 \leq g_2 - \gamma_2 \\ \frac{g_2P_T}{(1+\alpha)(g_2 + \gamma_1 + g_r\alpha)} & \text{for } g_2 - \gamma_2 \leq g_1 - \gamma_1 \end{cases} \quad (3.40)$$

$$P_2 = \begin{cases} \frac{(\gamma_1 + g_r\alpha)P_T}{(1+\alpha)(g_2 + g_r\alpha + \gamma_1)} & \text{for } g_1 - \gamma_1 \leq g_2 - \gamma_2 \\ \frac{g_1P_T}{(1+\alpha)(g_1 + g_r\alpha + \gamma_2)} & \text{for } g_2 - \gamma_2 \leq g_1 - \gamma_1 \end{cases}$$

**3.2.3 Partition 3:**  $\alpha_0 \leq \alpha \leq \frac{\max(g_1 - \gamma_1, g_2 - \gamma_2)}{g_r}$

Over this interval, this objective function is  $w_0(P_1, P_2, \alpha) = g_1P_1 + g_2P_2$ , and its monotonicity property is stated below.

*Lemma 3-3:* Let  $\alpha_1$  be another instance of  $\alpha$  and be defined as:

$$\alpha_1 \triangleq \begin{cases} \frac{-(g_2 + \gamma_2) + \sqrt{(g_1 - g_2)(g_r - g_2 - \gamma_2)}}{g_r} & \text{for } g_1 - \gamma_1 \leq g_2 - \gamma_2 \\ \frac{-(g_1 + \gamma_1) + \sqrt{(g_2 - g_1)(g_r - g_1 - \gamma_1)}}{g_r} & \text{for } g_2 - \gamma_2 \leq g_1 - \gamma_1 \end{cases} \quad (3.41)$$

Whenever  $\alpha_1$  is real and positive and lies in the interval  $[\alpha_1, \frac{\max(g_1 - \gamma_1, g_2 - \gamma_2)}{g_r}]$ , the objective

is a monotonically increasing function of  $\alpha$  over the interval  $[\alpha_0, \alpha_1]$  and decreases

monotonically over  $[\alpha_1, \frac{\max(g_1 - \gamma_1, g_2 - \gamma_2)}{g_r}]$ . Note that if such  $\alpha_1$  does exist, then the objective

is a decreasing function of  $\alpha$ .

*Proof of Lemma 3-3:* In this interval, the objective function becomes  $w_0(P_1, P_2, \alpha) = g_1P_1 + g_2P_2$ .

For  $g_1 - \gamma_1 \leq g_2 - \gamma_2$ , the fairness constraint and user powers are the same as in Eq. (3.30) and Eq.(3.34), respectively. Hence, the derivative of the objective function can be written as:

$$\begin{aligned} \frac{\partial w_0(P_1, P_2, \alpha)}{\partial \alpha} &= (g_2 - g_1) \frac{-g_1 P_T ((g_1 + g_r \alpha + \gamma_2) + (1 + \alpha)(g_r \alpha))}{(1 + \alpha)^2 (g_1 + g_r \alpha + \gamma_2)^2} - \frac{g_1 P_T (g_1 + g_r \alpha + \gamma_2)^2}{(1 + \alpha)^2 (g_1 + g_r \alpha + \gamma_2)^2} \\ &= \frac{P_T (A\alpha^2 + B\alpha + C)}{(1 + \alpha)^2 (g_1 + g_r \alpha + \gamma_2)^2} \end{aligned}$$

where

$$A = -g_1 g_r^2 \tag{3.42}$$

$$B = -2g_1 g_r (g_2 + \gamma_2)$$

$$C = -g_1 g_r (g_2 - g_1) - g_1 (\gamma_2 + g_2) (\gamma_2 + g_1)$$

$$= -g_1 (g_r - g_2 - \gamma_2) (g_2 - g_1)$$

It is obvious that  $A, B < 0$ , and therefore, the polynomial  $A\alpha^2 + B\alpha + C$  does not have any real positive root when  $C \leq 0$ . Hence, the positive root of  $A\alpha^2 + B\alpha + C$  may exist only when  $C > 0$  (i.e.  $(g_1 - g_2)(g_r - g_2 - \gamma_2) > 0$ ), for which the root can be derived as:

$$\alpha_1 = \frac{-(g_2 + \gamma_2) + \sqrt{(g_1 - g_2)(g_r - g_2 - \gamma_2)}}{g_r} \tag{3.43}$$

Since  $A < 0$ , the sign of the derivative in Eq. (3.42) is positive for  $\alpha \leq \alpha_1$ . Otherwise, it is negative. Hence, when there exists a real positive  $\alpha_1 \in [\alpha_0, \frac{\max(g_1 - \gamma_1, g_2 - \gamma_2)}{g_r}]$ , the objective function is an increasing function for  $\alpha \in [\alpha_0, \alpha_1]$  and is decreasing monotonically over  $[\alpha_1, \frac{\max(g_1 - \gamma_1, g_2 - \gamma_2)}{g_r}]$ . Therefore, when such  $\alpha_1$  does not exist, the objective function decreases monotonically. The existence of a real positive  $\alpha_1$ , which is greater than  $\alpha_0$ , requires the following conditions (assuming  $g_1 - \gamma_1 \leq g_2 - \gamma_2$ ) to be met:

$$g_2 + \gamma_2 + \frac{1}{g_1 - g_2} \left( g_2 + \gamma_2 + \frac{-(\gamma_1 + \gamma_2) + \sqrt{(\gamma_1 + \gamma_2)^2 - 4(\gamma_1 \gamma_2 - g_1 g_2)}}{2} \right)^2 \leq g_r \leq \frac{4g_2^2}{g_1 - g_2} + g_2 + \gamma_2$$

$g_2 < g_1$

(3.44)

For  $g_2 - \gamma_2 \leq g_1 - \gamma_1$ , the fairness constraint is  $w_3(P_1, P_2, \alpha) = \gamma_1 P_1 + g_r \alpha P_1 - g_2 P_2 = 0$ , where user powers are stated in Eq.(3.34). The derivative of the objective function can be derived as:

$$\frac{\partial w_0(P_1, P_2, \alpha)}{\partial \alpha} = \frac{P_r (A\alpha^2 + B\alpha + C)}{(1 + \alpha)^2 (\gamma_1 + g_r \alpha + g_2)^2}$$

where

$$A = -g_2 g_r^2 \quad (3.45)$$

$$B = -2g_2 g_r (g_1 + \gamma_1)$$

$$C = -g_2 g_r (g_1 - g_2) - g_2 (\gamma_1 + g_1) (\gamma_1 + g_2)$$

$$= -g_2 (g_r - g_1 - \gamma_1) (g_1 - g_2)$$

The real positive root of  $A\alpha^2 + B\alpha + C$  exists only when  $(g_2 - g_1)(g_r - g_1 - \gamma_1) > 0$ , for which the root can be expressed as:

$$\alpha_1 = \frac{-(g_1 + \gamma_1) + \sqrt{(g_2 - g_1)(g_r - g_1 - \gamma_1)}}{g_r} \quad (3.46)$$

Again, when there exists a real positive  $\alpha_1 \in [\alpha_0, \frac{\max(g_1 - \gamma_1, g_2 - \gamma_2)}{g_r}]$ , the objective function is

an increasing function over the interval  $[\alpha_0, \alpha_1]$  and decreases monotonically over  $[\alpha_1, \frac{\max(g_1 - \gamma_1, g_2 - \gamma_2)}{g_r}]$ . Such  $\alpha_1$ , which is greater than  $\alpha_0$  and less than

$\frac{\max(g_1 - \gamma_1, g_2 - \gamma_2)}{g_r}$ , does exist only when the following conditions are satisfied:

$$g_1 + \gamma_1 + \frac{1}{g_2 - g_1} \left( g_1 + \gamma_1 + \frac{-(\gamma_1 + \gamma_2) + \sqrt{(\gamma_1 + \gamma_2)^2 - 4(\gamma_1 \gamma_2 - g_1 g_2)}}{2} \right)^2 \leq g_r \leq \frac{4g_1^2}{g_2 - g_1} + g_1 + \gamma_1$$

$$g_1 < g_2 \quad (3.47)$$

Because of Lemma 3-3, the optimal solution over this interval can be obtained as:

$$\begin{aligned}
\alpha_1 &\triangleq \begin{cases} \frac{-(g_2 + \gamma_2) + \sqrt{(g_1 - g_2)(g_r - g_2 - \gamma_2)}}{g_r} & \text{for } g_1 - \gamma_1 \leq g_2 - \gamma_2 \\ \frac{-(g_1 + \gamma_1) + \sqrt{(g_2 - g_1)(g_r - g_1 - \gamma_1)}}{g_r} & \text{for } g_2 - \gamma_2 \leq g_1 - \gamma_1 \end{cases} \\
\alpha &= \begin{cases} \alpha_0 & \text{whenever a real positive } \alpha_1 \in [\alpha_0, \frac{\max(g_1 - \gamma_1, g_2 - \gamma_2)}{g_r}] \text{ does not exist} \\ \alpha_1, & \text{otherwise} \end{cases} \\
P_1 &= \begin{cases} \frac{(\gamma_2 + g_r \alpha) P_T}{(1 + \alpha)(g_1 + \gamma_2 + g_r \alpha)} & \text{for } g_1 - \gamma_1 \leq g_2 - \gamma_2 \\ \frac{g_2 P_T}{(1 + \alpha)(\gamma_1 + g_r \alpha + g_2)} & \text{for } g_2 - \gamma_2 \leq g_1 - \gamma_1 \end{cases} \\
P_2 &= \begin{cases} \frac{g_1 P_T}{(1 + \alpha)(g_1 + \gamma_2 + g_r \alpha)} & \text{for } g_1 - \gamma_1 \leq g_2 - \gamma_2 \\ \frac{(\gamma_1 + g_r \alpha) P_T}{(1 + \alpha)(\gamma_1 + g_r \alpha + g_2)} & \text{for } g_2 - \gamma_2 \leq g_1 - \gamma_1 \end{cases} \tag{3.48}
\end{aligned}$$

### 3.2.4 Partition 4: $\frac{\max(g_1 - \gamma_1, g_2 - \gamma_2)}{g_r} \leq \alpha$

*Lemma 3-4* : For this interval, the objective function is  $w_0(P_1, P_2, \alpha) = g_1 P_1 + g_2 P_2$  and is a monotonically decreasing function of  $\alpha$  with the following user powers, which satisfy the power and fairness constraints:

$$\begin{aligned}
P_1 &= \frac{P_T}{(1 + \alpha)} \frac{g_2}{g_1 + g_2} \\
P_2 &= \frac{P_T}{(1 + \alpha)} \frac{g_1}{g_1 + g_2} \tag{3.49}
\end{aligned}$$

*Proof of Lemma 3-4*: When  $\alpha \geq \frac{\max(g_1 - \gamma_1, g_2 - \gamma_2)}{g_r}$  is valid, the objective function and fairness

constraint can be expressed as:

$$\begin{aligned}
w_0(P_1, P_2, \alpha) &= g_1 P_1 + g_2 P_2 \\
w_3(P_1, P_2, \alpha) &= g_1 P_1 - g_2 P_2 = 0 \tag{3.50}
\end{aligned}$$

Using these constraints, the user powers can be written as:

$$\begin{aligned}
P_1 &= \frac{P_T}{(1+\alpha)} \frac{g_2}{g_1 + g_2} \\
P_2 &= \frac{P_T}{(1+\alpha)} \frac{g_1}{g_1 + g_2}
\end{aligned} \tag{3.51}$$

The derivative of objective function  $w_0(P_1, P_2, \alpha)$  can be given as:

$$\frac{\partial w_0(P_1, P_2, \alpha)}{\partial \alpha} = -2g_1g_2 \frac{P_T}{(1+\alpha)^2 (g_2 + g_1)} < 0 \tag{3.52}$$

Hence, the objective function in Eq. (3.50) decreases monotonically over **Partition 4**. Therefore, the optimal solution for this partition becomes

$$\begin{aligned}
\alpha &= \max\left(\frac{g_1 - \gamma_1}{g_r}, \frac{g_2 - \gamma_2}{g_r}\right) \\
P_1 &= \frac{P_T}{\left(1 + \max\left(\frac{g_1 - \gamma_1}{g_r}, \frac{g_2 - \gamma_2}{g_r}\right)\right)} \frac{g_2}{g_1 + g_2} \\
P_2 &= \frac{P_T}{\left(1 + \max\left(\frac{g_1 - \gamma_1}{g_r}, \frac{g_2 - \gamma_2}{g_r}\right)\right)} \frac{g_1}{g_1 + g_2}
\end{aligned} \tag{3.53}$$

After analyzing the monotonicity properties of the objective function and its optimal solution over various partitions, we state the solution of ROFPA (see Eq. (3.19) ) in the following theorem.

*Theorem 3-1:* The optimal solution of ROFPA in Eq. (3.19) is given as:

$$\begin{aligned}
\alpha_0 &\triangleq \frac{-(\gamma_1 + \gamma_2) + \sqrt{(\gamma_1 + \gamma_2)^2 - 4(\gamma_1\gamma_2 - g_1g_2)}}{2g_r} \\
\alpha_1 &\triangleq \begin{cases} \frac{-(g_2 + \gamma_2) + \sqrt{(g_1 - g_2)(g_r - g_2 - \gamma_2)}}{g_r} & \text{for } g_1 - \gamma_1 \leq g_2 - \gamma_2 \\ \frac{-(g_1 + \gamma_1) + \sqrt{(g_2 - g_1)(g_r - g_1 - \gamma_1)}}{g_r} & \text{for } g_2 - \gamma_2 \leq g_1 - \gamma_1 \end{cases} \\
\alpha &= \begin{cases} \alpha_0 & \text{whenever a real positive } \alpha_1 \in [\alpha_0, \frac{\max(g_1 - \gamma_1, g_2 - \gamma_2)}{g_r}] \text{ does not exist} \\ \alpha_1, & \text{otherwise} \end{cases} \\
P_1 &= \begin{cases} \frac{(\gamma_2 + g_r\alpha)P_T}{(1 + \alpha)(g_1 + \gamma_2 + g_r\alpha)} & \text{for } g_1 - \gamma_1 \leq g_2 - \gamma_2 \\ \frac{g_2P_T}{(1 + \alpha)(\gamma_1 + g_r\alpha + g_2)} & \text{for } g_2 - \gamma_2 \leq g_1 - \gamma_1 \end{cases} \\
P_2 &= \begin{cases} \frac{g_1P_T}{(1 + \alpha)(g_1 + \gamma_2 + g_r\alpha)} & \text{for } g_1 - \gamma_1 \leq g_2 - \gamma_2 \\ \frac{(\gamma_1 + g_r\alpha)P_T}{(1 + \alpha)(\gamma_1 + g_r\alpha + g_2)} & \text{for } g_2 - \gamma_2 \leq g_1 - \gamma_1 \end{cases} \tag{3.54}
\end{aligned}$$

Proof of Theorem 3-1: Due to the monotonicity properties of the objective function over various partitions, which are stated in Lemma 3-1-Lemma 3-4, and the continuity of the objective at the boundaries of all partitions, the optimal solution for Eq. (3.19) is obtained as stated in Eq.(3.54).

∴ QED

### 3.2.5 Justification of the Negligibility of the Cross-Term

In the previous section, we assumed that the cross-term  $P_1P_2(\sqrt{\gamma_2} - \sqrt{\gamma_1})^2$  is negligible compared to  $P_1 + P_2$  and came up with analytical results for Eq. (3.19). In this section, we shall justify this assumption over each of these partitions.

It is clear that the cross-term gets close to zero for all segments for  $\gamma_2 \approx \gamma_1$  due to its third component (i.e.,  $(\sqrt{\gamma_2} - \sqrt{\gamma_1})^2$ ). We shall show below that the cross-term becomes approximately

zero for  $\gamma_1 \ll \gamma_2$  or  $\gamma_1 \gg \gamma_2$  due to fact that the multiplication of user powers  $P_1 P_2$  is almost zero for these values of  $\gamma_1$  and  $\gamma_2$ .

Over the **Partition 1**, the multiplication of user powers can be written as:

$$P_1 P_2 = \frac{(\gamma_2 + g_r \alpha)}{(\gamma_1 + \gamma_2 + 2g_r \alpha)} \frac{(\gamma_1 + g_r \alpha)}{(\gamma_1 + \gamma_2 + 2g_r \alpha)} \frac{P_T^2}{(1 + \alpha)^2} \quad (3.55)$$

The first and second term in the RHS of Eq. (3.55) get close to zero for  $\gamma_1 \gg \gamma_2$  and  $\gamma_2 \gg \gamma_1$ , respectively.

Over the **Partitions 2** and **3**, the multiplication of user powers can be expressed as:

$$P_1 P_2 = \begin{cases} \frac{(\gamma_2 + g_r \alpha)}{(g_1 + \gamma_2 + g_r \alpha)} \frac{g_1}{(g_1 + \gamma_2 + g_r \alpha)} \frac{P_T^2}{(1 + \alpha)^2} & \text{for } g_1 - \gamma_1 \leq g_2 - \gamma_2 \\ \frac{g_2}{(\gamma_1 + g_r \alpha + g_2)} \frac{(\gamma_1 + g_r \alpha)}{(\gamma_1 + g_r \alpha + g_2)} \frac{P_T^2}{(1 + \alpha)^2} & \text{for } g_2 - \gamma_2 \leq g_1 - \gamma_1 \end{cases} \quad (3.56)$$

Note that the following inequality holds for these partitions:

$$\begin{aligned} g_1 &\leq \gamma_1 + g_r \alpha & \text{for } g_1 - \gamma_1 \leq g_2 - \gamma_2 \\ g_2 &\leq \gamma_2 + g_r \alpha & \text{for } g_2 - \gamma_2 \leq g_1 - \gamma_1 \end{aligned} \quad (3.57)$$

Also, the conditions of  $\gamma_1 \leq g_1$  and  $\gamma_2 \leq g_2$  are always valid. Hence, the expressions in Eq.(3.56) are bounded above as follows:

$$P_1 P_2 \leq \begin{cases} \frac{(\gamma_2 + g_r \alpha)}{(\gamma_1 + \gamma_2 + g_r \alpha)} \frac{(\gamma_1 + g_r \alpha)}{(\gamma_1 + \gamma_2 + g_r \alpha)} \frac{P_T^2}{(1 + \alpha)^2} & \text{for } g_1 - \gamma_1 \leq g_2 - \gamma_2 \\ \frac{(\gamma_2 + g_r \alpha)}{(\gamma_1 + g_r \alpha + \gamma_2)} \frac{(\gamma_1 + g_r \alpha)}{(\gamma_1 + g_r \alpha + \gamma_2)} \frac{P_T^2}{(1 + \alpha)^2} & \text{for } g_2 - \gamma_2 \leq g_1 - \gamma_1 \end{cases} \quad (3.58)$$

A similar analysis performed for **Partition 1** reveals that the first and second terms in the RHS of Eq. (3.58) get close to zero for  $\gamma_1 \gg \gamma_2$  and  $\gamma_2 \gg \gamma_1$ , respectively.

For the **Partition 4**, adding or removing does not change the objective since it is independent from the cross-term. Hence, we can do our calculations as if there is no cross-term

In short, these analyses show that ignoring the cross-term can be accurately justified for most of

the time. Also, our simulations show that the numerical difference between the optimal solution for Eq. (3.18) and that for Eq.(3.19) is negligibly small. Therefore, our analytical results can be considered as accurate and consistent with the true optimal solution of Eq. (3.18), which is numerically found.

### 3.3 Simulation Results

In this section, we investigate the bit error rate (BER) performance of CFNC-RAC channel by employing the proposed rate-optimal fair power adaptation (ROFPA) policy, in which the user  $S_1$  and user  $S_2$  utilize CFNC signatures as  $\theta_1 = e^{j0} = 1$  and  $\theta_2 = e^{j\frac{3\pi}{4}}$ , respectively, [20]. We then compare the performance of ROFPA with the equal power allocation (EPA) policy, where we make not only the total transmit power for each time slot to be equal but also the user powers in the first time slot to be the same (i.e.,  $P_1 = P_2$  is dedicated to each user, and  $P_1 + P_2$  is allocated to the relay using  $\alpha = 1$ ). In the sequel, we assume that the average transmit power of the network is 2 units (i.e.,  $P_T = (1 + \alpha)(P_1 + P_2) = 2$ ). For all numerical experiments presented in this part, we also assume that distance from the user-1-to-destination link is one and the corresponding path loss coefficient is unity (i.e.,  $\gamma_1 = 1$  or 0 dB) so that other path loss coefficients (i.e.,  $g_1$ ,  $g_2$ ,  $g_r$  and  $\gamma_2$ ) are interpreted as power gains or losses relative to the user-1-to-destination link. Also, the path-loss exponent is assumed to be 2, and the path-loss coefficients of the relay channel should satisfy the following geometrical constraints because of the two-triangle inequalities:

$$|g_1^{-0.5} - g_r^{-0.5}| < \gamma_1^{-0.5} < g_1^{-0.5} + g_r^{-0.5} \quad (3.59)$$

$$|g_2^{-0.5} - g_r^{-0.5}| < \gamma_2^{-0.5} < g_2^{-0.5} + g_r^{-0.5} \quad (3.60)$$

For this study, the signal-to noise ratio of the network is defined in dB as:

$$\text{SNR (in dB)} = 10 \log\left(\frac{P_T}{2\sigma^2}\right) \quad (3.61)$$

Since the power budget is fixed, we realize different SNR values by changing the variance of

electronics noise in Eq. (3.61). We also define the fairness metric (FAM) at each value of the SNR as:

$$\text{FAM}(\text{SNR}) = \left( 1 - \frac{\sqrt{\sum_{i=1}^2 (\text{BER}_{av}(\text{SNR}) - \text{BER}_i(\text{SNR}))^2}}{\text{BER}_{av}(\text{SNR})} \right) \times 100\% \quad (3.62)$$

where  $\text{BER}_i(\text{SNR})$  represents the BER of the  $i$ th user,  $\text{BER}_{av}(\text{SNR})$  is the average BER of the users as a function of SNR. Intuitively, FAM gets higher when the BERs of the users get closer to the average BER. In order to quantify the fairness among the users, we have considered the average fairness metric (AFAM) over all SNRs as:

$$\text{AFAM} = \frac{1}{K} \sum_{j=1}^K \text{FAM}(\text{SNR}_j) \quad (3.63)$$

where  $K$  is the number of BER measurements taken at SNR of  $\text{SNR}_j$ . In order to see the benefit of the power optimization, we first consider a CFNC-RAC where users and destination are placed on three corner of an equilateral triangle. We initially put the relay at the midpoint of altitude of the destination node, which is referred as “nominal position” (NOP) of the relay, and has path gains of  $\gamma_1=0$  dB,  $\gamma_2=0$  dB,  $g_1=g_2=3.60$  dB and  $g_r=7.27$  dB.

To analyze the effect of position of the relay, we change the position of the relay towards to the destination with of  $v_d$  units with respect to the NOP, which only changes  $g_1$ ,  $g_2$  and  $g_r$  to  $g_1=2.72$ dB,  $g_2=2.72$  dB and  $g_r= 9.55$  dB ;  $g_1=1.87$ dB,  $g_2=1.87$  dB and  $g_r= 12.65$  dB;  $g_1=1.04$ dB,  $g_2=1.04$  dB and  $g_r= 17.52$  dB, respectively, for  $v_d=0.1$  units, 0.2 units and 0.3 units. For this scenario, the optimal user and relay powers are tabulated in Table 3-1. Since, users are placed symmetric with respect to the relay and destination, and power values allocated to the users are same. As the relay gets closer and closer to the destination, the reliabilities of the user-to-relay and relay-to-destination links become more and more similar. Thus, it is more logical for the users to directly communicate with the destination rather than over the relay, and therefore, the relay power decreases.

After determining the optimal power values of ROFPA, its BER performance is obtained as given in Figure 3-2 for different SNR values, in which the BER simulations of EPA are also shown. As seen from this figure, the proposed ROFPA policy provides average BER performance improvements over EPA up to 59.70% ,71.53%, 80.50% and 86.00% for  $v_d=0$  units, 0.1 units, 0.2 units and 0.3 units respectively. For the target average BER of  $10^{-2}$ , employing ROFPA instead of EPA results in SNR improvements of 3 dB, 4 dB, 5.75 dB, and 6 dB for  $v_d = 0$  units, 0.1 units, 0.2 units and 0.3 units respectively. Similarly, ROFPA achieves an average BER of  $10^{-3}$  with the use of 4 dB, 4.75 dB, 7dB and 8.25 dB less SNR when compared to the EPA for  $v_d = 0$  units, 0.1 units, 0.2 units and 0.3 units respectively.

As a second scenario, we move the relay left from the nominal position (towards to the user 1) with an amount of  $v_r=0.2$  units, for which the path gains are  $g_1=5.57$  dB,  $g_2=1.70$  dB and  $g_r= 6.43$  dB. The optimal ROFPA parameters and the average BER simulations of the considered power allocation methods for this case can be found in Table 3-2 and Figure 3-3, respectively. From Table 3-2 , we observe that  $S_2$  has been allocated more power compared to  $S_1$  when relay move to left. This makes sense since  $S_1$  is closer to the relay and less power should be assigned in order to maintain the fairness between the users. We have also observed that the relay power has slightly been increased since its distance from the destination is increased as compared to the nominal relay position. As seen from Figure 3-3, employing ROFPA instead of EPA improves the average BER up to 60.28% when  $v_r=0.2$  units. The ROFPA reaches an average BER of  $10^{-2}$  and  $10^{-3}$  by utilizing 3 dB and 4 dB less SNR when compared to EPA. Next, we analyze the individual BER performances of the users as seen in Figure 3-4 and calculated the AFAM of the power allocation techniques. For the case where relay is at its nominal position BER performance of each user is same. However, for  $v_r = 0.2$  units, ROFPA and EPA result in an AFAM of 87.86 % and 60%, respectively.

On the other hand, to see the effect of optimization on sum rate which is the metric we try to

maximize, we calculate sum rate performances of ROFPA and EPA for the scenarios which relay move towards to the destination and  $S_1$  in Figure 3-5, Figure 3-6 respectively. As seen from Figure 3-5, the proposed ROFPA policy provides sum rate performance improvements over EPA up to 37.03% ,50.73%, 60.25% and 66.19% for  $v_d = 0$  units, 0.1 units, 0.2 units and 0.3 units respectively. For the sum rate of 2 bits/s/Hz, employing ROFPA instead of over EPA results in SNR improvements of 2 dB, 2.4 dB, 3 dB, and 3 dB for  $v_d = 0$  units, 0.1 units, 0.2 units and 0.3 units respectively. Similarly, ROFPA achieves the sum rate of 4 bits/s/Hz with the use of 2 dB, 2.5 dB, 3 dB and 3 dB less SNR when compared to the EPA for  $v_d = 0$  units, 0.1 units, 0.2 units and 0.3 units respectively. Also from Figure 3-6, one can see that the proposed ROFPA policy provides a sum rate performance improvement over EPA up to 67.78% when  $v_r = 0.2$  units. And, ROFPA achieves sum rate of 2 bits/s/Hz and 4 bits/s/Hz with the use of approximately 2 dB less SNR.

Lastly, to show fairness of ROFPA in terms of rates of users we give achievable rate of users as a function of SNR in Figure 3-7. This figure shows that when relay is at its nominal position each user have same achievable rate with ROFPA (EPA). On the other hand, when  $v_r = 0.2$  units, with ROFPA users achieve exactly same achievable rates (which is a constraint of the optimization problem proposed in this chapter) but with EPA this equality is broken in favor of  $S_1$ . Specifically, with EPA  $S_1$  has 45.56% achievable rate superiority over  $S_2$  on the average which shows that EPA is unfair to  $S_2$ .

These results suggest that ROFPA not only improves the average BER performance of the CFNC- RAC channel or provides a great deal of SNR gains to achieve a targeted average BER but also has an adaptation with respect to the network geometry to achieve the user fairness when allocating user powers when compared to the EPA method.

Table 3-1. The optimal user and relay powers obtained by ROFPA policy for various locations of relay

$v_d = 0$			$v_d = 0.1$			$v_d = 0.2$			$v_d = 0.3$		
$P_1$	$P_2$	$\alpha$	$P_1$	$P_2$	$\alpha$	$P_1$	$P_2$	$\alpha$	$P_1$	$P_2$	$\alpha$
0.80	0.80	0.24	0.91	0.91	0.09	0.97	0.97	0.03	0.99	0.99	0.01

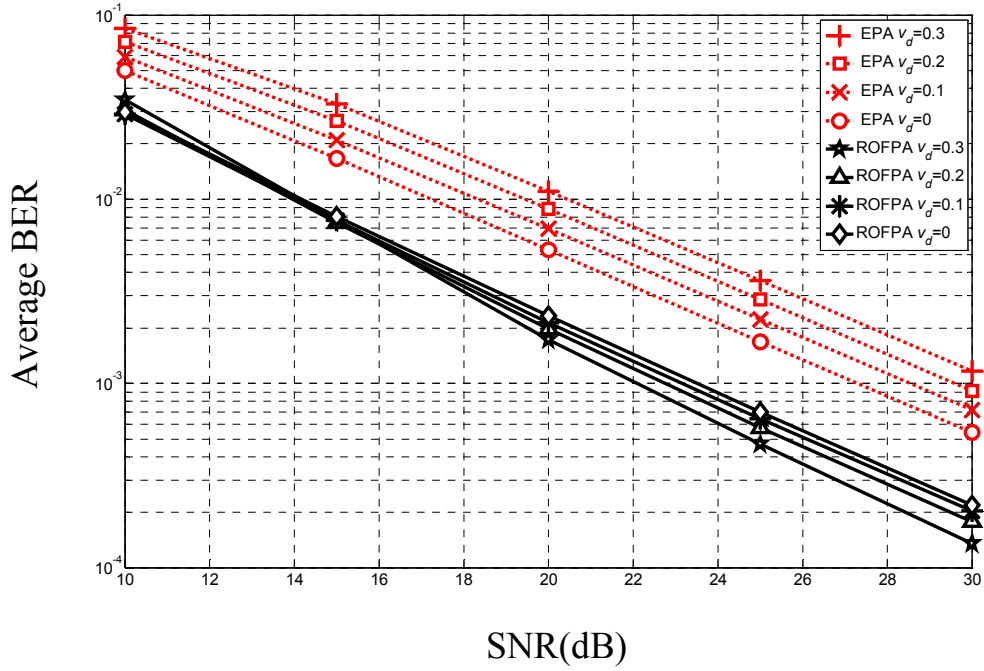


Figure 3-2. Average BER as a function of SNR of ROFPA and EPA method for various location of relay

Table 3-2 The optimal user and relay powers obtained by ROFPA for various location of relay

$v_l = 0$			$v_l = 0.2$		
$P_1$	$P_2$	$\alpha$	$P_1$	$P_2$	$\alpha$
0.80	0.80	0.24	0.60	0.94	0.29

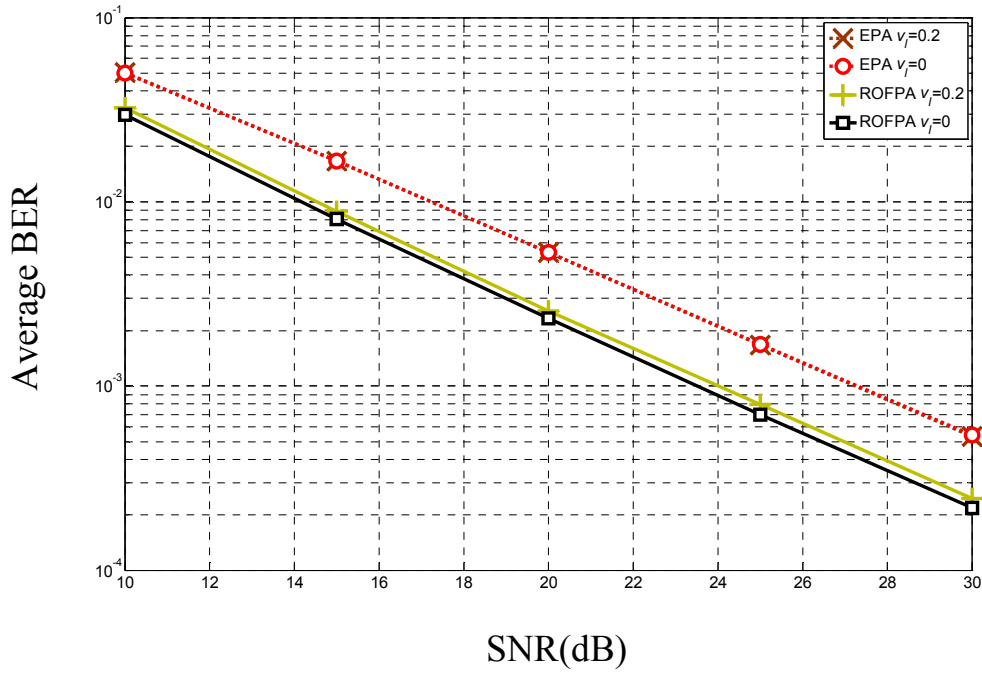


Figure 3-3. Average BER as a function of SNR of the proposed power optimization methods for cases  $g_1=5.57$  dB,  $g_2=1.70$  dB  $g_r=6.43$  dB and  $g_1=3.60$  dB,  $g_2=3.60$  dB  $g_r=7.27$  dB

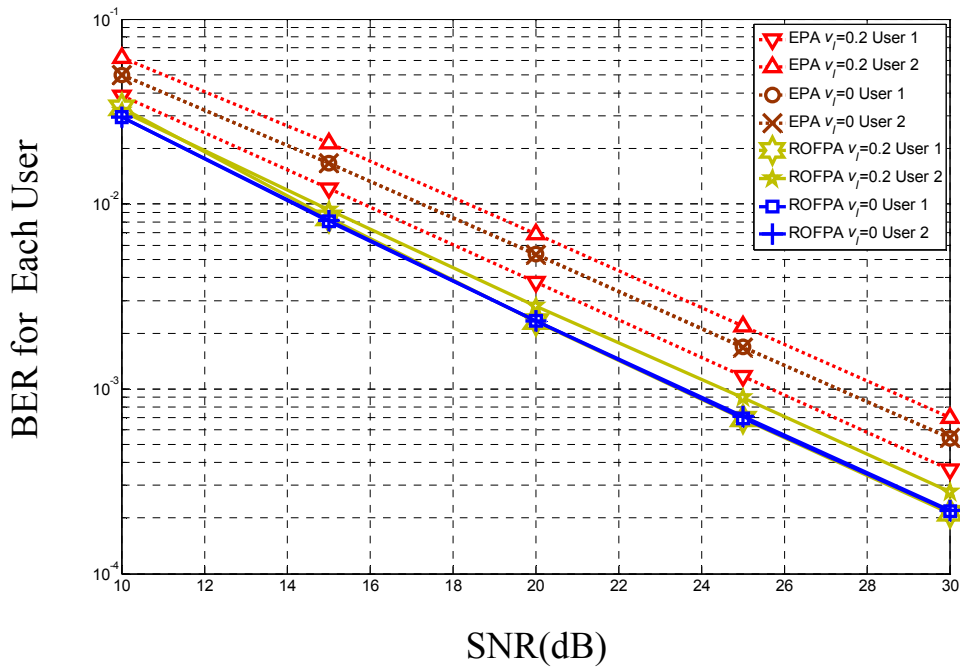


Figure 3-4. BER of each user for cases  $g_1=5.57$  dB,  $g_2=1.70$  dB  $g_r=6.43$  dB and  $g_1=3.60$  dB,  $g_2=3.60$  dB  $g_r=7.27$  dB

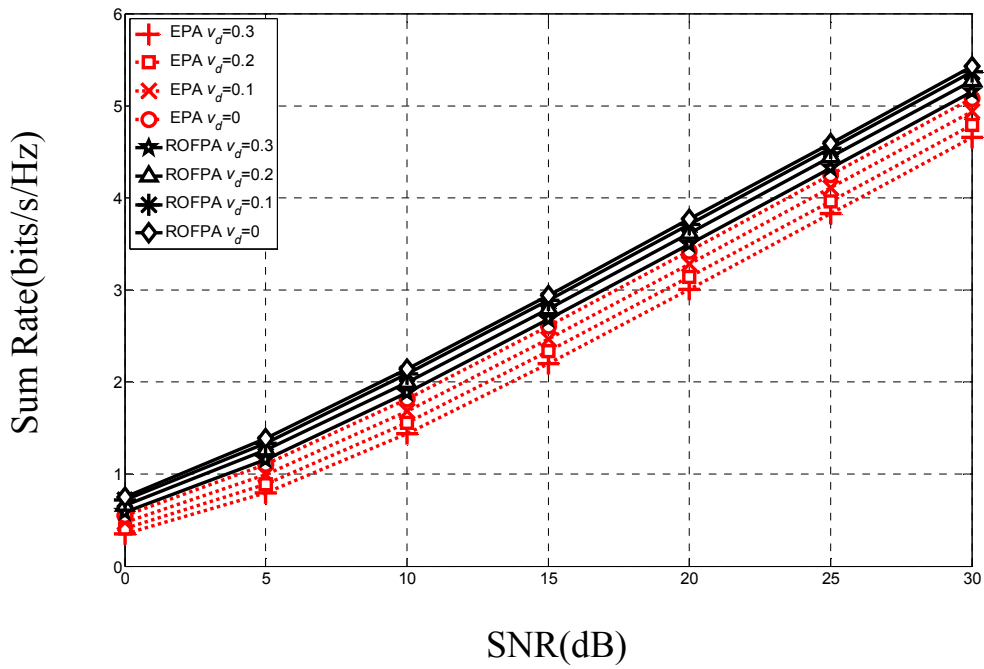


Figure 3-5. Sum rate as a function of SNR of ROFPA and EPA method for various location of relay

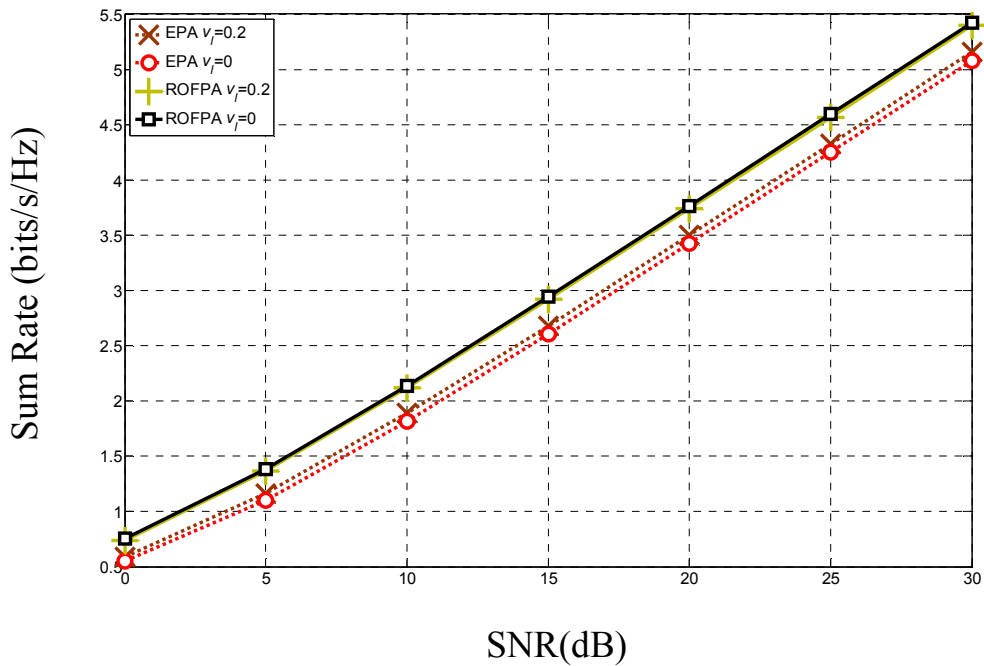


Figure 3-6. Sum rate as a function of SNR of the proposed power optimization methods for cases  $g_1= 5.57$  dB,  $g_2= 1.70$  dB  $g_r= 6.43$  dB and  $g_1= 3.60$  dB,  $g_2= 3.60$  dB  $g_r= 7.27$  dB

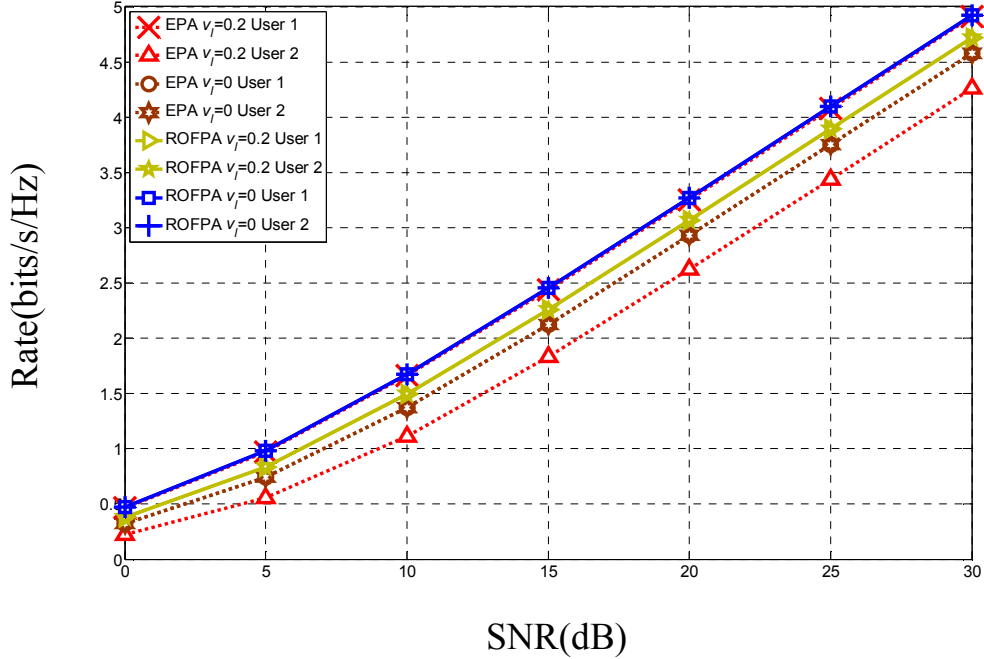


Figure 3-7. Rate of each user as a function of SNR of the proposed power optimization methods for cases  $g_1= 5.57$  dB,  $g_2= 1.70$  dB  $g_r= 6.43$  dB and  $g_1= 3.60$  dB,  $g_2= 3.60$  dB  $g_r= 7.27$  dB

### 3.4 Conclusions

In this chapter, we investigated the power allocation problem for CFNC coded relay assisted communication (CFNC-RAC) channel under the decode and forward type of relaying. While considering the user fairness in terms of the achievable information rates on the average, we proposed the rate-optimal fair power adaptation (ROFPA) method, which maximizes the sum-rate of users and also ensures the rate-fairness under the total transmit power constraint. We expressed ROFPA as a constraint optimization problem, which is a non-convex and non-linear program. Since the analytical solution to this non-convex program is not directly possible, we divided the parameter space into four disjoint regions, over which we derived an exact analytical solution by neglecting the cross-term in the objective function. The optimal power values in

ROFPA policy were determined over the segment, which resulted in the largest achievable sum-rate among all segments. Simulation results suggest that ROFPA can provide an sum rate improvement up to 66.19% while achieving an average BER improvement up to 86.00% with a very high average fairness metric when compared to EPA, and thus, it is a promising technique, which can be used in a high throughput next generation (CFNC-RAC) channel.

## 4. Symbol-Error Rate Optimized Complex Field Network Coding for Relay Assisted Communication Channels

In the previous chapter, we derived achievable rate bound of multi-access relay assisted channel which operates over non-orthogonal channels and then we propose a power allocation method for obtaining power values of source nodes and relay node which maximizes derived achievable rate bound. In this chapter, we study another performance metric: symbol error rate (SER) upper bound. Especially, in this chapter we propose an approach to obtain signatures for each source to minimize the SER bound metric when relay power is constant.

It should be noted that our approach can be seen as jointly optimizing signal constellation and power where the PNC for multiple access relay channel is employed. In the context of constellation optimization, Akino *et. al.* [71] proposed a method for the two-way relay channel where users employ the same QPSK modulation, and the modulation constellation and network coding under the denoise and forward relaying are optimized at the relay based on instantaneous channel state information (CSI) of users. Zaidi *et.al.* [72] considered an orthogonal additive white Gaussian noise (AWGN) multiple access relay channel employing PNC and then optimized the PNC by controlling the power of each user to maximize the achievable sum rate under the average power constraint of relay node, which was solved by a fixed point iteration method. Recently, Wang *et. al.* [73] considered a special communication scenario in which each destination node receives only the information of a single user in the first time slot while the PNC coded signal from the relay node is observed at all destination nodes in the second time slot. They developed a power control scheme to maximize the rate bound of each user under the peak power constraint by assuming that the complete CSI of communicating nodes is known at all nodes (i.e., transmitter CSI and receiver CSI are available). Compared to the previously mentioned studies, our work is completely different in many ways. Firstly, the receiving nodes (i.e., the relay node or the destination node) are assumed to solely know the CSI in our work

whereas the transmitting nodes do not have such knowledge. Secondly, we jointly optimize the signal constellation and power based on the average symbol-error probability bound, and this optimization results in different constellations for each user. Finally, in the channel model considered (also in [20]), both the relay and destination node observe the superposed signal in both time slots, and thus, it has completely different signal and symbol-error characteristics compared to [71]-[73] .

In this chapter, we give the system model for a basic CFNC coded relay channel. In Section 4.1. Then, the SER-optimized CFNC is developed in Section 4.2. Next, the approximate solution for the SER-optimized CFNC is derived in Section 4.3. Section 4.4 is devoted to present the average BER simulation results of the optimized CFNC. Finally, our major conclusions are included in Section 4.5.

## 4.1 A Basic Complex Field Network Coded Relay Channel Model

In this work, we consider a basic relay channel, as depicted in Figure 4-1, where there are two users  $S_1$  and  $S_2$ , one relay node  $R$  and one destination node  $D$ . In order to facilitate the CFNC, different signatures (denoted by  $\theta_1$  and  $\theta_2$  ) are assigned to user  $S_1$  and user  $S_2$  , respectively, and each user multiplies its information bearing signal (denoted as  $x_{s_1}[n]$  and  $x_{s_2}[n]$  respectively for the user  $S_1$  and user  $S_2$ ) by the associated signature. Then, the resultant signals are simultaneously sent in time slot 1 over non-orthogonal a channel, which causes multiuser interference both at the relay and at the destination. After employing ML detection, the relay node sends its CFNC code estimate to the destination node in time slot 2. In this figure, the path-loss coefficients of  $S_1$ -to- $D$  ,  $S_2$ -to- $D$  ,  $S_1$ -to- $R$  ,  $S_2$ -to- $R$  and  $R$ -to- $D$  links are represented by  $\gamma_1, \gamma_2$  ,  $g_1, g_2$  and  $g_r$  , respectively. Under the flat-fading wireless communications, the received signals at relay node and destination node in time slot 1 (represented by  $y_r[n]$  and  $y_{sd}[n]$  respectively) and the signal acquired by the destination due to the relaying in time slot 2 (denoted by  $y_{rd}[n]$  ) can be expressed as :

$$y_r[n] = \sqrt{g_1} h_{s_1r} \theta_1 x_{s_1}[n] + \sqrt{g_2} h_{s_2r} \theta_2 x_{s_2}[n] + z_r[n] \quad (4.1)$$

$$y_{sd}[n] = \sqrt{\gamma_1} h_{s_1d} \theta_1 x_{s_1}[n] + \sqrt{\gamma_2} h_{s_2d} \theta_2 x_{s_2}[n] + z_d[n] \quad (4.2)$$

$$y_{rd}[n] = \sqrt{g_r} h_{rd} x_r[n] + z_d[n] \quad (4.3)$$

where  $h_{s_1r}$ ,  $h_{s_2r}$ ,  $h_{s_1d}$ ,  $h_{s_2d}$  and  $h_{rd}$  are fading coefficient for  $S_1$ - $R$ ,  $S_2$ - $R$ ,  $S_1$ - $D$ ,  $S_2$ - $D$ ,  $R$ - $D$  links, respectively, which are modeled as complex Gaussian random variables with zero mean and unit variance, while  $z_r[n]$  and  $z_d[n]$  represent the noise at the relay node and destination node, respectively, which are modeled as additive white Gaussian noise (AWGN) with zero mean and variance of  $N_0/2$  per dimension.

It is assumed that the channel state information (CSI) of the users is known at both the relay node and the destination node (i.e., receiver CSI). To reduce the decoding complexity at the relay node, we employ only the ML estimation [20], in which the user messages are estimated as :

$$(\hat{x}_{s_1}[n], \hat{x}_{s_2}[n]) = \arg \min_{x_{s_1}[n], x_{s_2}[n]} \left\| y_r[n] - \sqrt{g_1} h_{s_1r} \theta_1 x_{s_1}[n] - \sqrt{g_2} h_{s_2r} \theta_2 x_{s_2}[n] \right\|^2 \quad (4.4)$$

Then, combining the ML estimates of user messages with the associated signatures, the relay signal is generated as:

$$x_r[n] = \theta_1 \hat{x}_{s_1}[n] + \theta_2 \hat{x}_{s_2}[n] \quad (4.5)$$

Next, the relay signal,  $x_r[n]$ , is forwarded to the destination according to Eq.(4.3) in time slot 2.

Finally, the destination node decodes the user messages jointly by using ML detection.

$$\begin{aligned} (\hat{x}_{s_1}[n], \hat{x}_{s_2}[n]) = \arg \min_{x_{s_1}[n], x_{s_2}[n]} & \left\| y_{sd}[n] - \sqrt{\gamma_1} h_{s_1d} \theta_1 x_{s_1}[n] - \sqrt{\gamma_2} h_{s_2d} \theta_2 x_{s_2}[n] \right\|^2 \\ & + \left\| y_{rd}[n] - \sqrt{g_r} h_{rd} (\theta_1 x_{s_1}[n] + \theta_2 x_{s_2}[n]) \right\|^2 \end{aligned} \quad (4.6)$$

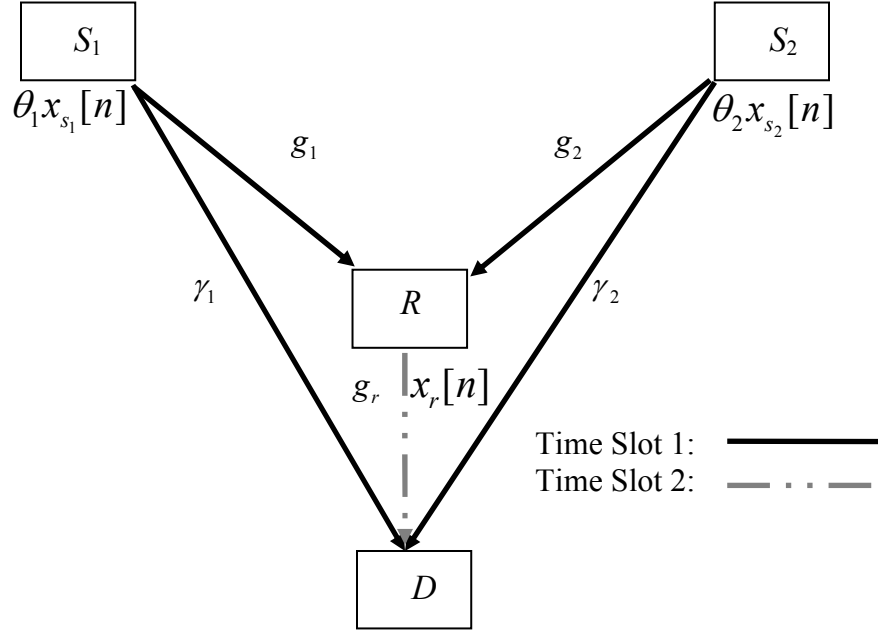


Figure 4-1 A basic complex field network coded relay channel with two users and one relay node.

## 4.2 Determination of SER-Optimized User-Signatures

According to [20], the CFNC coded signal refers to  $c[n] = \theta_1 x_{s_1}[n] + \theta_2 x_{s_2}[n]$  and the information of each user can be recovered uniquely from  $c[n]$  as long as  $\theta_1 \neq \theta_2$ . Thus, the user-signatures are important in order to extract the data of each user from the coded signal. As mentioned earlier, the user signatures in [20] are selected without considering detection performance of the relay network. To address that, we propose to obtain the optimal user-signatures by minimizing the ML bound on the SER of the network in this section. We assume that the information of each user is binary and is modulated using Binary Phase Shift Keying (BPSK), in which -1 and 1 represent the logical zero and logical one, respectively. The derived expressions can be straightforwardly extended to other types of modulations as well.

We denote the user signatures by  $\boldsymbol{\theta} = [\theta_1, \theta_2]^T$  and the vector of user-symbols by  $\mathbf{x} = [x_{s_1}[n], x_{s_2}[n]]^T$ . Since the information of each user is binary, there are four possible user

symbol vectors, which can be put in an ordered list. Let  $\mathbf{x}_i$  be the  $i^{\text{th}}$  possible symbol vector in the list for  $1 \leq i \leq 4$ . Since each signature is assigned uniquely to a specific user,  $c[n]$  takes one of four distinct values (i.e., CFNC symbols). The CFNC symbol regarding the symbol vector  $\mathbf{x}_i$  becomes

$$c_i = \boldsymbol{\theta}^T \mathbf{x}_i \quad (4.7)$$

Assuming CSI is known at the relay and ML relaying is used, an upper bound for the pair-wise symbol error probability at destination can be obtained by the use of  $y_{sd}[n]$  and  $y_{rd}[n]$  as follows.

First of all, pair-wise error probability (PEP) at the destination can be expressed as

$$P(c_i \rightarrow c_j \text{ at D} | c_i) = P(c_i \rightarrow c_i \text{ at R} | c_i) \times P(c_i \rightarrow c_j \text{ at D} | c_i \rightarrow c_i \text{ at R}, c_i) + P(c_i \rightarrow c_j \text{ at R} | c_i) \times (1 - P(c_i \rightarrow c_i \text{ at D} | c_i \rightarrow c_j \text{ at R}, c_i)) \quad (4.8)$$

where  $P(c_i \rightarrow c_i \text{ at R} | c_i)$  and  $P(c_i \rightarrow c_j \text{ at R} | c_i)$  denote the probability of correct decoding probability and PEP at the relay respectively when CFNC symbol  $c_i$  is sent. Also,  $P(c_i \rightarrow c_j \text{ at D} | c_i \rightarrow c_i \text{ at R}, c_i)$  represents the PEP at the destination given that  $c_i$  is sent and the decision of the relay is correct, whereas  $P(c_i \rightarrow c_i \text{ at D} | c_i \rightarrow c_j \text{ at R}, c_i)$  is the probability of making correct decision of the destination when  $c_i$  is sent and the relay reaches an erroneous decision.

The PEP of the relay (by assuming that CSI is known at the relay and ML relaying is used) becomes

$$\begin{aligned}
P(c_i \rightarrow c_j \text{ at R} \mid c_i, h_{s_1r}, h_{s_2r}) &= P\left( \left| \sum_{k=1}^2 \sqrt{g_k} h_{s_kr} \theta_k(\mathbf{x}_i)_k + z_r - \sum_{k=1}^2 \sqrt{g_k} h_{s_kr} \theta_k(\mathbf{x}_i)_k \right|^2 \geq \right. \\
&\quad \left. \left| \sum_{k=1}^2 \sqrt{g_k} h_{s_kr} \theta_k(\mathbf{x}_i)_k + z_r - \sum_{k=1}^2 \sqrt{g_k} h_{s_kr} \theta_k(\mathbf{x}_j)_k \right|^2 \right) \\
&= P\left( |z_r|^2 \geq \left| \sum_{k=1}^2 \sqrt{g_k} h_{s_kr} \theta_k(\mathbf{x}_i)_k + z_r - \sum_{k=1}^2 \sqrt{g_k} h_{s_kr} \theta_k(\mathbf{x}_j)_k \right|^2 \right) \\
&= P\left( - \left| \sum_{k=1}^2 \sqrt{g_k} h_{s_kr} \theta_k d_{ijk} \right|^2 \geq z_r^* \left( \sum_{k=1}^2 \sqrt{g_k} h_{s_kr} \theta_k d_{ijk} \right) + z_r \left( \sum_{k=1}^2 \sqrt{g_k} h_{s_kr} \theta_k d_{ijk} \right)^* \right)
\end{aligned} \tag{4.9}$$

where “\*” denotes the complex conjugation and the random variable

$z_r^* \left( \sum_{k=1}^2 \sqrt{g_k} h_{s_kr} \theta_k d_{ijk} \right) + z_r \left( \sum_{k=1}^2 \sqrt{g_k} h_{s_kr} \theta_k d_{ijk} \right)^*$  is Gaussian distributed with zero mean and variance

of  $4\sigma^2 \left| \sum_{k=1}^2 \sqrt{g_k} h_{s_kr} \theta_k d_{ijk} \right|^2$ . Therefore, the PEP in Eq. (4.9) can be found as

$$P(c_i \rightarrow c_j \text{ at R} \mid c_i, h_{s_1r}, h_{s_2r}) = Q\left( \frac{\left| \sum_{k=1}^2 \sqrt{g_k} h_{s_kr} \theta_k d_{ijk} \right|}{2\sigma} \right) \tag{4.10}$$

where  $d_{ijk}$  represents the  $k^{\text{th}}$  component of the difference vector between the  $i^{\text{th}}$  and  $j^{\text{th}}$  symbol vectors,  $\mathbf{d}_{ij} = (\mathbf{x}_i - \mathbf{x}_j)$ . This probability can be upper bounded using the Chernoff-bound as follows:

$$P(c_i \rightarrow c_j \text{ at R} \mid c_i, h_{s_1r}, h_{s_2r}) \leq \frac{1}{2} e^{-\frac{\left| \sum_{k=1}^2 \sqrt{g_k} h_{s_kr} \theta_k d_{ijk} \right|^2}{8\sigma^2}} \tag{4.11}$$

Consequently, a bound on the average PEP can be obtained by averaging the upper-bound in Eq. (4.11) over fading gains of the users-to-relay links as:

$$P(c_i \rightarrow c_j \text{ at R} \mid c_i, h_{s_1r}, h_{s_2r}) \leq E_{\mathbf{h}_{sr}} \left[ e^{-\frac{\left| \sum_{k=1}^2 \sqrt{g_k} h_{s_kr} \theta_k d_{ijk} \right|^2}{8\sigma^2}} \right] \tag{4.12}$$

$E_{\mathbf{h}_{sr}}[\cdot]$  represents the expectation operation with respect to the CSI vector  $\mathbf{h}_{sr}$ . Each fading coefficient  $h_{s_kr}$  is assumed to be a zero-mean complex Gaussian random variable with unit

variance, which is denoted by  $CN(0,1)$ . Hence, the distribution of random variable

$\sum_{k=1}^2 \sqrt{g_k} h_{s_k r} \theta_k d_{ijk}$  is  $CN\left(0, \sum_{k=1}^2 g_k |\theta_k|^2 d_{ijk}^2\right)$ , and the pdf of  $\left|\sum_{k=1}^2 \sqrt{g_k} h_{s_k r} \theta_k d_{ijk}\right|^2$  becomes

exponential with the mean of  $\sum_{k=1}^2 g_k |\theta_k|^2 d_{ijk}^2$ . Hence, the expectation term in Eq.(4.12) can be

deduced as:

$$\begin{aligned}
P(c_i \rightarrow c_j \text{ at R} | c_i) &\leq \int_0^\infty \frac{1}{2} e^{-\frac{t}{8\sigma^2}} \frac{1}{\sum_{k=1}^2 g_k |\theta_k|^2 d_{ijk}^2} e^{-\frac{t}{\sum_{k=1}^2 g_k |\theta_k|^2 d_{ijk}^2}} dt \\
&\leq \frac{0.5}{\left(1 + \frac{\sum_{k=1}^2 g_k |\theta_k|^2 d_{ijk}^2}{8\sigma^2}\right)} \tag{4.13}
\end{aligned}$$

Similar to Eq. (4.9), the PEP at the destination with complete CSI can be calculated, when it employs ML detection and the decoding of the relay is correct, as:

$$\begin{aligned}
P(c_i \rightarrow c_j \text{ at D} | c_i \rightarrow c_i \text{ at R}, c_i, \mathbf{h}_{sd}, h_{rd}) &= P\left(\left|\sum_{k=1}^2 \sqrt{\gamma_k} h_{s_k d} \theta_k (\mathbf{x}_i)_k + z_d - \sum_{k=1}^2 \sqrt{\gamma_k} h_{s_k d} \theta_k (\mathbf{x}_i)_k\right|^2\right. \\
&\quad \left. + \left|\sqrt{g_r} h_{rd} \sum_{k=1}^2 \theta_k (\mathbf{x}_i)_k + z_d - h_{rd} \sum_{k=1}^2 \theta_k (\mathbf{x}_i)_k\right|^2\right) \\
&\geq P\left(\left|\sum_{k=1}^2 \sqrt{\gamma_k} h_{s_k d} \theta_k (\mathbf{x}_i)_k + z_d - \sum_{k=1}^2 \sqrt{\gamma_k} h_{s_k d} \theta_k (\mathbf{x}_j)_k\right|^2\right. \\
&\quad \left. + \left|\sqrt{g_r} h_{rd} \sum_{k=1}^2 \theta_k (\mathbf{x}_i)_k + z_d - h_{rd} \sum_{k=1}^2 \theta_k (\mathbf{x}_j)_k\right|^2\right) \\
&= P(|z_d|^2 + |z_d|^2 \geq \left|\sum_{k=1}^2 \sqrt{\gamma_k} h_{s_k d} \theta_k d_{ijk} + z_d\right|^2 + \left|\sqrt{g_r} h_{rd} \sum_{k=1}^2 \theta_k d_{ijk} + z_d\right|^2) \\
&= P\left(-\left|\sum_{k=1}^2 \sqrt{\gamma_k} h_{s_k d} \theta_k d_{ijk}\right|^2 - \left|\sqrt{g_r} h_{rd} \sum_{k=1}^2 \theta_k d_{ijk}\right|^2 \geq\right. \\
&\quad \left.2\text{Re}\{z_d^* \sum_{k=1}^2 \sqrt{\gamma_k} h_{s_k d} \theta_k d_{ijk}\} + 2\text{Re}\{z_d^* \sqrt{g_r} h_{rd} \sum_{k=1}^2 \theta_k d_{ijk}\}\right) \tag{4.14}
\end{aligned}$$

Since  $z_d$  is assumed to be  $CN(0, 2\sigma^2)$ , the random

variable  $2\text{Re}\{z_d^* \sum_{k=1}^2 \sqrt{\gamma_k} h_{s_k d} \theta_k d_{ijk}\} + 2\text{Re}\{z_d^* \sqrt{g_r} h_{rd} \sum_{k=1}^2 \theta_k d_{ijk}\}$  is Gaussian with mean of zero and

variance of  $4\sigma^2 \left( \left| \sum_{k=1}^2 \sqrt{\gamma_k} h_{s_k d} \theta_k d_{ijk} \right|^2 + \left| \sqrt{g_r} h_{rd} \sum_{k=1}^2 \theta_k d_{ijk} \right|^2 \right)$ . Hence, the PEP in Eq. (4.14) can be

determined as

$$P(c_i \rightarrow c_j \text{ at D} | c_i \rightarrow c_i \text{ at R}, c_i, \mathbf{h}_{sd}, h_{rd}) = Q\left(\frac{\sqrt{\left| \sum_{k=1}^N \sqrt{\gamma_k} h_{s_k d} \theta_k d_{ijk} \right|^2 + \left| \sqrt{g_r} h_{rd} \sum_{k=1}^N \theta_k d_{ijk} \right|^2}}{2\sigma}\right) \quad (4.15)$$

which is upper bounded by

$$P(c_i \rightarrow c_j \text{ at D} | c_i \rightarrow c_i \text{ at R}, c_i, \mathbf{h}_{sd}, h_{rd}) \leq \frac{1}{2} e^{-\frac{\left| \sum_{k=1}^N \sqrt{\gamma_k} h_{s_k d} \theta_k d_{ijk} \right|^2 + \left| \sqrt{g_r} h_{rd} \sum_{k=1}^N \theta_k d_{ijk} \right|^2}{8\sigma^2}} \quad (4.16)$$

Again, a bound on the average PEP at the destination can be obtained by averaging the upper-bound in Eq.(4.16) over the fading coefficients  $h_{s_k d}, h_{rd}$ . Since fading coefficients are zero-mean

complex Gaussian random variables with unit variance,  $\left| \sum_{k=1}^N \sqrt{\gamma_k} h_{s_k d} \theta_k d_{ijk} \right|^2$  and

$\left| \sqrt{g_r} h_{rd} \sum_{k=1}^N \theta_k d_{ijk} \right|^2$  are exponential random variables with a mean of  $\lambda_1 = \sum_{k=1}^N \gamma_k |\theta_k|^2 d_{ijk}^2$  and

$\lambda_2 = g_r \sum_{k=1}^N |\theta_k|^2 d_{ijk}^2$ , respectively. So, the bound on the average PEP at the destination can be

obtained as:

$$\begin{aligned} P(c_i \rightarrow c_j \text{ at D} | c_i \rightarrow c_i \text{ at R}, c_i) &\leq \int_0^\infty \int_0^\infty 0.5 \exp\left(-\frac{t_1 + t_2}{8\sigma^2}\right) \frac{\exp\left(-\frac{t_1}{\lambda_1}\right)}{\lambda_1} \frac{\exp\left(-\frac{t_2}{\lambda_2}\right)}{\lambda_2} dt_1 dt_2 \\ &\leq \frac{0.5}{\left(1 + \frac{\sum_{k=1}^N \gamma_k |\theta_k|^2 d_{ijk}^2}{8\sigma^2}\right) \left(1 + \frac{\left| \sum_{k=1}^N \theta_k d_{ijk} \right|^2}{8\sigma^2}\right)} \end{aligned} \quad (4.17)$$

A similar analysis can be conducted to determine  $P(c_i \rightarrow c_i \text{ at D} | c_i \rightarrow c_i \text{ at R}, c_i)$ . Toward that

goal, we need to determine first,  $P(c_i \rightarrow c_j \text{ at D} | c_i \rightarrow c_i \text{ at R}, c_i)$  as :

$$\begin{aligned}
P(c_i \rightarrow c_i \text{ at D} | c_i \rightarrow c_i \text{ at R}, c_i, \mathbf{h}_{sd}, h_{rd}) &= P\left( \left| \sum_{k=1}^2 \sqrt{\gamma_k} h_{s_k d} \theta_k(\mathbf{x}_i)_k + z_d - \sum_{k=1}^2 \sqrt{\gamma_k} h_{s_k d} \theta_k(\mathbf{x}_i)_k \right|^2 \right. \\
&\quad \left. + \left| \sqrt{g_r} h_{rd} \sum_{k=1}^2 \theta_k(\mathbf{x}_i)_k + z_d - h_{rd} \sum_{k=1}^2 \theta_k(\mathbf{x}_i)_k \right|^2 \right) \\
&\leq \left| \sum_{k=1}^2 \sqrt{\gamma_k} h_{s_k d} \theta_k(\mathbf{x}_i)_k + z_d - \sum_{k=1}^2 \sqrt{\gamma_k} h_{s_k d} \theta_k(\mathbf{x}_j)_k \right|^2 \\
&\quad + \left| \sqrt{g_r} h_{rd} \sum_{k=1}^2 \theta_k(\mathbf{x}_i)_k + z_d - h_{rd} \sum_{k=1}^2 \theta_k(\mathbf{x}_j)_k \right|^2 \\
&= P(|z_d|^2 + |z_d|^2 \geq \left| \sum_{k=1}^2 \sqrt{\gamma_k} h_{s_k d} \theta_k d_{ijk} + z_d \right|^2 + \left| \sqrt{g_r} h_{rd} \sum_{k=1}^2 \theta_k d_{ijk} + z_d \right|^2) \\
&= P\left( - \left| \sum_{k=1}^2 \sqrt{\gamma_k} h_{s_k d} \theta_k d_{ijk} \right|^2 + \left| \sqrt{g_r} h_{rd} \sum_{k=1}^2 \theta_k d_{ijk} \right|^2 \geq \right. \\
&\quad \left. 2 \operatorname{Re}\{z_d^* \sum_{k=1}^2 \sqrt{\gamma_k} h_{s_k d} \theta_k d_{ijk}\} + 2 \operatorname{Re}\{z_d^* \sqrt{g_r} h_{rd} \sum_{k=1}^2 \theta_k d_{ijk}\} \right) \\
&= Q\left( \frac{- \left| \sum_{k=1}^2 \sqrt{\gamma_k} h_{s_k d} \theta_k d_{ijk} \right|^2 + \left| \sqrt{g_r} h_{rd} \sum_{k=1}^2 \theta_k d_{ijk} \right|^2}{2\sigma \sqrt{\left| \sum_{k=1}^2 \sqrt{\gamma_k} h_{s_k d} \theta_k d_{ijk} \right|^2 + \left| \sqrt{g_r} h_{rd} \sum_{k=1}^2 \theta_k d_{ijk} \right|^2}} \right)
\end{aligned} \tag{4.18}$$

In order to obtain a bound on the SER bound, we need to average Eq. (4.18) over CSI coefficients, which cannot be calculated analytically. For simplicity, we bound the fourth term in Eq. (4.8) as :

$$1 - P(c_i \rightarrow c_i \text{ at D} | c_i \rightarrow c_j \text{ at R}, c_i) \leq 1 \tag{4.19}$$

In parallel lines, the first term in Eq.(4.8) is also bounded as:

$$P(c_i \rightarrow c_i \text{ at R} | c_i) \leq 1 \tag{4.20}$$

Therefore, the upper bound for PEP at the destination in Eq.(4.8) can be re-written by combining Eq.(4.13),(4.17) ,(4.19) and (4.20) as:

$$P(c_i \rightarrow c_j \text{ at D} | c_i) \leq \frac{0.5}{1 + \frac{\sum_{k=1}^2 \gamma_k |\theta_k|^2 d_{ijk}^2}{8\sigma^2}} \frac{1}{1 + \frac{\sum_{k=1}^2 \theta_k d_{ijk}}{8\sigma^2}} + \frac{0.5}{1 + \frac{\sum_{k=1}^2 g_k |\theta_k|^2 d_{ijk}^2}{8\sigma^2}} \quad (4.21)$$

As a result, the upper bound for SEP ( $\bar{P}_e^D$ ) at the destination can be given as:

$$\bar{P}_e^D \leq \frac{1}{8} \sum_{i=1}^4 \sum_{\substack{j=1 \\ j \neq i}}^4 \frac{1}{1 + \frac{\sum_{k=1}^2 \gamma_k |\theta_k|^2 d_{ijk}^2}{8\sigma^2}} \frac{1}{1 + \frac{\sum_{k=1}^2 \theta_k d_{ijk}}{8\sigma^2}} + \frac{1}{1 + \frac{\sum_{k=1}^2 g_k |\theta_k|^2 d_{ijk}^2}{8\sigma^2}} \quad (4.22)$$

By expressing the signature  $\theta_k$  in the polar form as  $\theta_k = \sqrt{P_k} e^{j\phi_k}$ , Eq. (4.22) can be re-written

as:

$$\begin{aligned} \bar{P}_e^D &\leq \frac{1}{8} \sum_{i=1}^4 \sum_{\substack{j=1 \\ j \neq i}}^4 \frac{1}{1 + \frac{\sum_{k=1}^2 \gamma_k P_k d_{ijk}^2}{8\sigma^2}} \frac{1}{1 + \frac{\sum_{k=1}^2 \sqrt{P_k} e^{j\phi_k} d_{ijk}}{8\sigma^2}} + \frac{1}{1 + \frac{\sum_{k=1}^2 g_k P_k d_{ijk}^2}{8\sigma^2}} \\ &= \frac{1}{8} \sum_{i=1}^4 \sum_{\substack{j=1 \\ j \neq i}}^4 \frac{1}{1 + \frac{\sum_{k=1}^2 \gamma_k P_k d_{ijk}^2}{8\sigma^2}} \frac{1}{1 + \frac{g_r (P_1 d_{ij1}^2 + P_2 d_{ij2}^2 + 2\sqrt{P_1} d_{ij1} \sqrt{P_2} d_{ij2} \cos(\phi_1 - \phi_2))}{8\sigma^2}} + \frac{1}{1 + \frac{\sum_{k=1}^2 g_k P_k d_{ijk}^2}{8\sigma^2}} \end{aligned} \quad (4.23)$$

where  $\bar{P}_e^D$  is the average SER at the destination. It is important to note that the average SER-bound in Eq.(4.23) is a function of signature powers  $P_1$  and  $P_2$ , the cosine of the signatures' phase difference  $\delta \equiv \cos(\phi_1 - \phi_2)$ . In order to determine the SER-optimized signatures, both  $P_k$  and  $\phi_k$  need to be optimally decided to achieve the minimum SER-bound of the destination under the

total transmit-power constraint  $\sum_{k=1}^2 P_k = P_T$ . Additionally, since each user actively sends

information,  $P_1$  and  $P_2$  should be strictly greater than zero, and because of the cosine function, there is a box constraint on  $\delta$ , which can be expressed as  $-1 \leq \delta \leq 1$ . Therefore, the determination of SER-optimized signatures can be stated as a constrained optimization problem

as:

$$\begin{aligned} \underset{P_1, P_2, \delta}{\text{minimize}} f_0(P_1, P_2, \delta) &= \frac{1}{8} \sum_{i=1}^4 \sum_{\substack{j=1 \\ j \neq i}}^4 \frac{1}{1 + \frac{\sum_{k=1}^2 \gamma_k P_k d_{ijk}^2}{8\sigma^2}} \frac{1}{1 + \frac{g_r(P_1 d_{ij1}^2 + P_2 d_{ij2}^2 + 2\sqrt{P_1} d_{ij1} \sqrt{P_2} d_{ij2} \delta)}{8\sigma^2}} \\ &+ \frac{1}{1 + \frac{\sum_{k=1}^2 g_k P_k d_{ijk}^2}{8\sigma^2}} \end{aligned}$$

such that

$$\begin{aligned} f_1(P_1, P_2, \delta) &= P_T - \sum_{k=1}^2 P_k = 0 \\ f_2(P_1, P_2, \delta) &= P_1 > 0, \\ f_3(P_1, P_2, \delta) &= P_2 > 0, \\ f_4(P_1, P_2, \delta) &= \delta + 1 \geq 0, \\ f_5(P_1, P_2, \delta) &= 1 - \delta \geq 0, \end{aligned} \tag{4.24}$$

Since the objective function is convex and the constraints are affine, the optimization in Eq. (4.24) is a convex program, and its unique optimal global solution exists, which satisfies Karush-Kuhn-Tucker (KKT) conditions:

$$\begin{aligned} \nabla f_0(\mathbf{p}^*) - \sum_{i=1}^5 \lambda_i^* \nabla f_i(\mathbf{p}^*) &= \mathbf{0}, \\ f_1(\mathbf{p}^*) &= 0, \\ f_i(\mathbf{p}^*) &> 0, \text{ for } i = 2, 3 \\ f_i(\mathbf{p}^*) &\geq 0, \text{ for } i = 4, 5 \\ \lambda_i^* &\geq 0, \text{ for } i = 1, 2, 3, 4, 5 \\ \lambda_i^* f_i(\mathbf{p}^*) &= 0, \text{ for } i = 1, 2, 3, 4, 5 \end{aligned} \tag{4.25}$$

where  $\mathbf{p} = [P_1, P_2, \delta]^T$  is the vector of user signature parameters, and  $\mathbf{p}^*$  represents the corresponding optimal vector.

The KKT conditions in Eq.(4.25) result in the following equations as:

$$\begin{aligned}
& -\left(1+\frac{\gamma_1 P_1}{2\sigma^2}\right)^{-2}\left(\frac{\gamma_1}{4\sigma^2}\right)\left(1+\frac{g_r P_1}{2\sigma^2}\right)^{-1}-\left(1+\frac{\gamma_1 P_1}{2\sigma^2}\right)^{-1}\left(1+\frac{g_r P_1}{2\sigma^2}\right)^{-2}\frac{g_r}{4\sigma^2}-\left(1+\frac{g_1 P_1}{2\sigma^2}\right)^{-2}\left(\frac{g_1}{4\sigma^2}\right) \\
& -\left(1+\frac{g_1 P_1+g_2 P_2}{2\sigma^2}\right)^{-2}\left(\frac{g_1}{4\sigma^2}\right) \\
& -\left(1+\frac{\gamma_1 P_1+\gamma_2 P_2}{2\sigma^2}\right)^{-2}\left(\frac{\gamma_1}{8\sigma^2}\right)\left[\left(1+\frac{g_r(P_1+P_2+2\sqrt{P_1 P_2}\delta)}{2\sigma^2}\right)^{-1}+\left(1+\frac{g_r(P_1+P_2-2\sqrt{P_1 P_2}\delta)}{2\sigma^2}\right)^{-1}\right] \\
& -\left(1+\frac{\gamma_1 P_1+\gamma_2 P_2}{2\sigma^2}\right)^{-1} \\
& \times\left[\left(1+\frac{g_r(P_1+P_2+2\sqrt{P_1 P_2}\delta)}{2\sigma^2}\right)^{-2}\left(\frac{g_r\left(1+\frac{\sqrt{P_2}\delta}{\sqrt{P_1}}\right)}{8\sigma^2}\right)+\left(1+\frac{g_r(P_1+P_2-2\sqrt{P_1 P_2}\delta)}{2\sigma^2}\right)^{-2}\left(\frac{g_r\left(1-\frac{\sqrt{P_2}\delta}{\sqrt{P_1}}\right)}{8\sigma^2}\right)\right] \\
& -\lambda_1^*(-1)-\lambda_2^*(1)=0
\end{aligned} \tag{4.26}$$

$$\begin{aligned}
& -\left(1+\frac{\gamma_2 P_2}{2\sigma^2}\right)^{-2}\left(\frac{\gamma_2}{4\sigma^2}\right)\left(1+\frac{g_r P_2}{2\sigma^2}\right)^{-1}-\left(1+\frac{\gamma_2 P_2}{2\sigma^2}\right)^{-1}\left(1+\frac{g_r P_2}{2\sigma^2}\right)^{-2}\frac{g_r}{4\sigma^2}-\left(1+\frac{g_2 P_2}{2\sigma^2}\right)^{-2}\left(\frac{g_2}{4\sigma^2}\right) \\
& -\left(1+\frac{g_1 P_1+g_2 P_2}{2\sigma^2}\right)^{-2}\left(\frac{g_2}{4\sigma^2}\right) \\
& -\left(1+\frac{\gamma_1 P_1+\gamma_2 P_2}{2\sigma^2}\right)^{-2}\left(\frac{\gamma_2}{8\sigma^2}\right)\left[\left(1+\frac{g_r(P_1+P_2+2\sqrt{P_1 P_2}\delta)}{2\sigma^2}\right)^{-1}+\left(1+\frac{g_r(P_1+P_2-2\sqrt{P_1 P_2}\delta)}{2\sigma^2}\right)^{-1}\right] \\
& -\left(1+\frac{\gamma_1 P_1+\gamma_2 P_2}{2\sigma^2}\right)^{-1} \\
& \times\left[\left(1+\frac{g_r(P_1+P_2+2\sqrt{P_1 P_2}\delta)}{2\sigma^2}\right)^{-2}\left(\frac{g_r\left(1+\frac{\sqrt{P_1}\delta}{\sqrt{P_2}}\right)}{8\sigma^2}\right)+\left(1+\frac{g_r(P_1+P_2-2\sqrt{P_1 P_2}\delta)}{2\sigma^2}\right)^{-2}\left(\frac{g_r\left(1-\frac{\sqrt{P_1}\delta}{\sqrt{P_2}}\right)}{8\sigma^2}\right)\right] \\
& \lambda_1^*(-1)-\lambda_3^*(1)=0
\end{aligned} \tag{4.27}$$

$$\begin{aligned}
& -\left(1 + \frac{\gamma_1 P_1 + \gamma_2 P_2}{2\sigma^2}\right)^{-1} \\
& \times \left[ \left(1 + \frac{g_r (P_1 + P_2 + 2\sqrt{P_1 P_2} \delta)}{2\sigma^2}\right)^{-2} \left(\frac{g_r 2\sqrt{P_1 P_2}}{8\sigma^2}\right) + \left(1 + \frac{g_r (P_1 + P_2 - 2\sqrt{P_1 P_2} \delta)}{2\sigma^2}\right)^{-2} \left(\frac{-g_r 2\sqrt{P_1 P_2}}{8\sigma^2}\right) \right] \\
& -\lambda_4^* + \lambda_5^* = 0
\end{aligned} \tag{4.28}$$

Since  $P_1^* > 0$  and  $P_2^* > 0$ , both  $\lambda_2^*$  and  $\lambda_3^*$  become zero due to complementarity conditions. Also, because of the complementarity conditions  $\lambda_i^* f_i(\mathbf{p}^*) = 0$  for  $i=4$  and  $5$ ,  $\lambda_4^*$  and  $\lambda_5^*$  can be shown to be zero, otherwise  $\delta$  should be equal to either -1 or 1. We can prove this by contradiction. Assuming that  $\delta^*$  is -1,  $\lambda_5^*$  has to be zero due to complementarity slackness. Therefore, the following expression from Eq. (4.28) can be stated:

$$\left[ \left(1 + \frac{\gamma_1 P_1 + \gamma_2 P_2}{2\sigma^2}\right)^{-1} \left(\frac{g_r 2\sqrt{P_1 P_2}}{2\sigma^2}\right) \right] \times \left[ -\left(1 + \frac{g_r (P_1 + P_2 - 2\sqrt{P_1 P_2})}{2\sigma^2}\right)^{-2} + \left(1 + \frac{g_r (P_1 + P_2 + 2\sqrt{P_1 P_2})}{2\sigma^2}\right)^{-2} \right] = \lambda_4^* \tag{4.29}$$

Since  $\left(1 + \frac{g_r (P_1 + P_2 - 2\sqrt{P_1 P_2})}{2\sigma^2}\right)^{-2} > \left(1 + \frac{g_r (P_1 + P_2 + 2\sqrt{P_1 P_2})}{2\sigma^2}\right)^{-2}$ , the LHS of Eq. (4.29) is less than zero, which is a contradiction because  $\lambda_4^* \geq 0$ . Similarly, we can show that  $\lambda_4^*$  should be zero. Hence, by putting  $\lambda_4^* = \lambda_5^* = 0$  in Eq. (4.28), we obtain the following expression:

$$\left(1 + \frac{g_r (P_1 + P_2 + 2\sqrt{P_1 P_2} \delta)}{2\sigma^2}\right)^{-2} = \left(1 + \frac{g_r (P_1 + P_2 - 2\sqrt{P_1 P_2} \delta)}{2\sigma^2}\right)^{-2} \tag{4.30}$$

The only solution of Eq. (4.30) is  $\delta = 0$ , which implies

$$\phi_2^* - \phi_1^* = (2k + 1)\pi / 2 \text{ for any integer } k \tag{4.31}$$

Combining Eq.(4.30) with Eq.(4.26) and (4.27), the optimal powers  $P_1^*$  and  $P_2^*$  should satisfy the following expressions:

$$\begin{aligned}
& 0.5\left(1 + \frac{\gamma_1 P_1^*}{2\sigma^2}\right)^{-2} \frac{\gamma_1}{2\sigma^2} \left(1 + \frac{g_r P_1^*}{2\sigma^2}\right)^{-1} + 0.5\left(1 + \frac{\gamma_1 P_1^*}{2\sigma^2}\right)^{-1} \left(1 + \frac{g_r P_1^*}{2\sigma^2}\right)^{-2} \frac{g_r}{2\sigma^2} + \\
& 0.5\left(1 + \frac{\gamma_1 P_1^* + \gamma_2 P_2^*}{2\sigma^2}\right)^{-2} \frac{\gamma_1}{2\sigma^2} \left(1 + \frac{g_r (P_1^* + P_2^*)}{2\sigma^2}\right)^{-1} + 0.5\left(1 + \frac{g_1 P_1^*}{2\sigma^2}\right)^{-2} \frac{g_1}{2\sigma^2} + 0.5\left(1 + \frac{g_1 P_1^* + g_2 P_2^*}{2\sigma^2}\right)^{-2} \frac{g_1}{2\sigma^2} \\
& = 0.5\left(1 + \frac{\gamma_2 P_2^*}{2\sigma^2}\right)^{-2} \frac{\gamma_2}{2\sigma^2} \left(1 + \frac{g_r P_2^*}{2\sigma^2}\right)^{-1} + 0.5\left(1 + \frac{\gamma_2 P_2^*}{2\sigma^2}\right)^{-1} \left(1 + \frac{g_r P_2^*}{2\sigma^2}\right)^{-2} \frac{g_r}{2\sigma^2} + \\
& 0.5\left(1 + \frac{\gamma_1 P_1^* + \gamma_2 P_2^*}{2\sigma^2}\right)^{-2} \frac{\gamma_2}{2\sigma^2} \left(1 + \frac{g_r (P_1^* + P_2^*)}{2\sigma^2}\right)^{-1} + 0.5\left(1 + \frac{g_2 P_2^*}{2\sigma^2}\right)^{-2} \frac{g_2}{2\sigma^2} + 0.5\left(1 + \frac{g_1 P_1^* + g_2 P_2^*}{2\sigma^2}\right)^{-2} \frac{g_2}{2\sigma^2}
\end{aligned} \tag{4.32}$$

Equation (4.31) implies that phases of the user signatures should be separated by any odd multiples of  $90^\circ$ , which intuitively makes sense because it is logical to choose  $\cos(\phi_1 - \phi_2) = 1$ , whenever the product  $d_{ij1}d_{ij2}$  in Eq.(4.23) is positive, and to select  $\cos(\phi_1 - \phi_2) = -1$  otherwise. The average SER-bound is minimized by choosing  $\cos(\phi_1 - \phi_2) = 0$  since the product  $d_{ij1}d_{ij2}$  takes negative and positive values with equal frequency under the assumption of equally likely *priors* for the user decisions. This results in an increased minimum distance among CFNC symbols. For example, when BPSK is used, the minimum distance of PNC symbols becomes zero since  $x_{s_1} = 1$  and  $x_{s_2} = -1$  or  $x_{s_1} = -1$  and  $x_{s_2} = 1$  are mapped into the same symbol (i.e.,  $c_2 = c_3 = 0$ ), whereas the minimum distance of the optimized CFNC is two since the user 1 transmits symbols from the set  $\{-1, 1\}$ , and user 2 selects symbols from the set  $\{+j, -j\}$ .

In general, Eq. (4.32) is highly nonlinear, for which a closed form solution is not viable to obtain the optimal signature powers. For this purpose, we derive an approximate solution for the signature powers in the next section.

### 4.3 Determination of an Approximate Solution for the Signature Powers

The SER-optimized signature powers in Eq. (4.32) provide fairness among the users since the user powers become the same when they are located symmetrically with respect to both the relay and destination or when one of the users is positioned closer to the relay or destination, the other

user needs to consume more power in order to minimize the SER of the network. In parallel lines, we aim at devising an information theoretical power allocation scheme, which considers fairness among users and provides closed-form results. As pointed out earlier, we assume that the CSI due to the Rayleigh fading is available only at the receiver. Also, the fading gains of all communicating nodes are assumed to have unit energy for the sake of simplicity.

Since the users-to-relay channel is a multi-access channel (MAC), the achievable ergodic rates of users (denoted by  $R_1$  for user  $S_1$  and  $R_2$  for user  $S_2$ ) at the relay are upper bounded as :

$$R_1 \leq \frac{1}{2} \log \left( 1 + \frac{g_1 P_1}{2\sigma^2} \right) \quad (4.33)$$

$$R_2 \leq \frac{1}{2} \log \left( 1 + \frac{g_2 P_2}{2\sigma^2} \right) \quad (4.34)$$

$$R_1 + R_2 \leq \frac{1}{2} \log \left( 1 + \frac{g_1 P_1 + g_2 P_2}{2\sigma^2} \right) \quad (4.35)$$

By assuming perfect decoding at the relay, the signals received by the destination at both time slots (see Eqs. (4.2), (4.3), (4.5)) can be put in a matrix-vector form as

$$\underbrace{\begin{bmatrix} y_{sd}[n] \\ y_{rd}[n] \end{bmatrix}}_{\mathbf{y}} = \underbrace{\begin{bmatrix} \sqrt{\gamma_1} & \sqrt{\gamma_2} \\ \sqrt{g_r} & \sqrt{g_r} \end{bmatrix}}_{\mathbf{H}} \underbrace{\begin{bmatrix} \sqrt{P_1} x_{s_1}[n] \\ \sqrt{P_2} x_{s_2}[n] \end{bmatrix}}_{\mathbf{x}} + \underbrace{\begin{bmatrix} z_d[n] \\ z_d[n] \end{bmatrix}}_{\mathbf{z}} \quad (4.36)$$

where  $\mathbf{y}$  is the received signal vector at destination,  $\mathbf{H}$  is the channel matrix,  $\mathbf{x}$  is the user signal vector, and  $\mathbf{z}$  is the AWGN noise vector.

The single-user and joint-user rate-bounds of users  $S_1$  and  $S_2$  at the destination are therefore obtained as:

$$R_1 \leq \frac{1}{2} \log \left( 1 + \frac{\gamma_1 P_1 + g_r P_1}{2\sigma^2} \right) \quad (4.37)$$

$$R_2 \leq \frac{1}{2} \log \left( 1 + \frac{\gamma_2 P_2 + g_r P_2}{2\sigma^2} \right) \quad (4.38)$$

$$R_1 + R_2 \leq \frac{1}{2} \log \left( \det \left( \mathbf{I} + \frac{\mathbf{H}\mathbf{H}^T}{2\sigma^2} \right) \right) = \frac{1}{2} \log \left( 1 + \frac{\gamma_1 P_1 + \gamma_2 P_2 + g_r \left( P_1 + P_2 + P_1 P_2 (\sqrt{\gamma_2} - \sqrt{\gamma_1})^2 \right)}{2\sigma^2} \right) \quad (4.39)$$

where  $\mathbf{S} = E[\mathbf{xx}^T]$  is the input covariance matrix, which is a diagonal matrix of  $P_1$  and  $P_2$ .

Hence, combining Eqs. (4.33)-(4.35) with Eqs.(4.37)-(4.39), the following expressions are derived :

$$R_1 \leq \min \left\{ \frac{1}{2} \log \left( 1 + \frac{\gamma_1 P_1 + g_r P_1}{2\sigma^2} \right), \frac{1}{2} \log \left( 1 + \frac{g_1 P_1}{2\sigma^2} \right) \right\} \quad (4.40)$$

$$R_2 \leq \min \left\{ \frac{1}{2} \log \left( 1 + \frac{\gamma_2 P_2 + g_r P_2}{2\sigma^2} \right), \frac{1}{2} \log \left( 1 + \frac{g_2 P_2}{2\sigma^2} \right) \right\} \quad (4.41)$$

$$R_1 + R_2 \leq \min \left\{ \frac{1}{2} \log \left( 1 + \frac{\gamma_1 P_1 + \gamma_2 P_2 + g_r \alpha \left( P_1 + P_2 + P_1 P_2 (\sqrt{\gamma_2} - \sqrt{\gamma_1})^2 \right)}{2\sigma^2} \right), \frac{1}{2} \log \left( 1 + \frac{g_1 P_1 + g_2 P_2}{2\sigma^2} \right) \right\} \quad (4.42)$$

Since our aim is to determine an information theoretical optimum power allocation policy, which considers fairness among users, we equalize the maximum rate bounds of users in Eq. (4.40) and Eq. (4.42) as:

$$\min \left\{ \frac{1}{2} \log \left( 1 + \frac{\gamma_1 P_1 + g_r P_1}{2\sigma^2} \right), \frac{1}{2} \log \left( 1 + \frac{g_1 P_1}{2\sigma^2} \right) \right\} = \min \left\{ \frac{1}{2} \log \left( 1 + \frac{\gamma_2 P_2 + g_r P_2}{2\sigma^2} \right), \frac{1}{2} \log \left( 1 + \frac{g_2 P_2}{2\sigma^2} \right) \right\} \quad (4.43)$$

The expression above can be simplified further as

$$\min \{ \gamma_1 + g_r, g_1 \} P_1 = \min \{ \gamma_2 + g_r, g_2 \} P_2 \quad (4.44)$$

We can obtain the user powers using the total power constraint  $P_T - \sum_{k=1}^2 P_k = 0$  and Eq. (4.44) as:

$$\begin{aligned} \tilde{P}_1 &= \frac{\min \{ \gamma_2 + g_r, g_2 \}}{\min \{ \gamma_1 + g_r, g_1 \} + \min \{ \gamma_2 + g_r, g_2 \}} P_T \\ \tilde{P}_2 &= \frac{\min \{ \gamma_1 + g_r, g_1 \}}{\min \{ \gamma_1 + g_r, g_1 \} + \min \{ \gamma_2 + g_r, g_2 \}} P_T \end{aligned} \quad (4.45)$$

where  $\tilde{P}_1$  and  $\tilde{P}_2$  represent the rate-fair power values for user 1 and user 2, respectively.

The information theoretical result in Eq. (4.45) is beneficial to obtain approximately the SER-optimized signature powers with the use of Eq. (4.32) as explained below.

Using total power constraint  $P_1^* + P_2^* = P_T$ , we can eliminate  $P_2^*$  from Eq. (4.32), and the resultant

expression as a function of  $P_1^*$  becomes

$$\begin{aligned}
f(x) = & (1 + \frac{\gamma_1 x}{2\sigma^2})^{-2} \frac{\gamma_1}{2\sigma^2} (1 + \frac{g_r x}{2\sigma^2})^{-1} + (1 + \frac{\gamma_1 x}{2\sigma^2})^{-1} (1 + \frac{g_r x}{2\sigma^2})^{-2} \frac{g_r}{2\sigma^2} + \\
& (1 + \frac{\gamma_1 x + \gamma_2 (P_T - x)}{2\sigma^2})^{-2} \frac{\gamma_1}{2\sigma^2} (1 + \frac{g_r (P_T)}{2\sigma^2})^{-1} + (1 + \frac{g_1 x}{2\sigma^2})^{-2} \frac{g_1}{2\sigma^2} + (1 + \frac{g_1 x + g_2 (P_T - x)}{2\sigma^2})^{-2} \frac{g_1}{2\sigma^2} - \\
& (1 + \frac{\gamma_2 (P_T - x)}{2\sigma^2})^{-2} \frac{\gamma_2}{2\sigma^2} (1 + \frac{g_r (P_T - x)}{2\sigma^2})^{-1} - (1 + \frac{\gamma_2 (P_T - x)}{2\sigma^2})^{-1} (1 + \frac{g_r (P_T - x)}{2\sigma^2})^{-2} \frac{g_r}{2\sigma^2} - \\
& (1 + \frac{\gamma_1 x + \gamma_2 (P_T - x)}{2\sigma^2})^{-2} \frac{\gamma_2}{2\sigma^2} (1 + \frac{g_r (P_T)}{2\sigma^2})^{-1} - (1 + \frac{g_2 (P_T - x)}{2\sigma^2})^{-2} \frac{g_2}{2\sigma^2} - (1 + \frac{g_1 x + g_2 (P_T - x)}{2\sigma^2})^{-2} \frac{g_2}{2\sigma^2} = 0
\end{aligned} \tag{4.46}$$

where  $x = P_1^*$ .

We can obtain a quadratic approximation equation of Eq. (4.46) by obtaining its Taylor series expansion about  $x = \tilde{P}_1$  in Eq. (4.45) :

$$f(\tilde{P}_1) + f'(\tilde{P}_1)(x - \tilde{P}_1) + \frac{1}{2} f''(\tilde{P}_1)(x - \tilde{P}_1)^2 = 0 \tag{4.47}$$

where  $f'(x)$  and  $f''(x)$  represent the first and the second derivative of the function in Eq. (4.46), respectively, can be given as follows:

$$\begin{aligned}
f'(x) = & -(1 + \frac{g_1 x}{2\sigma^2})^{-3} \frac{2g_1^2}{4\sigma^4} - (1 + \frac{\gamma_1 x}{2\sigma^2})^{-1} (1 + \frac{g_r x}{2\sigma^2})^{-3} \frac{2g_r^2}{4\sigma^4} - (1 + \frac{\gamma_1 x}{2\sigma^2})^{-2} \frac{2\gamma_1 g_r}{4\sigma^4} (1 + \frac{g_r x}{2\sigma^2})^{-2} - \\
& (1 + \frac{\gamma_1 x}{2\sigma^2})^{-3} \frac{2\gamma_1^2}{4\sigma^4} (1 + \frac{g_r x}{2\sigma^2})^{-1} - (1 + \frac{g_2 (P_T - x)}{2\sigma^2})^{-3} \frac{2g_2^2}{4\sigma^4} - (1 + \frac{\gamma_2 (P_T - x)}{2\sigma^2})^{-1} (1 + \frac{g_r (P_T - x)}{2\sigma^2})^{-3} \\
& \times \frac{2g_r^2}{4\sigma^4} - (1 + \frac{\gamma_2 (P_T - x)}{2\sigma^2})^{-2} \frac{2\gamma_2 g_r}{4\sigma^4} (1 + \frac{g_r (P_T - x)}{2\sigma^2})^{-2} - (1 + \frac{\gamma_2 (P_T - x)}{2\sigma^2})^{-3} \frac{2\gamma_2^2}{4\sigma^4} (1 + \frac{g_r (P_T - x)}{2\sigma^2})^{-1} \\
& - (1 + \frac{g_1 x + g_2 (P_T - x)}{2\sigma^2})^{-3} \frac{2g_1 (g_1 - g_2)}{4\sigma^4} + (1 + \frac{g_1 x + g_2 (P_T - x)}{2\sigma^2})^{-3} \frac{2g_2 (g_1 - g_2)}{4\sigma^4} \\
& - (1 + \frac{\gamma_1 x + \gamma_2 (P_T - x)}{2\sigma^2})^{-3} \frac{2\gamma_1 (\gamma_1 - \gamma_2)}{4\sigma^4} (1 + \frac{g_r (P_T)}{2\sigma^2})^{-1} \\
& + (1 + \frac{\gamma_1 x + \gamma_2 (P_T - x)}{2\sigma^2})^{-3} \frac{2\gamma_2 (\gamma_1 - \gamma_2)}{4\sigma^4} (1 + \frac{g_r (P_T)}{2\sigma^2})^{-1}
\end{aligned} \tag{4.48}$$

$$\begin{aligned}
f''(x) = & \left(1 + \frac{g_1 x}{2\sigma^2}\right)^{-4} \frac{6g_1^3}{8\sigma^6} + \left(1 + \frac{\gamma_1 x}{2\sigma^2}\right)^{-1} \left(1 + \frac{g_r x}{2\sigma^2}\right)^{-4} \frac{6g_r^3}{8\sigma^6} + \left(1 + \frac{\gamma_1 x}{2\sigma^2}\right)^{-2} \left(1 + \frac{g_r x}{2\sigma^2}\right)^{-3} \frac{6\gamma_1 g_r^2}{8\sigma^6} + \\
& \left(1 + \frac{\gamma_1 x}{2\sigma^2}\right)^{-3} \frac{6\gamma_1^2 g_r}{8\sigma^6} \left(1 + \frac{g_r x}{2\sigma^2}\right)^{-2} + \left(1 + \frac{\gamma_1 x}{2\sigma^2}\right)^{-4} \frac{6\gamma_1^3}{8\sigma^6} \left(1 + \frac{g_r x}{2\sigma^2}\right)^{-1} - \\
& \left(1 + \frac{g_2(P_T - x)}{2\sigma^2}\right)^{-4} \frac{6g_2^3}{8\sigma^6} - \left(1 + \frac{\gamma_2(P_T - x)}{2\sigma^2}\right)^{-1} \left(1 + \frac{g_r(P_T - x)}{2\sigma^2}\right)^{-4} \frac{6g_r^3}{8\sigma^6} - \\
& \left(1 + \frac{\gamma_2(P_T - x)}{2\sigma^2}\right)^{-2} \frac{6\gamma_2^2 g_r}{8\sigma^6} \left(1 + \frac{g_r(P_T - x)}{2\sigma^2}\right)^{-3} - \left(1 + \frac{\gamma_2(P_T - x)}{2\sigma^2}\right)^{-3} \frac{6\gamma_2^2 g_r}{8\sigma^6} \left(1 + \frac{g_r(P_T - x)}{2\sigma^2}\right)^{-2} - \\
& \left(1 + \frac{\gamma_2(P_T - x)}{2\sigma^2}\right)^{-4} \frac{6\gamma_2^3}{8\sigma^6} \left(1 + \frac{g_r(P_T - x)}{2\sigma^2}\right)^{-1} + \left(1 + \frac{g_1 x + g_2(P_T - x)}{2\sigma^2}\right)^{-4} \frac{6g_1(g_1 - g_2)^2}{8\sigma^6} - \\
& \left(1 + \frac{g_1 x + g_2(P_T - x)}{2\sigma^2}\right)^{-4} \frac{6g_2(g_1 - g_2)^2}{8\sigma^6} + \left(1 + \frac{\gamma_1 x + \gamma_2(P_T - x)}{2\sigma^2}\right)^{-4} \frac{6\gamma_1(\gamma_1 - \gamma_2)^2}{8\sigma^6} \left(1 + \frac{g_r(P_T)}{2\sigma^2}\right)^{-1} - \\
& \left(1 + \frac{\gamma_1 x + \gamma_2(P_T - x)}{2\sigma^2}\right)^{-4} \frac{6\gamma_2(\gamma_1 - \gamma_2)^2}{8\sigma^6} \left(1 + \frac{g_r(P_T)}{2\sigma^2}\right)^{-1}
\end{aligned} \tag{4.49}$$

The roots of Eq. (4.47) can be expressed using Eq. (4.45) as :

$$\hat{P}_1^i = \tilde{P}_1 + \frac{-f'(\tilde{P}_1) + (-1)^{i+1} \sqrt{[f'(\tilde{P}_1)]^2 - 2f''(\tilde{P}_1)f(\tilde{P}_1)}}{f''(\tilde{P}_1)} \text{ for } i=1,2 \tag{4.50}$$

Although we have determined two roots, only one of them is close to the actual root of Eq.(4.46). At this point, it is important to note that the actual root from Eq. (4.46) is the minimizer of  $f^2(x)$ . Hence, the approximate optimal signature power of user 1 can be determined as the root minimizing  $f^2(x)$ .

$$\hat{P}_1 = \arg \min_{i=1,2} f^2(\hat{P}_1^i) \tag{4.51}$$

The signature power for user 2 can be obtained with the use of the total power constraint and Eq. (4.51) as

$$\hat{P}_2 = P_T - \hat{P}_1 \tag{4.52}$$

#### 4.4 Bit Error Rate Simulation Results of the SER-optimized CFNC

In this section, we investigate the performance of SER-optimized CFNC through simulations and compare it the conventional CFNC in [20] in which the user  $S_1$  and user  $S_2$  utilize non-optimal

signatures as  $\theta_1 = e^{j0}=1$  and  $\theta_2 = e^{j\frac{3\pi}{4}}$  respectively. To make a fair comparison between the optimal and non-optimal cases, we assume that the average transmit power of the network per time slot is 2 Watts (i.e.,  $P_T = P_1 + P_2 = 2$ ). For all numerical experiments along this chapter, we also assume that distance from the user-1-to-destination link is one and the corresponding path loss coefficient is unity (i.e.,  $\gamma_1 = 1$  or 0 dB) so that other path loss coefficients (i.e.,  $g_1$ ,  $g_2$ ,  $g_r$  and  $\gamma_2$ ) are interpreted as power gains or losses relative to the  $S_1$ -to-destination link. Also, the path-loss exponent is assumed to be 2 and the path-loss coefficients of the relay channel should satisfy the following geometrical constraints because of the two-triangle inequalities:

$$|g_1^{-0.5} - g_r^{-0.5}| < \gamma_1^{-0.5} < g_1^{-0.5} + g_r^{-0.5} \quad (4.53)$$

$$|g_2^{-0.5} - g_r^{-0.5}| < \gamma_2^{-0.5} < g_2^{-0.5} + g_r^{-0.5} \quad (4.54)$$

Moreover, the signal-to noise ratio (SNR) of the network is defined in dB as  $10\log(\frac{P_1+P_2}{2\sigma^2})$  for this study. Since the power budget is fixed, we realize different SNR values by changing the variance of electronic noise.

In order to see the benefit of the signature optimization, we have first considered a limiting case with the path-loss parameters  $g_1=30$  dB,  $g_2 = 0.14$  dB and  $g_r=0.27$  dB where the relay is very close to the destination. For this case, we obtain average BER of the network for both optimized and non-optimized CFNC schemes, in which the path-loss parameter  $\gamma_2$  is set first to 3 dB and is then increased to 6dB. The optimal signature powers for this case are put in Table 4-1

. For a fixed value of  $\gamma_2$ ,  $S_2$  has been allocated more power compared to user  $S_1$  for all SNR values. This makes sense, since  $S_1$  is closer to the relay, and therefore its BER is smaller than that of  $S_2$ . Hence, it is logical to assign more power to  $S_2$  in order to improve the overall network performance. The average BER simulations of the network for this case are illustrated in Figure 4-2 and the corresponding BER of individual nodes and the average BER of the network both with and without optimized CFNC are tabulated in Table 4-2 and Table 4-3. As can be observed

from these tables, (after signature optimization) the BER of  $S_2$  (shown by  $BER_2$ ) gets improved, whereas the BER of  $S_1$  (shown by  $BER_1$ ) worsen, but the overall average BER at the destination  $BER_D$  decreases, which is the main objective for this study. Particularly, the optimized CFNC achieves up-to 29% and 25% average BER improvements over the conventional CFNC for  $\gamma_2=3$  dB and  $\gamma_2=6$ dB, respectively, which proves the SER-optimized CFNC to be useful.

Next, we consider a more practical scenario, in which  $g_1$ ,  $g_2$  and  $g_r$  are selected as 3.10dB, 20 dB and 3.10 dB, respectively, while the path loss parameter  $\gamma_2$  is selected first as 1.94 dB and is then increased to 4.44 dB. The optimal signature magnitudes and the average BER simulations for this case can be found in Table 4-4 and Figure 4-3, respectively. In parallel lines with the previous observations,  $S_2$  has been allocated less power compared to user  $S_1$  for all SNR values, and the same value of  $\gamma_2$  since it is closer to the relay than  $S_1$ . Thus, the average network performance is improved by assigning more power to  $S_1$ , which is also verified by obtaining BER of individual nodes with and without optimized CFNC as shown in Table 4-5 and Table 4-6. Specifically, as can be seen from Figure 4-3, the optimized CFNC achieves up-to 25% and 24.5% average BER improvements over the conventional CFNC for  $\gamma_2=1.94$  dB and  $\gamma_2=4.44$  dB, respectively.

Table 4-1. The SER-optimized signature powers for  $g_1=30$  dB,  $g_2=0.14$  dB,  $g_r=0.27$  dB and various  $\gamma_2$  values

SNR (dB)	$\gamma_2=3$ dB		$\gamma_2=6$ dB	
	$P_1^*$	$P_2^*$	$P_1^*$	$P_2^*$
10	0.78	1.21	0.82	1.17
12.5	0.73	1.26	0.74	1.25
15	0.66	1.33	0.67	1.32
17.5	0.59	1.40	0.59	1.40
20	0.51	1.48	0.51	1.48
22.5	0.44	1.55	0.44	1.55
25	0.38	1.61	0.38	1.61

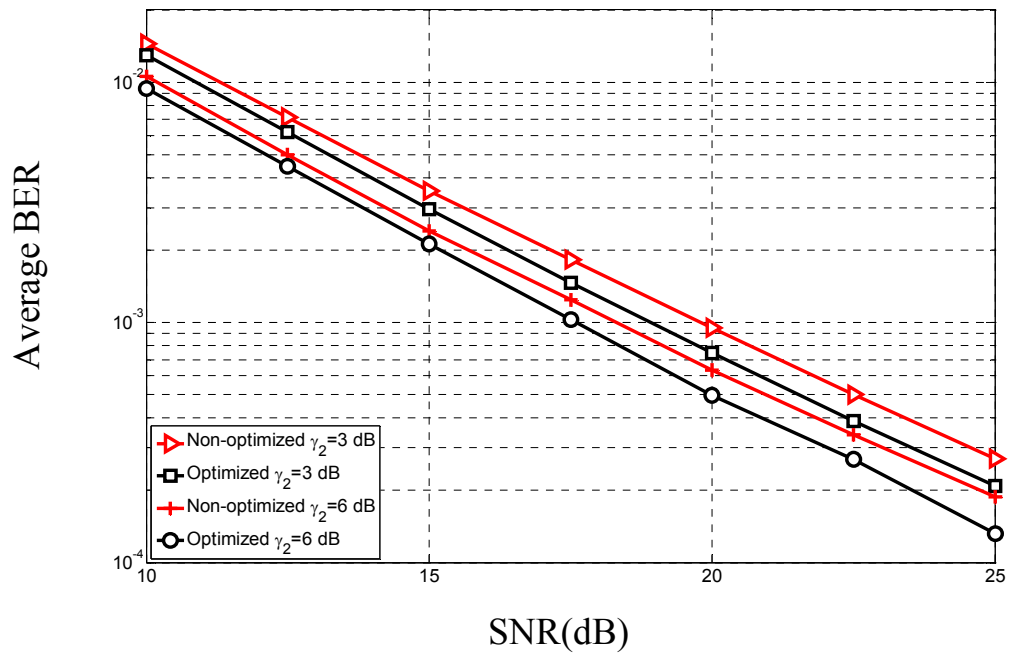


Figure 4-2 Average BER as a function of SNR of the optimized and non-optimized CFNC for  $g_1=30$  dB,  $g_2=0.14$  dB,  $g_r=0.27$  dB and various  $\gamma_2$  values

Table 4-2. BERs of Individual Users , the average BER and Its improvement at the destination with and without optimized CFNC for  $\gamma_2 = 3$  dB

	$\gamma_2 = 3$ dB				
	Optimized BER		Non-Optimized BER		BER <sub>D</sub> Imp.(%)
SNR (dB)	BER <sub>1</sub> /BER <sub>2</sub>	BER <sub>D</sub>	BER <sub>1</sub> /BER <sub>2</sub>	BER <sub>D</sub>	
10	1.0e-2/1.6e-2	1.29e-2	9.6e-3/1.9e-2	1.44e-2	11.16
12.5	4.3e-3/8.2e-3	6.20e-3	3.8e-3/1.1e-2	7.15e-3	13.24
15	1.8e-3/4.2e-3	3.00e-3	1.4e-3/5.6e-3	3.52e-3	14.68
17.5	0.7e-3/2.3e-3	1.49e-3	0.6e-3/3.1e-3	1.83e-3	18.54
20	3.2e-4/1.2e-3	7.47e-4	2.0e-4/1.7e-3	9.48e-4	21.22
22.5	1.5e-4/6.3e-4	3.86e-4	0.9e-4/9.1e-4	5.00e-4	22.74
25	0.6e-4/3.6e-4	2.11e-4	0.4e-4/5.1e-4	2.71e-4	22.17

Table 4-3. BERs of Individual Users , the average BER and Its improvement at the destination with and without optimized CFNC for  $\gamma_2 = 6$  dB

SNR (dB)	$\gamma_2 = 6$ dB				
	Optimized BER		Non-Optimized BER		BER <sub>D</sub> Imp.(%)
	BER <sub>1</sub> /BER <sub>2</sub>	BER <sub>D</sub>	BER <sub>1</sub> /BER <sub>2</sub>	BER <sub>D</sub>	
10	9.2e-3/9.6e-3	0.94e-2	9.5e-3/1.2e-2	1.06e-2	11.36
12.5	3.9e-3/5.0e-3	4.48e-3	3.7e-3/6.3e-3	4.98e-3	10.05
15	1.6e-3/2.6e-3	2.12e-3	1.4e-3/3.4e-3	2.41e-3	12.04
17.5	0.7e-3/1.4e-3	1.03e-3	0.5e-3/1.9e-3	1.24e-3	17.11
20	3.0e-4/6.9e-4	4.98e-4	2.4e-4/1.0e-3	6.33e-4	21.24
22.5	1.4e-4/3.9e-4	2.68e-4	1.1e-4/5.7e-4	3.40e-4	21.08
25	0.6e-4/2.0e-4	1.32e-4	0.5e-4/3.3e-4	1.88e-4	29.57

Table 4-4. The SER-optimized signature powers for  $g_1 = 3.10$  dB,  $g_2 = 20$  dB,  $g_r = 3.10$  dB and various  $\gamma_2$  values

SNR (dB)	$\gamma_2 = 1.44$ dB		$\gamma_2 = 4.44$ dB	
	$P_1^*$	$P_2^*$	$P_1^*$	$P_2^*$
10	1.27	0.72	1.33	0.66
12.5	1.31	0.68	1.38	0.61
15	1.36	0.63	1.43	0.56
17.5	1.42	0.57	1.48	0.51
20	1.48	0.51	1.53	0.46
22.5	1.53	0.46	1.57	0.42
25	1.57	0.42	1.60	0.39

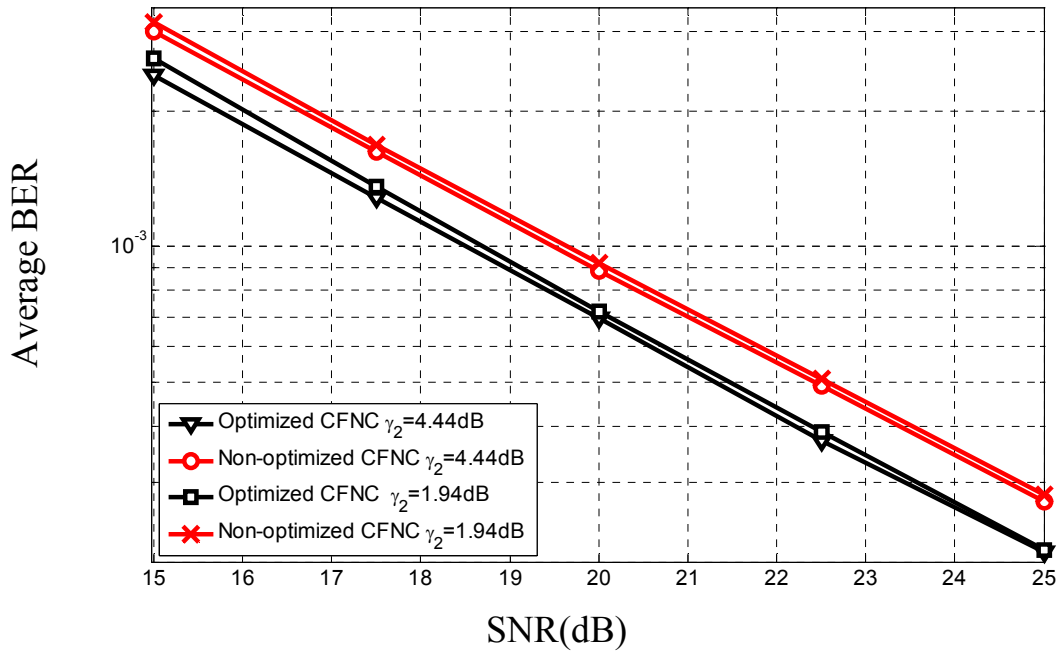


Figure 4-3. Average BER as a function of SNR of the optimized and non-optimized CFNC for  $g_1=3.10$  dB,  $g_2=20$  dB,  $g_r=3.10$  dB and various  $\gamma_2$  values

Table 4-5. BERs of Individual Users, the average BER and Its improvement at the destination with and without optimized CFNC for  $\gamma_2=1.94$  dB

SNR (dB)	$\gamma_2=1.94$ dB				
	Optimized CFNC		Non-Optimized CFNC		BER <sub>D</sub> Imp.(%)
	BER <sub>1</sub> /BER <sub>2</sub>	BER <sub>D</sub>	BER <sub>1</sub> /BER <sub>2</sub>	BER <sub>D</sub>	
10	1.5e-2/5.3e-3	1.02e-2	2.0e-2/4.3e-3	1.19e-2	13.97
12.5	8.0e-3/2.3e-3	5.14e-3	1.0e-2/1.7e-3	6.07e-3	15.39
15	4.2e-3/1.0e-3	2.61e-3	5.6e-3/6.6e-4	3.15e-3	16.90
17.5	2.2e-3/4.7e-4	1.35e-3	3.1e-3/2.6e-4	1.68e-3	19.42
20	1.2e-3/2.4e-4	7.18e-4	1.7e-3/1.1e-4	9.19e-4	21.89
22.5	6.5e-4/1.2e-4	3.88e-4	9.7e-4/5.2e-5	5.09e-4	23.71
25	3.6e-4/6.8e-5	2.11e-4	5.4e-4/2.6e-5	2.82e-4	24.95

Table 4-6. BERs of Individual Users , the average BER and Its improvement at the destination with and without optimized CFNC for  $\gamma_2 = 4.44$  dB

	$\gamma_2 = 4.44$ dB				
	Optimized CFNC		Non-Optimized CFNC		BER <sub>D</sub> Imp.(%)
SNR (dB)	BER <sub>1</sub> /BER <sub>2</sub>	BER <sub>D</sub>	BER <sub>1</sub> /BER <sub>2</sub>	BER <sub>D</sub>	
10	1.4e-2/4.1e-3	0.93e-2	1.9e-2/2.8e-3	1.11e-2	15.73
12.5	7.6e-3/1.8e-3	4.71e-3	1.0e-2/1.1e-3	5.69e-3	17.26
15	4.0e-3/0.8e-3	2.40e-3	5.6e-3/4.3e-4	3.01e-3	20.15
17.5	2.2e-3/4.0e-4	1.28e-3	3.1e-3/1.8e-4	1.63e-3	21.20
20	1.2e-3/2.0e-4	6.94e-4	1.7e-3/7.5e-5	8.85e-4	21.51
22.5	6.4e-4/1.1e-4	3.71e-4	9.5e-4/3.7e-5	4.92e-4	24.37
25	3.6e-4/5.9e-5	2.10e-4	5.3e-4/1.7e-5	2.72e-4	23.04

## 4.5 Conclusions

In this study, we have developed a SER-optimized CFNC for the relay channel, which employs ML detection at both the relay and destination. The proposed method optimally adjusts the user signatures by taking the topology of the relay network and the constraint on the total transmit power into account, and thus it minimizes the SER-bound of the system. We have formulated the optimal signature selection problem, as a convex program, and then obtained the KKT optimality conditions and stated them in a simplified form. Since KKT conditions provide a highly nonlinear relationship between signature powers, we have also developed an information theoretical approximate solution, which achieves fairness among users. Once after SER-optimal signature

powers are determined, we have investigated the average BER of the network for different values of system parameters. The results have indicated that the proposed SER optimized-CFNC could provide up-to 29 % enhancement in average BER over the conventional CFNC.

## 5. Joint Optimization of Complex-Field Network Coding and Relay Power for Multi-User Communications

In the previous chapter, we obtained optimum signatures for sources which minimize the derived SER upper bound in a MAR channel operates over non orthogonal-channels assuming that relay power is fixed. Therefore we show that, in contrast to [20], one can employ signature with non-unity magnitudes and optimize them according to certain criterion, which effectively not only rotate the signal constellation but also changes the transmit power of each user. In addition to signature optimization, the performance of the MAR-NOC channel can be further improved by appropriately allocating the relay power. With the use of these ideas, in this work, we jointly optimize the user signatures and the relay power by minimizing the symbol error rate (SER) of the CFNC coded MAR-NOC channel while taking the total transmit power and the network geometry into account. During our subsequent development, we assume that the transmitting nodes (e.g., the user nodes and relay node) have knowledge only on the path-losses dictated by the network geometry, and the complete knowledge on both path-losses and the channel state information (CSI) due to Rayleigh fading are available at the receiving nodes (e.g., the destination and relay node), which is more practical to implement since it does not require any feedback sent from the receiving node to the transmitting node(s). To achieve such an optimization, we first derive a symbol-error rate (SER) bound of the MAR-NOC channel by employing Maximum-Likelihood (ML) detection at both the relay and destination nodes. Then, we formulate the joint optimization of user signatures and the relay power as a convex optimization under the total transmit power constraint and consideration of the network geometry. From the Karush-Kuhn Tucker (KKT) condition, a simple analytical condition of the signature phases has been obtained while the solution for the signature magnitudes (and thus, the relay power) cannot be analytically viable since they satisfy a nonlinear relationship. Afterwards, we aim at solving the signature powers by the Sequential Quadratic Programming (SQP) [87], whose

the rate of convergence mainly depends on the closeness of the solution used in the initialization to the true optimal solution. For this purpose, we develop a heuristic initialization method, which has a basis from information theory, to speed up the convergence of SQP as compared to the initialization with equal power allocation (EPA) method. Next, we verify the efficacy of the proposed heuristic on the convergence of SQP through simulations while jointly obtaining the signature magnitudes and the relay power. Finally, we investigate the performance of the proposed SER-optimized joint signature and relay power, and compare it to the performance of non-optimized signatures used in [20] for various system parameters.

The rest of the chapter is organized as follows. In Section 5.1 we give system model for a basic CFNC coded MAR-NOC channel. We give an upper bound at SER at destination in Section 5.2. Then, the SER-optimized user signatures have been derived in Section 5.3 for the case which transmitters do not have CSI. In Section 5.4, we proposed a heuristic initialization method for the optimization problem considered to decrease the number of iterations. Section 5.5 is devoted to present the average BER simulation results of the optimized NC. Finally, our conclusions are summarized in Section 5.6.

## **5.1 System Model for A Basic CFNC Coded Multi-Access Relay Channel**

In sequel, we consider a basic CFNC coded MAR-NOC channel with two users  $S_1$  and  $S_2$ , one relay node  $R$  and one destination node  $D$ , which is illustrated in Figure 5-1. As seen from this figure, user  $S_1$  and user  $S_2$  are assigned signatures  $\theta_1$  and  $\theta_2$ , respectively, in order to employ the CFNC, in which each user first multiplies its message (denoted as  $x_{s_1}[n]$  and  $x_{s_2}[n]$  respectively for the user  $S_1$  and user  $S_2$ ) by its signature. After that, the resultant user signals are broadcasted simultaneously in time slot 1, which produces multiuser MAI at both the relay and destination nodes because of NOC. Next, the relay node decodes the user message by employing ML

detection as in [20], and then generates CFNC coded relay message and forwards it (after some power scaling in order to meet the total transmit power constraint) to the destination node in time slot 2 .

Referring to Figure 5-1 , the path-loss coefficients of  $S_1$ -to- $D$  ,  $S_2$ -to- $D$  ,  $S_1$ -to- $R$  ,  $S_2$ -to- $R$  and  $R$ -to- $D$  links are denoted by  $\gamma_1, \gamma_2$  ,  $g_1, g_2$  and  $g_r$  , respectively. Let  $y_r[n]$ ,  $y_{sd}[n]$  and  $y_{rd}[n]$  represent the signals received at the relay node in time slot 1, at the destination node in time slot 1 and time slot 2, respectively. Assume flat Rayleigh fading, these signals can be mathematically expressed as :

$$y_r[n] = \sqrt{g_1} h_{s_1r} \theta_1 x_{s_1}[n] + \sqrt{g_2} h_{s_2r} \theta_2 x_{s_2}[n] + z_r[n] \quad (5.1)$$

$$y_{sd}[n] = \sqrt{\gamma_1} h_{s_1d} \theta_1 x_{s_1}[n] + \sqrt{\gamma_2} h_{s_2d} \theta_2 x_{s_2}[n] + z_d[n] \quad (5.2)$$

$$y_{rd}[n] = \sqrt{g_r} h_{rd} \sqrt{\alpha} x_r[n] + z_d[n] \quad (5.3)$$

where  $h_{s_1r}$  ,  $h_{s_2r}$  ,  $h_{s_1d}$  ,  $h_{s_2d}$  and  $h_{rd}$  denote fading coefficient for  $S_1$ - $R$ ,  $S_2$ - $R$  ,  $S_1$ - $D$ ,  $S_2$ - $D$ ,  $R$ - $D$  links, respectively, which are modeled as complex Gaussian random variables with zero mean and unit variance, the parameter  $\alpha$  controls the relay power and determines the power allocated to the relay as a fraction of the total transmit power of all users, while  $z_r[n]$  and  $z_d[n]$  represent the noise at the relay node and destination node, respectively, which are modeled as additive white Gaussian noise (AWGN) with zero mean and variance of  $N_0/2$  per dimension.

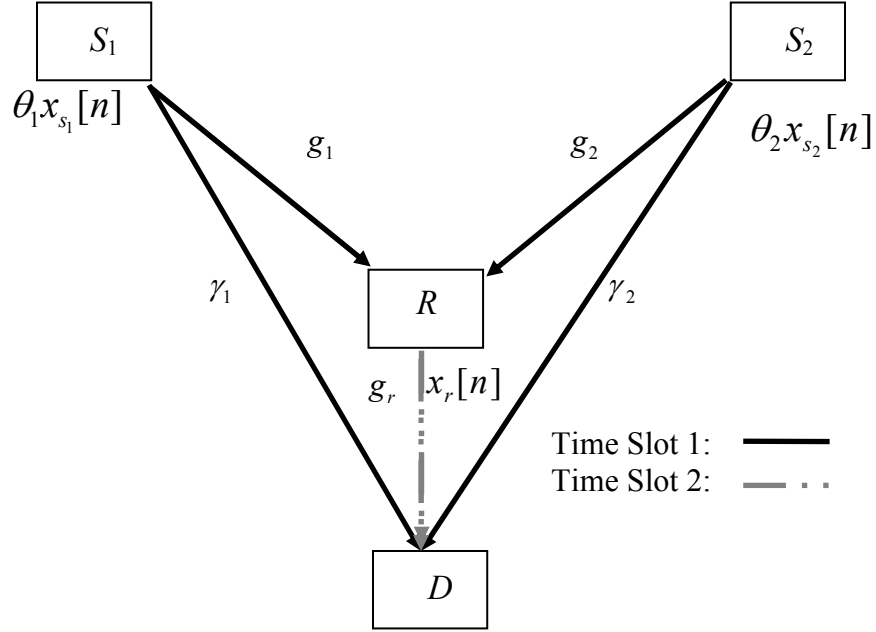


Figure 5-1. Schematic of a basic CFNC coded MAR-NOC channel with two users, one relay node and one destination node.

For the modeling of path gains, we assume the distance from the user-1-to-destination link is one and the corresponding path loss coefficient is unity (i.e.,  $\gamma_1 = 1$  or 0 dB) so that other path loss coefficients (i.e.,  $g_1$ ,  $g_2$ ,  $g_r$  and  $\gamma_2$ ) are interpreted as power gains or losses relative to the  $S_1$ -to-destination link. Also, the path-loss exponent is assumed to be 2 and the path-loss coefficients of the relay channel should satisfy the following geometrical constraints because of the two-triangle inequalities.

$$|g_1^{-0.5} - g_r^{-0.5}| < \gamma_1^{-0.5} < g_1^{-0.5} + g_r^{-0.5} \quad (5.4)$$

$$|g_2^{-0.5} - g_r^{-0.5}| < \gamma_2^{-0.5} < g_2^{-0.5} + g_r^{-0.5} \quad (5.5)$$

In this work, the state information (CSI) of wireless channels is assumed to be known only at the receiving nodes (i.e., the relay node and the destination node). To reduce the computational burden on the relay node, we just consider the ML detection as in [20], in which the user messages are decoded together as:

$$(\hat{x}_{s_1}[n], \hat{x}_{s_2}[n]) = \arg \min_{x_{s_1}[n], x_{s_2}[n]} \left\| y_r[n] - \sqrt{g_1} h_{s_1 r} \theta_1 x_{s_1}[n] - \sqrt{g_2} h_{s_2 r} \theta_2 x_{s_2}[n] \right\|^2 \quad (5.6)$$

Then, the relay signal is generated by incorporating the ML estimates of user messages to the user-signatures, and scaling the resultant signal to meet the total transmit power constraint as:

$$x_r[n] = \theta_1 \hat{x}_{s_1}[n] + \theta_2 \hat{x}_{s_2}[n] \quad (5.7)$$

Next, the relayed signal  $x_r[n]$  is forwarded to the destination according to Eq.(5.3) in time slot 2.

Finally, the destination node uses an ML detection to jointly decode the user messages by combining the signals it has received during both time slots as:

$$\begin{aligned} (\hat{x}_{s_1}[n], \hat{x}_{s_2}[n]) = \arg \min_{x_{s_1}[n], x_{s_2}[n]} & \left\| y_{sd}[n] - \sqrt{\gamma_1} h_{s_1 d} \theta_1 x_{s_1}[n] - \sqrt{\gamma_2} h_{s_2 d} \theta_2 x_{s_2}[n] \right\|^2 \\ & + \left\| y_{rd}[n] - \sqrt{g_r} h_{rd} \sqrt{\alpha} (\theta_1 x_{s_1}[n] + \theta_2 x_{s_2}[n]) \right\|^2 \end{aligned} \quad (5.8)$$

In the next section, we derive a bound on the average symbol-error rate (SER) of the system considered under the use of ML detection at both the relay node and destination node.

## 5.2 A Bound on Average SER under ML Detection and Receiver Channel State Information

As mentioned earlier, the user signatures in [20] are selected as purely complex exponentials, as long as  $\theta_1 \neq \theta_2$ , the information of each user can be recovered uniquely from the CFNC coded symbol sequence  $c[n] = \theta_1 x_{s_1}[n] + \theta_2 x_{s_2}[n]$ .

Alternatively, we can select the signatures as non-unity magnitude complex numbers, which can be optimized to minimize the decision errors while keeping the total transmit power of the network fixed. For this aim, in this part, we derive an average SER bound of CFNC coded MAR-NOC channel under the receiver CSI.

Although the information of each user is assumed to be modulated using Binary Phase Shift Keying (BPSK) for the subsequent analysis, in which -1 and 1 represent the logical zero and logical one, respectively, the derived expressions can be easily extended to other types of modulations as well.

The user signatures and symbols can be put into the signature vector  $\boldsymbol{\theta} = [\theta_1, \theta_2]^T$  and user symbol vector  $\mathbf{x} = [x_{s_1}[n], x_{s_2}[n]]^T$ , respectively, for the compactness of the resulting expressions. Since the modulation is binary, there are four possible realization of the user symbol vector, where the  $i^{\text{th}}$  possible user symbol vector can be represented by  $\mathbf{x}_i$  for  $1 \leq i \leq 4$ . The CFNC symbol corresponding to user symbol vector  $\mathbf{x}_i$  becomes

$$c_i = \boldsymbol{\theta}^T \mathbf{x}_i \quad (5.9)$$

where  $c_i$  takes one of four distinct values since each signature is assigned uniquely to a specific user. Assuming receiver CSI, the pair-wise error probability (PEP) of CFNC symbols at the destination which performs ML detection, can be written as

$$P(c_i \rightarrow c_j \text{ at D} | c_i) = P(c_i \rightarrow c_i \text{ at R} | c_i) \times P(c_i \rightarrow c_j \text{ at D} | c_i \rightarrow c_i \text{ at R}, c_i) + P(c_i \rightarrow c_j \text{ at R} | c_i) \times (1 - P(c_i \rightarrow c_i \text{ at D} | c_i \rightarrow c_j \text{ at R}, c_i)) \quad (5.10)$$

where  $P(c_i \rightarrow c_i \text{ at R} | c_i)$  and  $P(c_i \rightarrow c_j \text{ at R} | c_i)$  denote correctly decoding probability and PEP respectively at the relay when CFNC symbol  $c_i$  is sent. Also,  $P(c_i \rightarrow c_j \text{ at D} | c_i \rightarrow c_i \text{ at R}, c_i)$  is the PEP at the destination given that  $c_i$  is sent and the decoding at relay is correct, whereas  $P(c_i \rightarrow c_i \text{ at D} | c_i \rightarrow c_j \text{ at R}, c_i)$  is the probability of making correct decision of the destination when  $c_i$  is sent and the relay reaches an erroneous decision. Assuming that CSI is known at the relay and ML relaying is used, the PEP of the relay becomes

$$\begin{aligned} P(c_i \rightarrow c_j \text{ at R} | c_i, h_{s_{1r}}, h_{s_{2r}}) &= P\left( \left| \sum_{k=1}^2 \sqrt{g_k} h_{s_{kr}} \theta_k(\mathbf{x}_i)_k + z_r - \sum_{k=1}^2 \sqrt{g_k} h_{s_{kr}} \theta_k(\mathbf{x}_i)_k \right|^2 \geq \right. \\ &\quad \left. \left| \sum_{k=1}^2 \sqrt{g_k} h_{s_{kr}} \theta_k(\mathbf{x}_i)_k + z_r - \sum_{k=1}^2 \sqrt{g_k} h_{s_{kr}} \theta_k(\mathbf{x}_j)_k \right|^2 \right) \\ &= P\left( |z_r|^2 \geq \left| \sum_{k=1}^2 \sqrt{g_k} h_{s_{kr}} \theta_k(\mathbf{x}_i)_k + z_r - \sum_{k=1}^2 \sqrt{g_k} h_{s_{kr}} \theta_k(\mathbf{x}_j)_k \right|^2 \right) \\ &= P\left( - \left| \sum_{k=1}^2 \sqrt{g_k} h_{s_{kr}} \theta_k d_{ijk} \right|^2 \geq z_r^* \left( \sum_{k=1}^2 \sqrt{g_k} h_{s_{kr}} \theta_k d_{ijk} \right) + z_r \left( \sum_{k=1}^2 \sqrt{g_k} h_{s_{kr}} \theta_k d_{ijk} \right)^* \right) \end{aligned} \quad (5.11)$$

Where “\*” denotes the complex conjugation and random variable

$z_r^* (\sum_{k=1}^2 \sqrt{g_k} h_{s_{kr}} \theta_k d_{ijk}) + z_r (\sum_{k=1}^2 \sqrt{g_k} h_{s_{kr}} \theta_k d_{ijk})^*$  is Gaussian with zero mean and

$4\sigma^2 \left| \sum_{k=1}^2 \sqrt{g_k} h_{s_{kr}} \theta_k d_{ijk} \right|^2$  variance. Hence, PEP expression in Eq.(5.11) can be found as

$$P(c_i \rightarrow c_j \text{ at R} \mid c_i, h_{s_{1r}}, h_{s_{2r}}) = Q\left(\frac{\left| \sum_{k=1}^2 \sqrt{g_k} h_{s_{kr}} \theta_k d_{ijk} \right|}{2\sigma}\right) \quad (5.12)$$

where  $d_{ijk}$  represents the  $k^{\text{th}}$  component of the difference vector between the  $i^{\text{th}}$  and  $j^{\text{th}}$  decision vectors,  $\mathbf{d}_{ij} = (\mathbf{x}_i - \mathbf{x}_j)$ .

Similar to Eq.(5.11), the PEP of the destination given that the relay correctly decoded  $c_i$  (by assuming that CSI is known at the relay and ML decoding is used at destination) becomes

$$\begin{aligned} P(c_i \rightarrow c_j \text{ at D} \mid c_i \rightarrow c_i \text{ at R}, c_i, \mathbf{h}_{sd}, h_{rd}) &= P\left(\left|\sum_{k=1}^2 \sqrt{\gamma_k} h_{s_{kd}} \theta_k (\mathbf{x}_i)_k + z_d - \sum_{k=1}^2 \sqrt{\gamma_k} h_{s_{kd}} \theta_k (\mathbf{x}_i)_k\right|^2\right. \\ &\quad \left.+ \left|\sqrt{g_r} \alpha h_{rd} \sum_{k=1}^2 \theta_k (\mathbf{x}_i)_k + z_d - h_{rd} \sum_{k=1}^2 \theta_k (\mathbf{x}_i)_k\right|^2\right) \\ &\geq \left|\sum_{k=1}^2 \sqrt{\gamma_k} h_{s_{kd}} \theta_k (\mathbf{x}_i)_k + z_d - \sum_{k=1}^2 \sqrt{\gamma_k} h_{s_{kd}} \theta_k (\mathbf{x}_j)_k\right|^2 \\ &\quad \left.+ \left|\sqrt{g_r} \alpha h_{rd} \sum_{k=1}^2 \theta_k (\mathbf{x}_i)_k + z_d - h_{rd} \sum_{k=1}^2 \theta_k (\mathbf{x}_j)_k\right|^2\right) \\ &= P(|z_d|^2 + |z_d|^2 \geq \left|\sum_{k=1}^2 \sqrt{\gamma_k} h_{s_{kd}} \theta_k d_{ijk} + z_d\right|^2 \\ &\quad \left.+ \left|\sqrt{g_r} \alpha h_{rd} \sum_{k=1}^2 \theta_k d_{ijk} + z_d\right|^2\right) \\ &= P\left(-\left|\sum_{k=1}^2 \sqrt{\gamma_k} h_{s_{kd}} \theta_k d_{ijk}\right|^2 - \left|\sqrt{g_r} \alpha h_{rd} \sum_{k=1}^2 \theta_k d_{ijk}\right|^2 \geq\right. \\ &\quad \left.2\text{Re}\{z_d^* \sum_{k=1}^2 \sqrt{\gamma_k} h_{s_{kd}} \theta_k d_{ijk}\} + 2\text{Re}\{z_d^* \sqrt{g_r} \alpha h_{rd} \sum_{k=1}^2 \theta_k d_{ijk}\}\right) \end{aligned} \quad (5.13)$$

Since  $z_d$  is a complex Gaussian random variable with zero mean and  $2\sigma^2$  variance

$2\text{Re}\{z_d^* \sum_{k=1}^2 \sqrt{\gamma_k} h_{s_k d} \theta_k d_{ijk}\} + 2\text{Re}\{z_d^* \sqrt{g_r \alpha} h_{rd} \sum_{k=1}^2 \theta_k d_{ijk}\}$  is a Gaussian random variable with zero

mean and  $4\sigma^2 \left( \left| \sum_{k=1}^2 \sqrt{\gamma_k} h_{s_k d} \theta_k d_{ijk} \right|^2 + \left| \sqrt{g_r \alpha} h_{rd} \sum_{k=1}^2 \theta_k d_{ijk} \right|^2 \right)$  variance. Hence, the PEP in Eq.(5.13)

can be determined as

$$P(c_i \rightarrow c_j \text{ at D} | c_i \rightarrow c_i \text{ at R}, c_i, \mathbf{h}_{sd}, h_{rd}) = Q\left(\frac{\sqrt{\left| \sum_{k=1}^2 \sqrt{\gamma_k} h_{s_k d} \theta_k d_{ijk} \right|^2 + \left| \sqrt{g_r \alpha} h_{rd} \sum_{k=1}^2 \theta_k d_{ijk} \right|^2}}{2\sigma}\right) \quad (5.14)$$

A similar analysis can be conducted to determine  $P(c_i \rightarrow c_i \text{ at D} | c_i \rightarrow c_i \text{ at R}, c_i)$ . Toward that

goal, we need to determine first,  $P(c_i \rightarrow c_i \text{ at D} | c_i \rightarrow c_j \text{ at R}, c_i, \mathbf{h}_{sd}, h_{rd})$  as :

$$\begin{aligned}
P(c_i \rightarrow c_i \text{ at D} | c_i \rightarrow c_j \text{ at R}, c_i, \mathbf{h}_{sd}, h_{rd}) &= P\left( \left| \sum_{k=1}^2 \sqrt{\gamma_k} h_{s_k d} \theta_k(\mathbf{x}_i)_k + z_d - \sum_{k=1}^2 \sqrt{\gamma_k} h_{s_k d} \theta_k(\mathbf{x}_i)_k \right|^2 \right. \\
&\quad \left. + \left| \sqrt{g_r \alpha} h_{rd} \sum_{k=1}^2 \theta_k(\mathbf{x}_j)_k + z_d - \sqrt{g_r \alpha} h_{rd} \sum_{k=1}^2 \theta_k(\mathbf{x}_i)_k \right|^2 \right. \\
&\leq \left| \sum_{k=1}^2 \sqrt{\gamma_k} h_{s_k d} \theta_k(\mathbf{x}_i)_k + z_d - \sum_{k=1}^2 \sqrt{\gamma_k} h_{s_k d} \theta_k(\mathbf{x}_j)_k \right|^2 \\
&\quad \left. + \left| \sqrt{g_r \alpha} h_{rd} \sum_{k=1}^2 \theta_k(\mathbf{x}_j)_k + z_d - \sqrt{g_r \alpha} h_{rd} \sum_{k=1}^2 \theta_k(\mathbf{x}_i)_k \right|^2 \right) \\
&= P(|z_d|^2 + \left| \sqrt{g_r \alpha} h_{rd} \sum_{k=1}^2 \theta_k d_{jik} + z_d \right|^2) \\
&\geq \left| \sum_{k=1}^2 \sqrt{\gamma_k} h_{s_k d} \theta_k d_{ijk} + z_d \right|^2 + |z_d|^2) \\
&= P\left( - \left| \sum_{k=1}^2 \sqrt{\gamma_k} h_{s_k d} \theta_k d_{ijk} \right|^2 + \left| \sqrt{g_r \alpha} h_{rd} \sum_{k=1}^2 \theta_k d_{jik} \right|^2 \geq \right. \\
&\quad \left. 2 \operatorname{Re}\{z_d^* \sum_{k=1}^2 \sqrt{\gamma_k} h_{s_k d} \theta_k d_{ijk}\} - 2 \operatorname{Re}\{z_d^* \sqrt{g_r \alpha} h_{rd} \sum_{k=1}^2 \theta_k d_{jik}\} \right) \\
&= Q\left( \frac{- \left| \sum_{k=1}^2 \sqrt{\gamma_k} h_{s_k d} \theta_k d_{ijk} \right|^2 + \left| \sqrt{g_r \alpha} h_{rd} \sum_{k=1}^2 \theta_k d_{jik} \right|^2}{2\sigma \sqrt{\left| \sum_{k=1}^2 \sqrt{\gamma_k} h_{s_k d} \theta_k d_{ijk} \right|^2 + \left| \sqrt{g_r \alpha} h_{rd} \sum_{k=1}^2 \theta_k d_{jik} \right|^2}} \right)
\end{aligned} \tag{5.15}$$

Therefore, PEP at the destination which is given in Eq.(5.10) can be written as follows

$$\begin{aligned}
P(c_i \rightarrow c_j \text{ at D} | c_i) &= E_{\mathbf{h}} \left[ \left( 1 - Q\left( \frac{\left| \sum_{k=1}^2 \sqrt{g_k} h_{s_k r} \theta_k d_{ijk} \right|}{2\sigma} \right) \right) \times Q\left( \frac{\sqrt{\left| \sum_{k=1}^2 \sqrt{\gamma_k} h_{s_k d} \theta_k d_{ijk} \right|^2 + \left| \sqrt{g_r \alpha} h_{rd} \sum_{k=1}^2 \theta_k d_{jik} \right|^2}}{2\sigma} \right) \right. \\
&\quad \left. + Q\left( \frac{\left| \sum_{k=1}^2 \sqrt{g_k} h_{s_k r} \theta_k d_{ijk} \right|}{2\sigma} \right) \times Q\left( \frac{\left| \sum_{k=1}^2 \sqrt{\gamma_k} h_{s_k d} \theta_k d_{ijk} \right|^2 - \left| \sqrt{g_r \alpha} h_{rd} \sum_{k=1}^2 \theta_k d_{jik} \right|^2}{2\sigma \sqrt{\left| \sum_{k=1}^2 \sqrt{\gamma_k} h_{s_k d} \theta_k d_{ijk} \right|^2 + \left| \sqrt{g_r \alpha} h_{rd} \sum_{k=1}^2 \theta_k d_{jik} \right|^2}} \right) \right]
\end{aligned} \tag{5.16}$$

Each fading coefficient  $h_{s_k r}, h_{s_k d}, h_{rd}$  is assumed to be a zero-mean complex Gaussian random

variable with unit variance  $CN(0,1)$ . Hence,  $T_1 = \left| \sum_{k=1}^2 \sqrt{g_k} h_{s_k r} \theta_k d_{ijk} \right|^2$ ,  $T_2 = \left| \sum_{k=1}^2 \sqrt{\gamma_k} h_{s_k d} \theta_k d_{ijk} \right|^2$  and

$T_3 = \left| \sqrt{g_r} \alpha h_{rd} \sum_{k=1}^2 \theta_k d_{ijk} \right|^2$  random variables are exponential with a mean of

$\lambda_1 = \sum_{k=1}^2 g_k |\theta_k|^2 d_{ijk}^2$ ,  $\lambda_2 = \sum_{k=1}^2 \gamma_k |\theta_k|^2 d_{ijk}^2$  and  $\lambda_3 = g_r \left| \sum_{k=1}^2 \theta_k d_{ijk} \right|^2$  respectively. Therefore, PEP at the

destination can be rewritten as follows

$$\begin{aligned} P(c_i \rightarrow c_j \text{ at D} | c_i) &= (1 - \int_0^\infty Q\left(\frac{\sqrt{t_1}}{2\sigma}\right) \frac{1}{\lambda_1} e^{-\frac{t_1}{\lambda_1}} dt_1) \times \int_0^\infty \int_0^\infty Q\left(\frac{\sqrt{t_2+t_3}}{2\sigma}\right) \frac{1}{\lambda_2} e^{-\frac{t_2}{\lambda_2}} \frac{1}{\lambda_3} e^{-\frac{t_3}{\lambda_3}} dt_2 dt_3 \\ &\quad + \int_0^\infty Q\left(\frac{\sqrt{t_1}}{2\sigma}\right) \frac{1}{\lambda_1} e^{-\frac{t_1}{\lambda_1}} dt_1 \times \int_0^\infty \int_0^\infty Q\left(\frac{t_2-t_3}{2\sigma\sqrt{t_2+t_3}}\right) \frac{1}{\lambda_2} e^{-\frac{t_2}{\lambda_2}} \frac{1}{\lambda_3} e^{-\frac{t_3}{\lambda_3}} dt_2 dt_3 \end{aligned} \quad (5.17)$$

We can further this equation by using  $Q(\cdot)$  function with its alternative representation which can be given as [2]

$$Q(x) = \frac{1}{\pi} \int_0^{\pi/2} \exp\left(\frac{-x^2}{2\sin^2 \omega}\right) d\omega \quad \text{for } x > 0 \quad (5.18)$$

Hence, PEP in Eq.(5.17) can be calculated as:

$$\begin{aligned} P(c_i \rightarrow c_j \text{ at D} | c_i) &= (1 - \frac{1}{\pi} \int_0^{\pi/2} (1 + \frac{\lambda_1}{8\sigma^2 \sin^2 \omega})^{-1} d\omega) \times \frac{1}{\pi} \int_0^{\pi/2} (1 + \frac{\lambda_2}{8\sigma^2 \sin^2 \omega})^{-1} (1 + \frac{\lambda_3}{8\sigma^2 \sin^2 \omega})^{-1} d\omega \\ &\quad + \frac{1}{\pi} \int_0^{\pi/2} (1 + \frac{\lambda_1}{8\sigma^2 \sin^2 \omega})^{-1} d\omega \times \int_0^\infty \int_0^\infty Q\left(\frac{t_2-t_3}{2\sigma\sqrt{t_2+t_3}}\right) \frac{1}{\lambda_2} e^{-\frac{t_2}{\lambda_2}} \frac{1}{\lambda_3} e^{-\frac{t_3}{\lambda_3}} dt_2 dt_3 \end{aligned} \quad (5.19)$$

where  $\lambda_1 = \sum_{k=1}^2 g_k |\theta_k|^2 d_{ijk}^2$ ,  $\lambda_2 = \sum_{k=1}^2 \gamma_k |\theta_k|^2 d_{ijk}^2$  and  $\lambda_3 = g_r \left| \sum_{k=1}^2 \theta_k d_{ijk} \right|^2$ .

A closed form expression for this equation cannot be found analytically (it can be evaluated with numerical methods in MATLAB) but we can find a bound on this PEP at destination. For simplicity, we bound the fourth term in Eq. (5.10) as :

$$1 - P(c_i \rightarrow c_i \text{ at D} | c_i \rightarrow c_j \text{ at R}, c_i) \leq 1 \quad (5.20)$$

In parallel lines, the first term in Eq.(5.10) is also bounded as:

$$P(c_i \rightarrow c_i \text{ at R} | c_i) \leq 1 \quad (5.21)$$

Therefore, the upper bound for PEP at the destination can be re-written as

$$\begin{aligned} P(c_i \rightarrow c_j \text{ at D} | c_i) &\leq E_{\mathbf{h}} \left[ Q \left( \frac{\sqrt{\left| \sum_{k=1}^2 \sqrt{\gamma_k} h_{s_k d} \theta_k d_{ijk} \right|^2 + \left| \sqrt{g_r \alpha} h_{rd} \sum_{k=1}^2 \theta_k d_{ijk} \right|^2}}{2\sigma} \right) + Q \left( \frac{\left| \sum_{k=1}^2 \sqrt{g_k} h_{s_k r} \theta_k d_{ijk} \right|}{2\sigma} \right) \right] \\ &\leq E_{\mathbf{h}} \left[ 0.5 \exp \left( - \frac{\left| \sum_{k=1}^2 \sqrt{\gamma_k} h_{s_k d} \theta_k d_{ijk} \right|^2 + \left| \sqrt{g_r \alpha} h_{rd} \sum_{k=1}^2 \theta_k d_{ijk} \right|^2}{8\sigma^2} \right) + 0.5 \exp \left( - \frac{\left| \sum_{k=1}^2 \sqrt{g_k} h_{s_k r} \theta_k d_{ijk} \right|^2}{8\sigma^2} \right) \right] \\ &\leq \frac{0.5}{1 + \frac{\sum_{k=1}^2 \gamma_k |\theta_k|^2 d_{ijk}^2}{8\sigma^2}} \frac{1}{1 + \frac{g_r \alpha \left| \sum_{k=1}^2 \theta_k d_{ijk} \right|^2}{8\sigma^2}} + \frac{0.5}{1 + \frac{\sum_{k=1}^2 g_k |\theta_k|^2 d_{ijk}^2}{8\sigma^2}} \end{aligned} \quad (5.22)$$

Hence, SER-bound at the destination can be given as follows

$$\bar{P}_e^D \leq \frac{1}{8} \sum_{i=1}^4 \sum_{\substack{j=1 \\ j \neq i}}^4 \frac{1}{1 + \frac{\sum_{k=1}^2 \gamma_k |\theta_k|^2 d_{ijk}^2}{8\sigma^2}} \frac{1}{1 + \frac{g_r \alpha \left| \sum_{k=1}^2 \theta_k d_{ijk} \right|^2}{8\sigma^2}} + \frac{1}{1 + \frac{\sum_{k=1}^2 g_k |\theta_k|^2 d_{ijk}^2}{8\sigma^2}} \quad (5.23)$$

Performing the summations in Eq.(5.23) over the BPSK modulated CFNC symbols, bounds the average SER at the destination as:

$$\begin{aligned} \bar{P}_e^D &\leq \frac{1}{2} \left( 1 + \frac{\gamma_1 |\theta_1|^2}{2\sigma^2} \right)^{-1} \left( 1 + \frac{g_r \alpha |\theta_1|^2}{2\sigma^2} \right)^{-1} + \frac{1}{2} \left( 1 + \frac{g_1 |\theta_1|^2}{2\sigma^2} \right)^{-1} + \frac{1}{2} \left( 1 + \frac{\gamma_2 |\theta_2|^2}{2\sigma^2} \right)^{-1} \left( 1 + \frac{g_r \alpha |\theta_2|^2}{2\sigma^2} \right)^{-1} \\ &+ \frac{1}{2} \left( 1 + \frac{g_2 |\theta_2|^2}{2\sigma^2} \right)^{-1} + \frac{1}{4} \left( 1 + \frac{\gamma_1 |\theta_1|^2 + \gamma_2 |\theta_2|^2}{2\sigma^2} \right)^{-1} \times \left[ \left( 1 + \frac{g_r \alpha |\theta_1 + \theta_2|^2}{2\sigma^2} \right)^{-1} + \left( 1 + \frac{g_r \alpha |\theta_1 - \theta_2|^2}{2\sigma^2} \right)^{-1} \right] \\ &+ \frac{1}{2} \left( 1 + \frac{g_1 |\theta_1|^2 + g_2 |\theta_2|^2}{2\sigma^2} \right)^{-1} \end{aligned} \quad (5.24)$$

After deriving the exact PEP in Eq.(5.19), we perform some numerical experiments by placing the users and destination on the corners of an equilateral triangle with side length of unity, and by positioning the relay at the midpoint of altitude from the destination node, which results in  $\gamma_1=0$  dB,  $\gamma_2=0$  dB,  $g_1=g_2=3.60$  dB and  $g_r=7.27$  dB. We choose the signatures as  $\theta_1 = e^{j0} = 1$  and  $\theta_2 = e^{j\frac{3\pi}{4}}$ , which were used in [20]. Since we are interested in finding out an optimal but constant relay

power control  $\alpha$  during the subsequent developments  $\alpha=1$  is selected, in which the relay decodes the user symbols and forwards the CFNC symbols with no-power scaling.

Throughout this manuscript, we also define the signal-to-noise ratio (SNR) as the ratio of the total transmit power to the noise power as:

$$\text{SNR (in dB)} = 10 \log\left(\frac{P_T}{2\sigma^2}\right) \quad (5.25)$$

Since we assumed that the power budget  $P_T = (1 + \alpha)(|\theta_1|^2 + |\theta_2|^2)$  is 4 units and we obtain different SNR values by changing the variance of electronics noise.

It is important to note that the worst case PEP is because of the closest CFNC symbol pair, which result in difference vector  $\mathbf{d} = [-2, -2]^T$ . Hence, the exact PEP value in Eq. (5.19), its upper bound in Eq. (5.22) and the simulated PEP are numerically determined and plotted obtained in Figure 5-2 for this set of parameters under various SNRs. As seen from this figure, the proposed PEP bound lies within  $\sim 4$  dB of exact PEP and the simulated PEP perfectly matches with the exact analytical PEP. Another important observation is that the proposed PEP upper bound has same diversity order with the exact analytical PEP, which shows that proposed upper bound successfully mimics the diversity characteristics of the exact PEP.

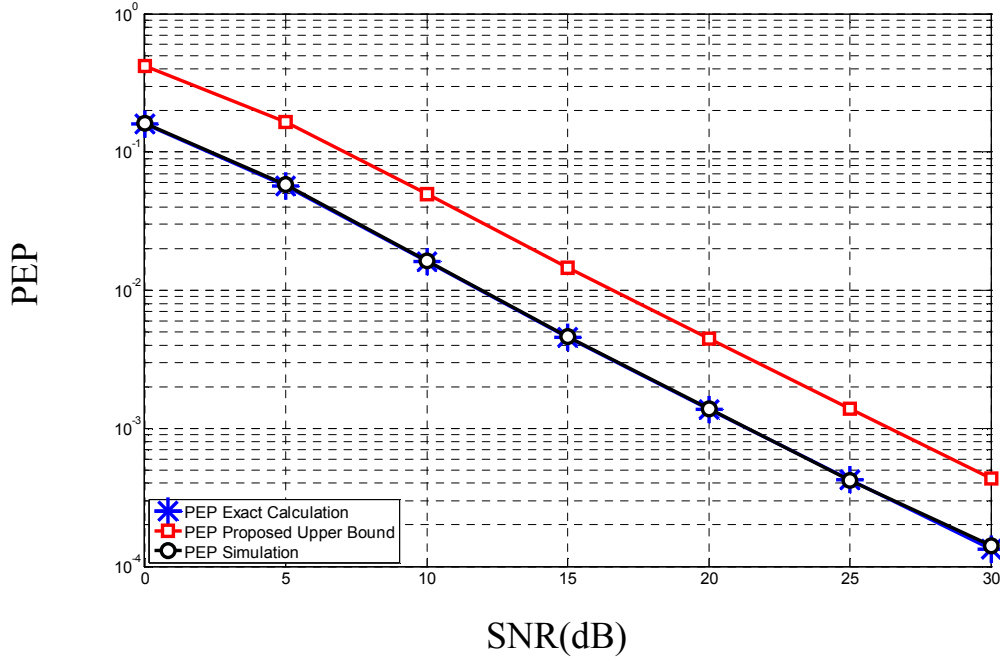


Figure 5-2 PEP as a function of SNR for  $\gamma_1=0\text{dB}$   $\gamma_2=0\text{dB}$   $g_1=g_2=3.60\text{ dB}$   $g_r=7.27\text{ dB}$

In addition, we also compare the proposed average SER bound in Eq. (5.23) with the one given in [20]. The average SER upper bound (see reference [20], p.564, Eqs(17) - (18)) is given in [20] as

$$\bar{P}_e^D \leq E \left[ (M-1)Q \left[ \sqrt{2(\Delta_{sd}\xi_{sd}^{\min} + \alpha\xi_{rd})} \right] \right] + E \left[ (M-1)^2 \exp(-\Delta_{sr}\xi_{sr}^{\min}) Q \left\{ \frac{\sqrt{2}[\Delta_{sd}\xi_{sd}^{\min} - \alpha\xi_{rd} 2\beta]}{\sqrt{\Delta_{sd}\xi_{sd}^{\min} + \alpha\xi_{rd} 2\beta}} \right\} \right] \quad (5.26)$$

where  $M$  is the cardinality of the CFNC constellation ;  $\xi_{sd}^{\min}$  and  $\xi_{sr}^{\min}$  are the minimum instantaneous SNR of the  $S$ - $D$  and  $S$ - $R$  links, respectively;  $\beta$  is the ratio of the maximum Euclidian distance  $d^{\max}$ , to the minimum Euclidean distance  $d^{\min}$  (i.e.,  $\beta = d^{\max}/d^{\min}$ ) in the CFNC constellation;  $\xi_{rd} = |h_{rd}|^2 (d^{\min}/2)^2 \bar{\xi}$  and  $|h_{rd}|^2 \bar{\xi}$  is the instantaneous SNR of the  $R$ - $D$  link where  $\bar{\xi} = \frac{P_x}{N_0}$  and  $P_x$  is average transmit power of source symbols ; parameters  $\Delta_{sr}$  and  $\Delta_{sd}$

are defined (see reference [20],p.570 Appendix A) respectively as:

$$\Delta_{sr} = \frac{\sin^2(\pi - (\arg(h_{s_2r}) + 3\pi/4))}{\beta^2}$$

$$\Delta_{sd} = \frac{\sin^2(\pi - (\arg(h_{s_2d}) + 3\pi/4))}{\beta^2}$$
(5.27)

where  $\arg(h_{s_2r})$  and  $\arg(h_{s_2d})$  represents the phases of CSI  $h_{s_2r}$  and  $h_{s_2d}$ , respectively. We numerically determine the SER-bound in Eq.(5.26) Through the Monte Carlo simulations, where the simulation parameters are taken the same as in the case when comparing the PEP bounds above (i.e.,  $\gamma_1=0\text{dB}$ ,  $\gamma_2=0\text{dB}$   $g_1=g_2=3.60\text{ dB}$   $g_r=7.27\text{ dB}$ ). Then, we have determined the exact average SER through simulation, and use it as a benchmark in order to compare the average SER bound in [20] and the proposed bound in Eq.(5.23), for which we show the simulation results in Figure 5-3.

As seen from this figure, the proposed average SER bound is closer to the exact numerical result as compared to average SER bound in [20], and the proposed and exact SER bound curves have similar slopes for all SNRs, which implies that the proposed bound captures the error characteristics of CFNC coded MAR-NOC channel better. Specifically, the proposed average SER bound lies within  $\sim 4\text{ dB}$  of the exact average SER bound for a target SER of  $10^{-1}$  while the upper bound in [20] requires approximately more than  $37.5\text{ dB}$  to achieve the same target as compared to the exact SER simulation.

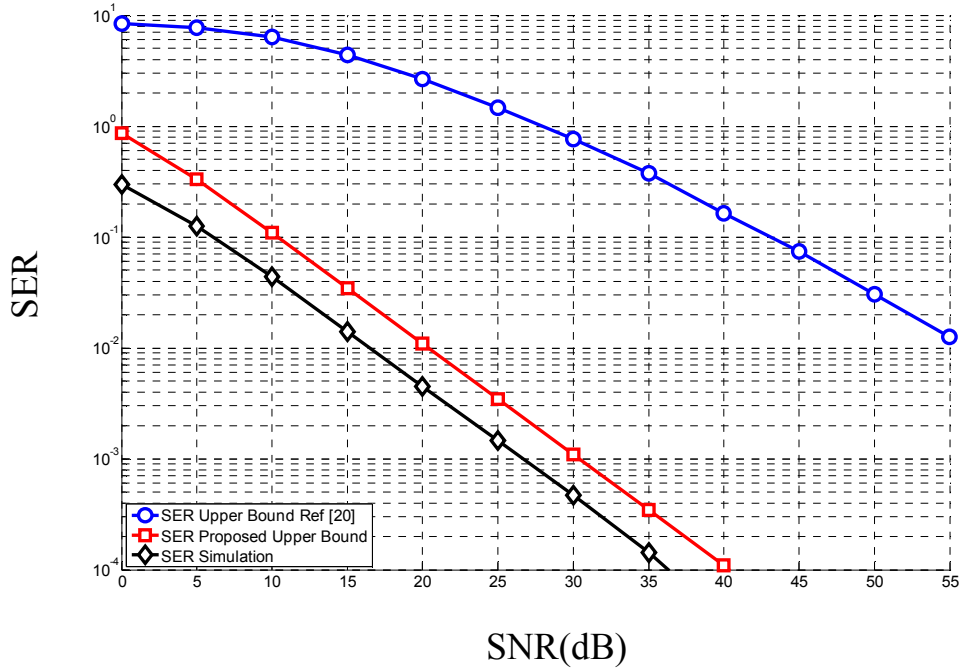


Figure 5-3 Average SER as a function of SNR for  $\gamma_1=0\text{dB}$   $\gamma_2=0\text{dB}$   $g_1=g_2=3.60\text{ dB}$   $g_r=7.27\text{ dB}$

### 5.3 Determination of SER-Optimized User-Signatures when Only Receivers Knows Channel State Information

Clearly,  $\sum_{k=1}^2 \gamma_k |\theta_k|^2 d_{ijk}^2$ ,  $|\sum_{k=1}^2 \theta_k d_{ijk}|^2$  and  $\sum_{k=1}^2 g_k |\theta_k|^2 d_{ijk}^2$  are convex functions of the user

signatures. Also,  $g_r \alpha |\sum_{k=1}^2 \theta_k d_{ijk}|^2$  is convex with respect to the parameter vector

$\mathbf{p}=[\theta_1, \theta_2, \alpha]^T$  since the multiplication of two convex scalar functions is also convex when both functions are non-decreasing (non-increasing) and positive [85]. Additionally,

$\left(1 + \frac{g_r \alpha |\sum_{k=1}^2 \theta_k d_{ijk}|^2}{8\sigma^2}\right)^{-1}$  is convex since  $f(x) = \frac{1}{1+x}$  is convex for  $x \geq 0$  and the composition of a

convex scalar function with another convex scalar function is convex. Therefore, the average

SER bound in Eq. (5.22) is convex.

Since the average SER bound in Eq. (5.24) is convex in both user signatures  $\theta_1$  and  $\theta_2$ , and in relay power control parameter  $\alpha$ , they can be jointly adjusted in order to minimize that bound under the total power constraint  $\sum_{k=1}^2 |\theta_k|^2 + \alpha (\sum_{k=1}^2 |\theta_k|^2) \leq P_T$ . Additionally, since the information of each user can be recovered from the CFNC coded symbol  $c[n]$  only if  $\theta_1 \neq \theta_2$ , there is a second constraint for the signatures, which can be expressed as  $|\theta_1 - \theta_2|^2 > 0$ . The third constraint is resultant from the fact that the relay actively sends information, and thus  $\alpha$  is strictly greater than zero. Therefore, the determination of joint SER-optimized signatures and the relay power can be stated as a constrained optimization problem as:

$$\begin{aligned} \underset{\theta_1, \theta_2, \alpha}{\text{minimize}} f_0(\theta_1, \theta_2, \alpha) &= \frac{1}{2} \left(1 + \frac{\gamma_1 |\theta_1|^2}{2\sigma^2}\right)^{-1} \left(1 + \frac{g_r \alpha |\theta_1|^2}{2\sigma^2}\right)^{-1} + \frac{1}{2} \left(1 + \frac{g_1 |\theta_1|^2}{2\sigma^2}\right)^{-1} + \frac{1}{2} \left(1 + \frac{\gamma_2 |\theta_2|^2}{2\sigma^2}\right)^{-1} \\ &+ \left(1 + \frac{g_r \alpha |\theta_2|^2}{2\sigma^2}\right)^{-1} + \frac{1}{2} \left(1 + \frac{g_2 |\theta_2|^2}{2\sigma^2}\right)^{-1} + \frac{1}{4} \left(1 + \frac{\gamma_1 |\theta_1|^2 + \gamma_2 |\theta_2|^2}{2\sigma^2}\right)^{-1} \times \left[ \left(1 + \frac{g_r \alpha |\theta_1 + \theta_2|^2}{2\sigma^2}\right)^{-1} \right. \\ &\left. + \left(1 + \frac{g_r \alpha |\theta_1 - \theta_2|^2}{2\sigma^2}\right)^{-1} \right] + \frac{1}{2} \left(1 + \frac{g_1 |\theta_1|^2 + g_2 |\theta_2|^2}{2\sigma^2}\right)^{-1} \end{aligned} \quad (5.28)$$

such that

$$\begin{aligned} f_1(\theta_1, \theta_2, \alpha) &= P_T - \sum_{k=1}^2 |\theta_k|^2 - \alpha \left(\sum_{k=1}^2 |\theta_k|^2\right) \geq 0 \\ f_2(\theta_1, \theta_2, \alpha) &= |\theta_1 - \theta_2|^2 > 0 \\ f_3(\theta_1, \theta_2, \alpha) &= \alpha > 0 \end{aligned}$$

The optimization in Eq. (5.28) is a convex program and thereby its unique global minimum exists, which should satisfy the following Karush-Kuhn-Tucker (KKT) conditions [87]. The KKT conditions for this problem can be expressed by using Wirtinger derivative of a complex function [90] as

$$\frac{\partial f(\theta)}{\partial \theta} = \frac{1}{2} \left( \frac{\partial f(\theta)}{\partial \theta_r} - j \frac{\partial f(\theta)}{\partial \theta_i} \right) \quad (5.29)$$

Where  $\theta$  is a complex number, whose real and imaginary parts are represented as  $\theta_r$  and  $\theta_i$ , respectively.

Based on the Wirtinger derivative, the KKT conditions of the considered optimization problem can be written as:

$$\begin{aligned}
& \frac{\gamma_1 \theta_1^*}{4\sigma^2} \left(1 + \frac{\gamma_1 |\theta_1|^2}{2\sigma^2}\right)^{-2} \left(1 + \frac{g_r \alpha |\theta_1|^2}{2\sigma^2}\right)^{-1} + \frac{g_r \alpha \theta_1^*}{4\sigma^2} \left(1 + \frac{\gamma_1 |\theta_1|^2}{2\sigma^2}\right)^{-1} \left(1 + \frac{g_r \alpha |\theta_1|^2}{2\sigma^2}\right)^{-2} + \frac{g_1 \theta_1^*}{4\sigma^2} \left(1 + \frac{g_1 |\theta_1|^2}{2\sigma^2}\right)^{-2} + \\
& \frac{\gamma_1 \theta_1^*}{8\sigma^2} \left(1 + \frac{\gamma_1 |\theta_1|^2 + \gamma_2 |\theta_2|^2}{2\sigma^2}\right)^{-2} \times \left[ \left(1 + \frac{g_r \alpha |\theta_1 + \theta_2|^2}{2\sigma^2}\right)^{-1} + \left(1 + \frac{g_r \alpha |\theta_1 - \theta_2|^2}{2\sigma^2}\right)^{-1} \right] + \\
& \left(1 + \frac{\gamma_1 |\theta_1|^2 + \gamma_2 |\theta_2|^2}{2\sigma^2}\right)^{-1} \times \left[ \frac{g_r \alpha (\theta_1 + \theta_2)^*}{8\sigma^2} \left(1 + \frac{g_r \alpha |\theta_1 + \theta_2|^2}{2\sigma^2}\right)^{-2} + \frac{g_r \alpha (\theta_1 - \theta_2)^*}{8\sigma^2} \left(1 + \frac{g_r \alpha |\theta_1 - \theta_2|^2}{2\sigma^2}\right)^{-2} \right] + \\
& \left[ \frac{g_1 \theta_1^*}{4\sigma^2} \left(1 + \frac{g_1 |\theta_1|^2 + g_2 |\theta_2|^2}{2\sigma^2}\right)^{-2} \right] + \lambda_1 (-\theta_1^* (1 + \alpha)) + \lambda_2 (\theta_1 - \theta_2)^* = 0
\end{aligned} \tag{5.30}$$

$$\begin{aligned}
& \frac{\gamma_2 \theta_2^*}{4\sigma^2} \left(1 + \frac{\gamma_2 |\theta_2|^2}{2\sigma^2}\right)^{-2} \left(1 + \frac{g_r \alpha |\theta_2|^2}{2\sigma^2}\right)^{-1} + \frac{g_r \alpha \theta_2^*}{4\sigma^2} \left(1 + \frac{\gamma_2 |\theta_2|^2}{2\sigma^2}\right)^{-1} \left(1 + \frac{g_r \alpha |\theta_2|^2}{2\sigma^2}\right)^{-2} + \frac{g_2 \theta_2^*}{4\sigma^2} \left(1 + \frac{g_2 |\theta_2|^2}{2\sigma^2}\right)^{-2} + \\
& \frac{\gamma_2 \theta_2^*}{8\sigma^2} \left(1 + \frac{\gamma_1 |\theta_1|^2 + \gamma_2 |\theta_2|^2}{2\sigma^2}\right)^{-2} \times \left[ \left(1 + \frac{g_r \alpha |\theta_1 + \theta_2|^2}{2\sigma^2}\right)^{-1} + \left(1 + \frac{g_r \alpha |\theta_1 - \theta_2|^2}{2\sigma^2}\right)^{-1} \right] + \\
& \left(1 + \frac{\gamma_1 |\theta_1|^2 + \gamma_2 |\theta_2|^2}{2\sigma^2}\right)^{-1} \times \left[ \frac{g_r \alpha (\theta_1 + \theta_2)^*}{8\sigma^2} \left(1 + \frac{g_r \alpha |\theta_1 + \theta_2|^2}{2\sigma^2}\right)^{-2} + \frac{g_r \alpha (-\theta_1 + \theta_2)^*}{8\sigma^2} \left(1 + \frac{g_r \alpha |\theta_1 - \theta_2|^2}{2\sigma^2}\right)^{-2} \right] + \\
& \left[ \frac{g_2 \theta_2^*}{4\sigma^2} \left(1 + \frac{g_1 |\theta_1|^2 + g_2 |\theta_2|^2}{2\sigma^2}\right)^{-2} \right] + \lambda_1 (-\theta_2^* (1 + \alpha)) + \lambda_2 (-\theta_1 + \theta_2)^* = 0
\end{aligned} \tag{5.31}$$

$$\begin{aligned}
& \frac{g_r |\theta_1|^2}{4\sigma^2} \left(1 + \frac{\gamma_1 |\theta_1|^2}{2\sigma^2}\right)^{-1} \left(1 + \frac{g_r \alpha |\theta_1|^2}{2\sigma^2}\right)^{-2} + \frac{g_r |\theta_2|^2}{4\sigma^2} \left(1 + \frac{\gamma_2 |\theta_2|^2}{2\sigma^2}\right)^{-1} \left(1 + \frac{g_r \alpha |\theta_2|^2}{2\sigma^2}\right)^{-2} + \\
& \left(1 + \frac{\gamma_1 |\theta_1|^2 + \gamma_2 |\theta_2|^2}{2\sigma^2}\right)^{-1} \times \left[ \frac{g_r |\theta_1 + \theta_2|^2}{8\sigma^2} \left(1 + \frac{g_r \alpha |\theta_1 + \theta_2|^2}{2\sigma^2}\right)^{-2} + \frac{g_r |\theta_1 - \theta_2|^2}{8\sigma^2} \left(1 + \frac{g_r \alpha |\theta_1 - \theta_2|^2}{2\sigma^2}\right)^{-2} \right] + \\
& \lambda_1 (-|\theta_1|^2 - |\theta_2|^2) + \lambda_3 (1) = 0
\end{aligned} \tag{5.32}$$

Since we assume that relay is located between users and destination  $\alpha$  have to be greater than zero which makes  $\lambda_3 = 0$ . Also,  $|\theta_1 - \theta_2|^2$  have to be greater than zero to recover each user's information so  $\lambda_2$  have to be equal to zero and . Hence, the Eq.(5.30) becomes

$$\begin{aligned}
& \frac{\gamma_1}{(1+\alpha)4\sigma^2} \left(1 + \frac{\gamma_1|\theta_1|^2}{2\sigma^2}\right)^{-2} \left(1 + \frac{g_r\alpha|\theta_1|^2}{2\sigma^2}\right)^{-1} + \frac{g_r\alpha}{(1+\alpha)4\sigma^2} \left(1 + \frac{\gamma_1|\theta_1|^2}{2\sigma^2}\right)^{-1} \left(1 + \frac{g_r\alpha|\theta_1|^2}{2\sigma^2}\right)^{-2} + \frac{g_i}{(1+\alpha)4\sigma^2} \\
& \times \left(1 + \frac{g_i|\theta_1|^2}{2\sigma^2}\right)^{-2} + \frac{\gamma_1}{(1+\alpha)8\sigma^2} \left(1 + \frac{\gamma_1|\theta_1|^2 + \gamma_2|\theta_2|^2}{2\sigma^2}\right)^{-2} \times \left[\left(1 + \frac{g_r\alpha|\theta_1 + \theta_2|^2}{2\sigma^2}\right)^{-1} + \left(1 + \frac{g_r\alpha|\theta_1 - \theta_2|^2}{2\sigma^2}\right)^{-1}\right] + \\
& \frac{\theta_1}{|\theta_1|^2(1+\alpha)} \left(1 + \frac{\gamma_1|\theta_1|^2 + \gamma_2|\theta_2|^2}{2\sigma^2}\right)^{-1} \times \left[\frac{g_r\alpha(\theta_1 + \theta_2)^*}{8\sigma^2} \left(1 + \frac{g_r\alpha|\theta_1 + \theta_2|^2}{2\sigma^2}\right)^{-2} \right. \\
& \left. + \frac{g_r\alpha(\theta_1 - \theta_2)^*}{8\sigma^2} \left(1 + \frac{g_r\alpha|\theta_1 - \theta_2|^2}{2\sigma^2}\right)^{-2}\right] + \frac{g_i}{(1+\alpha)4\sigma^2} \left(1 + \frac{g_i|\theta_1|^2 + g_2|\theta_2|^2}{2\sigma^2}\right)^{-2} = \lambda_1
\end{aligned} \tag{5.33}$$

Since  $\lambda_1$  is a real number, real part of the of left hand side of Eq.(5.30) have to be equal to  $\lambda_1$  and imaginary part have to be zero

$$\text{Im}\left\{\frac{g_r\alpha\theta_1\theta_2^*}{|\theta_1|^2(1+\alpha)8\sigma^2} \left(1 + \frac{g_r\alpha|\theta_1 + \theta_2|^2}{2\sigma^2}\right)^{-2} - \frac{g_r\alpha\theta_1\theta_2^*}{|\theta_1|^2(1+\alpha)8\sigma^2} \left(1 + \frac{g_r\alpha|\theta_1 - \theta_2|^2}{2\sigma^2}\right)^{-2}\right\} = 0 \tag{5.34}$$

We can rearrange this equation as

$$\text{Im}\left\{\frac{g_r\alpha\theta_1\theta_2^*}{|\theta_1|^2(1+\alpha)8\sigma^2} \left(\left(1 + \frac{g_r\alpha|\theta_1 + \theta_2|^2}{2\sigma^2}\right)^{-2} - \left(1 + \frac{g_r\alpha|\theta_1 - \theta_2|^2}{2\sigma^2}\right)^{-2}\right)\right\} = 0 \tag{5.35}$$

Since  $g_r, \alpha > 0$  we obtain the following equation

$$\left(\frac{1}{\left(1 + \frac{g_r\alpha|\theta_1 + \theta_2|^2}{2\sigma^2}\right)^2} - \frac{1}{\left(1 + \frac{g_r\alpha|\theta_1 - \theta_2|^2}{2\sigma^2}\right)^2}\right) \text{Im}\{\theta_1\theta_2^*\} = 0 \tag{5.36}$$

And this equation can be rewritten as follows

$$\begin{aligned}
& \left(\frac{|\theta_1||\theta_2|\sin(\arg(\theta_1) - \arg(\theta_2))}{\left(1 + \frac{g_r\alpha(|\theta_1|^2 + |\theta_2|^2 - 2|\theta_1||\theta_2|\cos(\arg(\theta_1) - \arg(\theta_2)))}{\sigma^2}\right)^2} \right. \\
& \left. - \frac{|\theta_1||\theta_2|\sin(\arg(\theta_1) - \arg(\theta_2))}{\left(1 + \frac{g_r\alpha(|\theta_1|^2 + |\theta_2|^2 + 2|\theta_1||\theta_2|\cos(\arg(\theta_1) - \arg(\theta_2)))}{\sigma^2}\right)^2}\right) = 0
\end{aligned} \tag{5.37}$$

Hence this equation can be satisfied when

$$\sin(\arg(\theta_1) - \arg(\theta_2)) = 0 \text{ or } \cos(\arg(\theta_1) - \arg(\theta_2)) = 0 \tag{5.38}$$

On the other hand, by analyzing objective function we can observe that only term affected by the

value of  $\arg(\theta_1) - \arg(\theta_2)$  is

$$\left[ \left(1 + \frac{g_r \alpha |\theta_1 + \theta_2|^2}{2\sigma^2}\right)^{-1} + \left(1 + \frac{g_r \alpha |\theta_1 - \theta_2|^2}{2\sigma^2}\right)^{-1} \right] \quad (5.39)$$

which is always positive. Therefore, we can find the optimum value of  $\arg(\theta_1) - \arg(\theta_2)$  selecting the one which minimizes in Eq.(5.39) from Eq.(5.38). If we rewrite Eq.(5.39) as follows

$$\begin{aligned} & \left[ \left(1 + \frac{g_r \alpha \left( |\theta_1|^2 + |\theta_2|^2 + 2|\theta_1||\theta_2| \cos(\arg(\theta_1) - \arg(\theta_2)) \right)}{2\sigma^2} \right)^{-1} \right. \\ & \left. + \left(1 + \frac{g_r \alpha \left( |\theta_1|^2 + |\theta_2|^2 - 2|\theta_1||\theta_2| \cos(\arg(\theta_1) - \arg(\theta_2)) \right)}{2\sigma^2} \right)^{-1} \right] \end{aligned} \quad (5.40)$$

we can see the effect of difference of argument of  $\theta_1$  and  $\theta_2$ . By taking the derivative of this term with respect to  $\cos(\arg(\theta_1) - \arg(\theta_2))$  and equating it to zero we have

$$\begin{aligned} & - \left(1 + \frac{g_r \alpha \left( |\theta_1|^2 + |\theta_2|^2 + 2|\theta_1||\theta_2| \cos(\arg(\theta_1) - \arg(\theta_2)) \right)}{2\sigma^2} \right)^{-2} \frac{g_r \alpha (2|\theta_1||\theta_2|)}{2\sigma^2} \\ & - \left(1 + \frac{g_r \alpha \left( |\theta_1|^2 + |\theta_2|^2 - 2|\theta_1||\theta_2| \cos(\arg(\theta_1) - \arg(\theta_2)) \right)}{2\sigma^2} \right)^{-2} \times \frac{-g_r \alpha (2|\theta_1||\theta_2|)}{2\sigma^2} = 0 \end{aligned} \quad (5.41)$$

By simplifying this equation we have

$$2|\theta_1||\theta_2| \cos(\arg(\theta_1) - \arg(\theta_2)) = -2|\theta_1||\theta_2| \cos(\arg(\theta_1) - \arg(\theta_2)) \quad (5.42)$$

which implies

$$\cos(\arg(\theta_1) - \arg(\theta_2)) = 0 \quad (5.43)$$

Hence we can conclude that the difference between phases of  $\theta_1$  and  $\theta_2$  have to be

$$\arg(\theta_1) - \arg(\theta_2) = (2k + 1)\pi / 2 \text{ for any integer } k \quad (5.44)$$

After simplifying KKT conditions of the program using Eq.(5.44), we show that the total power constraint become active at the optimal values of CFNC signatures and the relay power control parameter  $\alpha$ , should satisfy the following expression

$$\begin{aligned}
& \frac{\gamma_1}{(1+\alpha)4\sigma^2} \left(1 + \frac{\gamma_1|\theta_1|^2}{2\sigma^2}\right)^{-2} \left(1 + \frac{g_r\alpha|\theta_1|^2}{2\sigma^2}\right)^{-1} + \frac{g_r\alpha}{(1+\alpha)4\sigma^2} \left(1 + \frac{\gamma_1|\theta_1|^2}{2\sigma^2}\right)^{-1} \left(1 + \frac{g_r\alpha|\theta_1|^2}{2\sigma^2}\right)^{-2} + \frac{g_1}{(1+\alpha)8\sigma^2} \\
& \times \left(1 + \frac{g_1|\theta_1|^2}{2\sigma^2}\right)^{-2} + \frac{\gamma_1}{(1+\alpha)4\sigma^2} \left(1 + \frac{\gamma_1|\theta_1|^2 + \gamma_2|\theta_2|^2}{2\sigma^2}\right)^{-2} \left(1 + \frac{g_r\alpha(|\theta_1|^2 + |\theta_2|^2)}{2\sigma^2}\right)^{-1} + \frac{g_1}{(1+\alpha)4\sigma^2} \\
& \times \left(1 + \frac{g_1|\theta_1|^2 + g_2|\theta_2|^2}{2\sigma^2}\right)^{-2} \\
& = \frac{\gamma_2}{(1+\alpha)4\sigma^2} \left(1 + \frac{\gamma_2|\theta_2|^2}{2\sigma^2}\right)^{-2} \left(1 + \frac{g_r\alpha|\theta_1|^2}{2\sigma^2}\right)^{-1} + \frac{g_r\alpha}{(1+\alpha)4\sigma^2} \left(1 + \frac{\gamma_2|\theta_2|^2}{2\sigma^2}\right)^{-1} \left(1 + \frac{g_r\alpha|\theta_1|^2}{2\sigma^2}\right)^{-2} + \frac{g_2}{(1+\alpha)4\sigma^2} \\
& \times \left(1 + \frac{g_2|\theta_2|^2}{2\sigma^2}\right)^{-2} + \frac{\gamma_2}{(1+\alpha)4\sigma^2} \left(1 + \frac{\gamma_1|\theta_1|^2 + \gamma_2|\theta_2|^2}{2\sigma^2}\right)^{-2} \left(1 + \frac{g_r\alpha(|\theta_1|^2 + |\theta_2|^2)}{2\sigma^2}\right)^{-1} + \frac{g_2}{(1+\alpha)4\sigma^2} \\
& \times \left(1 + \frac{g_1|\theta_1|^2 + g_2|\theta_2|^2}{2\sigma^2}\right)^{-2} \\
& = \frac{g_r|\theta_1|^2}{4\sigma^2(|\theta_1|^2 + |\theta_2|^2)} \left(1 + \frac{\gamma_1|\theta_1|^2}{2\sigma^2}\right)^{-1} \left(1 + \frac{g_r\alpha|\theta_1|^2}{2\sigma^2}\right)^{-2} + \frac{g_r|\theta_2|^2}{4\sigma^2(|\theta_1|^2 + |\theta_2|^2)} \left(1 + \frac{\gamma_2|\theta_2|^2}{2\sigma^2}\right)^{-1} \left(1 + \frac{g_r\alpha|\theta_2|^2}{2\sigma^2}\right)^{-2} + \\
& \left(1 + \frac{\gamma_1|\theta_1|^2 + \gamma_2|\theta_2|^2}{2\sigma^2}\right)^{-1} \times \left[ \frac{g_r|\theta_1 + \theta_2|^2}{8\sigma^2(|\theta_1|^2 + |\theta_2|^2)} \left(1 + \frac{g_r\alpha|\theta_1 + \theta_2|^2}{2\sigma^2}\right)^{-2} + \frac{g_r|\theta_1 - \theta_2|^2}{8\sigma^2(|\theta_1|^2 + |\theta_2|^2)} \left(1 + \frac{g_r\alpha|\theta_1 - \theta_2|^2}{2\sigma^2}\right)^{-1} \right]
\end{aligned} \tag{5.45}$$

Hence, Eq.(5.44) implies that the phases of user signatures phases should be separated by any odd multiples of  $90^\circ$ . Obtaining a solution for the magnitude of user signatures together with relay power control parameter  $\alpha$  from Eq. (5.45) under the total power constraint is not, however, viable in general since it is highly nonlinear. Therefore, they can be determined numerically by using an iterative technique such as Sequential Quadratic Programming (SQP) kind of approach [87], which shall be investigated below.

After the use of the angle condition in Eq. (5.44), the objection function in Eq. (5.28) becomes

$$\begin{aligned}
f_0(\theta_1, \theta_2, \alpha) &= \frac{1}{2} \left(1 + \frac{\gamma_1|\theta_1|^2}{2\sigma^2}\right)^{-1} \left(1 + \frac{g_r\alpha|\theta_1|^2}{2\sigma^2}\right)^{-1} + \frac{1}{2} \left(1 + \frac{g_1|\theta_1|^2}{2\sigma^2}\right)^{-1} + \\
& \frac{1}{2} \left(1 + \frac{\gamma_2|\theta_2|^2}{2\sigma^2}\right)^{-1} \left(1 + \frac{g_r\alpha|\theta_2|^2}{2\sigma^2}\right)^{-1} + \frac{1}{2} \left(1 + \frac{g_2|\theta_2|^2}{2\sigma^2}\right)^{-1} + \\
& \frac{1}{2} \left(1 + \frac{\gamma_1|\theta_1|^2 + \gamma_2|\theta_2|^2}{2\sigma^2}\right)^{-1} \left(1 + \frac{g_r\alpha(|\theta_1|^2 + |\theta_2|^2)}{2\sigma^2}\right)^{-1} + \frac{1}{2} \left(1 + \frac{g_1|\theta_1|^2 + g_2|\theta_2|^2}{2\sigma^2}\right)^{-1}
\end{aligned} \tag{5.46}$$

By making a change of variables such that  $P_1 \triangleq |\theta_1|^2$ ,  $P_2 \triangleq |\theta_2|^2$  and  $P_r \triangleq \alpha(|\theta_1|^2 + |\theta_2|^2)$ , the total power constraint turns into  $P_1 + P_2 + P_r = P_T$  since the power constraint has shown to be active at

the optimal solution, and the  $l^{\text{th}}$  iteration of SQP utilizes the best quadratic approximation of the objective function around current iterate  $\mathbf{q}_l$  and solve the following sub-problem to obtain next iterate  $\mathbf{q}_{l+1}$ .

$$\begin{aligned} & \min f_0(\mathbf{q}_l) + \nabla f_0(\mathbf{q}_l)^T (\mathbf{q} - \mathbf{q}_l) + \frac{1}{2} (\mathbf{q} - \mathbf{q}_l)^T \nabla^2 f_0(\mathbf{q}_l) (\mathbf{q} - \mathbf{q}_l) \\ & \text{such that} \\ & \mathbf{a}^T \mathbf{q} = b \\ & \mathbf{c}^T \mathbf{q} > 0 \\ & \mathbf{d}^T \mathbf{q} > 0 \\ & \mathbf{e}^T \mathbf{q} > 0 \end{aligned} \quad (5.47)$$

where  $\mathbf{q} = [P_1, P_2, P_r]^T$ ,  $\nabla f_0(\mathbf{q}_l)^T$  and  $\nabla^2 f_0(\mathbf{q}_l)$  are the gradient vector and Hessian matrix of the objective function  $f_0(P_1, P_2, \alpha)$  around the solution  $\mathbf{q}_l = [P_{1,l}, P_{2,l}, P_{r,l}]^T$  at the  $l^{\text{th}}$  iteration, respectively, and  $\mathbf{a} = [1, 1, 1]^T$ ,  $b = P_r$ ,  $\mathbf{c} = [1, 0, 0]^T$ ,  $\mathbf{d} = [0, 1, 0]^T$ ,  $\mathbf{e} = [0, 0, 1]^T$ . Gradient vector can be written in detail as

$$\nabla f_0(\mathbf{q}_l)^T = [f_{P_1}, f_{P_2}, f_{P_r}] \quad (5.48)$$

where

$$\begin{aligned} f_{P_1} = & -\frac{\gamma_1}{4\sigma^2} \left(1 + \frac{\gamma_1 P_{1,l}}{2\sigma^2}\right)^{-2} \left(1 + \frac{g_r \alpha_l P_{1,l}}{2\sigma^2}\right)^{-1} - \frac{g_r \alpha_l}{4\sigma^2} \left(1 + \frac{\gamma_1 P_{1,l}}{2\sigma^2}\right)^{-1} \left(1 + \frac{g_r \alpha_l P_{1,l}}{2\sigma^2}\right)^{-2} - \frac{g_1}{4\sigma^2} \left(1 + \frac{g_1 P_{1,l}}{2\sigma^2}\right)^{-2} \\ & - \frac{\gamma_1}{4\sigma^2} \left(1 + \frac{\gamma_1 P_{1,l} + \gamma_2 P_{2,l}}{2\sigma^2}\right)^{-2} \left(1 + \frac{g_r \alpha_l (P_{1,l} + P_{2,l})}{2\sigma^2}\right)^{-1} - \frac{g_r \alpha_l}{4\sigma^2} \left(1 + \frac{\gamma_1 P_{1,l} + \gamma_2 P_{2,l}}{2\sigma^2}\right)^{-1} \left(1 + \frac{g_r \alpha_l (P_{1,l} + P_{2,l})}{2\sigma^2}\right)^{-2} \\ & - \frac{g_1}{4\sigma^2} \left(1 + \frac{g_1 P_{1,l} + g_2 P_{2,l}}{2\sigma^2}\right)^{-2} \end{aligned} \quad (5.49)$$

$$\begin{aligned} f_{P_2} = & -\frac{\gamma_2}{4\sigma^2} \left(1 + \frac{\gamma_2 P_{2,l}}{2\sigma^2}\right)^{-2} \left(1 + \frac{g_r \alpha_l P_{2,l}}{2\sigma^2}\right)^{-1} - \frac{g_r \alpha_l}{4\sigma^2} \left(1 + \frac{\gamma_2 P_{2,l}}{2\sigma^2}\right)^{-1} \left(1 + \frac{g_r \alpha_l P_{2,l}}{2\sigma^2}\right)^{-2} - \frac{g_2}{4\sigma^2} \left(1 + \frac{g_2 P_{2,l}}{2\sigma^2}\right)^{-2} \\ & - \frac{\gamma_2}{4\sigma^2} \left(1 + \frac{\gamma_1 P_{1,l} + \gamma_2 P_{2,l}}{2\sigma^2}\right)^{-2} \left(1 + \frac{g_r \alpha_l (P_{1,l} + P_{2,l})}{2\sigma^2}\right)^{-1} - \frac{g_r \alpha_l}{4\sigma^2} \left(1 + \frac{\gamma_1 P_{1,l} + \gamma_2 P_{2,l}}{2\sigma^2}\right)^{-1} \left(1 + \frac{g_r \alpha_l (P_{1,l} + P_{2,l})}{2\sigma^2}\right)^{-2} \\ & - \frac{g_1}{4\sigma^2} \left(1 + \frac{g_1 P_{1,l} + g_2 P_{2,l}}{2\sigma^2}\right)^{-2} \end{aligned} \quad (5.50)$$

$$f_{P_r} = \left( -\frac{g_r P_{1,l}}{4\sigma^2} \left(1 + \frac{\gamma_1 P_{1,l}}{2\sigma^2}\right)^{-1} \left(1 + \frac{g_r \alpha_l P_{1,l}}{2\sigma^2}\right)^{-2} - \frac{g_r P_{2,l}}{4\sigma^2} \left(1 + \frac{\gamma_2 P_{2,l}}{2\sigma^2}\right)^{-1} \left(1 + \frac{g_r \alpha_l P_{2,l}}{2\sigma^2}\right)^{-2} - \frac{g_r (P_{1,l} + P_{2,l})}{4\sigma^2} \left(1 + \frac{\gamma_1 P_{1,l} + \gamma_2 P_{2,l}}{2\sigma^2}\right)^{-1} \left(1 + \frac{g_r \alpha_l (P_{1,l} + P_{2,l})}{2\sigma^2}\right)^{-2} \right) \frac{P_T}{(P_T - P_r)^2} \quad (5.51)$$

Also, Hessian matrix can be written as

$$\nabla^2 f_0(\mathbf{q}_l) = \begin{bmatrix} f_{P_1 P_1} & f_{P_1 P_2} & f_{P_1 P_r} \\ f_{P_2 P_1} & f_{P_2 P_2} & f_{P_2 P_r} \\ f_{P_r P_1} & f_{P_r P_2} & f_{P_r P_r} \end{bmatrix} \quad (5.52)$$

Where

$$\begin{aligned} f_{P_1 P_1} &= \frac{\gamma_1^2}{4\sigma^4} \left(1 + \frac{\gamma_1 P_{1,l}}{2\sigma^2}\right)^{-3} \left(1 + \frac{g_r \alpha_l P_{1,l}}{2\sigma^2}\right)^{-1} + \frac{\gamma_1 g_r \alpha_l}{4\sigma^4} \left(1 + \frac{\gamma_1 P_{1,l}}{2\sigma^2}\right)^{-2} \left(1 + \frac{g_r \alpha_l P_{1,l}}{2\sigma^2}\right)^{-2} + \frac{g_r^2 \alpha_l^2}{4\sigma^4} \left(1 + \frac{\gamma_1 P_{1,l}}{2\sigma^2}\right)^{-1} \\ &\times \left(1 + \frac{g_r \alpha_l P_{1,l}}{2\sigma^2}\right)^{-3} + \frac{g_1^2}{4\sigma^4} \left(1 + \frac{g_1 P_{1,l}}{2\sigma^2}\right)^{-3} + \frac{\gamma_1^2}{4\sigma^4} \left(1 + \frac{\gamma_1 P_{1,l} + \gamma_2 P_{2,l}}{2\sigma^2}\right)^{-3} \left(1 + \frac{g_r \alpha_l (P_{1,l} + P_{2,l})}{2\sigma^2}\right)^{-1} \\ &+ \frac{\gamma_1 g_r \alpha_l}{4\sigma^4} \left(1 + \frac{\gamma_1 P_{1,l} + \gamma_2 P_{2,l}}{2\sigma^2}\right)^{-2} \left(1 + \frac{g_r \alpha_l (P_{1,l} + P_{2,l})}{2\sigma^2}\right)^{-2} + \frac{g_r^2 \alpha_l^2}{4\sigma^4} \left(1 + \frac{\gamma_1 P_{1,l} + \gamma_2 P_{2,l}}{2\sigma^2}\right)^{-1} \\ &\times \left(1 + \frac{g_r \alpha_l (P_{1,l} + P_{2,l})}{2\sigma^2}\right)^{-3} + \frac{g_1^2}{4\sigma^2} \left(1 + \frac{g_1 P_{1,l} + g_2 P_{2,l}}{2\sigma^2}\right)^{-3} \end{aligned} \quad (5.53)$$

$$\begin{aligned} f_{P_1 P_2} &= f_{P_2 P_1} \\ &= \frac{\gamma_1 \gamma_2}{4\sigma^4} \left(1 + \frac{\gamma_1 P_{1,l} + \gamma_2 P_{2,l}}{2\sigma^2}\right)^{-3} \left(1 + \frac{g_r \alpha_l (P_{1,l} + P_{2,l})}{2\sigma^2}\right)^{-1} + \frac{g_r (\gamma_1 + \gamma_2) \alpha_l}{8\sigma^4} \left(1 + \frac{\gamma_1 P_{1,l} + \gamma_2 P_{2,l}}{2\sigma^2}\right)^{-2} \\ &\times \left(1 + \frac{g_r \alpha_l (P_{1,l} + P_{2,l})}{2\sigma^2}\right)^{-2} + \frac{g_r^2 \alpha_l^2}{4\sigma^4} \left(1 + \frac{\gamma_1 P_{1,l} + \gamma_2 P_{2,l}}{2\sigma^2}\right)^{-1} \left(1 + \frac{g_r \alpha_l (P_{1,l} + P_{2,l})}{2\sigma^2}\right)^{-3} \\ &+ \frac{g_1 g_2}{4\sigma^4} \left(1 + \frac{g_1 P_{1,l} + g_2 P_{2,l}}{2\sigma^2}\right)^{-2} \end{aligned} \quad (5.54)$$

$$\begin{aligned}
f_{P_1 P_r} &= f_{P_r P_1} \\
&= \left( \frac{\gamma_1 g_r P_{1,l}}{8\sigma^4} \left(1 + \frac{\gamma_1 P_{1,l}}{2\sigma^2}\right)^{-2} \left(1 + \frac{g_r \alpha_l P_{1,l}}{2\sigma^2}\right)^{-2} - \frac{g_r}{4\sigma^2} \left(1 + \frac{\gamma_1 P_{1,l}}{2\sigma^2}\right)^{-1} \left(1 + \frac{g_r \alpha_l P_{1,l}}{2\sigma^2}\right)^{-2} + \frac{g_r^2 \alpha_l P_{1,l}}{4\sigma^4} \left(1 + \frac{\gamma_1 P_{1,l}}{2\sigma^2}\right)^{-1} \right. \\
&\quad \times \left(1 + \frac{g_r \alpha_l P_{1,l}}{2\sigma^2}\right)^{-3} + \frac{\gamma_1 g_r (P_{1,l} + P_{2,l})}{8\sigma^4} \left(1 + \frac{\gamma_1 P_{1,l} + \gamma_2 P_{2,l}}{2\sigma^2}\right)^{-2} \left(1 + \frac{g_r \alpha_l (P_{1,l} + P_{2,l})}{2\sigma^2}\right)^{-2} \\
&\quad - \frac{g_r}{4\sigma^2} \left(1 + \frac{\gamma_1 P_{1,l} + \gamma_2 P_{2,l}}{2\sigma^2}\right)^{-1} \left(1 + \frac{g_r \alpha_l (P_{1,l} + P_{2,l})}{2\sigma^2}\right)^{-2} + \frac{g_r^2 \alpha_l (P_{1,l} + P_{2,l})}{4\sigma^4} \left(1 + \frac{\gamma_1 P_{1,l} + \gamma_2 P_{2,l}}{2\sigma^2}\right)^{-1} \\
&\quad \left. \times \left(1 + \frac{g_r \alpha_l (P_{1,l} + P_{2,l})}{2\sigma^2}\right)^{-3} \right) \frac{P_T}{(P_T - P_r)^2}
\end{aligned} \tag{5.55}$$

$$\begin{aligned}
f_{P_2 P_2} &= \frac{\gamma_2^2}{4\sigma^4} \left(1 + \frac{\gamma_2 P_{2,l}}{2\sigma^2}\right)^{-3} \left(1 + \frac{g_r \alpha_l P_{2,l}}{2\sigma^2}\right)^{-1} + \frac{\gamma_2 g_r \alpha_l}{4\sigma^4} \left(1 + \frac{\gamma_2 P_{2,l}}{2\sigma^2}\right)^{-2} \left(1 + \frac{g_r \alpha_l P_{2,l}}{2\sigma^2}\right)^{-2} + \frac{g_r^2 \alpha_l^2}{4\sigma^4} \left(1 + \frac{\gamma_2 P_{2,l}}{2\sigma^2}\right)^{-1} \\
&\quad \times \left(1 + \frac{g_r \alpha_l P_{2,l}}{2\sigma^2}\right)^{-3} + \frac{g_2^2}{4\sigma^4} \left(1 + \frac{g_2 P_{2,l}}{2\sigma^2}\right)^{-3} + \frac{\gamma_2^2}{4\sigma^4} \left(1 + \frac{\gamma_1 P_{1,l} + \gamma_2 P_{2,l}}{2\sigma^2}\right)^{-3} \left(1 + \frac{g_r \alpha_l (P_{1,l} + P_{2,l})}{2\sigma^2}\right)^{-1} \\
&\quad + \frac{\gamma_2 g_r \alpha_l}{4\sigma^4} \left(1 + \frac{\gamma_1 P_{1,l} + \gamma_2 P_{2,l}}{2\sigma^2}\right)^{-2} \left(1 + \frac{g_r \alpha_l (P_{1,l} + P_{2,l})}{2\sigma^2}\right)^{-2} + \frac{g_r^2 \alpha_l^2}{4\sigma^4} \left(1 + \frac{\gamma_1 P_{1,l} + \gamma_2 P_{2,l}}{2\sigma^2}\right)^{-1} \\
&\quad \times \left(1 + \frac{g_r \alpha_l (P_{1,l} + P_{2,l})}{2\sigma^2}\right)^{-3} + \frac{g_2^2}{4\sigma^2} \left(1 + \frac{g_1 P_{1,l} + g_2 P_{2,l}}{2\sigma^2}\right)^{-3}
\end{aligned} \tag{5.56}$$

$$\begin{aligned}
f_{P_2 P_r} &= f_{P_r P_2} \\
&= \left( \frac{\gamma_2 g_r P_{2,l}}{8\sigma^4} \left(1 + \frac{\gamma_2 P_{2,l}}{2\sigma^2}\right)^{-2} \left(1 + \frac{g_r \alpha_l P_{2,l}}{2\sigma^2}\right)^{-2} - \frac{g_r}{4\sigma^2} \left(1 + \frac{\gamma_2 P_{2,l}}{2\sigma^2}\right)^{-1} \left(1 + \frac{g_r \alpha_l P_{2,l}}{2\sigma^2}\right)^{-2} + \frac{g_r^2 \alpha_l P_{2,l}}{4\sigma^4} \left(1 + \frac{\gamma_2 P_{2,l}}{2\sigma^2}\right)^{-1} \right. \\
&\quad \left. \left(1 + \frac{g_r \alpha_l P_{2,l}}{2\sigma^2}\right)^{-3} + \frac{\gamma_2 g_r (P_{1,l} + P_{2,l})}{8\sigma^4} \left(1 + \frac{\gamma_1 P_{1,l} + \gamma_2 P_{2,l}}{2\sigma^2}\right)^{-2} \left(1 + \frac{g_r \alpha_l (P_{1,l} + P_{2,l})}{2\sigma^2}\right)^{-2} - \frac{g_r}{4\sigma^2} \left(1 + \frac{\gamma_1 P_{1,l} + \gamma_2 P_{2,l}}{2\sigma^2}\right)^{-1} \right. \\
&\quad \left. \times \left(1 + \frac{g_r \alpha_l (P_{1,l} + P_{2,l})}{2\sigma^2}\right)^{-2} + \frac{g_r^2 \alpha_l (P_{1,l} + P_{2,l})}{4\sigma^4} \left(1 + \frac{\gamma_1 P_{1,l} + \gamma_2 P_{2,l}}{2\sigma^2}\right)^{-1} \left(1 + \frac{g_r \alpha_l (P_{1,l} + P_{2,l})}{2\sigma^2}\right)^{-3} \right) \frac{P_T}{(P_T - P_r)^2}
\end{aligned} \tag{5.57}$$

$$\begin{aligned}
f_{P_r, P_r} = & \left( \frac{g_r^2 P_{1,l}^2}{4\sigma^4} \left(1 + \frac{\gamma_1 P_{1,l}}{2\sigma^2}\right)^{-1} \left(1 + \frac{g_r \alpha_l P_{1,l}}{2\sigma^2}\right)^{-3} + \frac{g_r^2 P_{2,l}^2}{4\sigma^4} \left(1 + \frac{\gamma_2 P_{2,l}}{2\sigma^2}\right)^{-1} \left(1 + \frac{g_r \alpha_l P_{2,l}}{2\sigma^2}\right)^{-3} \right. \\
& \left. + \frac{g_r^2 (P_{1,l} + P_{2,l})^2}{4\sigma^4} \left(1 + \frac{\gamma_1 P_{1,l} + \gamma_2 P_{2,l}}{2\sigma^2}\right)^{-1} \left(1 + \frac{g_r \alpha_l (P_{1,l} + P_{2,l})}{2\sigma^2}\right)^{-3} \right) \left( \frac{P_r}{(P_T - P_r)^2} \right)^2 \\
& - \left( -\frac{g_r P_{1,l}}{4\sigma^2} \left(1 + \frac{\gamma_1 P_{1,l}}{2\sigma^2}\right)^{-1} \left(1 + \frac{g_r \alpha_l P_{1,l}}{2\sigma^2}\right)^{-2} - \frac{g_r P_{2,l}}{4\sigma^2} \left(1 + \frac{\gamma_2 P_{2,l}}{2\sigma^2}\right)^{-1} \left(1 + \frac{g_r \alpha_l P_{2,l}}{2\sigma^2}\right)^{-2} \right. \\
& \left. - \frac{g_r (P_{1,l} + P_{2,l})}{4\sigma^2} \left(1 + \frac{\gamma_1 P_{1,l} + \gamma_2 P_{2,l}}{2\sigma^2}\right)^{-1} \left(1 + \frac{g_r \alpha_l (P_{1,l} + P_{2,l})}{2\sigma^2}\right)^{-2} \right) \frac{P_r}{(P_T - P_r)^3}
\end{aligned} \tag{5.58}$$

Thus, we can solve the SQP in Eq. (5.47) iteratively as:

$$\begin{bmatrix} \mathbf{q}_{l+1} \\ \lambda_{l+1} \end{bmatrix} = \begin{bmatrix} \mathbf{q}_l \\ \lambda_l \end{bmatrix} + \begin{bmatrix} \Delta \mathbf{q}_l \\ \Delta \lambda_l \end{bmatrix} \tag{5.59}$$

where  $\lambda_l$ ,  $\Delta \mathbf{q}_l$  and  $\Delta \lambda_l$  are the Lagrange multiplier due to the total power constraint, the step vector for  $\mathbf{q}_l$  and the step for the Lagrange multiplier, respectively, at the  $l^{\text{th}}$  iteration. After we find the direction  $\Delta \mathbf{q}_l$ , we have decide how far we move along this direction considering non-negativeness of the elements of  $\mathbf{q}_{l+1}$ . If  $\mathbf{q}_l + \Delta \mathbf{q}_l$  is feasible we choose  $\mathbf{q}_{l+1} = \mathbf{q}_l + \Delta \mathbf{q}_l$  otherwise we use

$$\mathbf{q}_{l+1} = \mathbf{q}_l + \zeta_l \Delta \mathbf{q}_l \tag{5.60}$$

where  $\zeta_l$  is the step length at the  $l^{\text{th}}$  iteration, which should be chosen to be the largest number in the range  $[0, 1]$  that ensures the non-negativity of each component of the vector  $\mathbf{q}_{l+1}$  as:

$$\zeta_l = \min(1, \min_{\Delta \mathbf{q}_l: \mathbf{c}^T \Delta \mathbf{q}_l < 0, \mathbf{d}^T \Delta \mathbf{q}_l < 0, \mathbf{e}^T \Delta \mathbf{q}_l < 0} \left( \frac{0 - \mathbf{c}^T \mathbf{q}_l}{\mathbf{c}^T \Delta \mathbf{q}_l}, \frac{0 - \mathbf{d}^T \mathbf{q}_l}{\mathbf{d}^T \Delta \mathbf{q}_l}, \frac{0 - \mathbf{e}^T \mathbf{q}_l}{\mathbf{e}^T \Delta \mathbf{q}_l} \right)) \tag{5.61}$$

Hence, to obtain  $\Delta \mathbf{q}_l$  and  $\Delta \lambda_l$  we should solve the following KKT system.

$$\begin{bmatrix} \nabla^2 f_0(\mathbf{q}_l) & -\mathbf{a} \\ \mathbf{a}^T & 0 \end{bmatrix} \begin{bmatrix} \Delta \mathbf{q}_l \\ \Delta \lambda_l \end{bmatrix} = \begin{bmatrix} \boldsymbol{\kappa}_l \\ \mathcal{G}_l \end{bmatrix} \tag{5.62}$$

Where

$$\mathcal{G}_l = -\mathbf{a}^T \mathbf{q}_l + b, \quad \boldsymbol{\kappa}_l = -\nabla f_0(\mathbf{q}_l) + \mathbf{a} \lambda_l \tag{5.63}$$

Hence we have

$$\begin{bmatrix} \Delta \mathbf{q}_l \\ \Delta \lambda_l \end{bmatrix} = \begin{bmatrix} \nabla^2 f_0(\mathbf{q}_l) & -\mathbf{a} \\ \mathbf{a}^T & 0 \end{bmatrix}^{-1} \begin{bmatrix} \boldsymbol{\kappa}_l \\ \mathcal{G}_l \end{bmatrix} \quad (5.64)$$

Using block wise inversion [89] we have

$$\begin{bmatrix} \nabla^2 f_0(\mathbf{q}_l) & -\mathbf{a} \\ \mathbf{a}^T & 0 \end{bmatrix}^{-1} = \begin{bmatrix} \mathbf{D}(\mathbf{q}_l) - \frac{\mathbf{D}(\mathbf{q}_l)\mathbf{a}\mathbf{a}^T\mathbf{D}(\mathbf{q}_l)}{\mathbf{a}^T\mathbf{D}(\mathbf{q}_l)\mathbf{a}} & \frac{\mathbf{D}(\mathbf{q}_l)\mathbf{a}}{\mathbf{a}^T\mathbf{D}(\mathbf{q}_l)\mathbf{a}} \\ -\frac{\mathbf{a}^T\mathbf{D}(\mathbf{q}_l)}{\mathbf{a}^T\mathbf{D}(\mathbf{q}_l)\mathbf{a}} & \frac{1}{\mathbf{a}^T\mathbf{D}(\mathbf{q}_l)\mathbf{a}} \end{bmatrix} \quad (5.65)$$

where  $\mathbf{D}(\mathbf{q}_l) = \nabla^2 f_0(\mathbf{q}_l)^{-1}$  and the solution can be obtained as

$$\begin{aligned} \Delta \mathbf{q}_l &= \mathbf{D}(\mathbf{q}_l) \left( \boldsymbol{\kappa}_l - \frac{(\mathbf{a}^T \mathbf{D}(\mathbf{q}_l) \boldsymbol{\kappa}_l - \mathcal{G}_l) \mathbf{a}}{\mathbf{a}^T \mathbf{D}(\mathbf{q}_l) \mathbf{a}} \right) \\ \Delta \lambda_l &= \frac{\mathcal{G}_l - \mathbf{a}^T \mathbf{D}(\mathbf{q}_l) \boldsymbol{\kappa}_l}{\mathbf{a}^T \mathbf{D}(\mathbf{q}_l) \mathbf{a}} \end{aligned} \quad (5.66)$$

To obtain the solution in Eq.(5.66) we calculate  $\mathbf{D}(\mathbf{q}_l)$  as follows

$$\begin{aligned} \mathbf{D}(\mathbf{q}_l) &= \begin{bmatrix} d_{11} & d_{12} & d_{13} \\ d_{21} & d_{22} & d_{23} \\ d_{31} & d_{32} & d_{33} \end{bmatrix} \\ &= \frac{1}{\det(\nabla^2 f_0(\mathbf{q}_l))} \begin{bmatrix} f_{P_2 P_2} f_{P_r P_r} - (f_{P_2 P_r})^2 & f_{R P_r} f_{P_r P_2} - f_{R P_2} f_{P_r P_r} & f_{R P_2} f_{P_2 P_r} - f_{R P_r} f_{P_2 P_2} \\ f_{P_2 P_r} f_{P_r P_1} - f_{P_2 R} f_{P_r P_r} & f_{R P_1} f_{P_r P_r} - (f_{R P_r})^2 & f_{R P_r} f_{P_2 R} - f_{R P_r} f_{P_2 P_r} \\ f_{P_2 R} f_{P_r P_2} - f_{P_2 P_2} f_{P_r R} & f_{R P_2} f_{P_r R} - f_{R P_r} f_{P_r P_2} & f_{R R} f_{P_2 P_2} - (f_{R P_2})^2 \end{bmatrix} \end{aligned} \quad (5.67)$$

Where

$$\det(\nabla^2 f_0(\mathbf{q}_l)) = f_{R P_1} f_{P_2 P_2} f_{P_r P_r} + f_{P_2 P_1} f_{P_r P_2} f_{R P_r} + f_{P_r R} f_{R P_2} f_{P_2 P_r} - f_{R P_1} (f_{P_r P_2})^2 - (f_{P_r R})^2 f_{P_2 P_2} - (f_{P_2 R})^2 f_{P_r P_r} \quad (5.68)$$

Therefore we can write inverse of matrix in Eq.(5.65) as

$$\mathbf{E} = \begin{bmatrix} \nabla^2 f_0(\mathbf{q}_l) & -\mathbf{a} \\ \mathbf{a}^T & 0 \end{bmatrix}^{-1} = \begin{bmatrix} d_{11} - \frac{\sum_{i=1}^3 d_{1i} \sum_{j=1}^3 d_{j1}}{\sum_{i=1}^3 \sum_{j=1}^3 d_{ji}} & d_{12} - \frac{\sum_{i=1}^3 d_{1i} \sum_{j=1}^3 d_{j2}}{\sum_{i=1}^3 \sum_{j=1}^3 d_{ji}} & d_{13} - \frac{\sum_{i=1}^3 d_{1i} \sum_{j=1}^3 d_{j3}}{\sum_{i=1}^3 \sum_{j=1}^3 d_{ji}} & \frac{\sum_{i=1}^3 d_{1i}}{\sum_{i=1}^3 \sum_{j=1}^3 d_{ji}} \\ d_{21} - \frac{\sum_{i=1}^3 d_{2i} \sum_{j=1}^3 d_{j1}}{\sum_{i=1}^3 \sum_{j=1}^3 d_{ji}} & d_{22} - \frac{\sum_{i=1}^3 d_{2i} \sum_{j=1}^3 d_{j2}}{\sum_{i=1}^3 \sum_{j=1}^3 d_{ji}} & d_{23} - \frac{\sum_{i=1}^3 d_{2i} \sum_{j=1}^3 d_{j3}}{\sum_{i=1}^3 \sum_{j=1}^3 d_{ji}} & \frac{\sum_{i=1}^3 d_{2i}}{\sum_{i=1}^3 \sum_{j=1}^3 d_{ji}} \\ d_{31} - \frac{\sum_{i=1}^3 d_{3i} \sum_{j=1}^3 d_{j1}}{\sum_{i=1}^3 \sum_{j=1}^3 d_{ji}} & d_{32} - \frac{\sum_{i=1}^3 d_{3i} \sum_{j=1}^3 d_{j2}}{\sum_{i=1}^3 \sum_{j=1}^3 d_{ji}} & d_{33} - \frac{\sum_{i=1}^3 d_{3i} \sum_{j=1}^3 d_{j3}}{\sum_{i=1}^3 \sum_{j=1}^3 d_{ji}} & \frac{\sum_{i=1}^3 d_{3i}}{\sum_{i=1}^3 \sum_{j=1}^3 d_{ji}} \\ -\frac{\sum_{j=1}^3 d_{j1}}{\sum_{i=1}^3 \sum_{j=1}^3 d_{ji}} & -\frac{\sum_{j=1}^3 d_{j2}}{\sum_{i=1}^3 \sum_{j=1}^3 d_{ji}} & -\frac{\sum_{j=1}^3 d_{j3}}{\sum_{i=1}^3 \sum_{j=1}^3 d_{ji}} & \frac{1}{\sum_{i=1}^3 \sum_{j=1}^3 d_{ji}} \end{bmatrix} \quad (5.69)$$

Hence  $\Delta \mathbf{q}_l$  will be

$$\begin{bmatrix} \Delta \mathbf{q}_l \\ \Delta \lambda \end{bmatrix} = \begin{bmatrix} e_{11} & e_{12} & e_{13} & e_{14} \\ e_{21} & e_{22} & e_{23} & e_{24} \\ e_{31} & e_{32} & e_{33} & e_{34} \\ e_{41} & e_{42} & e_{43} & e_{44} \end{bmatrix} \begin{bmatrix} f_{P_1} - \lambda_l \\ f_{P_2} - \lambda_l \\ f_{P_r} - \lambda_l \\ 0 \end{bmatrix} \quad (5.70)$$

$$\Delta \mathbf{q}_l = \begin{bmatrix} e_{11}(f_{P_1} - \lambda_l) + e_{12}(f_{P_2} - \lambda_l) + e_{13}(f_{P_r} - \lambda_l) \\ e_{21}(f_{P_1} - \lambda_l) + e_{22}(f_{P_2} - \lambda_l) + e_{23}(f_{P_r} - \lambda_l) \\ e_{31}(f_{P_1} - \lambda_l) + e_{32}(f_{P_2} - \lambda_l) + e_{33}(f_{P_r} - \lambda_l) \end{bmatrix}$$

Note that, this solution is useful is when rate optimized solution is near the BER optimal solution where the Hessian is positive definite and quadratic model has a well defined minimize. On the other hand, when Hessian is not positive definite we use BFGS algorithm which replaces it by an approximation  $\mathbf{B}(\mathbf{q}_l)$  to guarantee that  $\Delta \mathbf{q}_l$  is a descent direction for objective function.

Approximation of Hessian can be given as follows using BFGS algorithm

$$\mathbf{B}(\mathbf{q}_{l+1}) = \mathbf{B}(\mathbf{q}_l) - \frac{\mathbf{B}(\mathbf{q}_l) \mathbf{s}_l \mathbf{s}_l^T \mathbf{B}(\mathbf{q}_l)}{\mathbf{s}_l^T \mathbf{B}(\mathbf{q}_l) \mathbf{s}_l} + \frac{\boldsymbol{\omega}_l \boldsymbol{\omega}_l^T}{\boldsymbol{\omega}_l^T \mathbf{s}_l} \quad (5.71)$$

where  $\mathbf{s}_l = \mathbf{q}_{l+1} - \mathbf{q}_l$  and  $\boldsymbol{\omega}_l = \nabla f_0(\mathbf{q}_{l+1}) - \nabla f_0(\mathbf{q}_l)$ .

Note that an initial solution for the signature and relay power is needed in order to run the SQP based iterative method above. One obvious choice would be to distribute the power equally per time slot and then allocate the signature powers equally (i.e.,  $P_1 = P_2 = P_T / 4$  and  $P_r = P_T / 2$ ), which shall be referred as equal power allocation (EPA). As in the all iterative techniques, selecting the initial solution in SQP is very crucial since the convergence is fast when the initial solution is close to the true-optimal solution. Therefore, we propose an information theoretical heuristic initialization technique to improve the convergence of EPA, which is explained in detail in the next section.

## 5.4 An Information Theoretical Heuristic Initialization Method

The SER-optimized signature powers satisfying Eq.(5.45) provide somehow user fairness to minimize the average SER of the network since the user powers become the same when they are located symmetrically with respect to both the relay and destination or when one of the users is positioned closer to the relay or destination, the other user needs to consume more power. We now look at the problem of determining the signature and relay powers while considering fairness from an information theoretical point of view. As pointed out earlier, we assume only the receiver-CSI and Rayleigh fading with unit energy for all communicating links along with the manuscript.

Since the users-to-relay channel is a MAC channel, the achievable ergodic rates of users (denoted by  $R_1$  for user  $S_1$  and  $R_2$  for user  $S_2$ ) at the relay are upper bounded as

$$R_1 \leq \frac{1}{2} \log \left( 1 + \frac{g_1 P_1}{2\sigma^2} \right) \quad (5.72)$$

$$R_2 \leq \frac{1}{2} \log \left( 1 + \frac{g_2 P_2}{2\sigma^2} \right) \quad (5.73)$$

$$R_1 + R_2 \leq \frac{1}{2} \log \left( 1 + \frac{g_1 P_1 + g_2 P_2}{2\sigma^2} \right) \quad (5.74)$$

By assuming perfect decoding at the relay, the signals at the destination in both time slots (see

Eqs. (5.2), (5.3) and (5.7)) can be put into a matrix-vector form as:

$$\underbrace{\begin{bmatrix} y_{sd}[n] \\ y_{rd}[n] \end{bmatrix}}_{\mathbf{y}} = \underbrace{\begin{bmatrix} \sqrt{\gamma_1} h_{s_1d} & \sqrt{\gamma_2} h_{s_2d} \\ \sqrt{g_r \alpha} h_{rd} & \sqrt{g_r \alpha} h_{rd} \end{bmatrix}}_{\mathbf{H}} \underbrace{\begin{bmatrix} \sqrt{P_1} x_{s_1}[n] \\ \sqrt{P_2} x_{s_2}[n] \end{bmatrix}}_{\mathbf{x}} + \underbrace{\begin{bmatrix} z_d[n] \\ z_d[n] \end{bmatrix}}_{\mathbf{z}} \quad (5.75)$$

where  $\mathbf{y}$  is the received signal vector at destination;  $\mathbf{H}$  is the channel gain matrix;  $\mathbf{x}$  is the user signal vector and  $\mathbf{z}$  is the AWGN noise vector.

The single-user and the joint-user rate-bounds of users  $S_1$  and  $S_2$  at the destination are obtained as:

$$R_1 \leq \frac{1}{2} \log \left( 1 + \frac{\gamma_1 P_1 + g_r \alpha P_1}{2\sigma^2} \right) \quad (5.76)$$

$$R_2 \leq \frac{1}{2} \log \left( 1 + \frac{\gamma_2 P_2 + g_r \alpha P_2}{2\sigma^2} \right) \quad (5.77)$$

$$\begin{aligned} R_1 + R_2 &\leq \frac{1}{2} E \left\{ \log \left( \det \left( \mathbf{I} + \frac{\mathbf{HSH}^\dagger}{2\sigma^2} \right) \right) \right\} \leq \frac{1}{2} \log \left( \det \left( \mathbf{I} + \frac{E\{\mathbf{HSH}^\dagger\}}{2\sigma^2} \right) \right) \\ &= \frac{1}{2} \log \left( 1 + \frac{\gamma_1 P_1 + \gamma_2 P_2 + g_r \alpha (P_1 + P_2 + P_1 P_2 (\sqrt{\gamma_2} - \sqrt{\gamma_1})^2)}{2\sigma^2} \right) \end{aligned} \quad (5.78)$$

where  $\dagger$  denotes the conjugate-transpose operation,  $\mathbf{S} = E[\mathbf{xx}^T]$  is the input covariance matrix, which is a diagonal matrix with  $P_1$  and  $P_2$  on its diagonal.

By combining Eqs. (3.8)- (3.7) with Eqs. (3.11)-(3.13), the single user and joint-user rate bounds in MAR-NOC channel can be derived as:

$$R_1 \leq \min \left\{ \frac{1}{2} \log \left( 1 + \frac{\gamma_1 P_1 + g_r \alpha P_1}{2\sigma^2} \right), \frac{1}{2} \log \left( 1 + \frac{g_1 P_1}{2\sigma^2} \right) \right\} \quad (5.79)$$

$$R_2 \leq \min \left\{ \frac{1}{2} \log \left( 1 + \frac{\gamma_2 P_2 + g_r \alpha P_2}{2\sigma^2} \right), \frac{1}{2} \log \left( 1 + \frac{g_2 P_2}{2\sigma^2} \right) \right\} \quad (5.80)$$

$$R_1 + R_2 \leq \min \left\{ \frac{1}{2} \log \left( 1 + \frac{\gamma_1 P_1 + \gamma_2 P_2 + g_r \alpha (P_1 + P_2 + P_1 P_2 (\sqrt{\gamma_2} - \sqrt{\gamma_1})^2)}{2\sigma^2} \right), \frac{1}{2} \log \left( 1 + \frac{g_1 P_1 + g_2 P_2}{2\sigma^2} \right) \right\} \quad (5.81)$$

To achieve fairness among users, the maximum rate bounds of users in Eqs. (5.79) and (5.80) can be equalized as:

$$\min \left\{ \frac{1}{2} \log \left( 1 + \frac{\gamma_1 P_1 + g_r \alpha P_1}{2\sigma^2} \right), \frac{1}{2} \log \left( 1 + \frac{g_1 P_1}{2\sigma^2} \right) \right\} = \min \left\{ \frac{1}{2} \log \left( 1 + \frac{\gamma_2 P_2 + g_r \alpha P_2}{2\sigma^2} \right), \frac{1}{2} \log \left( 1 + \frac{g_2 P_2}{2\sigma^2} \right) \right\} \quad (5.82)$$

The rate fairness in Eq. (5.82) can be simplified as

$$\min \{ \gamma_1 + g_r \alpha, g_1 \} P_1 = \min \{ \gamma_2 + g_r \alpha, g_2 \} P_2 \quad (5.83)$$

By combining the total power constraint (i.e.,  $(1 + \alpha)(P_1 + P_2) = P_T$ ) with the fairness condition in Eq. (5.83), the signature powers can be derived in terms of the relay power control parameter  $\alpha$  as:

$$P_1 = \frac{P_T \min \{ \gamma_2 + g_r \alpha, g_2 \}}{(1 + \alpha) (\min \{ \gamma_1 + g_r \alpha, g_1 \} + \min \{ \gamma_2 + g_r \alpha, g_2 \})} \quad (5.84)$$

$$P_2 = \frac{P_T \min \{ \gamma_1 + g_r \alpha, g_1 \}}{(1 + \alpha) (\min \{ \gamma_1 + g_r \alpha, g_1 \} + \min \{ \gamma_2 + g_r \alpha, g_2 \})}$$

Therefore, once we decide on the parameter  $\alpha$ , the signature powers automatically determined using Eq. (5.84). Heuristically, we propose to choose  $\alpha$  as:

$$\alpha = \min \left\{ \frac{g_1 - \gamma_1}{g_r}, \frac{g_2 - \gamma_2}{g_r} \right\} \quad (5.85)$$

The logic behind for selecting such  $\alpha$  in Eq. (5.85) can explained as follows. During the time slot 1, the expected received signature powers at the relay are  $g_1 P_1$  and  $g_2 P_2$  for user 1 and user 2, respectively, while these become  $\gamma_1 P_1$  and  $\gamma_2 P_2$  for user 1 and user 2, respectively, at the destination. In order to achieve rate fairness of the users, the expected received signal to noise ratios (SNR)s of the users should be the same, which can be done by carefully adjusting the relay power during the time slot 2 so that the relay can be able to compensate the difference between the expected SNRs of the users at the destination. Thus, the heuristic choice in Eq. (5.85) equates the expected received signatures powers of the users, which takes the smallest  $g_k - \gamma_k$  for  $k=1,2$  into account in order to tune the parameter  $\alpha$ . Thus, we can start SQP

in Eq. (5.60) using signature power values determined by Eqs.(5.84) and (5.85), which we refer as “fair-rate initialization (FARI)” method.

In order to quantify the convergence of the proposed heuristical initialization technique as compared to EPA initialization, we have first numerically solved Eq. (5.24) using "fmincon" command in MATLAB by setting termination tolerance argument “TolX” as  $10^{-12}$  in order to obtain the optimal signature powers (denoted by  $P_1^*$  and  $P_2^*$  for user 1 and 2 , respectively) and relay power  $P_r^*$  . Then, we have determined the percentage normalized root mean-square error (NRMSE) per user of the iterative methods at the  $k^{th}$  iteration as:

$$\text{NRMSE}(k) = \sqrt{\frac{1}{3} \sum_{i=1,2,r} \frac{(P_{i,k} - P_i^*)^2}{(P_i^*)^2}} \times 100\% \quad (5.86)$$

During our experiments, the total power budget  $P_T$  is taken to be 2 units and each iterative algorithm stops when the change in the power value  $P_{i,k}$  is less than  $10^{-12}$ .

We first consider a scenario where the users and destination are placed on the corners of an equilateral triangle with side length of unity, and the relay is positioned at the midpoint of altitude from the destination node, which results in  $\gamma_1=0$  dB,  $\gamma_2=0$  dB,  $g_1=g_2=3.60$  dB and  $g_r=7.27$  dB. For SNR of 10 dB and 15 dB, we then calculate the percentage NRMSE by employing both FARI and EPA initialization methods during SQP iterations, which is illustrated in Figure 5-4. As seen from this figure, FARI starts with a smaller NRMSE, and thus, converges quicker than EPA initialization. Specifically, for SNR of 10 dB, FARI and EPA initialization results in NRMSE of 0.1% and 13.7%, respectively, whereas the SQP with FARI and EPA initialization give rise to NRMSE of 8.9% and 31.3%, respectively.

Next, we adduct the relay towards to the destination by 0.1 units (compared to the previous scenario) along the altitude of the destination node, in which path gains become  $\gamma_1=0$  dB,  $\gamma_2=0$  dB,  $g_1=2.72$ dB,  $g_2=2.72$  dB,  $g_r= 9.55$  dB. As shown in Figure 5-5, FARI again convergences

faster than EPA initialization for this case. For SNR of 10 dB and the use of single iteration, NRMSEs of FARI and EPA initialization become 5.6% and 19.9%, respectively, whereas they are 0.05% and 42.3%, respectively, after performing one iteration for SNR of 15 dB.

Therefore, FARI with SQP iterations in Eq.(5.60) requires less number of iterations as compared to the EPA initialization. Once the convergence is reached, we end up with the joint SER-optimized signature and relay powers to be used in CFNC coded MAR-NOC channel. So, the next section is devoted to investigate the BER performance improvement obtained with the use of optimized parameters.

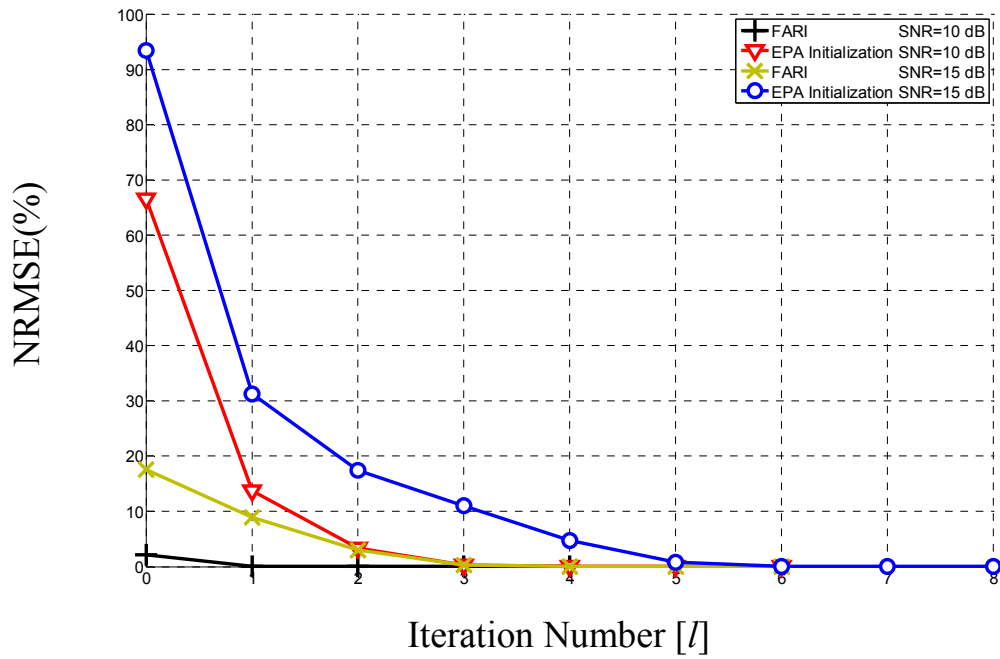


Figure 5-4. NMRS value at each iteration for the scenario  $g_1= 3.60$  dB,  $g_2= 3.60$  dB  $g_r= 7.27$  dB  $\gamma_1=0$  dB  $\gamma_2=0$  when only receivers have knowledge of CSI

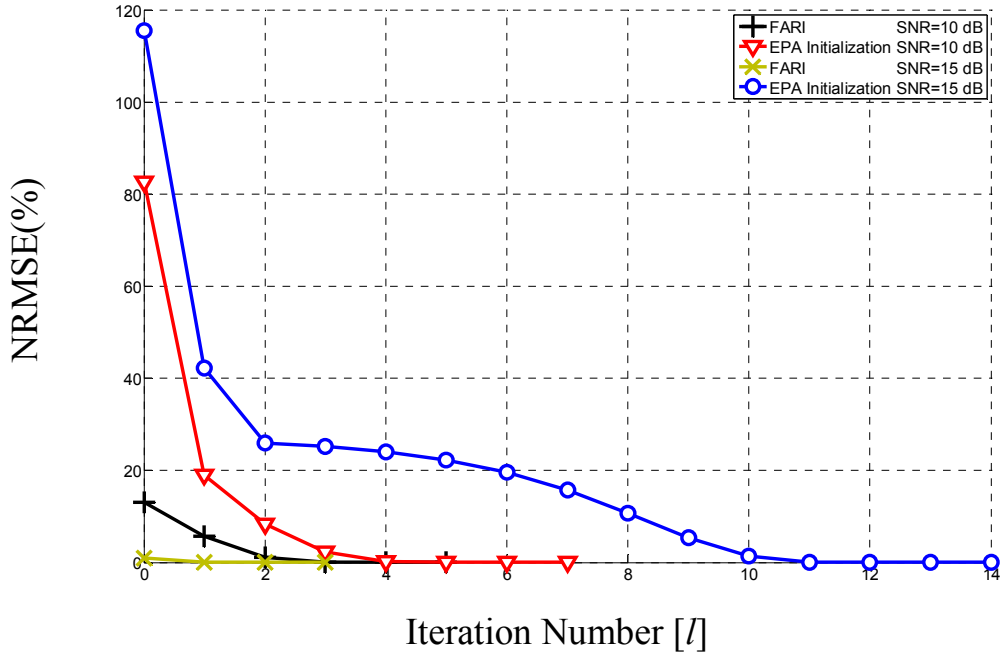


Figure 5-5. NRMSE value at each iteration for the scenario  $g_1=2.72$  dB,  $g_2=2.72$  dB  $g_r=9.55$  dB  $\gamma_1=0$  dB  $\gamma_2=0$  when only receivers have knowledge of CSI

### 5.5 Bit Error Rate Simulation Results For the SER-optimized CFNC Coded MAR-NOC Channel

In this section, we investigate the average bit error rate (BER) performance of proposed method , which is based on joint optimization of CFNC coding and relay power to minimize the average SER of MAR-NOC channel, through simulations, and compare it with the CFNC with EPA used in [20], where equal power allocation (EPA) policy is employed. To make a fair comparison between the EPA and the proposed methods, we assume that the average transmit power of the network per time slot is 2 units (i.e.,  $P_T = (1 + \alpha)(P_1 + P_2) = 2$ ).

For all numerical experiments presented in this part, we assume that users and destination are placed on three corner of an equilateral triangle. We initially put the relay at the midpoint of altitude of the destination node, which is referred as “nominal position” (NOP) of the relay, and has path gains of  $\gamma_1=0$  dB,  $\gamma_2=0$  dB,  $g_1=g_2=3.60$  dB and  $g_r=7.27$  dB.

To see the effect of the relay location on the performance of the techniques considered, we first move the relay towards to the destination with an amount of  $v_d$  units with respect to the NOP, which only changes  $g_1$ ,  $g_2$  and  $g_r$  to  $g_1=2.72\text{dB}$  ,  $g_2=2.72\text{ dB}$  and  $g_r= 9.55\text{ dB}$  ;  $g_1=1.87\text{dB}$ ,  $g_2=1.87\text{ dB}$  and  $g_r= 12.65\text{ dB}$ ;  $g_1=1.04\text{dB}$ ,  $g_2=1.04\text{ dB}$  and  $g_r= 17.52\text{ dB}$ , respectively, for  $v_d =0.1\text{units}$ ,  $0.2\text{units}$  and  $0.3\text{ units}$ . The optimal signature power and relay power control parameter  $\alpha$  for different amount of move from the nominal position to the destination are tabulated in Table 5-1. Since the relay is symmetrically located with respect to both the users, the proposed method makes the user signature powers equal according to the relay position and SNR. For a given SNR, as the relay gets closer and closer to the destination, the reliabilities of the user-to-relay and relay-to-destination links become more and more similar. Thus, it is more logical for the users to directly communicate with the destination rather than over the relay, and therefore, the relay power decreases. For a given relay location, as SNR increases, the amount of relay power required to reliably and fairly communicate with the destination decreases and the user signature powers increases and each of them is assigned powers according to their locations to have similar SER. We have also obtained the average BER curves in Figure 5-6 for the various relay positions considered in the first scenario. As seen from this figure, the proposed method achieves average BER performance improvements up to 90.32%, 90.63% , 89.22%, and 86.09% over the convention method for  $v_d =0\text{ units}$  ,  $0.1\text{units}$ ,  $0.2\text{units}$  and  $0.3\text{ units}$  , respectively. It is important to note that the average BER of each user is the same as the average BER of the network for this scenario since the user signature powers are equal owing to the symmetry of the relay position. For the target BER of  $10^{-2}$  employing proposed method instead of EPA results in an SNR improvement of 3.75 dB, 4.25 dB, 4.5 dB and 4.5 dB for  $v_d =0\text{ units}$  ,  $0.1\text{units}$ ,  $0.2\text{units}$  and  $0.3\text{ units}$  , respectively. Similarly, the proposed method achieves an average BER of  $10^{-3}$  with the use of 6.25 dB, 6.75 dB, 6.75 dB and 6.5 dB less SNR when compared to the convectional scheme for  $v_d =0\text{ units}$  ,  $0.1\text{units}$ ,  $0.2\text{units}$  and  $0.3\text{ units}$  , respectively. Therefore, the proposed technique is superior in performance as compared to the convention method since

the former jointly allocates power to the user signatures and relay by taking the network geometry and SNR into account.

As a second scenario, we move the relay left from the nominal position (towards to the user 1) with an amount of  $v_r=0.2$  units, for which the path gains are  $g_1=5.57$  dB,  $g_2=1.70$  dB and  $g_r= 6.43$  dB. The optimal signature and relay power parameters are obtained as in Table 5-2. From this table, we observe that user  $S_2$  has been allocated more power compared to user  $S_1$  for all SNR values. This makes sense since  $S_1$  is closer to the relay and so its expected BER is smaller than that of  $S_2$ . Therefore, it is logical to assign more power to  $S_2$  in order to improve the overall network performance. Hence, the user signature powers are distributed inversely proportional to the path gains of users with respect to the relay. We have also seen that the relay power has slightly been increased since its distance from the destination is increased as compared to the nominal relay position. We have also obtained the average BER performance of both the proposed method and the EPA method in Figure 5-7 for the second scenario. In particular, the proposed method achieves an average BER improvement up to 89.99% over the EPA technique when  $v_r=0.2$  units. The proposed method reaches an average BER of  $10^{-2}$  and  $10^{-3}$  by utilizing 3.75 dB and 6.25 dB less SNR when compared to EPA method. In order to see the fairness achieved by the proposed method, the average BER plots of each user is also shown in Figure 5-8. Specifically, when the relay is at the nominal position the average BER of users using both the EPA and proposed methods are same. However, when the relay is moved left from the nominal position with  $v_r=0.2$  units, the proposed technique adapts the signature and the relay powers according to the location of relay, and thus, makes the average BER of users similar. Therefore, the proposed method achieves higher fairness than the EPA method. To compare the techniques considered in terms of user fairness, we also define the fairness metric (FAM) at each value of the SNR as:

$$\text{FAM}(\text{SNR}) = \left( 1 - \frac{\sqrt{\sum_{i=1}^2 (\text{BER}_{av}(\text{SNR}) - \text{BER}_i(\text{SNR}))^2}}{\text{BER}_{av}(\text{SNR})} \right) \times 100\% \quad (5.87)$$

where  $\text{BER}_i(\text{SNR})$  represents the BER of the  $i$ th user,  $\text{BER}_{av}(\text{SNR})$  is the average BER of the users as a function of SNR. Intuitively, FAM gets higher when the BERs of the users get closer to the average BER. In order to quantify the fairness among the users, we have considered the average fairness metric (AFAM), which is obtained the FAM over all SNRs, as:

$$\text{AFAM} = \frac{1}{K} \sum_{j=1}^K \text{FAM}(\text{SNR}_j) \quad (5.88)$$

The proposed and EPA methods result in AFAM of 83% and 60%, respectively, which numerically validates that the proposed method is inherently fairer than the conventional technique. These results suggest that the idea of joint SER-optimization of CFNC signatures and relay power reduces not only the average BER of the network but also achieve higher fairness among users according to the network geometry and SNR as compared to the EPA method.

It is important to note that, proposed method in this chapter can be compared with the ROFPA in Chapter 3. When  $v_d = 0$  units, and 0.1 units proposed method performs better than ROFPA in terms of BER performance and BER performance increase increases with the SNR. On the other hand, for  $v_d = 0.2$  units, and 0.3 units, at low SNR (around 10 dB) ROFPA performs slightly better than proposed method in this chapter, but it performs ROFPA in the high SNR (30 dB and more) regime. Namely, when relay becomes closer to the destination ROFPA performs better when the SNR is low. This can be explained as follows: when we are deriving SER upper bound we used union bound which actually is an high SNR approximation which means our SER upper bound approximation performs well in high SNR regime. And, since we implicitly assume that relay decodes correctly, proposed method performs better for all SNR values when the relay is close to the users.

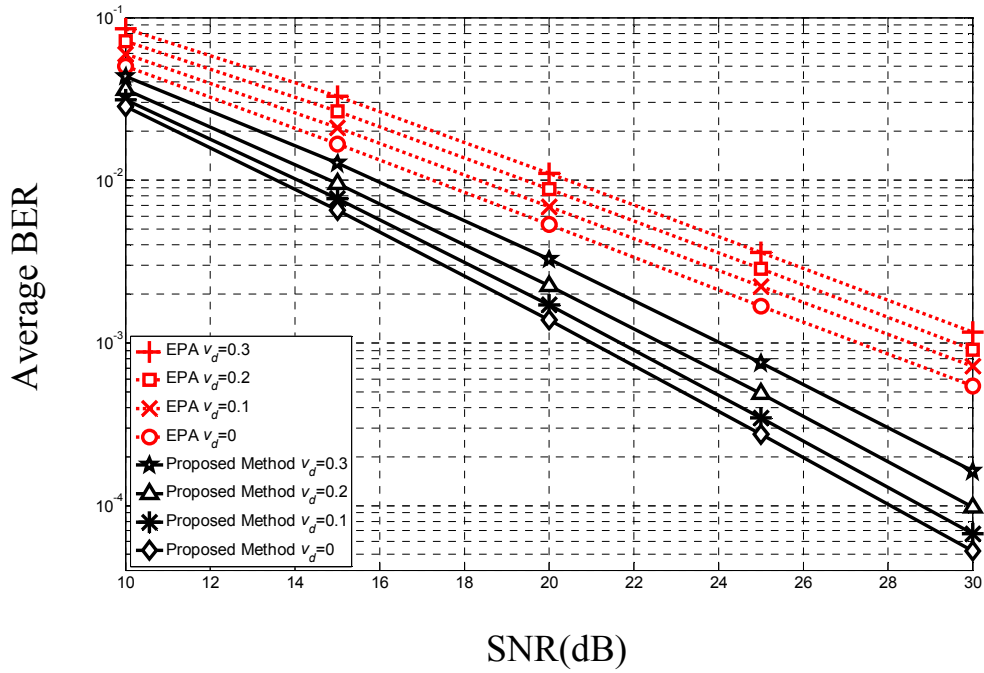


Figure 5-6. Average BER value of users for various location of relay

Table 5-1. SER Optimum Signature powers and  $\alpha$  for various location of relay node

$SNR[dB]$	$v_d = 0$			$v_d = 0.1$			$v_d = 0.2$			$v_d = 0.3$		
	$ \theta_1 ^2$	$ \theta_2 ^2$	$\alpha$	$ \theta_1 ^2$	$ \theta_2 ^2$	$\alpha$	$ \theta_1 ^2$	$ \theta_2 ^2$	$\alpha$	$ \theta_1 ^2$	$ \theta_2 ^2$	$\alpha$
10	0.82	0.82	0.23	0.86	0.86	0.17	0.90	0.90	0.11	0.94	0.94	0.06
15	0.88	0.88	0.14	0.91	0.91	0.10	0.94	0.94	0.07	0.97	0.97	0.04
20	0.92	0.92	0.08	0.94	0.94	0.06	0.96	0.96	0.04	0.98	0.98	0.02
25	0.95	0.95	0.05	0.97	0.97	0.03	0.98	0.98	0.02	0.99	0.99	0.01
30	0.97	0.97	0.03	0.98	0.98	0.02	0.99	0.99	0.01	0.99	0.99	0.01

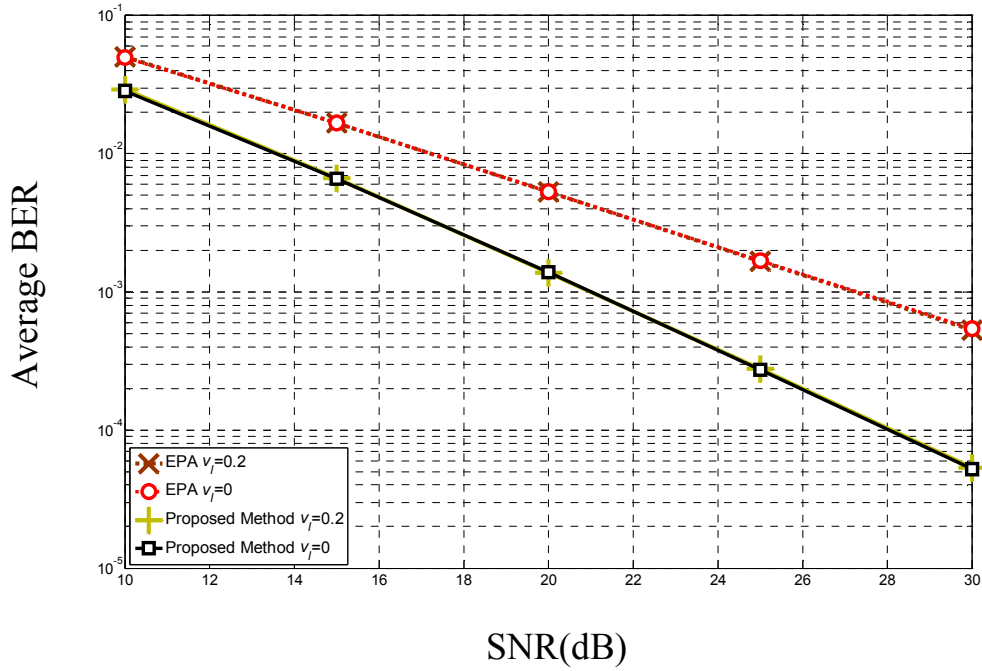


Figure 5-7. Average BER value of users for cases  $g_1= 5.57$  dB,  $g_2= 1.70$  dB  $g_r= 6.43$  dB and  $g_1= 3.60$  dB,  $g_2= 3.60$  dB  $g_r= 7.27$  dB

Table 5-2. SER Optimum Signature powers and  $\alpha$  for various location of relay node

$SNR[dB]$	$v_f = 0$			$v_f = 0.2$		
	$ \theta_1 ^2$	$ \theta_2 ^2$	$\alpha$	$ \theta_1 ^2$	$ \theta_2 ^2$	$\alpha$
10	0.82	0.82	0.23	0.75	0.86	0.24
15	0.88	0.88	0.14	0.78	0.96	0.15
20	0.92	0.92	0.08	0.80	1.03	0.09
25	0.95	0.95	0.05	0.81	1.08	0.05
30	0.97	0.97	0.03	0.82	1.12	0.03

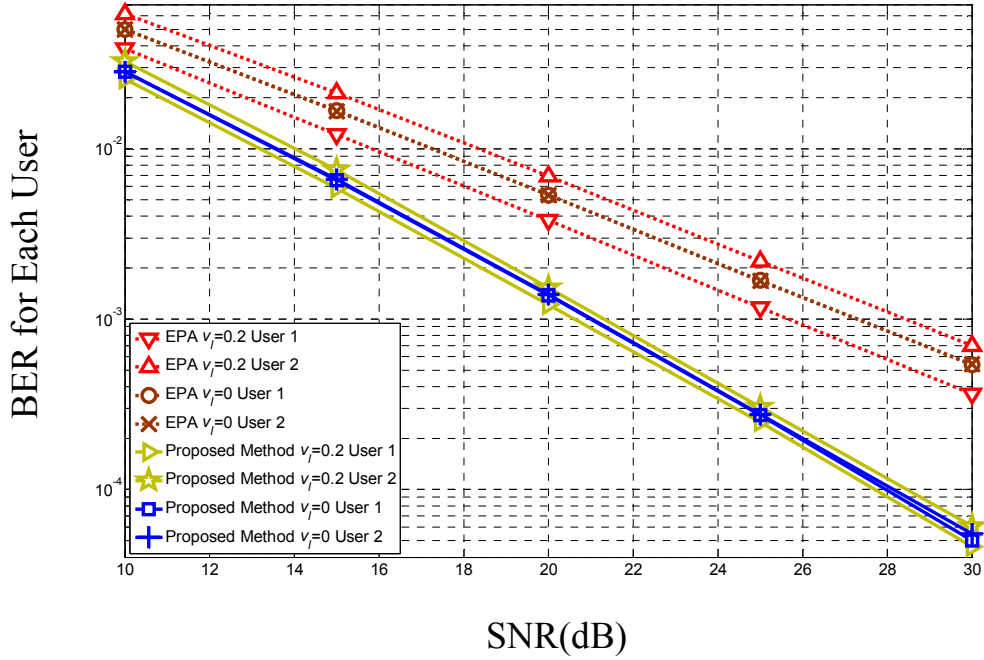


Figure 5-8. BER of each user for cases  $g_1= 5.57$  dB,  $g_2= 1.70$  dB  $g_1= 6.43$  dB and  $g_1= 3.60$  dB,  $g_2= 3.60$  dB  $g_1= 7.27$  dB

In addition to these, to analyze the effect of optimum signature angles we compare BER performance of users which use proposed signature angles and users which apply the angles derived from [20]. Specifically, user signature angles for proposed case are  $\arg(\theta_1)=0$ ,

$$\arg(\theta_2)=\frac{\pi}{4}, \quad \arg(\theta_3)=\frac{\pi}{2} \text{ and } \arg(\theta_4)=\frac{3\pi}{4} \quad \text{and, user signature angles given in [20] are}$$

$$\arg(\theta_1)=0, \quad \arg(\theta_2)=\frac{3\pi}{8}, \quad \arg(\theta_3)=\frac{6\pi}{8} \text{ and } \arg(\theta_4)=\frac{9\pi}{8}.$$

In our simulations, we use user signature powers which are obtained from proposed method for all cases. To make a fair comparison between cases, we assume that the average transmit power of the network is 4 units (i.e.,  $P_T = (1 + \alpha)(P_1 + P_2 + P_3 + P_4) = 4$ ) . For all numerical experiments presented for 4 users, we

again assume that distance from the user-1-to-destination link is one and the corresponding path loss coefficient is unity (i.e.,  $\gamma_1=1$  or 0 dB) so that other path loss coefficients

(i.e.,  $g_1, g_2, g_3, g_4, g_r$ , and  $\gamma_2, \gamma_3, \gamma_4$ ) are interpreted as power gains or losses relative to the user-1-to-destination link. Also, the path-loss coefficients of the relay channel should be satisfy

the following geometrical constraints because of the two-triangle inequalities

$$|g_i^{-0.5} - g_r^{-0.5}| < \gamma_i^{-0.5} < g_i^{-0.5} + g_r^{-0.5} \quad i = 1, 2, 3, 4 \quad (5.89)$$

We obtained average BER performance and BER performance of each user for the case where  $\gamma_2 = \gamma_3 = \gamma_4 = g_r = 0.91$  dB and  $g_1 = g_2 = g_3 = g_4 = 13.98$  dB.

TABLE 5-3 and TABLE 5-4 give BER performance of each user and average BER performance of users as a function of SNR for optimized and non-optimized angles respectively. Also, TABLE 5-5 gives BER improvement of each user and average BER improvement. We can conclude that using optimal angle provides an average BER performance improvement up to 18.96%. TABLE 5-5 also shows that signatures with optimized angles have BER performance improvement up to 20.69 %, 14.55%, 17.45% and 22.75% over signatures with angles derived from [20] for user 1, 2, 3 and 4 respectively. We can conclude that proposed method have less performance improvement for user 2 and 3. To explain this behavior we define  $\delta_{ij}$  as the distance between  $\theta_i x_{s_i}$  of user  $i$  and  $\theta_j x_{s_j}$  of user  $j$  which can be given as

$$\delta_{ij} = \left| \theta_i x_{s_i} - \theta_j x_{s_j} \right| \quad \text{for } i, j = 1, 2, 3, 4 \text{ and } i \neq j \quad (5.90)$$

Where  $x_{s_i}$  and  $x_{s_j}$  are BPSK symbols for  $i^{\text{th}}$  and  $j^{\text{th}}$  user respectively. Hence, when the signature powers are same and unit when angles in [20] is used minimum  $\delta_{ij}$  for user 1 and user 4 is

$\sqrt{2 - 2\cos\left(\frac{\pi}{8}\right)}$  and for user 2 and user 3 is  $\sqrt{2 - 2\cos\left(\frac{\pi}{4}\right)}$ . On the other hand, with the angles

used in the proposed angle the minimum  $\delta_{ij}$  for user each user is  $\sqrt{2 - 2\cos\left(\frac{\pi}{4}\right)}$ . Namely, when

we use proposed method, minimum  $\delta_{ij}$  increases for user 1 and 4 while staying same for user 2 and 3. Therefore, proposed method has greater performance improvement for user 1 and 4 compared to user 2 and 3.

TABLE 5-3 BER OF USERS WITH OPTIMIZED ANGLE

SNR(dB)	5	10	15	20	25	30
BER <sub>1</sub>	0.2221180	0.0928276	0.0239010	0.0042828	0.0007024	0.0001140
BER <sub>2</sub>	0.1969748	0.0867206	0.0223998	0.0040538	0.0006564	0.0001074
BER <sub>3</sub>	0.1968724	0.0866624	0.0224022	0.0040184	0.0006550	0.0001038
BER <sub>4</sub>	0.1966556	0.0867894	0.0225198	0.0040322	0.0006622	0.0001008
Average BER	0.2031552	0.0882500	0.0228057	0.0040968	0.0006690	0.0001065

TABLE 5-4 BER OF USERS WITH NON-OPTIMIZED ANGLE

SNR(dB)	5	10	15	20	25	30
BER <sub>1</sub>	0.2276909	0.0995625	0.0265395	0.0049971	0.0008338	0.0001438
BER <sub>2</sub>	0.1932098	0.0842518	0.0224916	0.0043177	0.0007434	0.0001257
BER <sub>3</sub>	0.1935401	0.0846732	0.0225842	0.0043636	0.0007413	0.0001258
BER <sub>4</sub>	0.2017480	0.0925900	0.0250788	0.0046908	0.0007740	0.0001305
Average BER	0.2040472	0.0902693	0.0241735	0.0045923	0.0007731	0.0001314

TABLE 5-5 BER IMPROVEMENT OF ANGLE OPTIMIZATION

SNR(dB)	5	10	15	20	25	30
BER <sub>1</sub> improvement (%)	2.44	6.76	9.94	14.29	15.75	20.69
BER <sub>2</sub> improvement (%)	-1.94	-2.93	0.40	6.11	11.70	14.55
BER <sub>3</sub> improvement (%)	-1.72	-2.34	0.80	7.90	11.63	17.45
BER <sub>4</sub> improvement (%)	2.52	6.26	10.20	14.03	14.44	22.75
Average BER improvement (%)	0.43	2.23	5.65	10.78	13.46	18.96

## 5.6 Conclusions

In this chapter, the joint optimization of the user signatures together with the relay power to minimize the average SER bound of the network was proposed for the CFNC coded multi-access relay channels with non-orthogonal communications (MAR-NOC). For this purpose, we first developed a new SER bound under the receiver-CSI for the system considered, where ML detection is assumed to be employed at both a the relay and destination nodes, and numerically shown that this SER-bound captures the error characteristics of the network for a wide range of SNR values. After that, we formulated the problem of jointly optimizing the user signatures and the relay power as a convex program while considering the network topology and the constraint

on total transmit power. Following that, we derived the KKT optimality conditions for the designed convex program, where it was shown that the optimal signature powers and the relay powers constitutes a highly nonlinear relationship whereas the requirement on the optimal user signature phases is simple. Then, we used Sequential Quadratic Programming (SQP) to numerically solve the optimal signature and the relay powers from their non-linear relationship, for which we analytically derived the optimal step direction. To ensure fast convergence of SQP iterations, we also proposed an information theoretical heuristics initialization, whose efficacy was shown through simulations. Once after SER-optimal parameters were determined, we investigated the average BER of the network by performing extensive numerical experiments for different relay positions and various SNR values. Simulation results indicate that the proposed technique improves the average BER of MAR-NOC by up to 90% with a very high average fairness metric as compared to the EPA method, and therefore, it is a promising method to be used in a high throughput next generation multi-access relay system, which operates over non-orthogonal channels.

## 6. Distributed Detection in Wireless Sensor Networks Using Complex Field Network Coding

In Chapter 2, we developed distributed decision fusion both under the perfect CSI and CS for WSNs with a hierarchical topology [91]. Also in Chapter 3, 4 and 5, we analyzed MAR communication which applies CFNC and operates over non-orthogonal channels. In this chapter, we propose to integrate these two contexts, namely we propose to handle distributed detection (DD) with the use of CFNC.

The DD is very useful to combat the adverse effects of fading channels (e.g., multipath-fading, shadowing, noise) in wireless sensor networks because the sensor nodes reaching the same decision provide spatial diversity since the FC is supplied with multiple copies of the transmitted signal over different channels that fade almost independently.

It is important to mention that in all previously mentioned studies in [10], [22]-[24], [29]-[32] the signal transmission and the information fusion are assumed to be accomplished by using orthogonal communications (OC) to avoid multi-access interference (MAI), where only one sensor sends its decision at a certain time while others wait. This, however, decreases the throughput of the system, which is also turns out to be bandwidth inefficient particularly for large networks.

To improve the throughput efficiency of WSNs, the decision fusion with the use of non-orthogonal communications (NOC) have been analyzed in [92]-[95], where the local sensors are directly send their decisions to the FC over a multiple-access channel (MAC).

The performance of the DD in WSNs can be also enhanced with the use of relaying, which has been proposed to achieve both spatial and time diversity in multi-user communications [19]. In the relaying, the sensors first send their decisions over wireless medium, and because of the broadcast nature of the wireless channel both the relay node and the FC hear the information bearing signals of the sensors. Then, the relay node extracts the necessary information about the

sensor decisions. Finally, in the subsequent time interval, the relay node forwards its signal to the FC by employing a relaying protocol [19].

Additionally, the use of relaying together with transmitting sensor decisions over a MAC channel improves both the reliability and the throughput of WSNs, which can be further increased by employing a network-coding (NC) scheme [20] such as physical layer network coding (PNC) (a.k.a analog network coding), complex field network coding (CFNC) [18], [20], [60]-[65] etc.

It is important to point out that although the works in ([92]-[95]) show that non-orthogonal signaling has a potential to improve error performance distributed detection, none of them has considered the use of the relaying. Therefore, in this work, we consider CFNC coded relay assisted communications over a MAC in a WSN with a parallel topology.

In the initial version of this work in [96], we proposed the idea of the use of the CFNC for relay assisted communications over a MAC since the CFNC provides the highest throughput (1/2 symbol per user per channel-use) compared to PNC and XOR methods for communications over non-orthogonal channels since it uniquely allows decoding of user messages under multi-access interference (MAI) [20].

In CFNC, each sensor is assigned a unique pre-determined complex number, which is referred as *signature*. Each signature is used to weight the signal of a particular sensor before the signal transmission and this provides robustness against the multi-access interference (MAI). Hence, the signature selection appears to become one of the important issues to improve the energy efficiency of the system considered. Wang *et.al.* [20] selected signatures based on linear constellation precoding, which is purely complex exponential and distinctively rotates the constellation of each sensor. In contrast to [20], one can also employ signatures with non-unity magnitudes and optimize them according to a certain criterion to enhance the system performance while keeping the average transmit power of the network limited. In addition to signature optimization, the performance of the network can be further improved by appropriately allocating the relay power. In [96], we proposed to optimize the sensor signatures and the relay power by

minimizing the symbol error rate (SER) bound of the network, which provided ,however, only numerical results since the problem is highly non-linear and there is no closed form solutions for the parameters that need to be optimized.

Contrary to [96], in this chapter, we aim at providing analytical solutions to the problem of jointly optimizing the sensor signatures and the relay power. Our main contribution in this work can be summarized as follows. We first derive the optimal LRT based fusion rule for a parallel WSN with a relay node that operates over non-orthogonal wireless channels. Then, we utilize the SER bound of the network together with information theoretical results, and make series of approximations to determine sensor signature and the relay power. Finally, we have shown through the numerical experiments that the proposed method outperforms the classical approach , where the former reaches the same performance of the latter while consuming less amount of energy.

In the next Section, we give a background on the classical distributed detection (CDD) for a parallel WSN. In Section 6.2, the system model for CFNC coded relay assisted communications in WSNs is described, and subsequently the LRT based optimum fusion rule is derived for the system considered. In Section 6.3, we present our analytical method for the selection of the sensor signatures and the relay power. Section 6.4 is devoted to investigate the performance of the proposed method through numerical simulations. Finally, we conclude in Section 6.5.

## **6.1 Overview of Classical Distributed Detection over Orthogonal Communication Channels**

In this part, we review the classical distributed detection (CDD) for orthogonal signaling (without a relay node) in WSNs with a parallel topology, where we focus on binary hypotheses:  $H_1$  and  $H_0$  (e.g., they may represent the existence and absence of a target, respectively) at the region of interest (ROI). Also, a network of  $N$  sensors and a FC (without a relay node) is considered as

shown in Figure 3-1., where the  $k^{\text{th}}$  sensor,  $S_k$ , first acquires its measurement  $m_k$  from the ROI and arrives at its decision  $u_k$ , which is later modulated to produce  $x_k$ . Then, the modulated signal  $x_k$  is distorted by the fading and noise and constitutes the signal  $y_k$  at the FC. Finally, the FC combines all of the signals it has received according to a fusion rule, and casts a final decision  $u_o$ . We assume throughout the manuscript that all fading coefficients are modeled as complex Gaussian random variables with zero mean and unit variance and the receiver electronics noise is modeled as additive white Gaussian noise (AWGN) channel. Furthermore, we also assume that the channel state information (CSI) is available at the FC. Note that we just consider binary phase shift keying (BPSK) modulation for the modulated signal, but extension of the results to other modulation schemes is straightforward.

Under the *orthogonal signaling*, the received signal at the the fusion due to the *transmission* of the  $k^{\text{th}}$  sensor can becomes:

$$y_k = \sqrt{\gamma_k} h_k x_k + z_k \quad (6.1)$$

where  $\gamma_k$  is the path loss coefficient of the link between the  $k^{\text{th}}$  sensor and FC;  $h_k$  is complex Gaussian channel coefficient,  $x_k$  is the BPSK modulated signal, which takes values of -1 and 1 respectively for  $k^{\text{th}}$  sensor decision  $u_k$  being 0 and 1 respectively,  $z_k$  is zero-mean AWGN sample with variance of  $\sigma^2 = N_0 / 2$  per dimension.

For this network topology and orthogonal signaling model, the optimal likelihood ratio (LRT) based fusion rule is given in [40]<sup>2</sup> as:

$$\begin{aligned} \Lambda(\mathbf{y}) &= \prod_{k=1}^N \frac{f(y_k | H_1, h_k)}{f(y_k | H_0, h_k)} \\ &= \prod_{k=1}^N \frac{P_{D_k} e^{-\frac{|y_k - \sqrt{\gamma_k} h_k|^2}{2\sigma^2}} + (1 - P_{D_k}) e^{-\frac{|y_k + \sqrt{\gamma_k} h_k|^2}{2\sigma^2}}}{P_{F_k} e^{-\frac{|y_k - \sqrt{\gamma_k} h_k|^2}{2\sigma^2}} + (1 - P_{F_k}) e^{-\frac{|y_k + \sqrt{\gamma_k} h_k|^2}{2\sigma^2}}} \end{aligned} \quad (6.2)$$

<sup>2</sup> The phase coherent detection formulation in reference [40] is equivalent to the complex representation in Eq.(6.2)

where  $\mathbf{y} = [y_1 \dots y_N]^T$  denotes the received signal vector,  $P_{D_k}$  and  $P_{F_k}$  denote the probability of detection and the probability of false alarm respectively of the sensor  $S_k$ , which can be expressed respectively as:

$$\begin{aligned} P_{D_k} &= \mathbb{P}(u_k = 1 | H_1) \\ P_{F_k} &= \mathbb{P}(u_k = 1 | H_0) \end{aligned} \quad (6.3)$$

So, the conventional strategy for the parallel network assumes that the transmission from each sensor is accomplished over orthogonal channels in time. As a result of that, one-symbol information in regard to the hypothesis testing of each sensor is transmitted by  $N$  channel-uses, each of which has duration of  $T_0$  seconds. Therefore, the information rate or throughput for the CDD using orthogonal signaling can be written as :

$$R_{CDD} = \frac{1}{NT_0} \text{ symbols/sec per sensor per channel use} \quad (6.4)$$

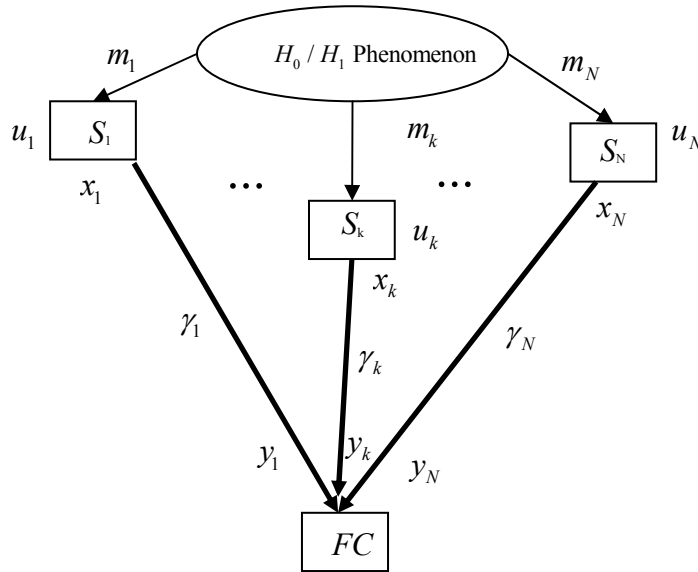


Figure 6-1. The Schematic of Classical Parallel Distributed Detection.

## 6.2 Distributed Detection for Complex Field Network Coded Relay Assisted Communication Over Multi-access Channels

In this section, we first propose to use relaying over a MAC for WSNs and then incorporate

complex field network coding (CFNC) to such a network. Finally, we investigate distributed detection for CFNC coded relay assisted multi-access communication channel.

As mentioned earlier, the use of relay is beneficial to achieve cooperative diversity in order to combat the detrimental effects of fading channels. Hence, in this work, we propose to incorporate CFNC to the parallel WSN with a relay node ( $R$ ) as depicted in Figure 6-2 where all of information signals are transmitted over MAC channels.

In this method, each sensor  $S_k$  is assigned a unique signature  $\theta_k$ . Then the modulated decisions of sensors,  $x_k$ 's, are multiplied by the associated signature and the resultant signals of sensors are sent over non-orthogonal channels simultaneously in time slot 1, which causes interference both at the relay and at the FC. After that, based on the relaying policy (e.g., amplify and forward, estimate and forward etc.), the relay node sends its output to the FC in time slot 2. Therefore, the signals resultant from the non-orthogonal communications under the flat-fading can be written as

$$y_r = \sum_{k=1}^N \sqrt{g_k} h_{s_k r} \theta_k x_k + z_r \quad (6.5)$$

$$y_{sd} = \sum_{k=1}^N \sqrt{\gamma_k} h_{s_k d} \theta_k x_k + z_d \quad (6.6)$$

$$y_{rd} = \sqrt{g_r} h_{rd} \sqrt{\alpha} x_r + z_d \quad (6.7)$$

where  $y_r$  and  $y_{sd}$  are the received signals at the relay node and the FC in time slot 1 respectively;  $y_{rd}$  is the signal acquired at the FC in time slot 2 due to the relaying;  $h_{s_k r}$ ,  $h_{s_k d}$ , and  $h_{rd}$  denote the fading gains of  $S_k$ - $R$ ,  $S_k$ - $FC$  and  $R$ - $FC$  links respectively, which are modeled as complex Gaussian random variables with zero mean and unit variance; the parameter  $\alpha$  determines the power allocated to the relay as a fraction of the total transmit power of sensors;  $\gamma_k$ ,  $g_k$  and  $g_r$  denote respectively as the path-loss coefficients of  $S_k$ - $FC$ ,  $S_k$ - $R$ , and  $R$ - $FC$  links;  $z_r$  and  $z_d$  represent the noise samples at the relay node and FC respectively, which are modeled as additive white Gaussian noise (AWGN) with zero mean and variance of  $N_0/2$  per dimension.

Hence, each sensor transmits one-symbol information in two channel uses each with a duration of

$T_0$  seconds, for which the information-rate becomes

$$R_{CFNC} = \frac{1}{2T_0} \text{ symbols/sec per sensor per channel use} \quad (6.8)$$

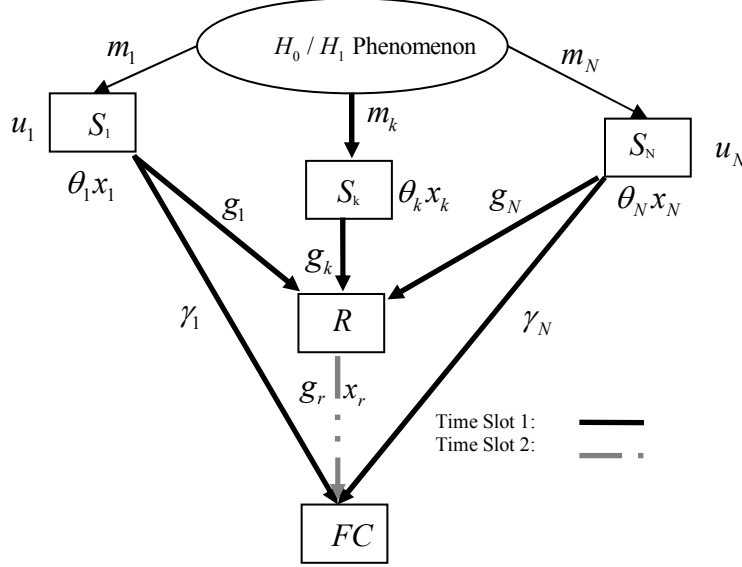


Figure 6-2. The schematic of a CFNC coded relay assisted parallel sensor network, which communicates over MAC channels, with  $N$  sensors, one relay node and a FC.

It is important to point out that in this work, the channel state information (CSI) is assumed to be known at all receiving nodes (i.e., the relay node and the FC). As in [20], we employ estimate and forward type of relaying based on maximum likelihood (ML) detection (i.e., ML relaying). For this relaying policy, the sensor messages are estimated as

$$\hat{\mathbf{x}} \triangleq (\hat{x}_1, \dots, \hat{x}_N) = \arg \min_{x_1, \dots, x_N} \left\| y_r - \sum_{k=1}^N \sqrt{g_k} h_{s_k r} \theta_k x_k \right\|^2 \quad (6.9)$$

Then, the relay signal is generated by incorporating the ML estimates of sensor messages with the sensor-signatures as

$$x_r = \sum_{k=1}^N \theta_k \hat{x}_k \quad (6.10)$$

After that, the relay signal  $x_r$  is forwarded to the FC according to (6.7) in time slot 2. Finally, the FC combines all of the signals it has received in time slot 1 and time slot 2 in Bayesian sense.

Specifically, the optimal LRT based fusion rule is

$$\begin{aligned}\hat{\Lambda}(\mathbf{y}_d) &= \frac{f(\mathbf{y}_d | H_1)}{f(\mathbf{y}_d | H_0)} \\ &= \frac{\sum_{\mathbf{x}} f(y_{sd} | H_1, \mathbf{x}) \left( \sum_{\hat{\mathbf{x}}} f(y_{rd} | H_1, \hat{\mathbf{x}}) P(\hat{\mathbf{x}} | \mathbf{x}) \right) P(\mathbf{x} | H_1)}{\sum_{\mathbf{x}} f(y_{sd} | H_0, \mathbf{x}) \left( \sum_{\hat{\mathbf{x}}} f(y_{rd} | H_1, \hat{\mathbf{x}}) P(\hat{\mathbf{x}} | \mathbf{x}) \right) P(\mathbf{x} | H_0)}\end{aligned}\quad (6.11)$$

where  $\mathbf{y}_d = [y_{sd}, y_{rd}]$ ,  $\mathbf{x} = [x_1, \dots, x_N]^T$ . Also,  $P(\hat{\mathbf{x}} | \mathbf{x})$  is the probability that the relay decides  $\hat{\mathbf{x}}$ , although  $\mathbf{x}$  is transmitted. To simplify the analysis, we assume that the decoding at the relay is perfect<sup>3</sup> (i.e.,  $\hat{\mathbf{x}} = \mathbf{x}$ ) and thus the following LRT rule is employed at the FC.

$$\Lambda(\mathbf{y}_d) = \frac{f(\mathbf{y}_d | H_1)}{f(\mathbf{y}_d | H_0)} = \frac{\sum_{\mathbf{x}} f(y_{sd} | H_1, \mathbf{x}) f(y_{rd} | H_1, \mathbf{x}) P(\mathbf{x} | H_1)}{\sum_{\mathbf{x}} f(y_{sd} | H_0, \mathbf{x}) f(y_{rd} | H_0, \mathbf{x}) P(\mathbf{x} | H_0)} \quad (6.12)$$

Since the conditional probability density function of  $y_{sd}$  ( $y_{rd}$ ) is independent of hypothesis when  $\mathbf{x}$  is given and sensor decisions are conditionally independent, the conditional distributions or probabilities in Eq. (6.12) can be written as

$$f(y_{sd} | \mathbf{x}) = \frac{1}{2\pi\sigma^2} \exp\left\{-\frac{\left|y_{sd} - \sum_{k=1}^N \sqrt{\gamma_k} h_{s_k d} \theta_k x_{s_k}\right|^2}{2\sigma^2}\right\} \quad (6.13)$$

$$f(y_{rd} | \mathbf{x}) = \frac{1}{2\pi\sigma^2} \exp\left\{-\frac{\left|y_{rd} - \sqrt{g_r} h_{rd} \sqrt{\alpha} x_r\right|^2}{2\sigma^2}\right\} \quad (6.14)$$

$$\begin{aligned}P(\mathbf{x} | H_1) &= \prod_{k=1}^N P_{D_k}^{u_k} (1 - P_{D_k})^{1-u_k} \\ P(\mathbf{x} | H_0) &= \prod_{k=1}^N P_{F_k}^{u_k} (1 - P_{F_k})^{1-u_k}\end{aligned}\quad (6.15)$$

The FC produces its final decision  $u_0$  as

$$\Lambda(\mathbf{y}_d) \underset{u_0=0}{\overset{u_0=1}{\geq}} \tau \quad (6.16)$$

where  $\tau$  is the optimal threshold value used at the FC. In this paper, we consider minimum error probability detection at the FC. Hence, the optimal threshold value can be determined in terms of *a priori probability* of the event at the ROI as

<sup>3</sup> This assumption can be justified under high SNR or by using an error correction code.

$$\tau = \frac{P(H_0)}{P(H_1)} \quad (6.17)$$

where  $P(H_0)$  and  $P(H_1)$  are *a priori* probabilities of  $H_0$  and  $H_1$  respectively. The average probability of error of the network can be determined as

$$P_e = P(H_0)P_F + P(H_1)(1 - P_D) \quad (6.18)$$

where  $P_F$  and  $P_D$  are the false alarm and detection probability of the FC respectively, which can be expressed as

$$P_F = P(\Lambda(\mathbf{y}_d) > \tau | H_0) \quad (6.19)$$

$$P_D = P(\Lambda(\mathbf{y}_d) > \tau | H_1) \quad (6.20)$$

Note that the complexity of the fusion in CDD is linear in  $N$  whereas its complexity in CFNC-DD is exponential in  $N$ . Although the CFNC-DD seems to be more complex, it has a better detection performance than CDD as we show in Section 6.4. This computation burden can be alleviated with the use of clustering [42]-[43].

### 6.3 Determination of Sensor Signatures and the Relay Power for Complex Field Network Coded Relay Assisted Communications in WSNs

In this section, we propose a way to select the sensor-signatures optimally by minimizing the ML bound on the symbol error probability of the network. We denote the vector of signatures by  $\boldsymbol{\theta} = [\theta_1, \dots, \theta_N]^T$ . Since each sensor decision is binary, there are  $2^N$  possibilities for the sensor decision vector which can be put in an ordered list. Let  $\mathbf{x}_i$  be the  $i^{\text{th}}$  possible decision vector in the list for  $1 \leq i \leq 2^N$ . The CFNC coded symbol for the decision vector  $\mathbf{x}_i$  due to the non-orthogonal signaling becomes

$$c_i = \boldsymbol{\theta}^T \mathbf{x}_i \quad (6.21)$$

Hence, the CFNC coded symbol takes  $2^N$  distinct values. Assuming CSI is known at the relay

and ML relaying is used, the pair-wise symbol error probability (PEP) of the relay node is

$$\text{PEP}^r(c_i, c_j) \triangleq P(c_i \rightarrow c_j | c_i, \mathbf{h}_{\text{sr}}) = Q\left(\frac{|\sum_{k=1}^N \sqrt{g_k} h_{s_k r} \theta_k d_{ijk}|}{2\sigma}\right) \quad (6.22)$$

where  $\mathbf{h}_{\text{sr}} = [h_{s_1 r}, \dots, h_{s_N r}]^T$ ,  $P(c_i \rightarrow c_j | c_i, \mathbf{h}_{\text{sr}})$  is the probability of deciding symbol  $c_j$  given that symbol  $c_i$  is transmitted under the CSI vector  $\mathbf{h}_{\text{sr}}$ ,  $Q(x) \equiv (1/\sqrt{2\pi}) \int_x^\infty \exp(-t^2/2) dt$  and  $\mathbf{d}_{ij}$  is the difference between the  $i^{\text{th}}$  and  $j^{\text{th}}$  decision vectors i.e.,  $\mathbf{d}_{ij} = (\mathbf{x}_i - \mathbf{x}_j)$ ,  $d_{ijk}$  represents the  $k^{\text{th}}$  component of  $\mathbf{d}_{ij}$ . Hence, the instantaneous CFNC symbol error rate (SER) at the relay can be bounded as

$$P_e^r(\mathbf{h}_{\text{sr}}) \leq \sum_{i=1}^{2^N} \sum_{\substack{j=1 \\ j \neq i}}^{2^N} P(c_i) Q\left(\frac{|\sum_{k=1}^N \sqrt{g_k} h_{s_k r} \theta_k d_{ijk}|}{2\sigma}\right) \quad (6.23)$$

where  $P(c_i)$  is the probability of the CFNC coded symbol for  $1 \leq i \leq 2^N$ , which depends on the false alarm and detection probabilities of the sensors as follows

$$\begin{aligned} P(c_i) &= P(c_i | H_0)P(H_0) + P(c_i | H_1)P(H_1) \\ &= P(\mathbf{x}_i | H_0)P(H_0) + P(\mathbf{x}_i | H_1)P(H_1) \\ &= \prod_{k=1}^N P_{F_k}^{u_k} (1 - P_{F_k})^{1-u_k} P(H_0) + \prod_{k=1}^N P_{D_k}^{u_k} (1 - P_{D_k})^{1-u_k} P(H_1) \end{aligned} \quad (6.24)$$

By using the Chernoff-bound [5] (i.e.,  $Q(x) \leq \frac{1}{2} e^{-\frac{x^2}{2}}$ ), the instantaneous PEP and SER of the relay node is further upper-bounded, respectively, as:

$$\text{PEP}^r(c_i, c_j) \leq \frac{1}{2} e^{-\frac{|\sum_{k=1}^N \sqrt{g_k} h_{s_k r} \theta_k d_{ijk}|^2}{8\sigma^2}} \quad (6.25)$$

$$P_e^r(\mathbf{h}_{\text{sr}}) \leq \frac{1}{2} \sum_{i=1}^{2^N} \sum_{\substack{j=1 \\ j \neq i}}^{2^N} P(c_i) e^{-\frac{|\sum_{k=1}^N \sqrt{g_k} h_{s_k r} \theta_k d_{ijk}|^2}{8\sigma^2}} \quad (6.26)$$

Consequently, bounds on the average PEP and SER can be obtained by averaging the upper-bounds in Eqs.(6.25)-(6.26) over fading gains of the sensors-to-relay links, respectively, as:

$$APEP^r(c_i, c_j) \leq \frac{0.5}{1 + \frac{\sum_{k=1}^N g_k |\theta_k|^2 d_{ijk}^2}{8\sigma^2}} \quad (6.27)$$

$$\bar{P}_e^r \leq \frac{1}{2} \sum_{i=1}^{2^N} \sum_{\substack{j=1 \\ j \neq i}}^{2^N} P(c_i) \frac{1}{1 + \frac{\sum_{k=1}^N g_k |\theta_k|^2 d_{ijk}^2}{8\sigma^2}} \quad (6.28)$$

Also, pair-wise error probability (PEP) at the fusion center (FC), which is denoted by  $D$ , can be written as

$$P(c_i \rightarrow c_j \text{ at } D | c_i) = P(c_i \rightarrow c_i \text{ at } R | c_i) P(c_i \rightarrow c_j \text{ at } D | c_i \rightarrow c_i \text{ at } R, c_i) + P(c_i \rightarrow c_j \text{ at } R | c_i) \left(1 - P(c_i \rightarrow c_i \text{ at } D | c_i \rightarrow c_j \text{ at } R, c_i)\right) \quad (6.29)$$

where  $P(c_i \rightarrow c_i \text{ at } R | c_i)$  and  $P(c_i \rightarrow c_j \text{ at } R | c_i)$  denote correctly decoding probability and PEP respectively at the relay when  $c_i$  is sent. Also,  $P(c_i \rightarrow c_j \text{ at } D | c_i \rightarrow c_i \text{ at } R, c_i)$  denotes the PEP at the FC given that  $c_i$  is sent and the relay correctly decoded,  $P(c_i \rightarrow c_i \text{ at } D | c_i \rightarrow c_j \text{ at } R, c_i)$  denotes the probability of correctly decoding  $c_i$  at the FC given that  $c_i$  is sent and the relay erroneously decode  $c_i$ . Assuming CSI is known at the relay and ML relaying is used, the PEP of the relay node  $R$  is given in (6.22). In addition to that, assuming CSI is available and ML estimator is used at the FC; PEP at the FC given that the relay correctly decoded  $c_i$  will be

$$\begin{aligned}
& P(c_i \rightarrow c_j \text{ at D} | c_i \rightarrow c_i \text{ at R}, c_i, \mathbf{h}_{sd}, h_{rd}) \\
&= P \left( \left| \sum_{k=1}^N \sqrt{\gamma_k} h_{s_k d} \theta_k(\mathbf{x}_i)_k + z_d - \sum_{k=1}^N \sqrt{\gamma_k} h_{s_k d} \theta_k(\mathbf{x}_i)_k \right|^2 + \left| \sqrt{g_r \alpha} h_{rd} \sum_{k=1}^N \theta_k(\mathbf{x}_i)_k + z_d - h_{rd} \sum_{k=1}^N \theta_k(\mathbf{x}_i)_k \right|^2 \right. \\
&\quad \left. \geq \left| \sum_{k=1}^N \sqrt{\gamma_k} h_{s_k d} \theta_k(\mathbf{x}_i)_k + z_d - \sum_{k=1}^N \sqrt{\gamma_k} h_{s_k d} \theta_k(\mathbf{x}_j)_k \right|^2 + \left| \sqrt{g_r \alpha} h_{rd} \sum_{k=1}^N \theta_k(\mathbf{x}_i)_k + z_d - \sqrt{g_r \alpha} h_{rd} \sum_{k=1}^N \theta_k(\mathbf{x}_j)_k \right|^2 \right) \\
&= P \left( |z_d|^2 + |z_d|^2 \geq \left| \sum_{k=1}^N \sqrt{\gamma_k} h_{s_k d} \theta_k d_{ijk} + z_d \right|^2 + \left| \sqrt{g_r \alpha} h_{rd} \sum_{k=1}^N \theta_k d_{ijk} + z_d \right|^2 \right) \\
&= P \left( - \left| \sum_{k=1}^N \sqrt{\gamma_k} h_{s_k d} \theta_k d_{ijk} \right|^2 - \left| \sqrt{g_r \alpha} h_{rd} \sum_{k=1}^N \theta_k d_{ijk} \right|^2 \geq 2 \operatorname{Re} \left\{ z_d^* \sum_{k=1}^N \sqrt{\gamma_k} h_{s_k d} \theta_k d_{ijk} \right\} + 2 \operatorname{Re} \left\{ z_d^* \sqrt{g_r \alpha} h_{rd} \sum_{k=1}^N \theta_k d_{ijk} \right\} \right) \\
&\quad (6.30)
\end{aligned}$$

Since  $z_d$  has a complex Gaussian distribution with zero mean and  $2\sigma^2$  variance which can be denoted as  $CN(0, 2\sigma^2)$ , distribution of random variable

$2 \operatorname{Re} \left\{ z_d^* \sum_{k=1}^N \sqrt{\gamma_k} h_{s_k d} \theta_k d_{ijk} \right\} + 2 \operatorname{Re} \left\{ z_d^* \sqrt{g_r \alpha} h_{rd} \sum_{k=1}^N \theta_k d_{ijk} \right\}$  will be a Gaussian with zero mean and

$4\sigma^2 \left( \left| \sum_{k=1}^N \sqrt{\gamma_k} h_{s_k d} \theta_k d_{ijk} \right|^2 + \left| \sqrt{g_r \alpha} h_{rd} \sum_{k=1}^N \theta_k d_{ijk} \right|^2 \right)$  variance. Therefore, error probability at the FC

given that the relay decoded correctly can be written as

$$\begin{aligned}
& P(c_i \rightarrow c_j \text{ at D} | c_i \rightarrow c_i \text{ at R}, c_i, \mathbf{h}_{sd}, h_{rd}) \\
&= Q \left( \frac{\sqrt{\left| \sum_{k=1}^N \sqrt{\gamma_k} h_{s_k d} \theta_k d_{ijk} \right|^2 + \left| \sqrt{g_r \alpha} h_{rd} \sum_{k=1}^N \theta_k d_{ijk} \right|^2}}{2\sigma} \right) \quad (6.31)
\end{aligned}$$

Also, by a similar analysis as in Eq.(6.30) we can obtain the probability of decoding  $c_i$  correctly at the FC when it is given that relay decode  $c_i$  erroneously

$$\begin{aligned}
& P(c_i \rightarrow c_i \text{ at D} | c_i \rightarrow c_j \text{ at R}, c_i, \mathbf{h}_{sd}, h_{rd}) \\
&= P \left( \left| \sum_{k=1}^N \sqrt{\gamma_k} h_{s_k d} \theta_k(\mathbf{x}_i)_k + z_d - \sum_{k=1}^N \sqrt{\gamma_k} h_{s_k d} \theta_k(\mathbf{x}_i)_k \right|^2 + \left| \sqrt{g_r \alpha} h_{rd} \sum_{k=1}^N \theta_k(\mathbf{x}_j)_k + z_d - \sqrt{g_r \alpha} h_{rd} \sum_{k=1}^N \theta_k(\mathbf{x}_i)_k \right|^2 \right. \\
&\quad \left. \leq \left| \sum_{k=1}^N \sqrt{\gamma_k} h_{s_k d} \theta_k(\mathbf{x}_i)_k + z_d - \sum_{k=1}^N \sqrt{\gamma_k} h_{s_k d} \theta_k(\mathbf{x}_j)_k \right|^2 + \left| \sqrt{g_r \alpha} h_{rd} \sum_{k=1}^N \theta_k(\mathbf{x}_j)_k + z_d - \sqrt{g_r \alpha} h_{rd} \sum_{k=1}^N \theta_k(\mathbf{x}_j)_k \right|^2 \right) \\
&= P \left( |z_d|^2 + \left| \sqrt{g_r \alpha} h_{rd} \sum_{k=1}^N \theta_k d_{jik} + z_d \right|^2 \geq \left| \sum_{k=1}^N \sqrt{\gamma_k} h_{s_k d} \theta_k d_{ijk} + z_d \right|^2 + |z_d|^2 \right) \\
&= P \left( - \left| \sum_{k=1}^N \sqrt{\gamma_k} h_{s_k d} \theta_k d_{ijk} \right|^2 + \left| \sqrt{g_r \alpha} h_{rd} \sum_{k=1}^N \theta_k d_{jik} \right|^2 \geq 2 \operatorname{Re} \left\{ z_d^* \sum_{k=1}^N \sqrt{\gamma_k} h_{s_k d} \theta_k d_{ijk} \right\} - 2 \operatorname{Re} \left\{ z_d^* \sqrt{g_r \alpha} h_{rd} \sum_{k=1}^N \theta_k d_{jik} \right\} \right) \\
&= Q \left( \frac{- \left| \sum_{k=1}^N \sqrt{\gamma_k} h_{s_k d} \theta_k d_{ijk} \right|^2 + \left| \sqrt{g_r \alpha} h_{rd} \sum_{k=1}^N \theta_k d_{jik} \right|^2}{2\sigma \sqrt{\left| \sum_{k=1}^N \sqrt{\gamma_k} h_{s_k d} \theta_k d_{ijk} \right|^2 + \left| \sqrt{g_r \alpha} h_{rd} \sum_{k=1}^N \theta_k d_{jik} \right|^2}} \right) \\
&\tag{6.32}
\end{aligned}$$

Therefore, PEP at the FC which is given in Eq.(6.29) can be written as follows

$$\begin{aligned}
& P(c_i \rightarrow c_j \text{ at D} | c_i) = \\
& APEP^D(c_i, c_j) = E_{\mathbf{h}} \left[ \left( 1 - Q \left( \frac{\left| \sum_{k=1}^N \sqrt{g_k} h_{s_k r} \theta_k d_{ijk} \right|}{2\sigma} \right) \right) Q \left( \frac{\sqrt{\left| \sum_{k=1}^N \sqrt{\gamma_k} h_{s_k d} \theta_k d_{ijk} \right|^2 + \left| \sqrt{g_r \alpha} h_{rd} \sum_{k=1}^N \theta_k d_{jik} \right|^2}}{2\sigma} \right) \right. \\
&\quad \left. + Q \left( \frac{\left| \sum_{k=1}^N \sqrt{g_k} h_{s_k r} \theta_k d_{ijk} \right|}{2\sigma} \right) Q \left( \frac{\left| \sum_{k=1}^N \sqrt{\gamma_k} h_{s_k d} \theta_k d_{ijk} \right|^2 - \left| \sqrt{g_r \alpha} h_{rd} \sum_{k=1}^N \theta_k d_{jik} \right|^2}{2\sigma \sqrt{\left| \sum_{k=1}^N \sqrt{\gamma_k} h_{s_k d} \theta_k d_{ijk} \right|^2 + \left| \sqrt{g_r \alpha} h_{rd} \sum_{k=1}^N \theta_k d_{jik} \right|^2}} \right) \right] \\
&\tag{6.33}
\end{aligned}$$

Each fading coefficient  $h_{s_k r}, h_{s_k d}, h_{rd}$  is assumed to be a zero-mean complex Gaussian random variable with unit variance, which is denoted by  $CN(0,1)$ . Hence, distribution of the random

variable  $T_1 = \left| \sum_{k=1}^N \sqrt{g_k} h_{s_k r} \theta_k d_{ijk} \right|^2$ ,  $T_2 = \left| \sum_{k=1}^N \sqrt{\gamma_k} h_{s_k d} \theta_k d_{ijk} \right|^2$  and  $T_3 = \left| \sqrt{g_r \alpha} h_{rd} \sum_{k=1}^N \theta_k d_{jik} \right|^2$  are exponential

random variables with means  $\lambda_1 = \sum_{k=1}^N g_k |\theta_k|^2 d_{ijk}^2$   $\lambda_2 = \sum_{k=1}^N \gamma_k |\theta_k|^2 d_{ijk}^2$

and  $\lambda_3 = g_r \left| \sum_{k=1}^N \theta_k d_{ijk} \right|^2$  respectively.

Also, pairwise error probability in Eq.(6.33) can be upper bounded as

$$\begin{aligned}
P(c_i \rightarrow c_j \text{ at D} | c_i) &= APEP^D(c_i, c_j) \\
&\leq E_{\mathbf{h}} \left[ Q \left( \frac{\sqrt{\left| \sum_{k=1}^N \sqrt{\gamma_k} h_{s_k d} \theta_k d_{ijk} \right|^2 + \left| \sqrt{g_r \alpha} h_{rd} \sum_{k=1}^N \theta_k d_{ijk} \right|^2}}{2\sigma} \right) + Q \left( \frac{\left| \sum_{k=1}^N \sqrt{g_k} h_{s_k r} \theta_k d_{ijk} \right|}{2\sigma} \right) \right] \\
&\leq E_{\mathbf{h}} \left[ 0.5 \exp \left( -\frac{\left| \sum_{k=1}^N \sqrt{\gamma_k} h_{s_k d} \theta_k d_{ijk} \right|^2 + \left| \sqrt{g_r \alpha} h_{rd} \sum_{k=1}^N \theta_k d_{ijk} \right|^2}{8\sigma^2} \right) + 0.5 \exp \left( -\frac{\left| \sum_{k=1}^N \sqrt{g_k} h_{s_k r} \theta_k d_{ijk} \right|^2}{8\sigma^2} \right) \right] \quad (6.34) \\
&\leq \frac{0.5}{1 + \frac{\sum_{k=1}^N \gamma_k |\theta_k|^2 d_{ijk}^2}{8\sigma^2}} + \frac{1}{1 + \frac{g_r \alpha \left| \sum_{k=1}^N \theta_k d_{ijk} \right|^2}{8\sigma^2}} + \frac{0.5}{1 + \frac{\sum_{k=1}^N g_k |\theta_k|^2 d_{ijk}^2}{8\sigma^2}}
\end{aligned}$$

Hence, PEP and SER at the FC respectively, as:

$$APEP^D(c_i, c_j) \leq \frac{0.5}{1 + \frac{\sum_{k=1}^N \gamma_k |\theta_k|^2 d_{ijk}^2}{8\sigma^2}} + \frac{1}{1 + \frac{g_r \alpha \left| \sum_{k=1}^N \theta_k d_{ijk} \right|^2}{8\sigma^2}} + \frac{0.5}{1 + \frac{\sum_{k=1}^N g_k |\theta_k|^2 d_{ijk}^2}{8\sigma^2}} \quad (6.35)$$

$$\begin{aligned}
\bar{P}_e^D &\leq B_e^D(\mathbf{\theta}, \alpha) \\
&= \frac{1}{2} \sum_{i=1}^{2^N} \sum_{j \neq i}^{2^N} P(c_i) \left( \frac{1}{1 + \frac{\sum_{k=1}^N \gamma_k |\theta_k|^2 d_{ijk}^2}{8\sigma^2}} + \frac{1}{1 + \frac{g_r \alpha \left| \sum_{k=1}^N \theta_k d_{ijk} \right|^2}{8\sigma^2}} + \frac{1}{1 + \frac{\sum_{k=1}^N g_k |\theta_k|^2 d_{ijk}^2}{8\sigma^2}} \right) \quad (6.36)
\end{aligned}$$

where  $B_e^D(\mathbf{\theta}, \alpha)$  denotes the SER upper bound at the FC. Note that, we do not consider any specific type of modulation while we are deriving this bound.

Authors in [96], proposed to determine the sensor signatures and the relay power by minimizing the average SER bound in Eq. (6.36) under the constraints on the total transmit power and the

network geometry as:

$$\begin{aligned}
& \underset{\boldsymbol{\theta}, \alpha}{\text{minimize}} B_e^D(\boldsymbol{\theta}, \alpha) \\
& \text{such that} \\
& P_T - \sum_{k=1}^N |\theta_k|^2 - \alpha \left( \sum_{k=1}^N |\theta_k|^2 \right) \geq 0 \\
& |\theta_k - \theta_l|^2 > 0 \text{ for } k \neq l \\
& \alpha > 0
\end{aligned} \tag{6.37}$$

where the first and second are due to the total transmit power budget and the distinctiveness of the signatures whereas the third constraint stems from the fact that the relay actively sends information.

Clearly,  $\sum_{k=1}^N \gamma_k |\theta_k|^2 d_{ijk}^2$ ,  $|\sum_{k=1}^N \theta_k d_{ijk}|^2$  and  $\sum_{k=1}^N g_k |\theta_k|^2 d_{ijk}^2$  are convex functions of the user signatures. Also,  $g_r \alpha |\sum_{k=1}^N \theta_k d_{ijk}|^2$  is convex with respect to the parameter vector  $\mathbf{p} = [\boldsymbol{\theta}, \alpha]^T$  since

the multiplication of two convex scalar functions is also convex when both functions are non-

decreasing (non-increasing) and positive [85]. Additionally,  $\left( 1 + \frac{g_r \alpha |\sum_{k=1}^N \theta_k d_{ijk}|^2}{8\sigma^2} \right)^{-1}$  is convex

since  $f(x) = \frac{1}{1+x}$  is convex for  $x \geq 0$  and the composition of a convex scalar function with

another convex scalar function is convex. Therefore, the average SER-bound  $B_e^D(\boldsymbol{\theta}, \alpha)$  is convex in both signatures  $\theta_k$  and parameter  $\alpha$ , Eq.(6.37) is a convex program.

As pointed out in [96], deriving closed form analytical results for the sensor signatures and the relay power are cumbersome since the Karush Khun Tucker (KKT) conditions for the convex program (please see the convexity proof in Appendix II) in Eq. (6.37) result in highly nonlinear equations.

Instead of pursuing this direction, we follow another approach, in which we have first expressed

the signatures in the polar form as  $\theta_i = \sqrt{P_i} e^{j\phi_i}$  where  $P_i$  and  $\phi_i$  represent the magnitude-square and phase of the  $i^{\text{th}}$  sensor signature. It is important to note that the signature phases does not have any effect on the average pair-wise error probability (APEP) at the relay (i.e., it is the second term inside the sum of Eq.(6.28)) whereas they affect the at the FC as seen from the second term inside the sum of Eq. (6.36). Following that, we heuristically select the phases of the signatures to increase the separation between CFNC coded symbols using BPSK modulated decisions for unit magnitude sensor signatures, which produces equally separated phases as:

$$\phi_i = \frac{\pi}{N}(i-1) \text{ for } i=1, \dots, N \quad (6.38)$$

In order to optimize the signature magnitudes, we next consider a network of a sensor node called super node (SN), which transmits CFNC symbol  $\theta_1 x_1 + \theta_2 x_2 + \dots + \theta_N x_N$ , a relay with a power control parameter  $\alpha$ , and a FC. The average transmit power,  $P_{SN}$ , of the super node should satisfy

$$P_{SN} = \sum_{k=1}^N P_k \quad (6.39)$$

which is because the decision symbols have unit powers.

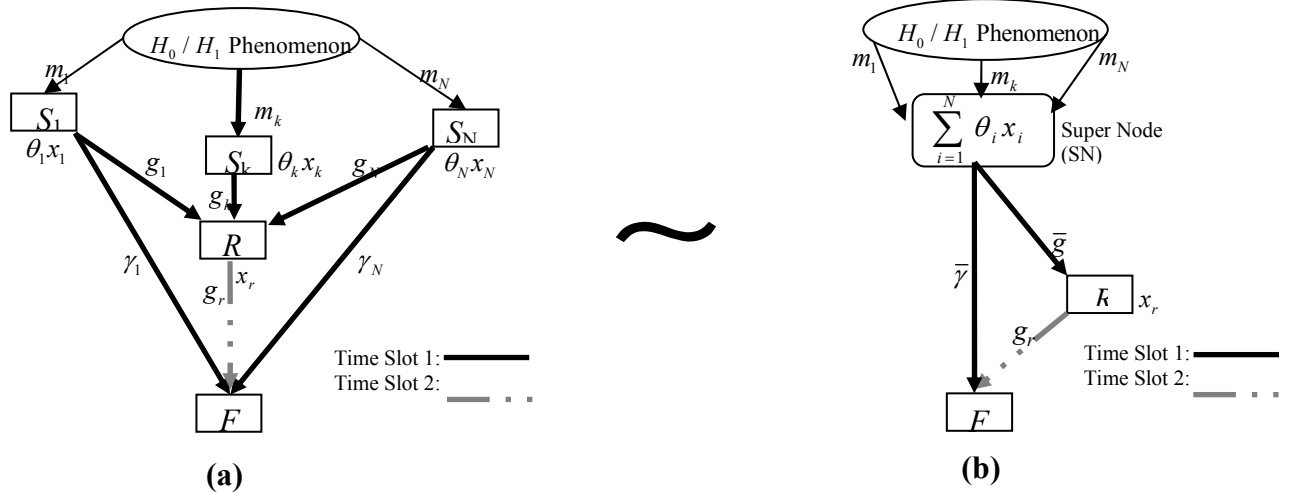


Figure 6-3. An  $N$  node CFNC coded WSN shown in (a) and its approximation by the Super Node (SN) network illustrated in (b).

By performing a similar analysis while deriving Eq.(6.35) and considering the worst symbol pair

that gives the maximum APEP bound at the FC, the APEP of the SN network becomes

$$APEP_{SN}^D(c_i, c_j) \leq B_{SN}^D = \frac{0.5}{1 + \frac{\bar{\gamma} P_{SN} d_{\min}^2}{8\sigma^2}} \frac{1}{1 + \frac{g_r \alpha P_{SN} d_{\min}^2}{8\sigma^2}} + \frac{0.5}{1 + \frac{\bar{g} P_{SN} d_{\min}^2}{8\sigma^2}} \quad \text{for all } i \neq j \quad (6.40)$$

where  $B_{SN}^D$  represents the maximum APEP bound of the SN network,  $\bar{g}$  and  $\bar{\gamma}$  represent the gains of the  $SN-R$  link and  $SN-FC$  link, respectively, and  $d_{\min}$  is the minimum distance in the constellation formed by  $e^{j\phi_1} x_1 + e^{j\phi_2} x_2 + \dots + e^{j\phi_N} x_N$ , which is mathematically represented as:

$$d_{\min} = \min_{i \neq j} |\tilde{c}_i - \tilde{c}_j| \quad (6.41)$$

where  $\tilde{c}_i = [e^{j\phi_1}, e^{j\phi_2}, \dots, e^{j\phi_N}]^T \mathbf{x}_i$  (i.e., CFNC symbols obtained by normalizing the magnitude of each sensor signature to unity).

Assuming that the path gains of all sensor-to-relay links and sensor-to-FC links in the original  $N$  node WSN are close to  $\bar{g}$  and  $\bar{\gamma}$ , respectively, (i.e.,  $g_1 \approx g_2 \approx \dots \approx g_N \approx \bar{g}$  and  $\gamma_1 \approx \gamma_2 \approx \dots \approx \gamma_N \approx \bar{\gamma}$ ), the maximum APEP bound in Eq. (6.35) of the  $N$  node network is close to the maximum APEP bound of the SN network in Eq. (6.35), which implies

$$B^D \approx B_{SN}^D \quad (6.42)$$

where  $B^D$  is the maximum of the APEP bound of the  $N$  node network in Eq. (6.35).

Therefore, approximating the  $N$ -node WSN by the SN network is accurate when path gains of all sensor-to-relay links and sensor-to-FC links are close to  $\bar{g}$  and  $\bar{\gamma}$ , respectively. For a general setting in which these gains may vary, the average of path gains in dB scale is used to determine the path gains of  $SN-R$  link and  $SN-FC$  link, respectively, as:

$$\bar{g} \text{ (in dB)} = \frac{1}{N} \sum_{i=1}^N g_i \text{ (in dB)} \quad \text{and} \quad \bar{\gamma} \text{ (in dB)} = \frac{1}{N} \sum_{i=1}^N \gamma_i \text{ (in dB)} \quad (6.43)$$

where  $\bar{g} = 10^{\frac{\bar{g} \text{ (in dB)}}{10}}$  and  $\bar{\gamma} = 10^{\frac{\bar{\gamma} \text{ (in dB)}}{10}}$ .

After determining the parameters of SN network in terms of parameters of  $N$  node WSN, we are ready to determine optimal transmit powers of the SN and the relay node under the total transmit power constraint stated as:

$$(1 + \alpha) \left( \sum_{k=1}^N P_k \right) = (1 + \alpha) P_{SN} = P_T \quad (6.44)$$

The total power constraint in Eq. (6.44) can be used to replace  $\alpha P_{SN}$  by  $P_T - P_{SN}$  for the bound in Eq.(6.40), which results in

$$B_{SN}^D = \frac{0.5}{1 + \frac{\bar{\gamma} P_{SN} d_{\min}^2}{8\sigma^2}} \frac{1}{1 + \frac{g_r (P_T - P_{SN}) d_{\min}^2}{8\sigma^2}} + \frac{0.5}{1 + \frac{\bar{g} P_{SN} d_{\min}^2}{8\sigma^2}} \quad (6.45)$$

When  $\frac{d_{\min}^2}{\sigma^2}$  is high, a further simplification can be obtained as :

$$B_{SN}^D \approx \frac{32\sigma^4}{(\bar{\gamma} P_{SN} d_{\min}^2)(g_r (P_T - P_{SN}) d_{\min}^2)} + \frac{4\sigma^2}{\bar{g} P_{SN} d_{\min}^2} \quad (6.46)$$

The optimal total power reserved for the transmission of all sensors, which minimizes the maximum pair-wise error probability bound in Eq. (6.46), is obtained by the derivative of Eq. (6.46) with respect to  $P_{SN}$ , and then by equating to zero as:

$$-\frac{32\sigma^4}{\bar{\gamma} P_{SN}^2 g_r (P_T - P_{SN}) d_{\min}^4} + \frac{32\sigma^4}{\bar{\gamma} P_{SN} g_r (P_T - P_{SN})^2 d_{\min}^4} - \frac{4\sigma^2}{\bar{g} P_{SN}^2 d_{\min}^2} = 0 \quad (6.47)$$

Multiplying both sides of Eq. (6.47) by  $P_{SN}^2 (P_T - P_{SN})^2 / 4$  and dividing produces

$$-\frac{8\sigma^4 (P_T - P_{SN})}{\bar{\gamma} g_r d_{\min}^4} + \frac{8\sigma^4 P_{SN}}{\bar{\gamma} g_r d_{\min}^4} - \frac{\sigma^2 (P_T - P_{SN})^2}{\bar{g} d_{\min}^2} = 0 \quad (6.48)$$

The roots of the quadratic relationship in Eq.(6.48) with respect to  $P_{SN}$  can be found as:

$$P_{SN} = P_T + \frac{(8\sigma^2/d_{\min}^2) 2\bar{g} \pm \sqrt{(2\bar{\gamma} g_r P_T + (8\sigma^2/d_{\min}^2) 2\bar{g})^2 - 4\bar{\gamma}^2 g_r^2 P_T^2}}{2\bar{\gamma} g_r} \quad (6.49)$$

The only root satisfying the power constraint  $0 < P_{SN} < P_T$  is

$$P_{SN} = P_T + \frac{(8\sigma^2/d_{\min}^2) \bar{g}}{\bar{\gamma} g_r} - \frac{\sqrt{4\bar{g}\bar{\gamma} g_r P_T (8\sigma^2/d_{\min}^2) + 4\bar{g}^2 (8\sigma^2/d_{\min}^2)^2}}{2\bar{\gamma} g_r} \quad (6.50)$$

The approximate relay power control parameter is determined using the total power constraint in Eq.(6.44) as:

$$\alpha \approx \frac{P_r}{P_r + \frac{(8\sigma^2/d_{\min}^2)2\bar{g} \pm \sqrt{4\bar{g}\bar{\gamma}g_r P_r (8\sigma^2/d_{\min}^2) + 4\bar{g}^2 (8\sigma^2/d_{\min}^2)^2}}{2\bar{\gamma}g_r}} - 1 \quad (6.51)$$

Therefore, the SN network approximation allows us to determine the relay power parameter and the total transmit power of all sensors in Eq. (6.50), which does not, however, specify the individual transmit power of each sensor. The next sub-section is devoted to talk about an information theoretical power allocation method for each sensor by using the total transmit power result in Eq. (6.50).

### 6.3.1 Information Theoretical Determination of Individual Sensor Powers

While allocating an optimal power to each of the sensors is important, maintaining the fairness among sensors is also very crucial in realizing a practical communication network [3], which ensures that the access of any sensor to the network is not denied or overly penalized [67]. For resource allocation in communication systems, various fairness criteria are considered in the literature such as max-min fairness [68], proportional fairness [69] and fairness in information rate (a.k.a symmetric capacity) [70]. Since the symmetric capacity represents the fairest maximum common rate [70], we consider a fairness criterion based on the notion of symmetric capacity and aim to develop a fair power allocation policy for sensor nodes in this study, which ensures fairness among sensors in terms of their average rates and is referred as ‘‘average-rate fairness’’.

For this purpose, we first consider the users-to-relay channel, which is a MAC channel, and thus, the achievable average sum-rate of sensors (the average rates of sensor  $S_i$  is denoted by  $R_i$ ) at the relay is upper bounded as:

$$\begin{aligned}
R_1 + R_2 + \dots + R_N &\leq \frac{1}{2} E \left\{ \log \left( 1 + \frac{\sum_{i=1}^N g_i |\theta_i h_{s,r}|^2}{2\sigma^2} \right) \right\} \\
&\leq \frac{1}{2} \log \left( 1 + \frac{\sum_{i=1}^N g_i P_i E \{ |h_{s,r}|^2 \}}{2\sigma^2} \right) = \frac{1}{2} \log \left( 1 + \frac{\sum_{i=1}^N g_i P_i}{2\sigma^2} \right)
\end{aligned} \tag{6.52}$$

Note that the first line of Eq. (3.7) is because of the ergodic sum-capacity of the MAC channel, while the second line follows from the Jensen's inequality since the ergodic sum-capacity is a log-concave function, and the third line is a resultant from the assumption of independently identically distribution (i.i.d) fading gains with unit energy. Also, the factor of  $\frac{1}{2}$  in the rate calculations results from the normalization due to the use of two time-slots during the communications.

Hence, the average (or ergodic) single user rate bounds can be obtained as:

$$R_i \leq \frac{1}{2} \log \left( 1 + \frac{g_i P_i}{2\sigma^2} \right) \text{ for } i=1,2,\dots,N \tag{6.53}$$

Assuming that the relay decodes the user messages perfectly (which can be achieved by adjusting the user powers appropriately), the signals received at the destination in both time slots (see Eq.(6.6) and Eq.(6.7)) can be written as:

$$\underbrace{\begin{bmatrix} y_{sd}[n] \\ y_{rd}[n] \end{bmatrix}}_{\mathbf{y}} = \underbrace{\begin{bmatrix} \sqrt{\gamma_1} h_{s_1d} & \sqrt{\gamma_2} h_{s_2d} \cdots & \sqrt{\gamma_N} h_{s_Nd} \\ \sqrt{g_r} \alpha h_{rd} & \sqrt{g_r} \alpha h_{rd} \cdots & \sqrt{g_r} \alpha h_{rd} \end{bmatrix}}_{\mathbf{H}} \underbrace{\begin{bmatrix} \theta_1 x_{s_1}[n] \\ \theta_2 x_{s_2}[n] \\ \vdots \\ \theta_N x_{s_N}[n] \end{bmatrix}}_{\mathbf{x}} + \underbrace{\begin{bmatrix} z_d[n] \\ z_d[n] \end{bmatrix}}_{\mathbf{z}} \tag{6.54}$$

where  $\mathbf{y}$  is the received signal vector at destination;  $\mathbf{H}$  is the channel gain matrix;  $\mathbf{x}$  is the power scaled and signature multiplied user message vector, and  $\mathbf{z}$  is the AWGN noise vector.

Therefore, the this channel can be modeled as a  $2 \times N$  *Virtual-MIMO* system, since we consider the dependency of the relayed signal on the sensor messages in Eq. (6.10) under the assumption of perfect relay decoding.

The average joint-sensor rate-bound at the FC is obtained as:

$$R_1 + R_2 + \dots + R_N \leq \frac{1}{2} E \left\{ \log \left( \det \left( \mathbf{I} + \frac{\mathbf{H}\mathbf{S}\mathbf{H}^\dagger}{2\sigma^2} \right) \right) \right\} \leq \frac{1}{2} \log \left( \det \left( \mathbf{I} + \frac{E\{\mathbf{H}\mathbf{S}\mathbf{H}^\dagger\}}{2\sigma^2} \right) \right) \quad (6.55)$$

where  $\dagger$  denotes the conjugate-transpose operation,  $\mathbf{S} = E[\mathbf{x}\mathbf{x}^T]$  is the input covariance matrix, which is a diagonal matrix with  $P_1, P_2, \dots, P_N$  on its diagonal.

Using Eq. (6.55), the average rate of individual sensor can be derived as:

$$R_i \leq \frac{1}{2} \log \left( 1 + \frac{\gamma_i P_i + g_r \alpha P_i}{2\sigma^2} \right) \quad (6.56)$$

By combining Eqs. (3.7)-(3.8) with Eqs. (6.55)-(6.56), the average single-sensor and joint-user rate bounds, respectively, becomes

$$R_i \leq \min \left\{ \frac{1}{2} \log \left( 1 + \frac{\gamma_i P_i + g_r \alpha P_i}{2\sigma^2} \right), \frac{1}{2} \log \left( 1 + \frac{g_i P_i}{2\sigma^2} \right) \right\} \text{ for } i = 1, 2, \dots, N \quad (6.57)$$

$$R_1 + R_2 + \dots + R_N \leq \min \left\{ \frac{1}{2} \log \left( \det \left( \mathbf{I} + \frac{E\{\mathbf{H}\mathbf{S}\mathbf{H}^\dagger\}}{2\sigma^2} \right) \right), \frac{1}{2} \log \left( 1 + \frac{\sum_{i=1}^N g_i P_i}{2\sigma^2} \right) \right\} \quad (6.58)$$

In order to realize the average-rate fairness, we equalize the maximum average rate bounds of sensors in Eqs. (6.57) as:

$$\min \left\{ \frac{1}{2} \log \left( 1 + \frac{\gamma_i P_i + g_r \alpha P_i}{2\sigma^2} \right), \frac{1}{2} \log \left( 1 + \frac{g_i P_i}{2\sigma^2} \right) \right\} = \min \left\{ \frac{1}{2} \log \left( 1 + \frac{\gamma_{i+1} P_{i+1} + g_r \alpha P_{i+1}}{2\sigma^2} \right), \frac{1}{2} \log \left( 1 + \frac{g_{i+1} P_{i+1}}{2\sigma^2} \right) \right\} \quad (6.59)$$

for  $i = 1, 2, \dots, N-1$

which can be further simplified as:

$$\min \{ \gamma_i + g_r \alpha, g_i \} P_i = \min \{ \gamma_{i+1} + g_r \alpha, g_{i+1} \} P_{i+1} \text{ for } i = 1, 2, \dots, N-1 \quad (6.60)$$

By considering Eq.(5.83) , the total transmit power of the sensors in Eq. (6.51) and the solution for the relay control parameter in Eq.(6.51) , the optimal power allocation with the average-rate fairness criterion can be derived as:

$$P_i = \frac{P_{SN}}{\left( \sum_{j=2}^N \frac{1}{\min\{\gamma_j + g_r \alpha, g_j\}} \right) (\min\{\gamma_i + g_r \alpha, g_i\})} \text{ for } i=1,2,\dots,N \quad (6.61)$$

As a result of our analysis, we determine the signature phases, the sensor powers using the notion of average-rate fairness, and the relay power control parameter in Eq. (6.38), Eq.(6.61) and Eq. (6.51), respectively, which shall be used in CFNC-DD. In the next section, we compare the performance of the proposed CFNC-DD with that of the CDD.

## 6.4 Simulation Results

In this part, we investigate the performances of the CFNC-DD over non-orthogonal signaling and CDD over orthogonal signaling by obtaining and comparing their probability of error plots and their receiver operating characteristics (ROC) curves. It is critical to note that the probability of error plots are obtained with the assumption of equal likely priors for various  $SNRs$  while each simulated points on ROC curves is resultant by using a different prior probability. Throughout our discussion, we assume that sensors are identical in terms of their false alarm and detection probabilities as  $P_{F_j} = 0.05$  and  $P_{D_j} = 0.5$ . To make a fair comparison between the Classical-DD (CDD and CFNC-DD, we keep the average transmit power of the network per time slot the same, which is assumed to be 2 units (i.e.,  $P_T = 2$ ). For all numerical simulations presented in this part, we also assume that distance from the sensor  $S_1$ -to-FC link is one and the corresponding path loss coefficient is unity (i.e.,  $\gamma_1 = 1$  or 0 dB) so that other path loss coefficients (i.e.,  $g_k$ ,  $g_r$  and  $\gamma_k$ ) are interpreted as power gains or losses relative to the sensor  $S_1$ -to-FC link. Also, the path-loss exponent is assumed to be 2 and the path-loss coefficients of the relay channel should satisfy the following geometrical constraints because of triangle inequalities.

$$|g_k^{-0.5} - g_r^{-0.5}| < \gamma_k^{-0.5} < g_k^{-0.5} + g_r^{-0.5} \quad (6.62)$$

For the simulations considered, the signal-to noise ratio values given in dB calculated as:

$$SNR \text{ (in dB)} \triangleq 10 \log_{10} \left( \frac{P_r T_0}{2\sigma^2} \right) \quad (6.63)$$

To compare both schemes under the information rate of unity (i.e.,  $R=1$  symbol/sec/channel use), we set the duration of each channel use,  $T_0$ , to  $1/N$  by using Eq.(6.4) and to  $1/2$  by using Eq.(6.8) for CDD or CFNC-CDD, respectively. Since the power budget is fixed, we realize different SNR values by changing the variance of electronics noise in Eq. (6.63).

In order to see the benefit of CFNC-DD over CDD, we first obtain probability of error as a function of  $SNR$  for a WSN with 2 sensors (i.e.,  $N=2$ ) and  $\gamma_1 = \gamma_2 = 0$  dB,  $g_1 = g_2 = 10.45$  dB and  $g_r = 3.10$  dB, which assumes that sensor nodes are equally separated from FC and the distance from the relay node to each sensor node is same. One can see from Figure 6-4 that CFNC-DD outperforms CDD for all  $SNR$  values considered. Specifically, the CFNC-DD has provided an improvement up-to 20.74% in average error probability over CDD. In addition to average error probability plots, we also obtained ROC curves as depicted in Figure 6-5 for same network and different  $SNR$  values of -5, 0 and 5 dB. The proposed CFNC-DD method can obtain up to 10.34%, 11.76%, and 37.77% detection performance improvement over CDD for 5, 0 and -5 dB  $SNR$  respectively.

From the observations made above, we can say that by employing the proposed method, the probability of error gets better especially in the low- $SNR$  regime as compared to using CDD, which can be explained as follows. In the CDD, each sensor signal is sent over an orthogonal channel and disturbed by one noise sample at the FC, which results in the availability of  $N$  noisy measurements at the FC. Contrary to that, CFNC-DD allows interference of sensor signals both at the relay and the FC but each of the interference signals in each time slot of CFNC-DD experiences a distortion due to one noise sample at the FC and thereby there are only two noisy measurements, which carry all sensor data, at the FC. Therefore, the noise has a worse impact on the performance of CDD. Moreover, CDD provides only spatial diversity using the sensors that give the same decision whereas CFNC-DD also achieves time diversity in addition to the spatial

diversity since the relay node in CFNC-DD sends its decision to the FC at a different time slot. This is very beneficial to reduce the negative effect of the interference and noise on the detection performance of the network.

Secondly, we consider a scenario where sensors are located asymmetric with respect to the FC and relay node is closer to  $S_1$  and accordingly, parameters  $g_1, g_2$  and  $g_r$  are selected as 10.45 dB, 3.10 dB and 3.10 dB respectively. The value of  $\gamma_2$  is varied and decided to satisfy the triangle inequality in Eq. (6.62). Then, we obtain the probability of error results as a function of  $SNR$  for various values of  $\gamma_2$ , which are shown in Figure 6-6. Again, CFNC-DD outperforms CDD using the same  $\gamma_2$  value in all  $SNR$  regimes. For example, CFNC-DD has a error performance improvement of 8.43%, 20.92% and 22.98% respectively for  $\gamma_2$  value of 20 dB, 7.96 dB and -2.28 dB under the  $SNR$  of -5 dB. After that, the ROC curves are presented in Figure 6-7 for different  $\gamma_2$  values and  $SNR$  of -5 dB. Consistently, CFNC-DD has a better detection performance than CDD for each  $\gamma_2$  value and a given false alarm probability. In particular, CFNC-DD results in detection performance improvements up to 32.14%, 42.10% and 105.50% can be obtained for 20 dB, 7.96 dB and -2.28 dB  $\gamma_2$  respectively. Therefore, our proposed method performs better even if sensor nodes are located far from the FC. As pointed out earlier, this is because the CFNC-DD results in both spatial diversity and the time diversity.

Next, we increase the number of sensors to  $N=4$  and select  $g_1= g_2= g_3= g_4=13.98$  dB in which the relay node is separated from the sensors equally. Also, the parameters  $\gamma_1, \gamma_2, \gamma_3, \gamma_4$  and  $g_r$  should be chosen to satisfy the triangle inequalities in Eq. (6.62) for which  $\gamma_1=0$  dB,  $\gamma_2=0.91$  dB,  $\gamma_3=0.91$  dB,  $g_r=0.91$  dB are used and the value of  $\gamma_4$  has let to change during the numerical experiments without conflicting the triangle inequalities. Then, we obtain the probability of error versus  $SNR$  curves for various values of  $\gamma_4$  as shown in Figure 6-8. One can see from this figure that CFNC-DD decreases the error probability of CDD up-to 29.10%, 34.40% and 31.61% for  $\gamma_4$  value of 20 dB, 6.02 dB and 0.91 dB respectively for 0 dB  $SNR$ . Finally, we obtain the ROC curves in

Figure 6-9 by changing the a priori probability of the event in the region of interest for SNR of 0 dB and different values of  $\gamma_4$ . CFNC-DD has a detection performance increase up to 34.73%, 54.23% and 57.86% detection performance improvement over CDD for 20 dB, 6.02 dB and 0.91 dB  $\gamma_4$  respectively.

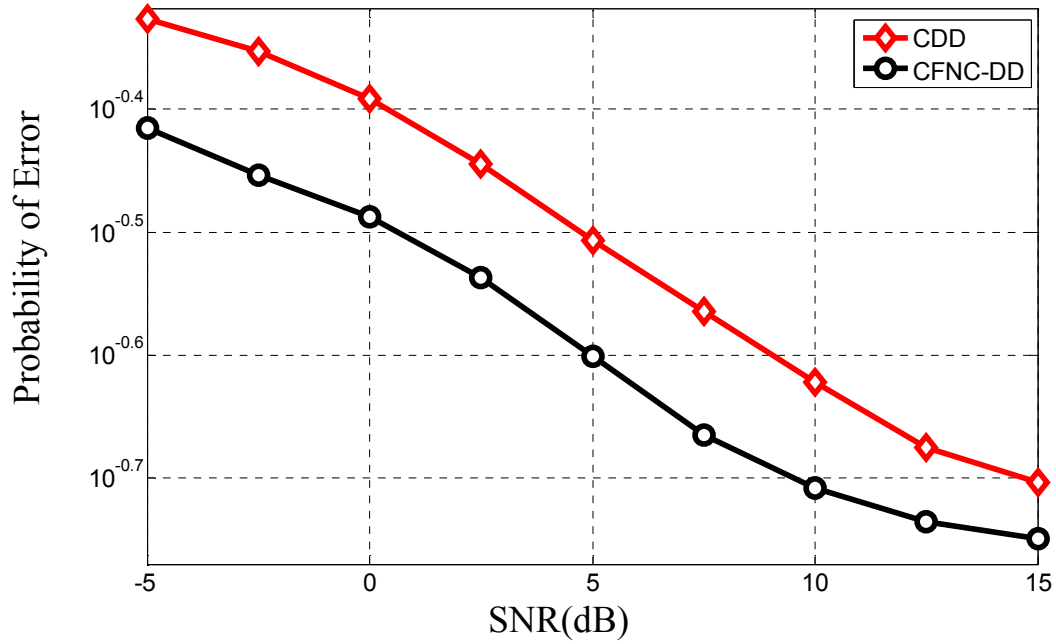


Figure 6-4 Probability of error versus SNR curves of CFNC-DD and CDD for  $N=2$ ,  $\gamma_1 = \gamma_2 = 0$  dB,  $g_1 = g_2 = 10.45$  dB,  $g_r = 3.10$  dB.

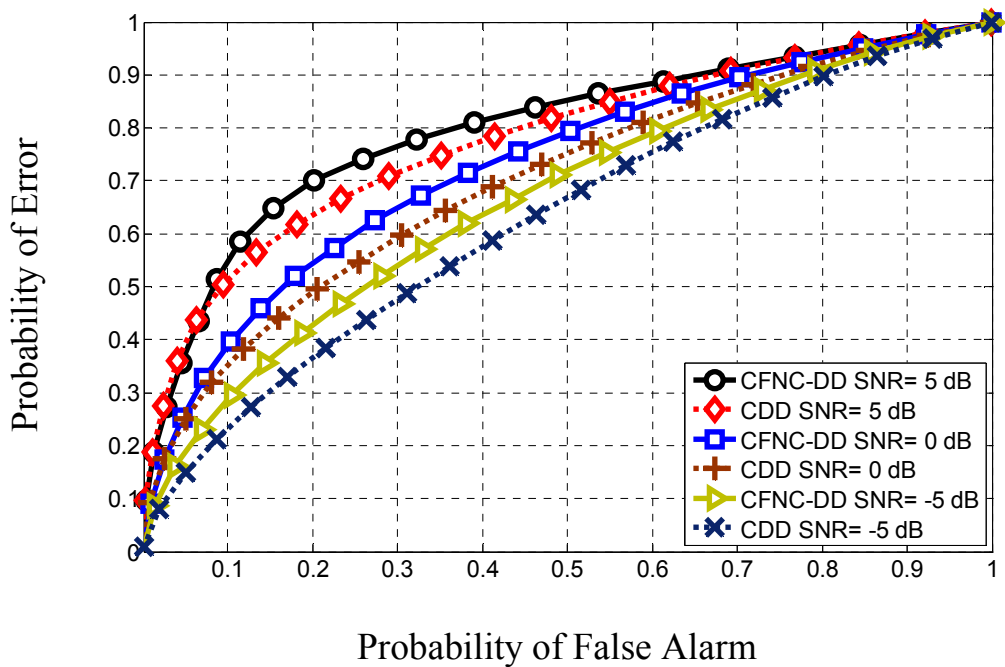


Figure 6-5. ROC curves of CFNC-DD and CDD under different SNRs for  $N=2$ ,  $\gamma_1=\gamma_2=0$  dB,  $g_1=g_2=10.45$  dB,  $g_r=3.10$  dB

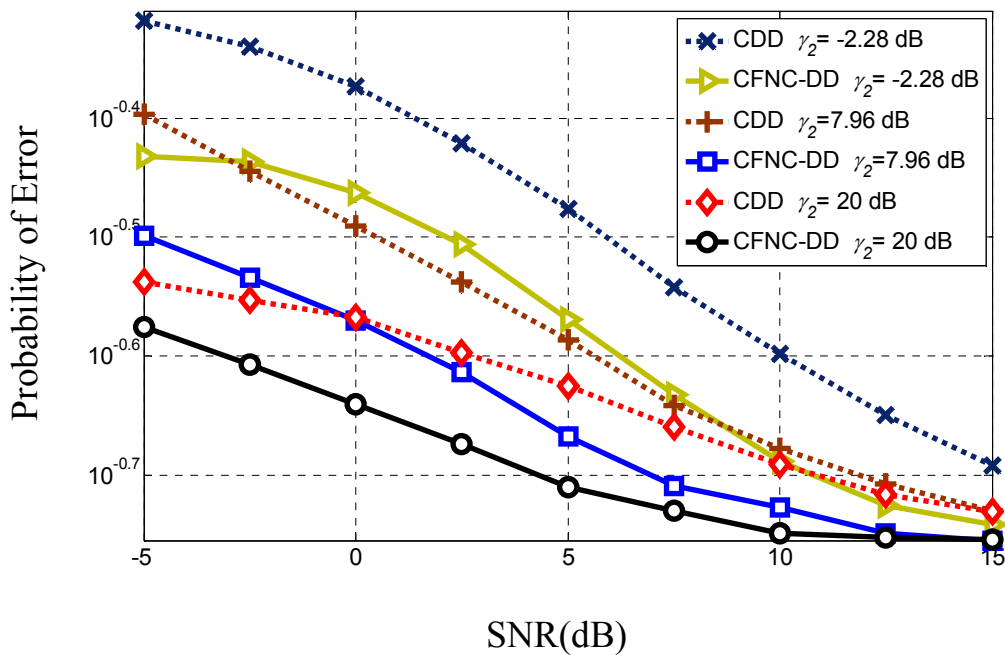


Figure 6-6. Probability of error versus SNR curves of CFNC-DD and CDD under various  $\gamma_2$  values for  $N=2$ ,  $\gamma_1=0$  dB  $g_1=10.45$  dB  $g_2=3.10$  dB  $g_r=3.10$  dB

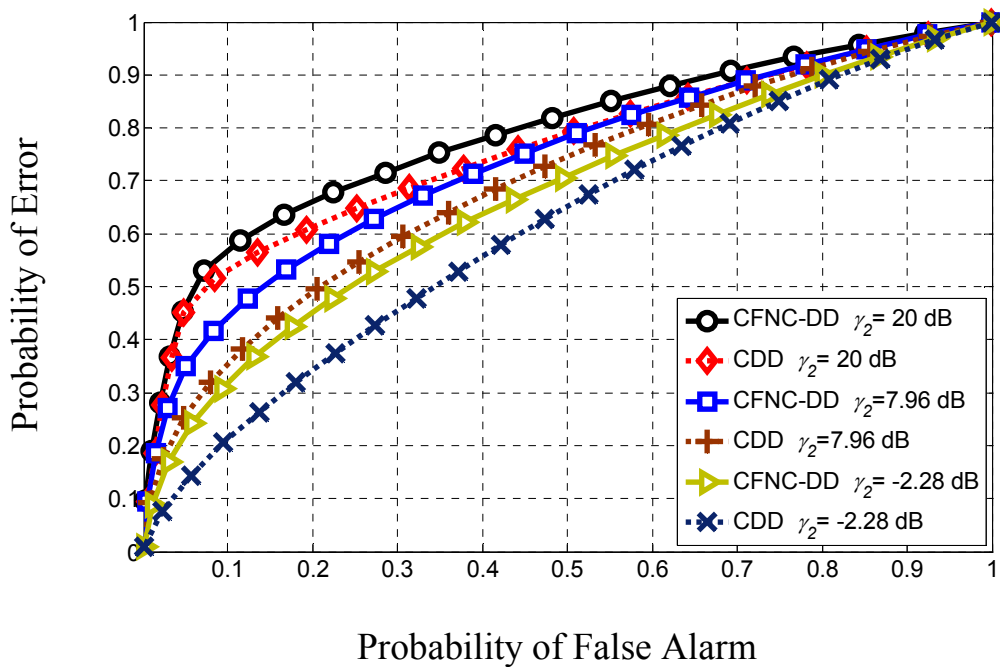


Figure 6-7. ROC curves of CFNC-DD and CDD under various  $\gamma_2$  values for  $N=2$ ,  $\gamma_1=0$  dB  $g_1=10.45$  dB  $g_2=3.10$  dB  $g_r=3.10$  dB and  $SNR=-5$  dB

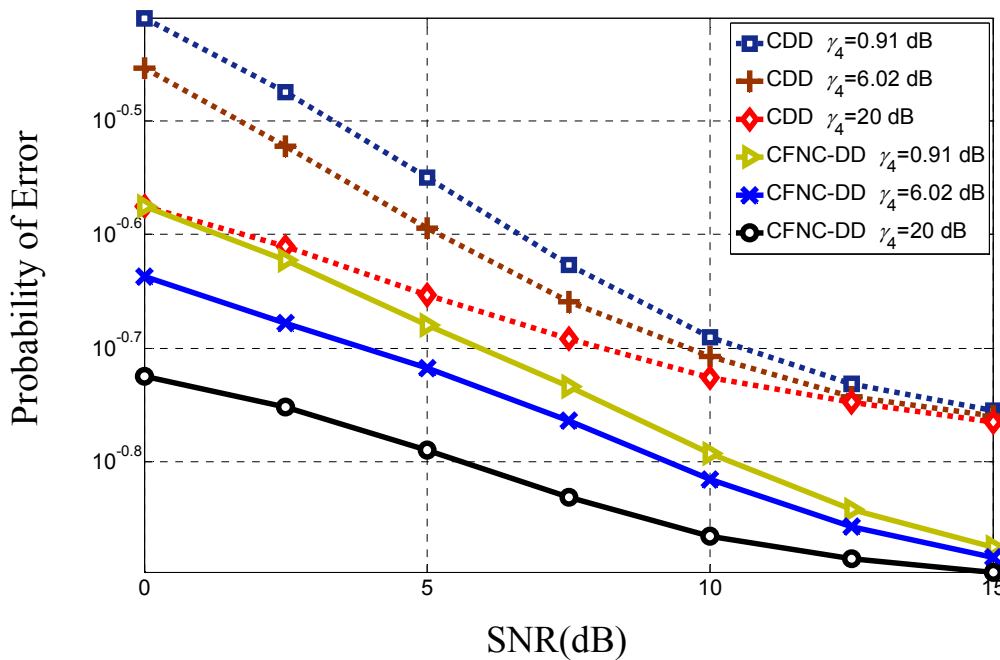


Figure 6-8. Probability of error versus  $SNR$  curves of CFNC-DD and CDD under various  $\gamma_4$  values for  $N=4$ ,  $\gamma_1=0$  dB,  $\gamma_2=0.91$  dB,  $\gamma_3=0.91$  dB, and  $g_1=g_2=g_3=g_4=13.98$  dB,  $g_r=0.91$  dB

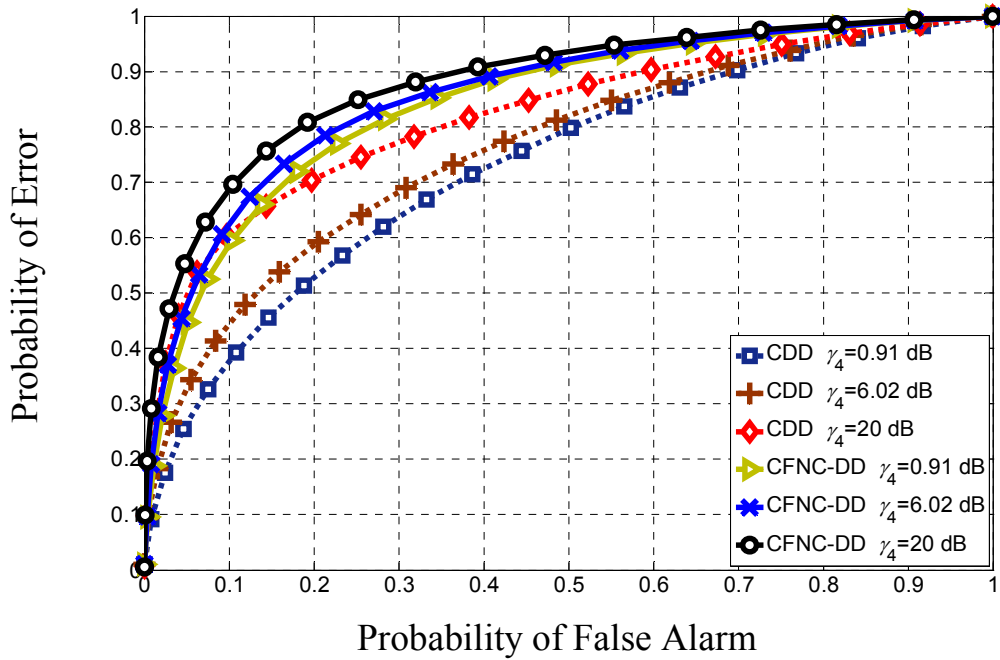


Figure 6-9. ROC curves of CFNC-DD and CDD under various  $\gamma_4$  values for  $N=4$ ,  $\gamma_1=0$  dB,  $\gamma_2=0.91$  dB,  $\gamma_3=0.91$  dB, and  $g_1=g_2=g_3=g_4=13.98$  dB, and  $SNR=0$  dB

## 6.5 Conclusions

In this work, we considered the complex field network coded (CFNC) relay assisted communications in order to improve the performance and energy efficiency of the parallel wireless sensor networks (WSN) under fading and noise. We derived the optimal LRT based fusion rule for the proposed system. Then, we proposed an analytical method to jointly determine the sensor signatures and the relay power by utilizing an upper bound on symbol error probability of the network together with some information theoretical results. Finally, we have shown through that numerical simulation that the proposed method significantly outperforms the classical distributed detection (CDD) in terms of detection performance or energy efficiency. Therefore, the proposed signature selection method in the system considered is a promising technique to be used in a high energy efficient next generation wireless sensor networks, which operates over non-orthogonal channels.

## 7. Conclusion and Future Work

In this thesis, power allocation, network coding and distributed decision fusion is investigated for multi source communication over a relay. The target of this thesis is to understand and analyze relay assisted multi source communication systems and then propose methods to improve the network performance in terms of detection probability, BER and achievable rate.

We first studied decision fusion over fading channels for a hierarchical WSN. We derived optimum fusion rules for a WSN with hierarchical topology under two distinct assumptions: (1) receiving nodes have exact knowledge of CSI or (2) receiving nodes have exact phase information and statistics of the channel gain. It turns out that, although the fusion rule under the assumption of exact CSI knowledge performs better in terms of detection probability, it is much more complex than the fusion rule with exact phase knowledge and channel statistics. We, also show that cluster size of a hierarchical WSN with same total number of sensors affects the detection probability performance of network for each fusion rule. Our simulations confirm that selecting smaller cluster sizes boosts the detection performance of network. An extension to our work may be integrating the path loss coefficients of randomly deployed nodes in the network into the decision fusion process and deriving simpler fusion rules to decrease computational complexity. Also, as we mentioned in Chapter 2, for the fusion rule with exact CSI, GFC have to know the CSIs between sensor nodes and CLHs exactly. But in practice, due to communication and feedback errors it is not possible. Therefore, another extension for this work may be the analysis of optimum fusion rule with CSI considering feedback and quantization errors for CSI [5].

Next, we analyzed power allocation problem for CFNC-RAC channel under decode and forward type of relaying. We present non-convex non-linear sum rate maximization problem which considers fairness among users for the CFNC-RAC under the total power constraint. As the solution to this problem, we propose rate-optimal fair power adaptation (ROFPA) where we

obtained power values for users and relay by dividing the parameter space properly. The optimal power values in ROFPA policy were determined over the segment, which resulted in the largest achievable sum-rate among all segments. Our simulations validate that proposed ROFPA, which is fair to the users in terms of achievable rate, approach have better performance in both BER and sum rate when compared to EPA. Then, for the same CFNC-RAC channel we come up with the SER upper bound problem when ML is employed both in relay and destination. We derived SER upper bound for CFNC-RAC channel, and we define signature optimization problem which minimizes the derived SER upper bound under total power constraint for the cases where relay power is fixed and adjustable. For the fixed relay power case, we show that minimizing the SER upper bound problem is convex and applying KKT conditions optimum angle difference between users signatures can be obtained directly. On the other hand, it is not possible to reach optimum signature powers analytically since the relation between them is highly non-linear. Hence, using Taylor expansion we decrease the level of nonlinearity and we obtained best solutions around ROFPA solution. In our simulations we observed that proposed method overcomes the conventional method EPA in terms of BER. Also, for the adjustable relay power case, obviously obtaining the user signature and relay powers is much more complicated than the fixed relay case. Therefore, starting from ROFPA solution we applied SQP to get user signature and relay powers. And we observed from simulations that, our method has great superiority on EPA case. Finally, we suggest integrating CFNC in decision fusion process of WSNs. Considering performance indexes of sensor nodes we derive SER upper bound at the FC under adjustable relay power assumption. To minimize the decision fusion failures based on the communication errors, we come up with the idea of selection of sensor signature which minimizes the SER upper bound and we end up with more complicated relations between sensors' powers and relay power. Then, we proposed a method to obtain user signature powers and relay power by making an analogy between MAR channel and single user (super node) relay channel. As a future work, proposed methods for both sum rate and SER upper bound optimization can be extended to the cases where

transmitters have CSI and effect of imperfect feedback from receiving nodes to transmitting nodes can be analyzed for both optimization problems. Sum rate and SER upper bound derivations should be revisited to make this extension.

## REFERENCES

- [1] H. Walke et al, "Relay-based deployment concepts for wireless and mobile broadband radio," *IEEE Commun. Mag.*, vol.40, no.8, pp. 102–114, Aug. 2002.
- [2] A. Goldsmith, *Wireless Communications*. 1<sup>st</sup> ed. Cambridge UK: Cambridge University Press, 2005.
- [3] D. Tse and P. Viswanath, *Fundamentals of Wireless Communication*, 1<sup>st</sup> ed. Cambridge UK: Cambridge University Press, 2005.
- [4] A. Sendonaris, E. Erkip, B. Aazhang, "User cooperation diversity. Part I. System description," *IEEE Trans. Commun.* vol.51, no.11, pp.1927-1938, Nov. 2003
- [5] J. G. Proakis, *Digital Communications*, 4<sup>th</sup> ed. New York: McGraw-Hill, 2001.
- [6] V. Tarokh, N. Seshadri, A.R. Calderbank, "Space-time codes for high data rate wireless communication: performance criterion and code construction," *IEEE Trans. Inf. Theory*, vol.44, no.2, pp.744-765, Mar. 1998
- [7] E. Van der Meulen, "Three-terminal communication channels," *Advances in Applied Probability*, vol.3, pp,120-154, 1971
- [8] W. Guan, "Cooperative communication with wireless network coding," Ph.D. Thesis, University of Maryland, USA, 2013.
- [9] J. N. Laneman, D. N. C. Tse, and G. W. Wornell, "Cooperative diversity in wireless networks: efficient protocols and outage behavior," *IEEE Trans. Inform. Theory*, vol. 50, no.12, pp. 3062-3080, Dec. 2004.
- [10] P. K. Varshney, "*Distributed detection and data fusion*," 1<sup>st</sup> ed. New York:Springer,1996.
- [11] I.F. Akyildiz, W. Su, Y. Sankarasubramaniam, E. Cayirci, "A survey on sensor networks," *IEEE Commun. Mag.*, vol.42, no.9, pp. 80–89, Sep. 2004.

- [12] B. Rankov and A. Wittneben, "Achievable rate regions for the two-way relay channel," in *Proc. IEEE International Symposium on Information Theory (ISIT '06)*, Seattle, USA, Jul. 2006), p.1668-1672.
- [13] B. Rankov and A. Wittneben, "Spectral efficient protocols for half-duplex fading relay channels," *IEEE J. Sel. Areas Commun.*, vol. 25, no. 2, pp.378-389, Feb. 2007.
- [14] T.Ho and D. S. Lun, *Network Coding: An Introduction*, 1<sup>st</sup> ed. Cambridge UK: Cambridge University Press, 2008.
- [15] S. Zhang and S. C. Liew, and P. P. Lam " Hot topic: physical layer network coding for the two-way relay channels," in *Proc. 12th MobiCom*, Los Angeles, CA,USA, Sep.2006, 358-365.
- [16] M. Pischella, and D.L.Ruyet, "Optimal power allocation for the two-way relay channel with data fairness," *IEEE Commun. Letters*, vol.15, no.9, pp. 959-961, Sep. 2011.
- [17] R. Ahlswede, N. Cai, S. Y. R. Li, and R. W. Yeung, "Network information flow," *IEEE Trans. Inf. Theory*, vol. 46, no. 4, pp. 1204–1216, Jul. 2000.
- [18] S. Y. R. Li, R. W. Yeung, and N. Cai, "Linear network coding," *IEEE Trans. Inf. Theory*, vol. 49, no. 2, pp. 371–381, Feb. 2003.
- [19] T.M.Cover and J.A. Thomas, *Elements of Information Theory*, 1<sup>st</sup> ed. New York: Wiley, 1991.
- [20] T. Wang and G. B. Giannakis, "Complex field network coding for multiuser cooperative communications," *IEEE J. Sel. Areas Commun.*, vol. 26, no. 3, pp.561-571, Apr. 2008.
- [21] R.R.Tenney and N.R. Sandell Jr., "Detection with distributed sensors," *Trans. Aerosp. Electron. Syst.*, vol.17, no.4, pp.501-510, Jul. 1981.
- [22] I.Y. Hoballah, P.K. Varshney, "Distributed Bayesian signal detection," *IEEE Trans. Inf.Theory*, vol. 35, no.5 pp. 995–1000, Sep. 1989.

- [23] S.C.A Thomopoulos., R. Viswanathan , D.K. Bougoulas, "Optimal distributed decision fusion," *IEEE Trans. Aerosp. Electron. Syst.*, vol. 25, no.5, pp. 761–765, Sep. 1989.
- [24] Z. Chair, P.K. Varshney, "Optimal data fusion in multiple sensor detection system," *IEEE Trans. Aerosp. Electron. Syst.*, vol. 22, no.1, pp.98-101, Jan. 1986.
- [25] Z.B.Tang, K. Pattipatti, and D.L. Kleinman, "An algorithm for determining the detection thresholds in a distributed detection problem," *IEEE Trans. Syst. Man Cybern.*, vol.21, no.1, pp231-237, Jan./Feb. 1991.
- [26] C.W. Helstrom, "Gradient algorithms for quantization levels in distributed systems" *IEEE Trans. Aerosp. Electron. Syst.*, vol. 31, no. 1, pp390-398, Jan.1995.
- [27] G. S. Lauer and N. R. Sandell, "*Distributed detection of known signal in correlated noise*," Rep. ALPHATECH, Burlington, MA Mar. 1982.
- [28] V. Aalo, R. Viswanathan, "On distributed detection with correlated sensors: Two examples," *IEEE Trans. Aerosp. Electron. Syst.* vol.25, no.3, pp.414-421, May. 1989.
- [29] M. Kam, W. Chang, and Q. Zhu, "Hardware complexity of binary distributed detection systems with isolated local Bayesian detectors," *IEEE Trans. Syst., Man, Cybern.*, vol. 21, no. 3, pp. 565–571, May/Jun. 1991.
- [30] E. Drakopoulos and C. C. Lee, "Optimum multisensor fusion of correlated local decisions," *IEEE Trans. Aerosp. Electron. Syst.*, vol. 27, no. 4, pp. 593–605, Jul. 1991.
- [31] M. Kam, Q. Zhu, and W. S. Gray, "Optimal data fusion of correlated local decisions in multiple sensor detection systems," *IEEE Trans. Aerosp. Electron. Syst.*, vol. 28, no. 3, pp. 916–920, Jul. 1992.
- [32] P. K. Willett, P. F. Swaszek, and R. S. Blum, "The good, bad, and ugly: Distributed detection of a known signal in dependent Gaussian noise," *IEEE Trans. Signal Process.*, vol. 48, no. 12, pp. 3266–3279, Dec. 2000.

- [33] C. Rago, P. K. Willett, and Y. Bar-Shalom, "Censoring sensors: A low-communication-rate scheme for distributed detection," *IEEE Trans. Aerosp. Electron. Syst.*, vol. 32, no. 2, pp. 554–568, Apr. 1996.
- [34] C. T. Yu and P. K. Varshney, "Paradigm for distributed detection under communication constraints," *Opt. Eng.*, vol. 37, no. 2, pp. 417–426, Feb. 1998.
- [35] F. Gini, F. Lombardini and L. Verrazzani, "Decentralised detection strategies under communication constraints," in *Proc. Inst. Elect. Eng., Part F: Radar, Sonar, Navigation*, vol. 145, Aug. 1998, pp. 199–208.
- [36] J. Chamberland and V. V. Veeravalli, "Decentralized detection in sensor networks," *IEEE Trans. Signal Process.*, vol. 51, no. 2, pp. 407–416, Feb. 2003.
- [37] S. Appadwedula, V.V. Veeravalli and D.L. Jones, "Robust and locally-optimum decentralized detection with censoring sensors," in *Proc. Int. Conf. on Inform. Fusion*, Annapolis, MD, USA, Jul. 2002 pp.56-63.
- [38] S. C. A. Thomopoulos and L. Zhang, "Distributed decision fusion networking delays and channel errors," *Inf. Sci.*, vol. 66, pp. 91–118, Dec. 1992.
- [39] B. Chen and P. K. Willet, "On the optimality of the likelihood-ratio test for local sensor decision rules in the presence of nonideal channels," *IEEE Trans. Inf. Theory*, vol. 51, no. 2, pp. 693–699, Feb. 2005.
- [40] B. Chen, R. Jiang, T. Kasetkasem and P.K. Varshney, "Channel aware decision fusion in wireless sensor networks," *IEEE Trans. Signal Process.* vol.52, no. 12, pp.3454-3458, Dec. 2004.
- [41] R. Niu, B. Chen, P.K. Varshney, "Fusion of decisions transmitted over Rayleigh fading channels in wireless sensor networks," *IEEE Trans. Signal Process.*, vol. 54, no. 3, pp. 1018-1027, Mar. 2006.

- [42] Q. Tian, E. J. Coyle, "Optimal distributed detection in clustered wireless sensor networks," *IEEE Trans. Signal Process.* vol.55, no. 7, pp.3892-3904, Jul. 2007.
- [43] G. Ferrari, M. Martalo, R. Pagliari, "Decentralized detection in clustered sensor networks," *IEEE Trans. Aerosp. Electron. Syst.*, vol. 47, no. 2, pp. 959–973, Apr. 2011.
- [44] J.N. Tsitsiklis, "Decentralized detection," *Advances in Stat. Signal Process.*, Vol.2, pp. 297-334, 1993.
- [45] Y. Lin, B. Chen, and P. K. Varshney, "Decision fusion rules in multi-hop wireless sensor networks," *IEEE Trans. Aerosp. Electron. Syst.*, vol. 41, no.2, pp. 475-488, Apr. 2005.
- [46] W.H. Press, S. A. Teukolsky, W. T. Vetterling and B. P. Flannery, *Numerical Recipes in C*, 2<sup>nd</sup> ed. New York: Cambridge University Press, 1997.
- [47] Ye Nong (Ed.), *The Handbook of Data Mining*, 1<sup>st</sup> ed. New Jersey:Lawrance Erlbaum Associates, 2003.
- [48] T. M. Cover and A. E. Gamal, "Capacity theorems for the relay channel," *IEEE Trans. Inf. Theory*, vol. 25, no. 5, pp. 572-584, Sep. 1979.
- [49] A. Host-Madsen and J. Zhang, "Capacity bounds and power allocation for wireless relay channels," *IEEE Trans. Inf. Theory*, vol. 51, no. 6, pp. 2020-2040, June 2005.
- [50] M. O. Hasna and M. S. Alouini, "End-to-end performance of transmission systems with relays over Rayleigh fading channels," *IEEE Trans. Wireless Commun.*, vol. 2, no.6, pp. 1126-1131, Nov. 2003.
- [51] P. A. Anghel and M. Kaveh, "Exact symbol error probability of a cooperative network in a Rayleigh-fading environment," *IEEE Trans. Wireless Commun.*, vol. 3, no.5, pp. 1416-1421, Sep. 2004.
- [52] S. Ikki and M. H. Ahmed, "Performance analysis of cooperative diversity wireless networks over Nakagami-m fading channel," *IEEE Commun. Lett.*, vol. 11, no.4, pp. 334-336, Jul. 2007.

- [53] N. C. Beaulieu and J. Hu, "A closed-form expression for the outage probability of decode-and-forward relaying in dissimilar Rayleigh fading channels," *IEEE Commun. Lett.*, vol. 10, no.12, pp. 813-815, Dec. 2006.
- [54] Y. Li, B. Vucetic, Z. Zhou and M. Dohler, "Distributed adaptive power allocation for wireless relay networks," *IEEE Trans. Wireless Commun.*, vol. 6, no.3, pp. 948-958, Mar. 2007.
- [55] M. Chen, S. Serbetli, and A. Yener, "Distributed power allocation for parallel relay networks," *IEEE Trans. Wireless Commun.*, vol.7, no.2, pp.552-561, Feb.2008.
- [56] X. Deng and A. M. Haimovich, "Power allocation for cooperative relaying in wireless networks," *IEEE Commun. Lett.*, vol. 9, no.11, pp. 994-996, Nov. 2005.
- [57] A. H. Madsen and J. Zhang, "Capacity bounds and power allocation for wireless relay channels," *IEEE Trans. Inf. Theory*, vol. 51, no.6, pp. 2020-2040, Jun. 2005.
- [58] Y. Liang and V. Veeravalli, "Gaussian orthogonal relay channel: optimal resource allocation and capacity," *IEEE Trans. Inf. Theory*, vol. 51, no.9, pp. 3284-3289, Sep. 2005.
- [59] Y. Zhao, R. S. Adve, and T. J. Lim, "Improving amplify-and-forward relay networks: optimal power allocation versus selection," *IEEE Trans. Wireless Commun.*, vol. 6, no.8, pp. 3114-3123, Aug. 2007.
- [60] Y. Chen, S. Kishore, and J. Li, "Wireless diversity through network coding," in *Proc. Wireless Commun. Networking Conf.*, vol. 3, Apr. 2006, pp. 1681-1686.
- [61] S. Katti, H. Rahul, W. Hu, D. Katabi, M. Médard, and J. Crowcroft, "XORs in the air: Practical wireless network coding," in *Proc. ACM SIGCOMM*, Pisa, Italy, Sep. 2006 pp. 243-254.

- [62] S. Zhang and S. C. Liew, "Channel coding and decoding in a relay system operated with physical layer network coding," *IEEE J. Sel. Areas Commun.*, vol.27, no.5, pp.788-796, Jun. 2009.
- [63] Z. Guo, B. Wang, P. Xie, W. Zeng and J. Cui, "Efficient error recovery with network coding in underwater sensor networks", *Ad Hoc Networks*, vol. 7, no. 4, pp. 791-802, Jun. 2009.
- [64] U. Bhat, T. M.Duman, "Decoding strategies at the relay with physical-layer network coding," *IEEE Trans. Wireless Commun.*, vol.11, no.12, pp. 4503-4513, Dec. 2012.
- [65] S. C. Liew, S. Zhang and L. Lu, "Physical-layer network coding: Tutorial, survey, and beyond", *Physical Commun.*, vol. 6, pp.4-42, Mar. 2013.
- [66] L. Lu, T. Wang, S. C. Liew, S. Zhang, "Implementation of physical-layer network coding", *Physical Commun.*, vol. 6, pp. 74-87, Mar. 2013.
- [67] R. Mazumdar, L. Mason and C. Douligeris, "Fairness in the Network Optimal Flow Control: Optimality of Product Forms," *IEEE Trans. Commun.*, vol.39, no.5, pp.775-782, May 1991.
- [68] D. Bertsekas and R. Gallager, *Data Networks*. 2<sup>nd</sup> ed. Upper Saddle River, NJ: Prentice Hall Inc., 1992.
- [69] F. P. Kelly, A. K. Maulloo and D. K. H. Tan, "Rate control in communication networks: shadow prices, proportional fairness and stability," *J.Operational Research Soc.*, vol. 49, no. 3, pp. 237-252, Mar. 1998.
- [70] J. Lee and N. Jindal, "Symmetric Capacity of MIMO Downlink Channels," in *Proc. ISIT 2006*, Seattle USA Jul. 2006 pp. 1031-1035.
- [71] T.K. Akino, P. Popovski and V. Tarokh, "Optimized constellations for two-way wireless relaying with physical network coding," *IEEE J. Sel. Areas Commun.*, vol.27, no.5, pp. 773-787, Jun.2009.

- [72] A.A. Zaidi, M.N. Khormuji, S.Yao and M.Skoglund, "Optimized analog network coding strategies for the white Gaussian multiple-access relay channel," *IEEE ITW*, Taormina, Italy, Oct. 2009, pp. 460-464.
- [73] S. Wang, Q. Song, X. Wang and A. Jamalipour, "Rate and power adaptation for analog network coding," *IEEE Trans. Veh. Technol.*, vol.60, no.5, pp.2302-2313, Jun. 2011.
- [74] Y. Yang, H. Hu, J. Xu, and G. Mao, "Relay Technologies for WIMAX and LTE-advanced mobile systems" *IEEE Commun. Mag.*, vol.47, no.10, pp. 100–105, Oct. 2009.
- [75] A. Bleicher, "4G gets real" *IEEE Spectr.*, vol.51, no.1, pp. 38-62, Jan. 2014
- [76] G. Kramer, M. Gastpar and P. Gupta, "Cooperative strategies and capacity theorems for relay networks," *IEEE Trans. Inf. Theory*, vol. 51, no. 9, pp. 3037–3063, Aug. 2005.
- [77] G. Kramer and A. J. Van Wijngaarden, "On the white Gaussian multiple-access relay channel," in *Proc. IEEE International Symposium on Information Theory (ISIT '00)*, Sorrento, Italy, Jun. 2000), p.40.
- [78] L. Sankaranarayanan, G. Kramer and N. B. Mandayam, "Capacity theorems for the multiple-access relay channels," in *Proc. of the 42nd Annu. Allerton Conf. on Commun., Control and Computing*, Monticello, USA, Sep. 2004 pp.1782-1791.
- [79] L. Sankaranarayanan, G. Kramer and N. B. Mandayam, "Cooperation vs. hierarchy: an information-theoretic comparison," in *Proc. IEEE Int. Symp. on Inform. Theory (ISIT '05)*, Adelaide, Australia, Sep. 2005 pp. 411–415.
- [80] W. Mesbah and T. N. Davidson, "Power and resource allocation for orthogonal multiple access relay systems," *EURASIP J. Adv. Signal. Process.*, vol. 2008, no. 476125, pp. 1-15, May 2008.

- [81] S. Serbetli and A. Yener, "Relay assisted F/TDMA ad hoc networks: node classification, power allocation and relaying strategies," *IEEE Trans. Commun.*, vol.56, no.6, pp.937-947, Jun. 2008
- [82] K. Phan, T. Le-Ngoc, S. A. Vorobyov, C. Tellambura, "Power allocation in wireless multi-user relay networks," *IEEE Trans. Wireless Commun.*, vol. 8, no.5, pp. 2535-2545, May 2009.
- [83] J. Schaefferle and A. Ruegg, " Enhancement of throughput and fairness in 4G wireless access systems by non-orthogonal signaling," *Bell Labs Tech. J.*, vol.13, no.4, pp.59-77, Feb. 2009.
- [84] P.Gong, P. Xue, D. Park, and D. K. Kim, "Optimum power allocation in a nonorthogonal amplify-and-forward relay-assisted network," *IEEE Trans. Veh. Technol.*, vol. 60, no.3, pp.890-900 Mar. 2011
- [85] S. Boyd and I. Vandenberghe, *Convex Optimization*. 1<sup>st</sup> ed. Cambridge UK: Cambridge University Press 2004.
- [86] X. Wang, A. V. Vasilakos, M. Chen ,Y. Liu and T. T. Kwon, "A survey of green mobile networks: opportunities and challenges," *Mobile Networks and Applicat.*, vol. 17. no.1, pp.4-20, Feb. 2012.
- [87] J. Nocedal and S.J. Wright, *Numerical Optimization*, 2<sup>nd</sup> ed. New York: Springer, 2006.
- [88] X. Wang, A. V. Vasilakos ,M. Chen ,Y. Liu and T. T. Kwon, "A Survey of Green Mobile Networks: Opportunities and Challenges," *Mobile Networks and Applicat.*, vol. 17. no.1, pp.4-20, Feb. 2012.
- [89] B. Bernstein, *Matrix Mathematics: Theory, Facts, and Formulas*. 2<sup>nd</sup> ed. NJ: Princeton University Press, 2009.
- [90] R.F.H. Fisher, *Precoding and Signal Shaping for Digital Transmission*. 1<sup>st</sup> ed. New York: Wiley, 2002.

- [91] K. Eritmen, M. Keskinöz, "Distributed Decision Fusion for Hierarchical Wireless Sensor Networks," to Appear in *Wireless Networks*, Springer, 2013 [published online 2013 DOI: 10.1007/s11276-013-0649-y].
- [92] C.R. Berger, M. Guerriero, S. Zhou, P. Willett, "PAC vs. MAC for decentralized detection using noncoherent modulation," *IEEE Trans. Signal Process.*, vol. 57, no. 9, pp.3562-3575, Sep. 2009.
- [93] D. Ciuonzo, G. Romano, P. S. Rossi, "Optimality of received energy in decision fusion over Rayleigh fading diversity MAC with non-identical sensors," *IEEE Trans. Signal Process.*, vol.61, no.1, pp.22-27, Jan. 2013.
- [94] W. Li and H. Dai, "Distributed detection in wireless sensor networks using a multiple access channel," *IEEE Trans. Signal Process.*, vol. 55, no.3, pp. 822 -833, Mar. 2007.
- [95] D. Ciuonzo, G. Romano, P. S. Rossi, "Channel-aware decision fusion in distributed MIMO wireless sensor networks: decode-and-fuse vs. decode-then-fuse," *IEEE Trans. Wireless Commun.*, vol.11, no.8, pp.2976-2985, Aug. 2012.
- [96] K. Eritmen, M. Keskinöz, "Distributed Detection in Wireless Sensor Networks Using Complex Field Network Coding," *16<sup>th</sup> International Conference on Information Fusion (FUSION)*, Istanbul Turkey Apr. 2013 pp.989-996.